FLUXES, DYNAMICS AND CHEMISTRY OF SUSPENDED PARTICUALATE MATTER IN A SOUTHEAST ALASKAN FJORD

FLUXES, DYNAMICS AND CHEMISTRY OF SUSPENDED PARTICULATE MATTER IN A SOUTHEAST ALASKAN FJORD

A

THESIS

Presented to the Faculty of the University of Alaska

in Partial Fulfillment of the Requirements

for the Degree of

DOCTOR OF PHILOSOPHY

By

Gi Hoon Hong, B.S., M.S.

Fairbanks, Alaska

August 1986

FLUXES, DYNAMICS AND CHEMISTRY OF SUSPENDED PARTICULATE MATTER IN A SOUTHEAST ALASKAN FJORD

RECOMMENDED:

George W. Happhut

Susan A. Taneda

Wm. A. Reed

Vern Alverson

D. C. Burrell
Chairman, Advisory Committee

Vern Alverson
Director, Institute of Marine Science

H. J. Simpson
Head, Department of Marine Sciences and Limnology

APPROVED:

E. Dayaee
Dean, College of Natural Sciences

Director of Graduate Programs

Date

ABSTRACT

Sedimentation dynamics of suspended particulate matter (SPM) were investigated in the central basin of Boca de Quadra, a southeast Alaskan fjord.

The weighted mean fluxes over the June 1982-October 1983 were 290, 519, 812, 1124 g m^{-2} yr^{-1}, respectively, determined using sediment traps deployed at 40, 120, 300 and 375 m depth in the 380 m water column. The long-term sedimentation rate was estimated at average 589 g m^{-2} yr^{-1} from sediment ^{210}Pb profiles. Substantial SPM input to mid-depths (below 100 m) from the side arms was noted. Thus, the flux measured at 120 m depth was designated as the primary flux of the SPM to the basin. The sediment focusing resulting from the "V" shaped basin does not appear to be important. Using particulate Al as a tracer, resuspension rate was estimated at some 30-80% of the vertical flux below 280 m depth.

Based on the SPM dynamics, the non-conservative behavior of particulate biogenic matter, Mn and Fe was investigated using a primary-resuspended-altered flux model. Degradation rates of settling POC, PN and biogenic Si were estimated at about 0.85, 0.11, and 0.57 mol m^{-2} yr^{-1}, respectively, in the water column, with maxima at the time of the spring phytoplankton bloom. The "positive alteration" flux of particulate Mn was

estimated at 12-34 mg m^{-2} d^{-1} due to the active recycling of Mn in the benthic regime.

Settling fluxes of particulate biogenic matter show strong seasonality due to the precipitation and primary production pattern. The three methods for estimating sources of organic matter (C/N, $\delta^{13}C$, the riverine SPM input and primary productivity) suggest that phytoplankton primary production *in situ* provides the major portion of settling particulate organic matter (about 70%).

Of the 6.6 mol m^{-2} yr^{-1} of POC raining at 375 m depth, approximately 67% is recycled to overlying waters mainly *via* sediment resuspension, and around 30% is incorporated into the sediments. Sediment diagenesis accounts for about 8%, and around 21% is buried below 50 cm in the sediments. The distribution of pore water solute concentrations was apparently affected by nonlocal exchange processes.

TABLE OF CONTENTS

Page

Page

Page

LIST OF FIGURES

Page

Page

LIST OF TABLES

LIST OF PLATES

ACKNOWLEDGEMENTS

I express my sincere gratitude and appreciation to my major professor, Dr. David C. Burrell, under whose supervision this study has been carried out. My deepest gratitude and appreciation are likewise extended to members of the advisory committee: Drs. Vera Alexander, Susan Henrichs, George Kipphut, and Keith Van Cleve for their valuable suggestions, constructive criticism, patience and encouragement.

I am greatly indebted also to many others, too numerous to mention individually. Particularly noted here are John Smithhisler, Norma Haubenstock, Barry Hogarty, and the late Kurt DeSombre for their valuable assistance during field operations; Dr. Ken Dunton for stable carbon isotope measurements; Drs. Lee Cooper and Peter McRoy for use of the vacuum line; Mike McCrum for allowing to use of the high pressure ion chromatography; Dr. Mary Ann Borchert's help for scanning electron microscope operation; Dr. Donald Shell for contribution of dissolved oxygen meter; David Nebert and Warren Lee for physical oceanographic services in the Boca de Quadra fjord; Dr. Hasong Pak of Oregon State University for discussion of transmissometer results; and Mrs. Eleanor Kelley for proofreading.

Research assistantships were provided by the Institute of Marine Science through awards to Dr. Burrell. Fellowships were granted by the U.S. Borax and Chemical Company. Also, the College of Natural Science provided additional support through provision of a teaching assistant. This research was funded by the U.S. Borax and Chemical Company and the Office of the Vice Chancellor for Research and Advanced Study.

I am also grateful to the Institute of Marine Science for the opportunity to undertake graduate study. And finally, I thank my friends and family for helping me to enjoy these past years in Fairbanks.

CHAPTER 1. INTRODUCTION

Settling organic matter in oceans and estuaries is the major source of food and energy to the benthos. The composition of suspended particulate matter (SPM) is a result of ongoing physical, chemical, biological and geological processes. In the subarctic estuarine environment, these may include: inorganic and organic substances derived from river runoff; aeolian fallout and coastal erosion; resuspension of previously deposited sediments; production *in situ* and decomposition or dissolution of biogenic material; and physical-chemical adsorption-desorption processes related to redox reactions near the sediment-water interface. Most of these processes vary seasonally. Therefore, we can elucidate many of the important biological and geochemical processes occurring in coastal waters by studying the composition and temporal and spatial distribution of SPM.

It is generally impossible to collect biogenic and non-biogenic particulate material separately. Therefore it is necessary to study SPM bulk properties and dynamics in the water column and in the sediment. Parameters such as sources, transport, resuspension, sedimentation rate and sediment mixing are needed to study the non-

conservative behavior of particular constituents among the solid phase elements.

The simultaneous study of SPM dynamics and dynamics of non-conservative elements in the marine environment has been rarely attempted. However, in this thesis, it is proposed that knowledge of the bulk sedimentation dynamics is essential to an understanding of the non-conservative particulate constituents.

The purpose of this study is to describe and explain the temporal variability of settling fluxes of biogenic matter (particulate organic C and N, and biogenic Si) and of bulk SPM in the central basin of Boca de Quadra, a southeast Alaska fjord. In addition, sedimentation processes were investigated in terms of their relationship to settling fluxes. Four major goals of this work are:

1. To characterize the natural sedimentation dynamics in a non-glacial Alaskan fjord.

2. To quantify the physical, chemical and biological processes controlling the fate of particulate organic C, N, biogenic Si, Mn, and Fe within the basin water column.

3. To determine the energy transfer to the benthic community.

4. To elucidate the early diagenesis of biogenic material in the sediments.

Since U.S. Borax and Chemical Corporation intends to develop a molybdenum mine adjacent to Boca de Quadra, this work may also be useful in developing a monitoring strategy for the proposed disposal of mine tailings into this particular fjord.

Fjords in general have one or more sills which restrict the free exchange of water for periods of the year. During "stagnant" periods, chemical and biogeochemical reaction products may accumulate in the fjord basin, which thus acts as a "geochemical bucket" (Heggie, 1977). That is, the fjord basin below sill depth (including bottom sediments) approximates a bucket-like chemical system with one open boundary. Material and energy can be transported only across the boundary (generally around the sill depth horizon), and these fluxes can be easily accounted for.

Fjords are deep and steep-sided so that primary production occurs only in surface waters, with respiration dominating below the surface layers, including the entire benthic regime. The *in situ* primary production is mainly due to planktonic algae because of the extremely limited availability of substrate for littoral communities. The comparatively great depth of fjords permits collection of settling SPM free of

contamination by resuspended materials. Nearly constant temperatures in the deep waters provide a natural thermostat for chemical reactions occurring in the water column and sediments. Since stratification is usually weak below the sill, the vertical component of water movement is relatively large compared to shallow-water estuaries where the horizontal component dominates; hence, the vertical flux of reaction products is magnified. The subarctic latitude causes strong climatic seasonality due to a changing light regime which, in turn, produces strong seasonal changes in freshwater flow, *in situ* primary productivity, and surface water temperatures.

The pristine nature of Boca de Quadra fjord removes complexities introduced by human activity, such as pollutants and cultivated land erosion, and thus provides an environment suited to studying natural processes occurring at the land-sea interface. The pristine subartic fjord is a relatively simple system, similar in some ways to the open ocean, but the processes are occurring in a dramatic fashion. These typical fjord characteristics provide an excellent opportunity for examination of the oceanographic processes controlling the natural fate of non-conservative chemicals.

Among the three basins of Boca de Quadra, the

central basin is a logical choice for study. The outer basin is well-mixed with outside water year-round and behaves as an extension of the shelf waters, whereas, due to the direct influence of the river and the relatively small size of the basin, the inner basin is more akin to the typical shallow (non-fjord type) estuary. The central basin is 10 times larger by volume than is the inner basin, ensuring a relatively long water residence time, and, although separated from the river mouth, is close enough to reflect terrestrial forcing with little lag time. Therefore, the central basin provides a stable water body that retains reaction products for a relatively long period of time.

During the course of this study, most of these potential advantages of the study area have been realized. However, the complex bottom topography has made the task of understanding the dynamics of suspended sediments very difficult.

STUDY APPROACH AND DESIGN

In designing this study of Boca de Quadra sedimentation dynamics, it was proposed that a through understanding of the behavior of bulk particulate matter is essential to understanding the behavior of non-conservative constituents. Thus, to characterize

processes affecting the bulk SPM such as vertical flux, lateral transport and resuspension, measurements of the flux and standing stock of SPM at various depths in the basin water column were made using a sediment trap array and transmissometer, respectively. Scanning electron microscope observations were made on the sediments settling in the water column and on the basin floor to help elucidate the nature and means of transport (*e.g.*, fecal matter) of SPM. Since Al is a conservative element in suspended particles and surface sediments, particulate Al in sediment trap particles was utilized as a tracer for estimation of resuspension. ^{210}Pb activity profiles in the sediments were obtained to measure sedimentation rates of bulk SPM in the sediments for comparison with water column SPM fluxes, and particularly to help determine the primary flux of particles, free from resuspension effects. ^{137}Cs activities in the sediments were measured to complement ^{210}Pb sedimentation rates, and specifically to estimate the sediment mixing coefficient and determine its effects on ^{210}Pb sediment accumulation rates. The transmissometer data were collected in order to seek evidence from SPM distributions for sediment resuspension from the bottom (and to determine its vertical extent), and for lateral

input of sediment from fjord side arms.

Settling fluxes of particulate organic carbon and nitrogen were selected for study from among the non-conservative elements because they are the food and energy source to the benthos. Also, oxidation of organic matter generates most of the redox changes seen in surface sediments. Biogenic Si was chosen to monitor the seasonal effect of phytoplankton growth in the euphotic zone on SPM fluxes in the deep basin because the phytoplankton bloom is dominated by diatoms in this subarctic coastal basin. In order to estimate the provenance of organic matter introduced in the study area, the C/N ratio and $\delta^{13}C$ values of settling particulate organic matter were measured. Particulate Mn and Fe were also investigated because they act as electron-acceptors for organic matter decomposition in the suboxic zone of sediment and because reduction results in their remobilization. Because this work included study of the bulk suspended sedimentation dynamics in the deep basin (primary and resuspension fluxes), a major realizable objective has been the semi-quantitative estimation of non-conservative or alteration fluxes of settling POC, PN, biogenic Si, and particulate Mn and Fe. In the absence of such background data, non-conservative behavior would have been masked by depth

variability in the bulk sediment flux.

To further examine the fate of biogenic matter, the study included measurements of TOC, TN and biogenic Si in the sediments to determine their relationship to settling fluxes in the water column. This aspect of the work provided a means of comparing the rates of alteration processes in the water column and sediments to determine the most important sites of reaction. Concurrently, concentrations of the electron acceptors and diagenetic reaction products in the interstitial water were measured. Settling flux measurements, sedimentation and sediment mixing rates were essential for computing the mass balance of biogenic matter in the sediments.

The underlying rationale for this study can be summarized as follows: The Boca de Quadra fjord, as a pristine marine system with a physically bounded basin, offered a favorable site for the investigation of non-conservative processes affecting biologically important constituents of suspended particulate matter. However, in order to detect, identify, and quantify non-conservative processes, information on the behavior of bulk particulate matter is essential. The bottom sediments are an important reaction site and the ultimate repository for settling particulate matter, and thus must

be included in the investigation of SPM dynamics.

PREVIOUS WORK IN FJORDS

Recently, various aspects of the oceanography of fjords have been discussed extensively in *Fjords: Processes and Products* written by Syvitski, Burrell and Skei (1986). Previous work in fjords related to this thesis will be reviewed briefly in the following paragraphs.

SPM dynamics have been studied elsewhere in order to characterize natural sedimentation dynamics, and because of their influence on water quality. Sources, dispersal pathways, deposition rates and rates of sediment accumulation in glacially-fed fjords have been studied in Alaska (Hoskin *et al.*, 1976; Hoskin *et al.*, 1978) and on the Pacific coast of Canada (Syvitski and Murray, 1981; Syvitski *et al.*, 1986). Sources, distributions, reservoirs, and modes of sedimentation of SPM in non-glacial fjords have been examined in Alaskan fjords (Robb, 1981; Burrell, 1983b). Comprehensive observations on the distribution of SPM, water properties, circulation characteristics, and vertical and lateral SPM fluxes have been examined in Elliot Bay, Puget Sound (Baker *et al.*, 1983).

Settling fluxes of organic matter have been measured

in a number of fjords world-wide in order to estimate the energy transfer from the euphotic zone to the basin floor, and to follow pollutants introduced to surface waters. The flux of organic matter has been directly measured in non-glacial fjords, such as in a Scottish sea loch (Davis, 1975), in St. Margaret's Bay, Nova Scotia (Webster *et al.*, 1975), in Dabob Bay (Prahl *et al.*, 1980; Lorenzen *et al.*, 1981), and the main basin of Puget Sound (Baker *et al.*, 1985). To my knowledge, the settling flux of biogenic silica has not been measured in any fjord. Settling fluxes of particulate Mn and Fe have been directly measured in a very few fjords: in Puget Sound (Feely *et al.*, 1986) and the Laurentian Trough, Canada (Sundby and Silverberg, 1985).

STUDY AREA

Boca de Quadra fjord is located immediately north of the Alaska - British Columbia border (55 °N; Fig. 1.1). It is some 60 km long, and has three sills which divide the fjord into three partly separated basins. The outer basin is about 18 km long and 360 m deep. The central basin (32 km long, 2-3 km wide and 380 m deep) is isolated from the outer basin by the Kite Island sill, which is 85 m deep, and from the inner basin by a 140 m sill. The small inner basin is only 10 km long and 180 m

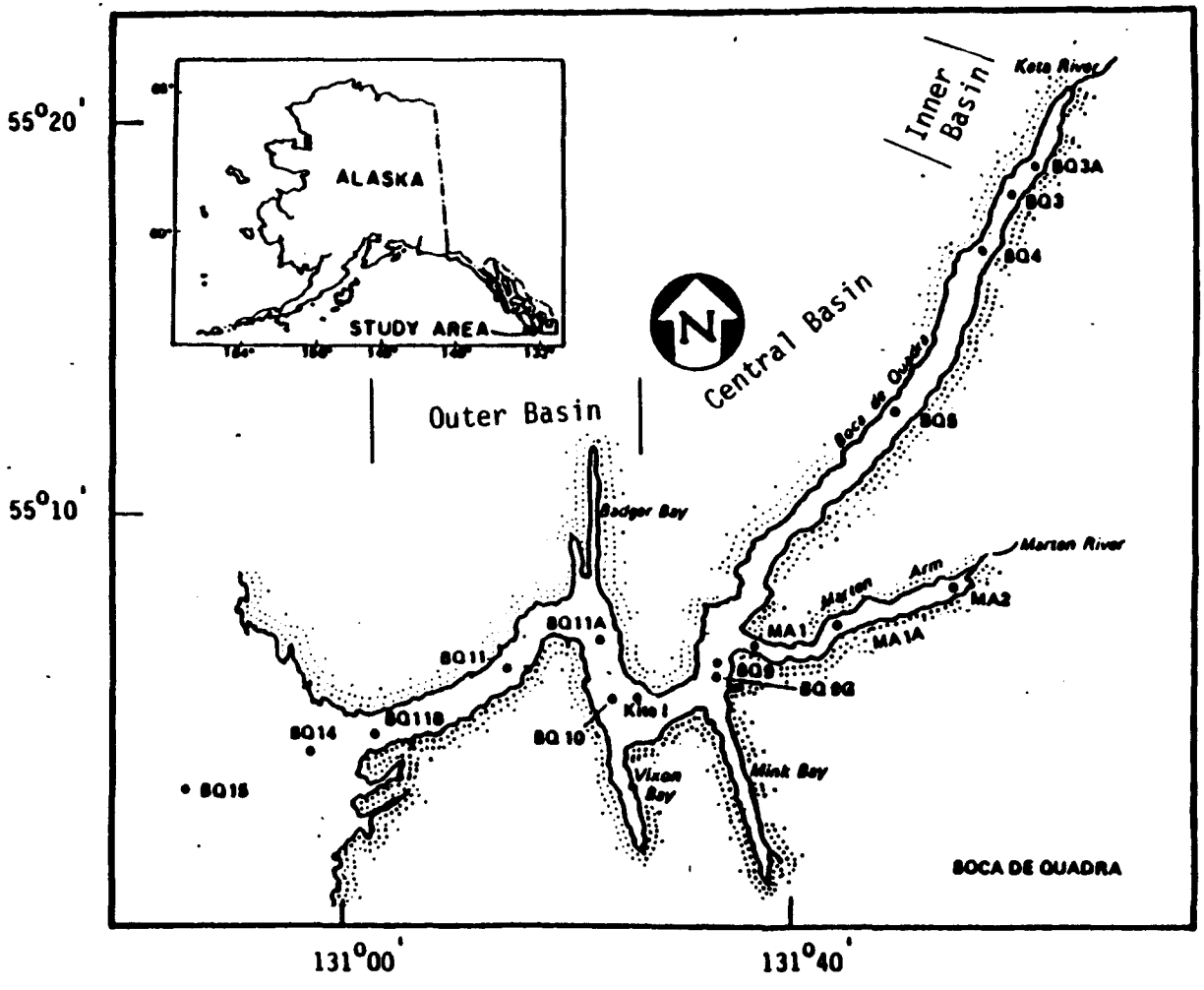

Fig. 1.1. Boca de Quadra fjord system: Location of oceanographic stations (from Burrell, 1983b).

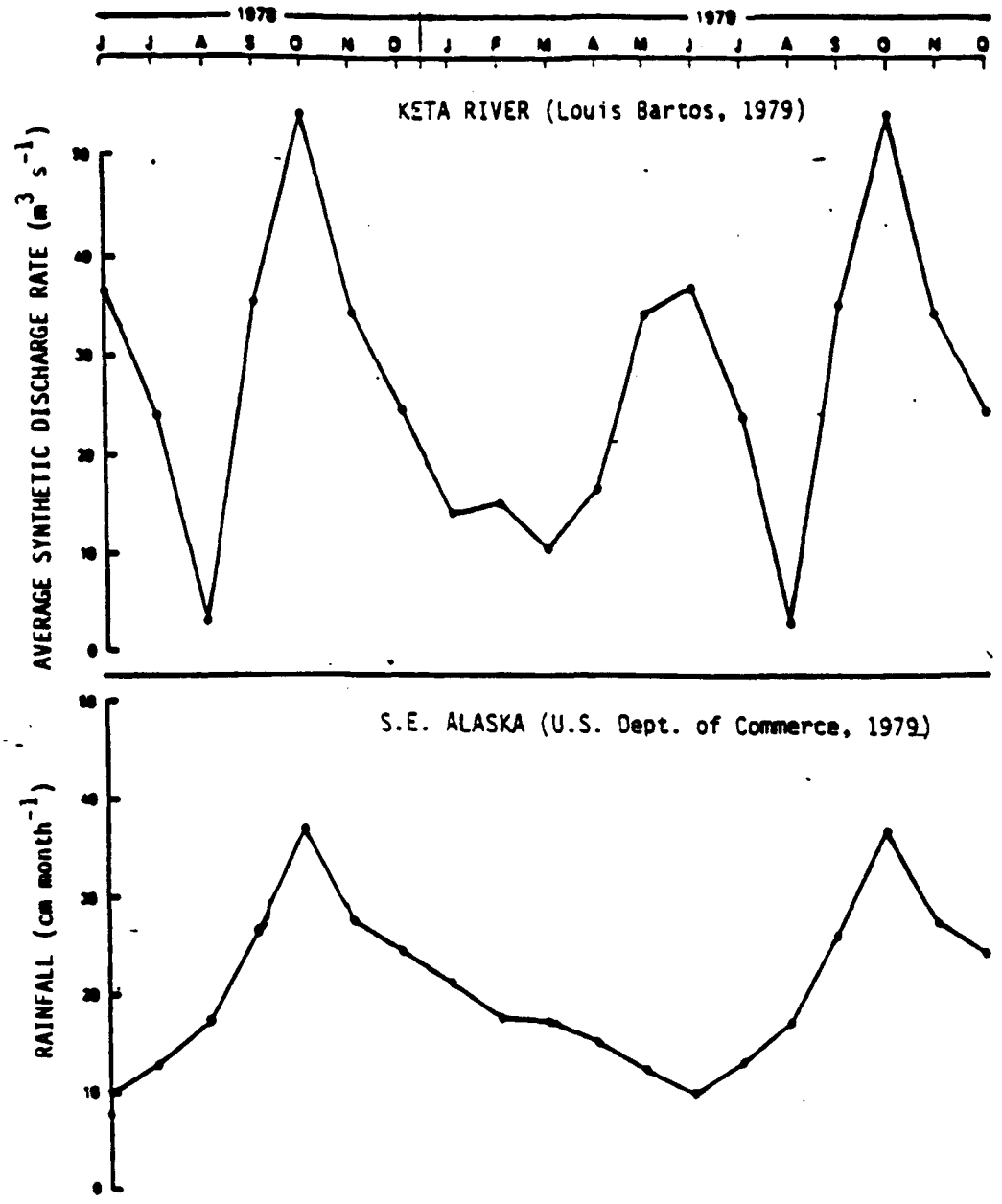

Fig. 1.2. Average synthetic discharge for the Keta River. Average records of rainfall for southeast Alaska (from Burrell et al., 1980).

deep. The major rivers which impinge on the fjord are the Keta River at the head, and the Marten and Red Rivers *via* Marten Arm. Both the Keta and Marten Rivers erode a grandiorite complex and quartzofeldspathic schists and gneisses associated with it (Robb, 1981). The rivers show a bimodal peak flow pattern, with maxima in the spring (April - May) due to snow melt and in late fall due to the precipitation maximum (Fig. 1.2). Because of the rugged terrain within the catchment area, the discharge rate into the head of the fjord is relatively low, despite the high mean precipitation rate over the region (up to 4 m yr^{-1}); and the residence time of rainfall is very short. Thus the daily variation in river discharge may be extremely large. During periods of high river discharge, freshwater input amounts to only 1.5 to 2% of the tidal volume (up-fjord from the Kite Island sill; Burrell, 1986).

The region is characterized by dry summers and wet winters. The vegetation is dominated by a dense forest of Sitka spruce (*Picea sicheness*) and western hemlock (*Tsuga heterphylla*) with extensive regions of poorly drained muskeg. Soils are highly leached, with a low pH and nutrient concentrations (Sugai, 1985), and are characteristic of spodosols.

Hydrography and Circulation Features

A comprehensive description of the hydrography and circulation of Boca de Quadra has been given by Burrell *et al.* (1980), Nebert (1984) and Kowalik (1984). Only a brief review of features relevant to suspended sediment dynamics will be given here.

Hydrography

The surface salinity in the central basin of Boca de Quadra (Station BQ9) is lower than elsewhere in the fjord due to the influence of Marten Arm, which is the major source of freshwater. Overall, the temperature ranges from 6.3-7.4 °C and salinity from 32.4-32.6 °/oo in the deep basin. The presence of the Kite Island sill (85 m), the small river flow relative to the tidal prism, and the very deep basin (380 m), result in the large differences in hydrographic characteristics between the surface layer (upper 50 m) and the deep layer beneath.

In the surface layer, water column stability exhibits a strong seasonal cycle. The poorest stratification occurs in winter when freshwater input is at a minimum and coastal downwelling is at a maximum. In addition, winds are greater in winter. During summer, the addition of freshwater at the surface and the intrusion of dense water from the adjacent continental

shelf due to the relaxation of downwelling tends to strengthen the overall water column stability. However, the deep water column (deeper than 50 m) tends to be most stable (stratified) during winter when renewal is not occurring, and least stable during the summer-fall renewal period. This is due to the nature of the renewal process: the water in the deep central basin becomes homogeneous during the deep water renewal period because water of greater density is introduced at sill depth. This creates instabilities which result in downward mixing and the formation of a homogeneous water column below sill depth. When nearly homogeneous, a relatively lower level of turbulent energy is able to provide sufficient mixing energy to maintain the deep region of low stability during fall and winter. The renewal period is characterized by this nearly homogeneous layer which grows in thickness downwards until it extends to the bottom of the central basin. Once the mixed layer reaches the bottom, currents in excess of 50 cm s^{-1} associated with the renewal process can occur at the bottom. The homogeneous deep basin waters tend to change with time because the stability of the water column decreases through mixing with overlying water. The low stability within the deep waters of the central basin results in a rapid reduction of the salt within the basin

during the non-renewal period.

No evidence of large scale mixing in the upper water column (above 50 m) was found. However, the deep basin waters experience vertical mixing, both during deep water renewal and during the winter period of relative isolation. Such deep mixing is limited in vertical extent during summer-fall by increased stability of the water column above the sill depth.

Circulation

Estuarine circulation in the surface layer is not well-developed due to a freshwater discharge into the head of the fjord which is insignificant compared with tidal flow. The surface waters of the fjord (upper 10 m) are very sluggish, and net transport is often upfjord (above Marten Arm). Below Marten Arm the surface outflow seems to be better developed due to the increased freshwater input from Marten Arm, and because of entrainment of subsurface waters. Below this surface outflow, the net near surface current (*ca.* 30 m depth) flow is inward at moderate speeds (5-10 cm s^{-1}). Near the 100 m depth, water flows upfjord during the early phase of deep water renewal (from April to June), but seawards for the rest of the year. This coincides with the observed net outflow at sill depth across the Kite

Island sill (Nebert, 1984).

The deep basin waters tend to be "quiet" except for periodic deep water renewal events. In general, Alaskan fjords exhibit a strong seasonality with a period of deep water renewal followed by a period of relative isolation (Muench and Heggie, 1978). Seasonal deep water renewal depends on non-local forcing over the adjacent continental shelf and on turbulent mixing within the fjord. In Boca de Quadra, the non-local forcing is thought to be due mainly to upwelling and downwelling phenomena in the Gulf of Alaska as described for the northeast Gulf region by Royer (1975). During the winter (October-April), regional winds lead to coastal downwelling, moving dense oceanic water down below sill depth, separating it from the deep basin water inside the fjord. In summer, wind-driven coastal downwelling is relaxed due to relaxation of the Aleutian low pressure system, and more dense oceanic water reappears at sill height, initiating renewal of basin water in the deep fjord. Currents during the renewal events may be very strong in the sill area (70-80 cm s^{-1}), lessening to 50 -60 cm s^{-1} at 310 m depth close to the sill, and gradually diminishing (5-10 cm s^{-1}) at 370 m depth in the BQ9 area (Nebert, 1984). However, occasional strong

currents in excess of 50 cm s^{-1} have been reported at the bottom in the BQ9 area. Currents are thought to be larger at the bottom than within most of the overlying basin waters because of bathymetric constraints: the bottom of the central basin of Boca de Quadra is "V" shaped (Fig. 1.3). However, current velocity is generally very small (0-5 cm s^{-1}) within the water column. During the renewal period, dense oceanic water displaces the resident water in the deep basin, causing upwelling in the fjord.

The general circulation of Boca de Quadra is shown schematically in Fig. 1.3. The solid arrows here indicate features which are thought to be relatively persistent, while dashed arrows suggest the intermittent currents. However it must be kept in mind that short term variability is generally great enough to reverse most of the features shown. Recent findings also show that deep water renewal may not necessarily occur annually (Nebert, 1984) and it may be related to long term density fluctuations in the northeast Pacific (*e.g.*, El Nino; Burrell, 1986).

Marine Biology

Burrell (1983b) has reviewed the ecology of marine biota in Boca de Quadra extensively. A brief summary

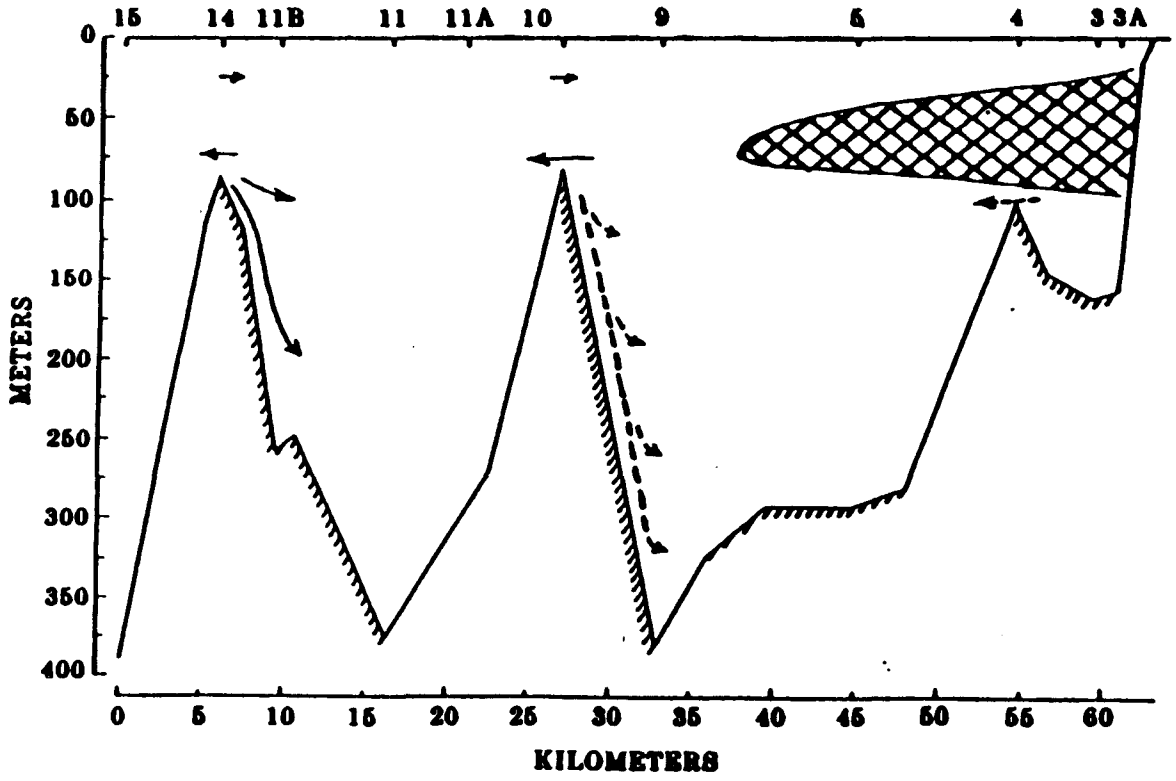

Fig. 1.3. Stylized dominant flow features in Boca de Quadra (from Nebert, 1984).

related to this study is given here.

In general, a relatively rapid and intense blooming of diatoms occurs each spring - early summer. This vernal bloom, which spans a few weeks or less, is the most distinctive feature of phytoplankton growth at high latitudes. In Boca de Quadra, it is often dominated by a single neritic diatom such as *Skeletonema costatum* (1980), *Thalassiosira* spp. (1981), or *Chaetoceros* spp (1982). These diatoms are succeeded by flagellates during the summer, which is a transition from "net" to "ultra" phytoplankton, but diatom densities may rise again as part of a secondary bloom in late summer. In winter phytoplankton growth virtually stops due to the lack of light and water column instability. The early phase is primarily fueled by "new" nutrients and summer primary production sustained by "regenerated" nutrients. The supply of "new" nutrients *via* increased mixing and from the rivers in late summer fuels the late summer bloom. The integrated ^{14}C uptake rate in Boca de Quadra has been measured from 1980 through 1982 (Fig. 1.4). During these years, the annual depth-integrated photosynthetic carbon uptake rate at Station BQ 9 within the central basin of Boca de Quadra was 140 $\pm$ 5 g C m^{-2} yr^{-1} (about 12 mol C m^{-2} yr^{-1}). In 1982, approximately 40% of this was due to the spring bloom. These annual

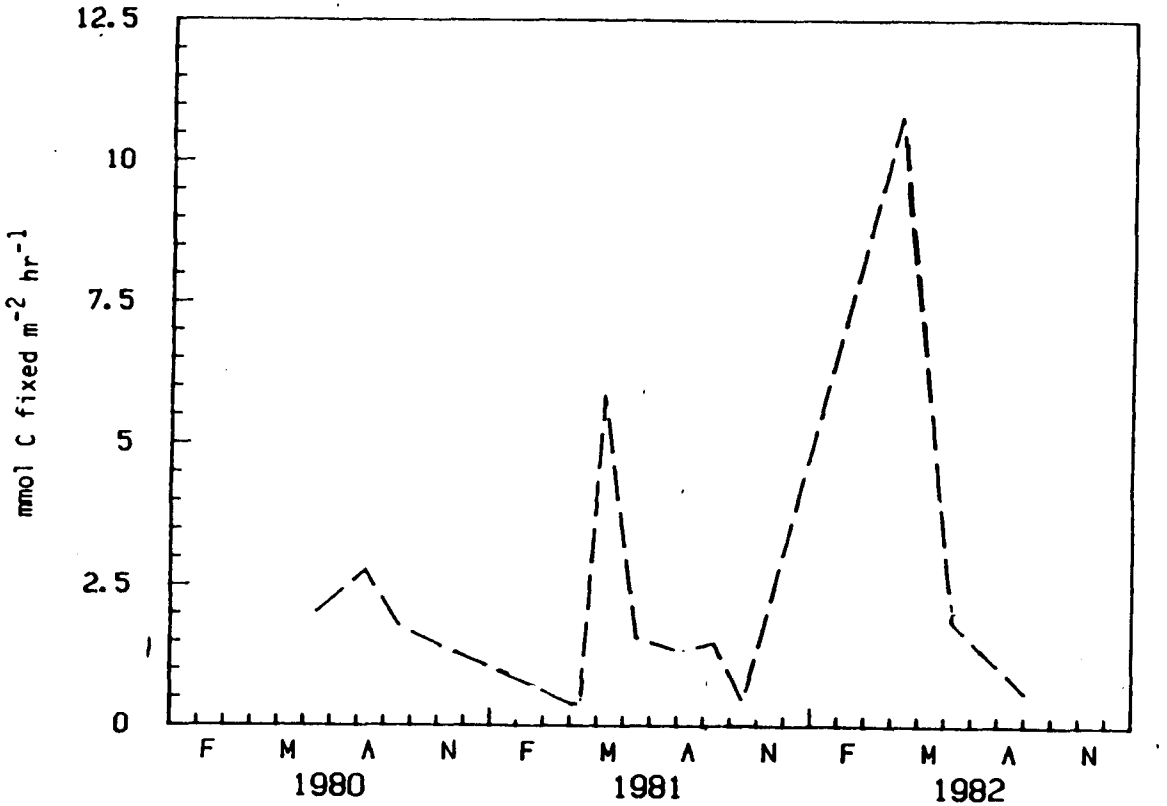

Fig. 1.4. Depth-integrated ^{14}C uptake rate through the euphotic zone at the Station BQ9 (from Burrell, 1983b).

uptake values are within the mean range cited for other fjords in the northern hemisphere (Syvitski *et al.*, 1986).

Small copepods (*Pseudocalanus* and *Acartia*) dominate the zooplankton in this area. The zooplankton populations remain very low during the winter, and increase substantially in the early or mid-summer after the spring phytoplankton bloom. The annual mean biomass of zooplankton is estimated at 0.32 g C m^{-2}.

The benthic community has not been well studied. A large echinoderm contribution to the benthic carbon utilization was noted (18 g C m^{-2} yr^{-1}), and deposit feeders are expected to be dominant in the deep central basin of Boca de Quadra (*e.g.*, Fauchauld and Jumars, 1977).

DISSERTATION OUTLINE

The following chapter describes the sediment trap construction and its operation in the sea. Chapter 3 describes the temporal variation of bulk SPM distribution, and settling fluxes at depth. Hydrography, water circulation features, and climate patterns are examined in the context of the dynamics of SPM. Mass balance computations are made by delineating various

sources and sinks of SPM using sedimentation rates, riverine influx of SPM, and SPM production *in situ*. Sources of biogenic matter in surface waters and the seasonal pattern of particulate biogenic matter fluxes out of the euphotic zone are presented in Chapter 4. The relative importance of autochthonous and allochthonous organic matter is discussed. The non-conservative behavior of biogenic matter and particulate Mn and Fe are examined using the primary flux and the estimated resuspension flux derived from Chapter 3. To further elucidate the fate of biogenic matter, the early diagenesis of this material in sediments is examined in Chapter 5. The relative importance of organic matter oxidation at or near the sediment-water interface and within the sediment, and processes which regulate pore water concentrations, are examined *via* modeling and mass balance computations using sedimentation rates and sediment mixing coefficients derived from Chapter 3, and settling fluxes from Chapter 4. The final chapter presents conclusions that were generated from the results of this work, and includes some thoughts for future studies.

CHAPTER 2. SEDIMENT TRAP CONSTRUCTION AND OPERATION

Particulate sediment material is transported according to the prevailing hydrodynamic flow pattern, which may vary in time and space. This feature may limit determination of vertical fluxes using sediment traps placed at different depths in the water if horizontal water velocities are much greater than vertical components. However, various sediment trap intercalibration studies - though usually carried out in low velocity regimes (*e.g.* Bruland *et al.*, 1982) - show that sediment trap results approximate the true vertical flux in many marine environments because the vertical mass flux is attributed mainly to scarce, large, rapidly sinking macro-particles (McCave, 1975). Deep fjords are especially good places to deploy sediment traps because the vertical component is significant compared with horizontal water velocities.

SEDIMENT TRAP DESIGN

A sediment trap disturbs the natural turbulent pattern and creates an artificial depositional environment in the trap. Suspended particles are collected through a process of fluid exchange rather than falling freely into a trap. Thus, the efficiency of a trap in collecting suspended sediment depends on the

residence time and circulation pattern of a fluid within the trap, which, in turn, are controlled by trap geometry and by the ambient current velocity. Various sediment trap designs have been used in the sea (reviewed by Gardner, 1977; Blomqvist and Hakanson, 1981). Gardner (1980) showed experimentally that a funnel-shape sediment trap generally under-traps due to resuspension losses caused by eddy penetration down into the funnel. In addition, the trapping area varies between the mouth and base of the trap under turbulent conditions, which may also lead to under-trapping (Hargrave and Burns, 1979). The reverse (over-trapping) occurs when bottle-shaped traps are used.

The most favorable form of sediment trap is a simple cylinder, which avoids the uncertainty of the effective collection area in turbulent waters (Gardner, 1980; Hargrave and Burns, 1979). Also, sediment traps must have a stagnant region in the bottom of the trap which protects the settled material from resuspension and scouring. Lau (1979) demonstrated that particle motion in the trap is governed by two dimensionless variables: the aspect ratio (H/D) and the Reynolds number (UD/V), where H and D are the height and diameter of the sediment trap, respectively; U is the ambient current velocity,

and V is the molecular kinematic viscosity of seawater. The effect of orifice size on the trapping efficiency has also been investigated. A small trap with a diameter of less than 4.5 cm was biased towards collection of lighter organic matter (Blomqvist and Kofoed, 1981).

The current speed varies from about 2 to 30 cm s^{-1} in the central basin of Boca de Quadra (Nebert, 1984). Assuming a kinematic molecular viscosity of 10^{-6} m^2 s^{-1} (Pond and Pickard, 1981), a maximum Reynolds number (*ca.* 3 x 10^4) may be computed. In this case, applying the formula of Lau (1979), the aspect ratio should be greater than 7 in order to retain the settled particulates on the floor of trap. In this study an aspect ratio of 8 and a 10 cm diameter trap have been selected. The existence of a stagnant bottom region in the sediment trap has been tested using a salt lump tracer. A substantial portion of the salt remained undissolved even after one month of *in situ* deployment. Furthermore, when the traps were retrieved, there were no signs of resuspension of particulates in the traps. Baffle system cells having an aspect ratio greater than 4 and cell diameter less than 1 cm have been reported to prevent frictional drag from inducing horizontal currents or vertical turbulence (Soutar *et al.*, 1977). A baffle system, consisting of a bundle of 0.7 cm diameter cells having an aspect ratio of

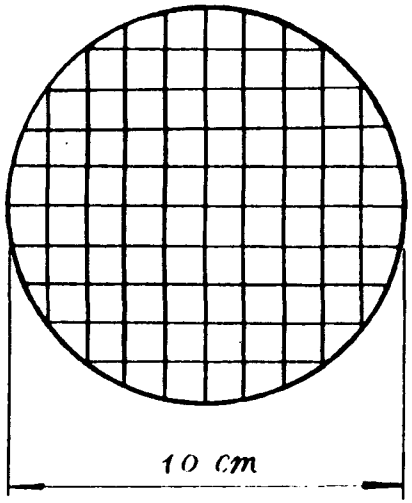

top view

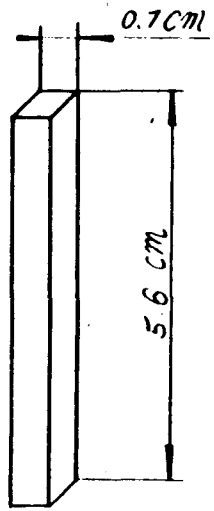

a baffle unit

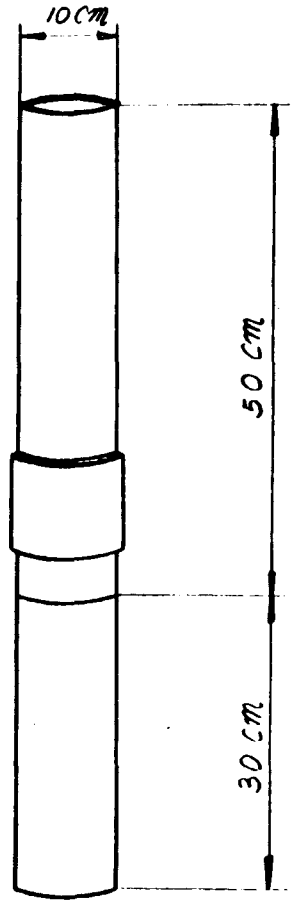

a sediment trap

Fig. 2.1. Schematic diagram of sediment trap.

8, was employed in the mouth of the sediment traps. Using this system, it was not necessary to close the trap during retrieval. The absence of a lid eliminates various mechanical and electrical malfunctions which have been frequently reported. In addition, the baffle system discourages swimming organisms from entering the trap. A schematic diagram of the sediment trap used in this study is given in Fig. 2.1. The semi-transparent PVC trap consists of two parts which can be easily detached. The baffle system inserted in the mouth is easily removable to facilitate sampling and cleaning. A sediment trap of similar design has been successfully used by Knauer et al. (1979) in the northeast Pacific.

SEDIMENT TRAP MOUNTING

The traps were mounted on a vertical taut-wire mooring, and gimballed to maintain the trap mouth in a horizontal plane. The stainless steel gimbal bracket and current vane made of high density plastic (Aanderra Co. Products) were supported by a stainless steel swivel incorporated in the mooring line. The entire array was free to rotate about the mooring line, so that the traps were always oriented upstream, thus avoiding the wake created by the mooring system itself. This attachment method was used also to prevent possible inclination of

the sediment trap due to waves or currents. It is very important to keep the trap upright because a tilted trap usually over-traps particles. Gardner (1985) extensively discussed the effect of tilt on sediment trap efficiency: The particle flux increased with tilt up to about 45°, and then decreased. Gardner further observed that the gimballed cylinder tilted about 10-20° in a flow of 12 cm s^{-1}. Lowering the center of gravity, however, limited the oscillations to 2-3° upstream even at 20 cm s^{-1}. Strong currents (about 30 cm s^{-1}) and large internal waves are frequently observed in the central basin of Boca de Quadra (Nebert, 1984). The degree of tilting of the sediment trap has not been evaluated.

Dacron rope was used for the entire mooring line, which was anchored with a 600 lb. weight. The number of buoys to be incorporated was calculated from the standard Aanderraa current meter mooring configuration (J. Smithhisler, Univ. of Alaska, 1982, pers. comm.). The vertical locations of buoys were largely dictated by the convenience of deployment and retrieval of the arrays. In order to facilitate assembling and disassembling of the mooring unit, a minimum number of stainless steel shackles and sling links was used.

MOORING POSITIONS OF SEDIMENT TRAPS

As particles settle by gravity, or by downward water movement through the water column (Brewer *et al.*, 1976), their concentration and composition are altered by zooplankton grazing and by aggregation, disaggregation, decomposition, and dissolution. Since the alteration of particles continues during passage to the sea floor, it seems reasonable to determine the sedimentation rate by measuring or calculating the flux of suspended sediments just above the sediment-water interface. However, an increase in suspended particle concentration, forming a nepheloid layer, occurs as the bottom is approached. This nepheloid layer is sustained mainly by resuspended material from the bottom due to various stresses. At times, resuspended material may occur almost up to sill depth in Boca de Quadra (Burrell, 1981).

Because of the presence of such a nepheloid layer, the best place to measure the primary flux of particles reaching the sea floor is just above the maximum height of resuspension of particles (Gardner, 1977). Biscaye and Eittreim (1977) show that this depth coincides with the level of minimum light scattering (nepheloid minimum or clear water) above the bottom nepheloid layer. Assuming that there is no decomposition or dissolution of particles from the nepheloid minimum to the sea floor,

the primary and resuspended vertical flux within the nepheloid layer can be separated by determining the primary flux. Further if the net standing crop of particles in suspension in the nepheloid layer is determined, gross estimates can be made of the residence time of the nepheloid layer at chosen depths, assuming steady-state and uniform deposition and erosion in the sea floor. Such assumptions of a steady-state nepheloid layer are, however, open to criticism (*e.g.* Feely, 1976). Numerous determinations of standing stock *via* discrete load determinations (Burrell, 1983b) suggest that at around 40 meters depth a "clear-water particle minimum" zone can be recognized. The sediment trap (#1) located at 40 m depth is expected to measure "primary" flux (F_P) uncontaminated by particles resuspended from the bottom (F_R). Traps deployed below the clear-water particle minimum will collect both F_P and F_R. The mooring positions were determined for the best evaluation of suspended sediment dynamics. A set of sediment trap arrays was moored in the central basin of Boca de Quadra at Station BQ9G. Individual trap positions in the water column are shown in Fig. 2.2.

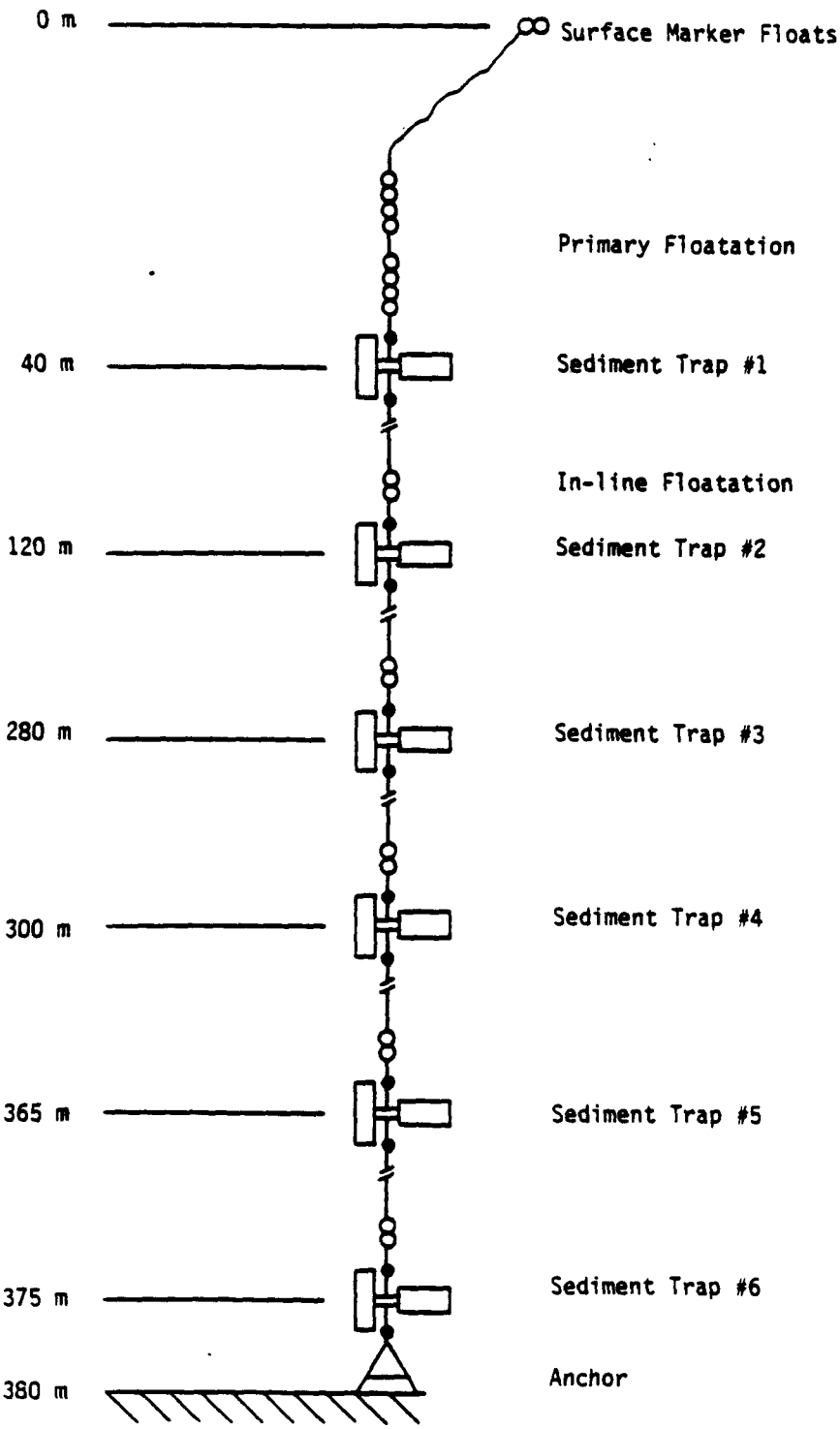

Fig. 2.2. Mooring design for the sediment trap array deployed at BQ9G.

PREPARATION OF SEDIMENT TRAP FOR DEPLOYMENT

All traps were thoroughly cleaned with laboratory detergent and distilled water. Prior to deployment, they were filled with high density reagent grade NaCl solution to reduce the chance of flushing *in situ* and during recovery. The resulting density of water inside the trap was 1.035 g cm^{-3}, significantly higher than ambient seawater, but sufficiently low compared to the densities of marine particles (Table 2.1). The traps were closed during their descent by placing a plastic sheet with punched holes on top of the sediment trap, secured by rubber bands and a candy product (which usually took a half an hour to dissolve in seawater) as a soluble link.

POISON

A small cup was packed with sodium azide and mounted to the bottom of each trap. The azide diffused through a membrane filter into the sample to provide a continuous antibacterial effect. The effects of sodium azide on the preservation of organic matter have been discussed by Lee *et al.* (1983).

DEPLOYMENT AND RECOVERY OF SEDIMENT TRAPS

Sediment traps were deployed by first stringing them out in the water and then lowering the anchor slowly to the bottom using a tension release made at the Institute

Table 2.1. Densities of marine particulates.

	Density ($g\ cm^{-3}$)	References
alluminosilicates	1.6	Lambert et al., 1981
quartz	2.65	Lerman, 1979
carbonate particles	1.3	Berger and Piper, 1972
inorganic aggregates	1.64-1.056	Krone, 1972*
2-6 um size particles	1.152	Riley, 1970*
>60 um size particles	1.032	Riley, 1970*
salp fecal matter	1.10	Bruland and Silver, 1981
copepod and euphausiid fecal pellet	1.23	Komar et al., 1981

* references in McCave (1975)

of Marine Science, University of Alaska. On retrieval, the entire mooring array was slowly pulled out from the water until the uppermost trap was on board. This trap was then covered with a plastic envelope and disassembled from the mooring array. The process was repeated until all the traps were recovered. Retrieved sediment traps were allowed to sit for a few hours in a cool area so that any sediment which might have been stirred up during the recovery could settle to the bottom. Overlying water was then discarded and the sediment trap body removed from the collection cup. The remaining sediment samples were inspected and zooplankton were carefully picked out before freezing. The frozen sample was returned to the laboratory (Institute of Marine Science, University of Alaska) and filtered using pre-combusted, pre-weighed glass fiber filters. All the samples on the filters were rinsed several times with distilled water and dried in a desiccator.

CHAPTER 3. SEDIMENTATION DYNAMICS OF BULK SUSPENDED PARTICULATE MATTER

INTRODUCTION

Marine particulate matter is of considerable geochemical importance. It acts as a carrier phase for the transport of chemical elements from the surface waters of the ocean to the sediments. It is also a site for heterogeneous chemical reactions. Thus it is important to understand the sources and physical processes that control the distributions and transport of this material. Sources of marine particulate matter within a fjord basin may be divided into two categories: that carried in from outside the basin (allochthonous) and that produced *in situ* (autochthonous). The bulk of allochthonus sediment is supplied by freshwater input *via* suspended load and bed-load transport. Suspended and bed load are here defined following Komar (1976): "The *suspended load* is transported within the water column, maintained above the bottom by the turbulence of the water. The *bed load* comprises the concentrated sediment that moves on or in close proximity to the bottom, maintained in a dispersed state by grain to grain contacts". Another possible source of allochthonous material is the influx of dense water during the periods

of basin water renewal (see Chapter 1). The most important source of autochthonous sediment material is biological production, primarily by phytoplankton. A possible minor source is the precipitation-flocculation of riverine dissolved and colloidal material (Burrell, 1983b). The primary sinks of sediment material introduced to the fjord basin are (i) burial at the basin floor and (ii) export out of the basin *via* efflux of basin water. The distribution of suspended sediment material may be affected by local input and transport *via* gravitational settling, advection and diffusion as well as by resuspension from the bottom sediments through erosion.

In general, the size distribution of particles in the oceans may be represented by a power function (Lal, 1977). Such a particle size distribution follows from the abundance of fine particulate matter (<10 um in diameter), and the rarity of coarse particulate matter (>10 um, but mostly in the 30 to 300 um diameter range). The coarser particulate matter in estuarine waters is made up almost entirely of biological particles, such as organisms and fecal matter, and various kinds of aggregates (Syvitski *et al.*, 1986). However, most of the settling flux of particulate matter is due to the rare, coarser particulates (McCave, 1975). Therefore, samples

collected in the sediment trap are biased towards this fraction. In this chapter, operational definitions of the suspended and settling particulates are used: *suspended particulate matter (SPM)* is defined as the particles collected in water sampling bottles, and *settling particulates* as the particles collected in the sediment traps. The concentration of suspended particulate matter (SPM) is further operationally defined as the dry weight of the SPM in a 1-liter seawater sample which is retained on a 0.4 um pore size Nuclepore filter.

The objectives of this chapter are:

1. To describe the temporal distribution pattern of bulk SPM in the basin water column.

2. To describe temporal variations in the vertical flux of settling particulates in the basin water column.

3. To elucidate the sources and sinks of settling particulates in the basin.

4. To elucidate the vertical flux patterns of settling particulates in the basin water column.

5. To describe the burial of bulk settling particulates in the bottom sediments.

To achieve the first objective, measurements of SPM made with a transmissometer will be used, taking into account the hydrography and circulation characteristics

of the basin. A continuous recording transmissometer has been used to give vertical resolution similar to the continuous-recording STD in order to study the distribution of SPM. The second objective requires utilizing the results of sediment trap deployments at various depths in the water column. The third objective will be achieved through a mass balance computation, based on the settling flux measurements made using sediment traps and sedimentation rates determined by the ^{210}Pb radiometric method. The fourth objective will be discussed in terms of the basin physiography, settling flux measurements, and sedimentation rates. The final objective will be addressed using ^{210}Pb and ^{137}Cs activity profiles within the sediments.

METHODS AND MATERIALS

Stability Values

Brunt-Väisälä frequencies were calculated employing a centered difference method (W. Johnson, Univ. of Alaska, 1984, pers. comm.) using STD data obtained by Nebert (1984).

Transmissometer

A Sea Tech transmissometer (Bartz *et al.*, 1978) coupled to the STD system was used to obtain SPM profiles

simultaneously with STD data. This transmissometer employs a LED light source at a wave length of 660 nm. The transmissometer was calibrated by comparing the beam attenuation at the particular station and depth to measured discrete SPM concentrations (w/v) at the same location. SPM concentrations were determined by water bottle sampling and immediate filtering through pre-weighed 0.4 um pore-size Nuclepore filters *via* a "whole-bottle" filtration system in order to avoid the possible incomplete extraction of rapidly settling large particles from the water samples (Gardner, 1977). The precision for the "whole-bottle" filtration was $\pm$ 0.02 mg l^{-1} or better (Burrell, 1983b).

Settling Particulates

Settling particulates were sampled using sediment traps at Station BQ9G (Chapter 2). The sampling precision was estimated to be better than 17% by comparing results from paired sediment traps deployed at the same depth.

Sediment Samples

Sediment samples were collected using a Benthos gravity corer with 6.7 cm internal diameter plastic core liners operated without core catcher, nose cone or pipe

barrel. Cores were extruded directly into PVC squeezers (Reeburgh, 1967) constructed with an internal diameter virtually identical to that of the core liner, thereby minimizing exposure to the air. Interstitial water was immediately squeezed from the sediment using 5 to 30 psi of ultrapure nitrogen gas pressure. Two precombusted Whatman EPM 1000 filters were used in the squeezer. The same procedures had been employed previously by Sugai (1985). A separate sediment core was sectioned completely to obtain the cumulative mass distribution.

Particulate Al

The content of Al in sediment trap and bottom sediment samples was determined using a Kevex X-ray fluorescence (XRF) unit, calibrated against NBS reference material #1646 (Estuarine Sediment) with a precision of 6 to 8%.

^{210}Pb and ^{137}Cs Activity in the Sediments

An alpha-emitting daughter radionuclide of ^{210}Pb, ^{210}Po, was extracted from the sediment to determine ^{210}Pb activity in the sediment, following the procedures of Kipphut (1978) and using ^{208}Po as a yield tracer. Counting was done using Ortec alpha counters (Si surface barrier detectors). Secular equilibrium between ^{210}Po and ^{210}Pb was assumed, and all activities are referred to

as ^{210}Pb. Counting precision is given in Appendix E with the data. ^{137}Cs activity was obtained using a Ge(Li) detector.

^{210}Pb Sedimentation Rate Calculation

Apparent sedimentation rates were obtained by applying the constant activity - constant sedimentation model (Robbins, 1978) within the core sections where the ^{210}Pb decreased exponentially with depth. For steady-state sedimentation:

$$(A_z - A_\infty) = (A_o - A_\infty)\exp(-\lambda w/z) \qquad (3.1)$$

where A_z and A_o are the ^{210}Pb activities at z and 0 cm depths, respectively, w is the average sedimentation rate, λ is the decay constant (0.0311 yr^{-1}), and A_∞ is the supported ^{210}Pb activity.

Porosity Calculation

Porosity was calculated from the sediment water content assuming the density of the solid material to be 2.5 g cm^{-3}.

RESULTS

Beam Attenuation *versus* Concentration of SPM

Results of simple linear least squares regressions for attenuation *versus* particle mass concentration in the

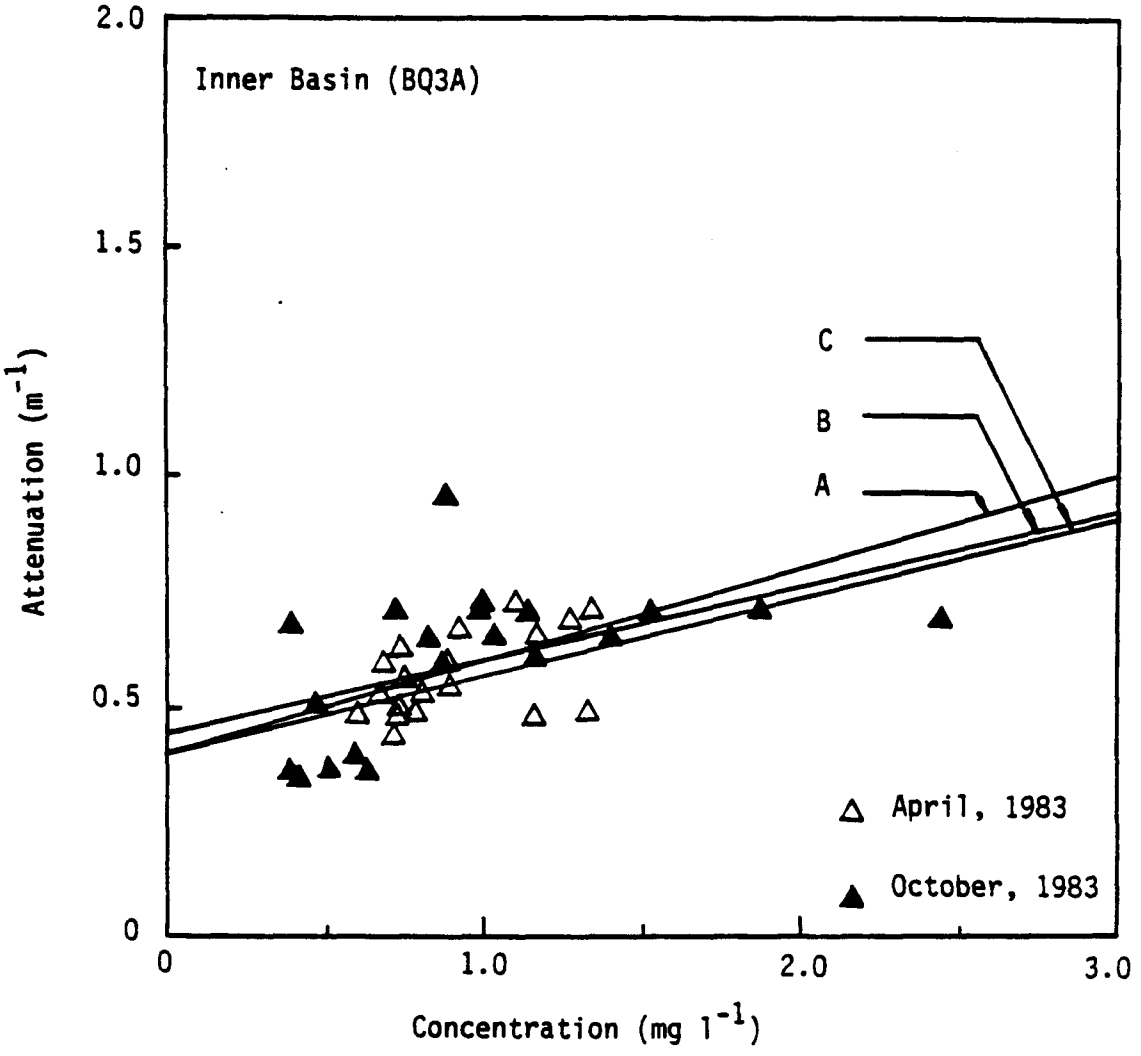

Line A (April, 1983) :A = 0.40 + 0.18C
Line B (October, 1983) :A = 0.46 + 0.15C
Line C (Lab. Calibration) :A = 0.40 + 0.17C

Fig. 3.1. Transmissometer calibration curves for the inner basin.

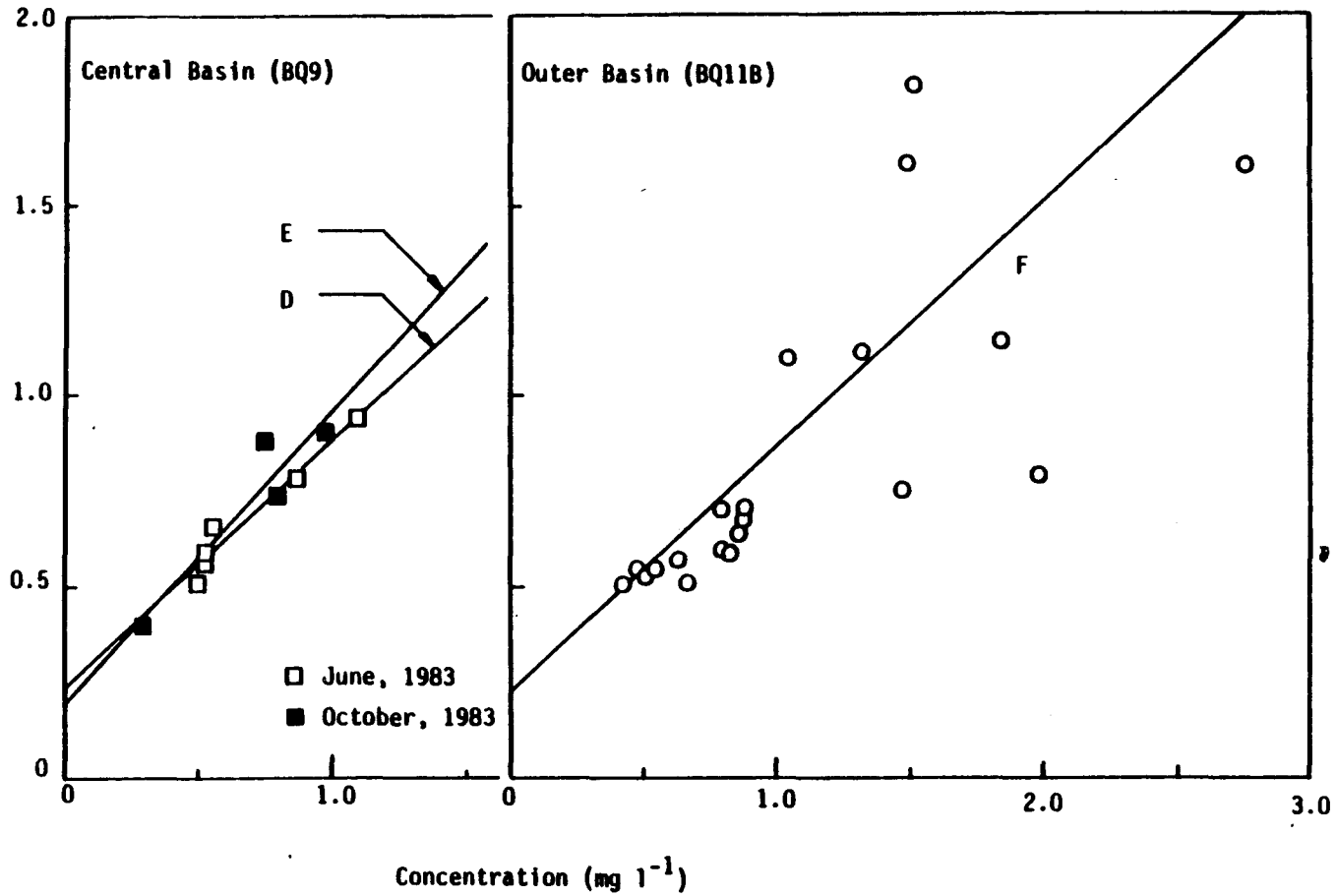

Line D (June 1983) :A = 0.24 + 0.64C
Line E (October 1983) :A = 0.22 + 0.65C
Line F (June 1983) :A = 0.22 + 0.65C

Fig. 3.2. Transmissometer calibration curves for the central and outer basins.

Table 3.1. Least square regression statistics for attenuation coefficient *versus* particulate mass concentration in Boca de Quadra.

		R	Sample size
Inner Basin			
April	A = 0.40 + 0.18C	0.41	23
October	A = 0.46 + 0.15C	0.48	20
Central Basin			
April	No significant correlation was found		
June	A = 0.24 + 0.64C	0.97	6
October	A = 0.22 + 0.65C	0.94	6
Outer Basin			
June	A = 0.22 + 0.65C	0.74	24
Laboratory Calibration*			
	A = 0.40 + 0.17C	1.0	

* Laboratory calibration of transmissometer was made with dried bottom sediments in filtered seawater (both obtained in Boca de Quadra).

Boca de Quadra fjord are shown in Figs. 3.1-3.2 and tabulated in Table 3.1. A is the beam attenuation coefficient (m^{-1}), C is SPM concentration (mg l^{-1}), and R is the correlation coefficient. All the correlation coefficients are significant at the 95% confidence level. The regression equation for attenuation *versus* SPM concentration for the inner basin is nearly identical with the results of a laboratory calibration of transmissometer readings using Boca de Quadra bottom sediment in filtered seawater. But the regression equations for beam attenuation *versus* SPM concentration in the inner basin differ from those in the central and outer basins throughout the year. No significant correlation was found between beam attenuation and particle mass concentration in April 1983 in the central basin of Boca de Quadra. It is interesting to note that optical properties of SPM (as shown by the regression equations) in the central basin and outer basin are very similar in June 1983. The regression equations are identical in June and October 1983 in the central basin of Boca de Quadra.

Distribution of SPM

Seasonal vertical profiles of beam attenuation coefficients (m^{-1}) together with temperature profiles are shown in Fig. 3.3. The temperature parameter was chosen here because, although density is primarily a function of salinity in cold water, temperature is a very useful tracer of the seasonal water masses in this fjord. In the fall, warm water is injected from the outside into the basin, and a subsurface temperature maximum forms due to surface cooling until spring, when it begins to decrease. The subsurface maximum disappears before deep basin water renewal starts again in summer (Fig. 3.3; Creswell and Nebert, 1986).

Fig. 3.3 shows that the principal reservoirs of SPM in Boca de Quadra are a thin (<20 m) surface layer, and a thicker (*ca.* 250 m) benthic nepheloid layer (BNL) below the 50 m depth. These zones are separated by a stable, mid-depth, low-turbidity layer. The SPM minimum zone is centered between about 10 and 40 m depth. This three-layer distribution is directly related to the hydrography and circulation patterns of Boca de Quadra (Chapter 1). SPM concentrations below the thin surface layer decrease rapidly, reaching a minimum in the pycnocline (thermocline in Fig. 3.3). The data of Fig. 3.4 were obtained in late oceanographic winter before deep water

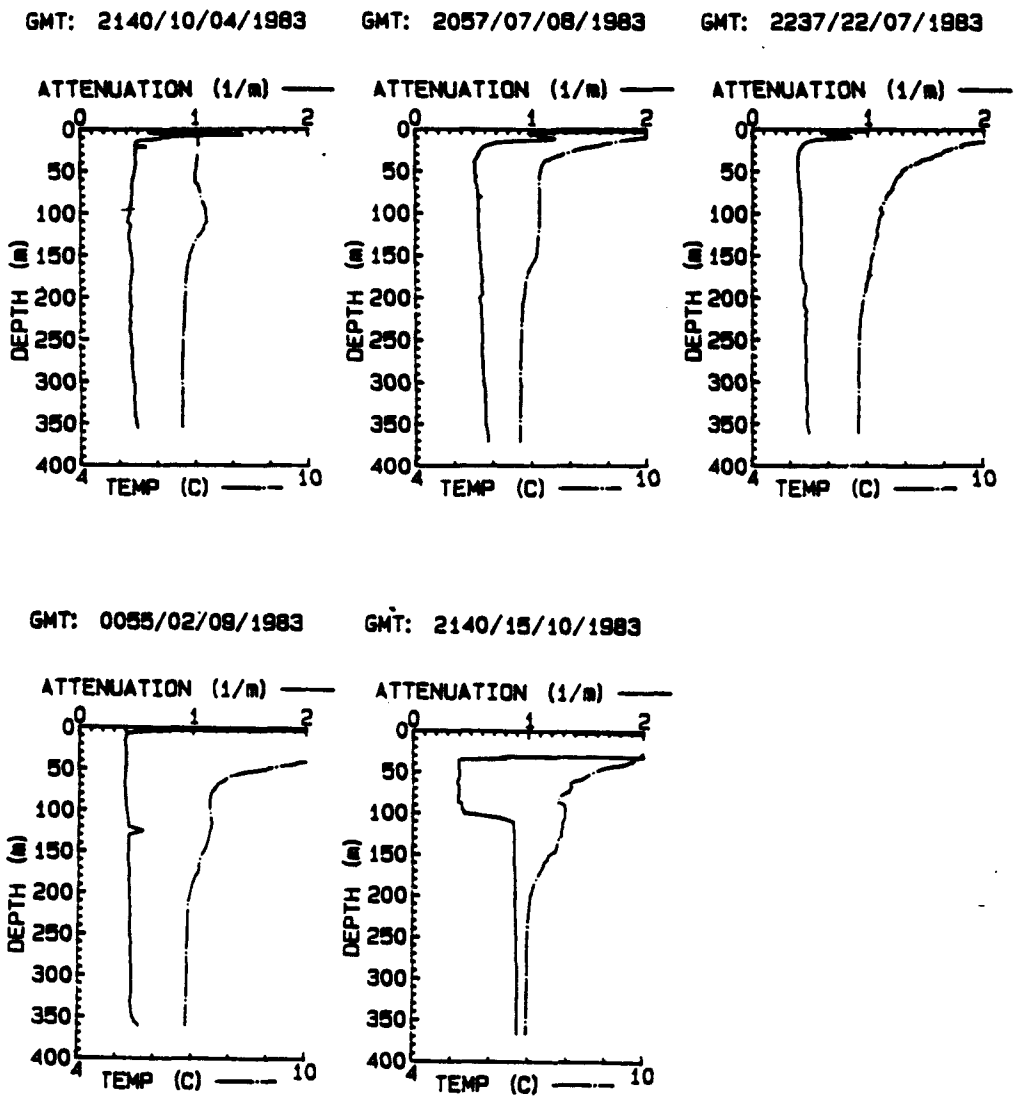

Fig. 3.3. Time series vertical profiles of the attenuation coefficient and temperature in the central basin (Station BQ9), April-October 1983.

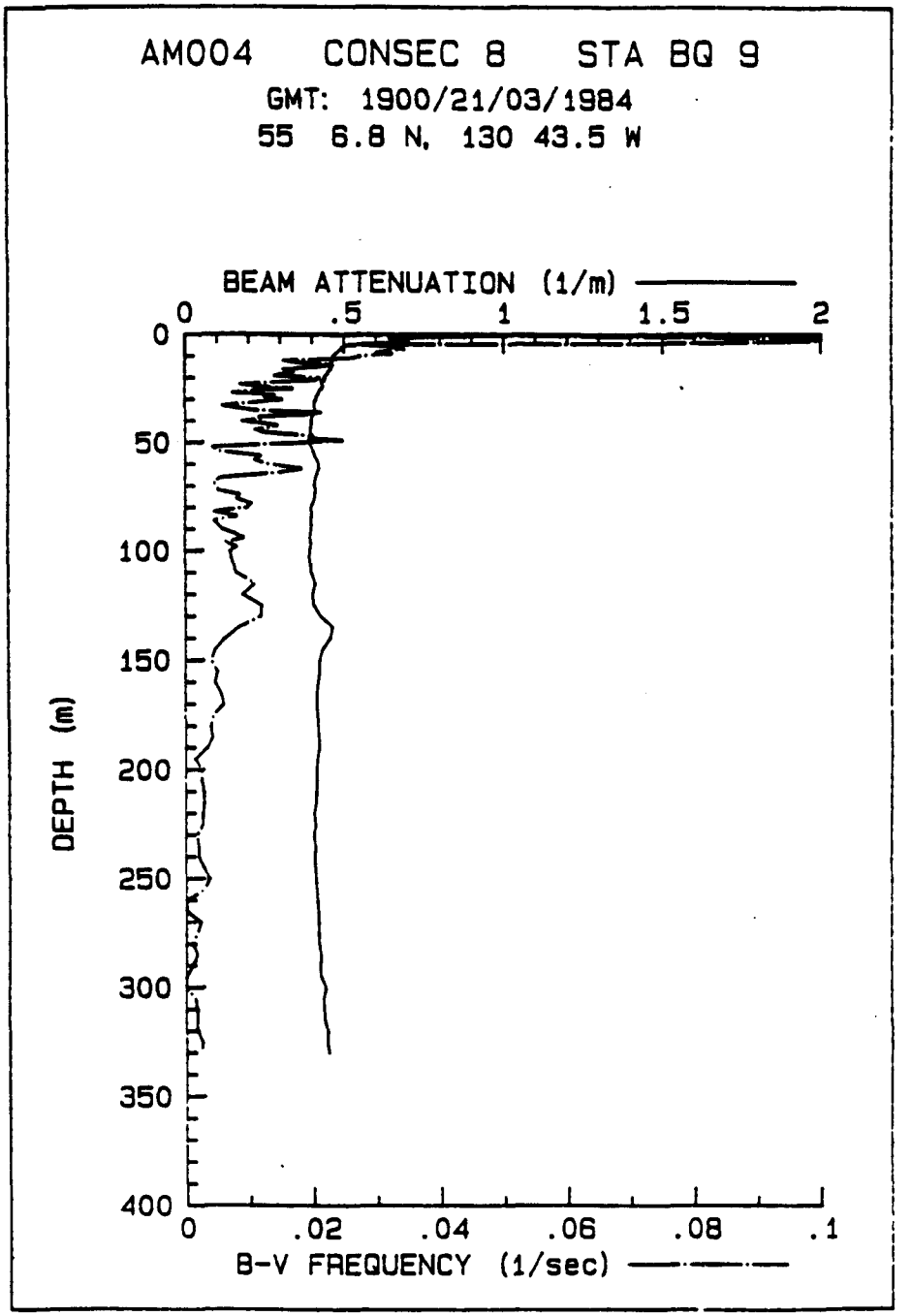

Fig. 3.4. Vertical profiles of the attenuation coefficient and Brunt-Väisälä frequency in the central basin during March 1984.

renewal began in the central basin of Boca de Quadra. At this time a pycnocline at 130 m coincides closely with the subsurface maximum of the transmissometer profile. This may mean that at the 130 m depth horizon, fine sediments are concentrated because the gravitational settling force of particulates is significantly reduced by the buoyancy force created by the density stratification of the water column. The latter peak in SPM concentration becomes weak and disappears as the water column becomes less stratified and homogeneous during deep water renewal in summer.

Vertical Flux of Settling Particulates

Fig. 3.5 shows the mean downward flux of sediment at several depths over the periods indicated. The weighted mean of the "primary" flux at 40 m over the one-year period 9 June 1982 to 7 June 1983 (10 sampling periods totaling 309 days) is 290 g m^{-2} yr^{-1}. The mean value over the period extending up to 18 October 1983 is 332 g m^{-2} yr^{-1}. Fig. 3.5 clearly demonstrates that the settling flux at various horizons below the Kite Island sill height (80 m) within the basin is far greater than that recorded just below the euphotic zone. The weighted mean fluxes at 300 m and adjacent to the sediment floor at 365 m between 22 September 1982 and 18 October 1983

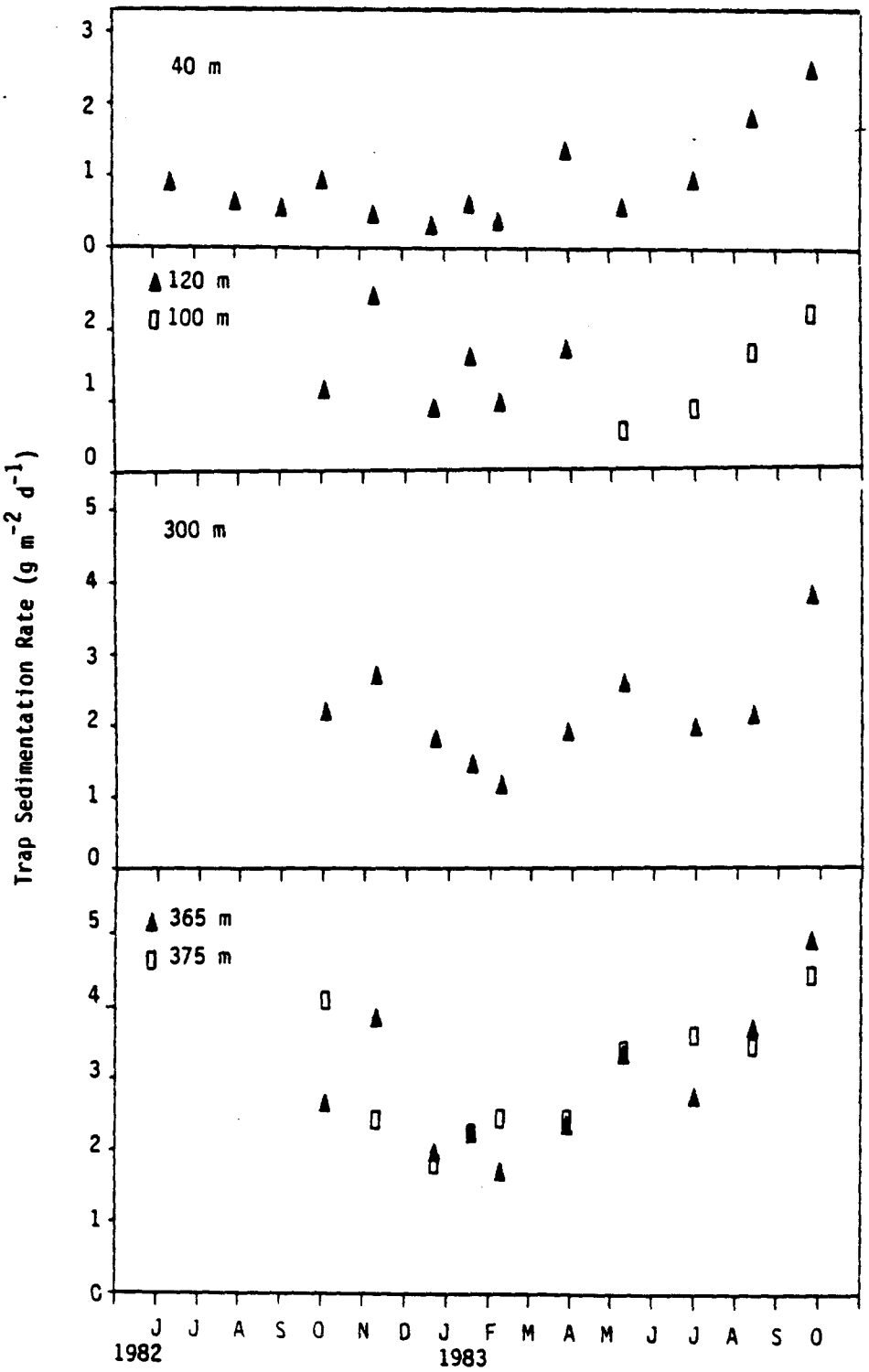

Fig. 3.5. Depth distribution of vertical flux of settling particulates.

(367 actual sampling days) are 812 and 1124 g m^{-2} yr^{-1}, respectively. At 375 m, just 5 m above the sediment surface, the weighted mean settling flux is 1151 g m^{-2} yr^{-1}, nearly the same as that at 15 m above the bottom.

A bimodal distribution of vertical fluxes also may be seen in Fig. 3.5. There is one small maximum in the spring-summer phytoplankton bloom period and a pronounced maximum in the fall-winter season of high precipitation and storms. The minimum flux at all depths over the approximately one-year observation period is in February 1983.

Particulate Al Distribution and Flux

The content of Al in settling particulates, and settling fluxes of Al at depth, are shown in Fig. 3.6 and listed in Appendix B. The Al content of the settling particulates collected at the 40 m depth horizon was nearly constant throughout the sampling period, ranging from 1.6 to 2.0% in the spring-summer period (13 March-9 April and 11 April-7 June 1983), and from 1.8 to 1.9% in the fall-winter period (18 October-1 December 1982 and 2 September-18 October 1983). The Al content increased markedly toward the 100 or 120 m depth horizons (2.2-2.5 and 3.1-3.5% in the spring-summer and fall-winter periods, respectively). In the spring-summer

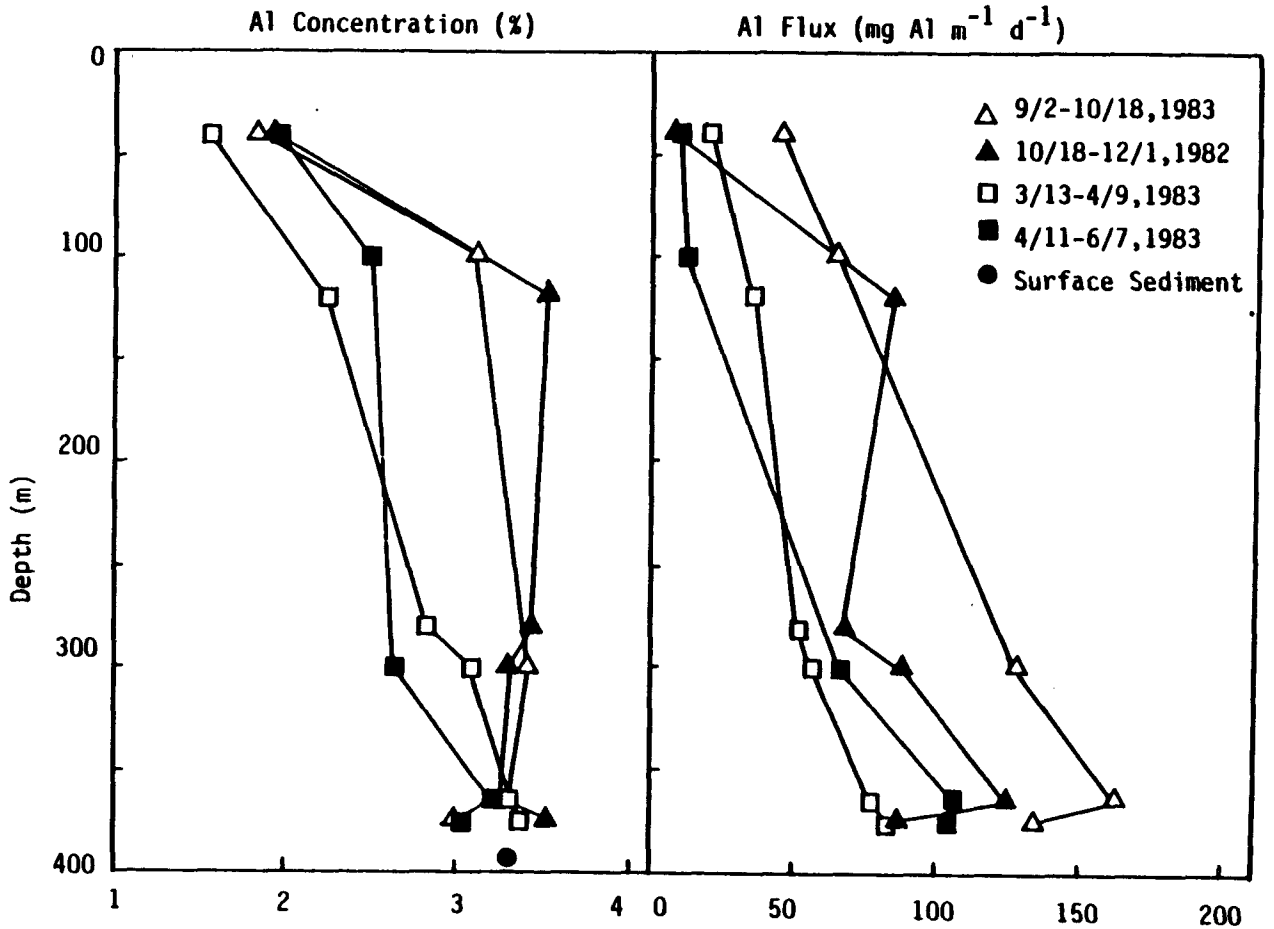

Fig. 3.6. The concentration of Al in settling particulates and particulate Al settling flux at various depths.

period, Al contents increased gradually down to the 300 m depth and then markedly toward the bottom. In the fall-winter period, however, Al contents were essentially the same throughout the entire water column below the 120 m depth. All the samples collected at a depth of 375 m depth, just 5 m above the bottom, contained nearly as much Al as did the bottom sediment. The Al content of the surface sediments is 3.3 $\pm$ 0.3%.

Settling fluxes of Al increased with depth throughout the sampling period. The gradient of Al flux with depth was smallest in the period 13 March - 9 April 1983. This may reflect the stable water column at the end of the winter isolation period, increasing towards the fall-winter season. Al fluxes at 40 m depth horizon ranged from 7-45 and from 10-21 mg Al m^{-2} d^{-1} in the fall-winter and spring-summer periods, respectively. Although Al contents increase with depth, a marked increase in the Al flux at 120 m depth was visible only during the sampling period from 18 October to 1 December 1982. Al fluxes at 365 or 375 m depth ranged from 124-162 and from 84-104 mg Al m^{-2} d^{-1} in the fall-winter and spring-summer periods, respectively. The deposition rate of particulate Al in the bottom sediments is calculated to be 53 $\pm$ 11 mg Al m^{-2} d^{-1} using the long-term

sedimentation rate (589 ± 131 g m^{-2} yr^{-1}; Table 3.2) and the average Al content in surface sediments.

Porosity and Cumulative Mass in the Sediment

The porosity of the sediment was about 0.92 in the top 4 cm, decreasing to 0.86-0.90 and remaining essentially constant between 4 and 50 cm (Fig. 3.7; data listed in Appendix D). This indicates that significant compaction has not occurred in the upper 50 cm of sediment in this region (Station BQ9G). The cumulative mass of bulk sediment per unit area appears to increase fairly linearly with depth.

^{210}Pb Sedimentation Rates

Profiles of the natural log of excess ^{210}Pb with depth in the central basin of Boca de Quadra are shown in Fig. 3.8, and data are tabulated in Appendix E. All the vertical distributions of unsupported ^{210}Pb appear to decrease exponentially with depth below a surface layer which is around 10-20 cm deep. The surface layers of the cores show very complex features. For example, the ^{210}Pb profile at Station BQ9G-2 shows that ^{210}Pb activity increases to a subsurface maximum at around 20 cm depth. The calculated sediment accumulation rates in the central basin of Boca de Quadra are 450-720 g m^{-2} yr^{-1} (mean of 589 ± 131 g m^{-2} yr^{-1}) which is equivalent to 0.2-0.3 cm

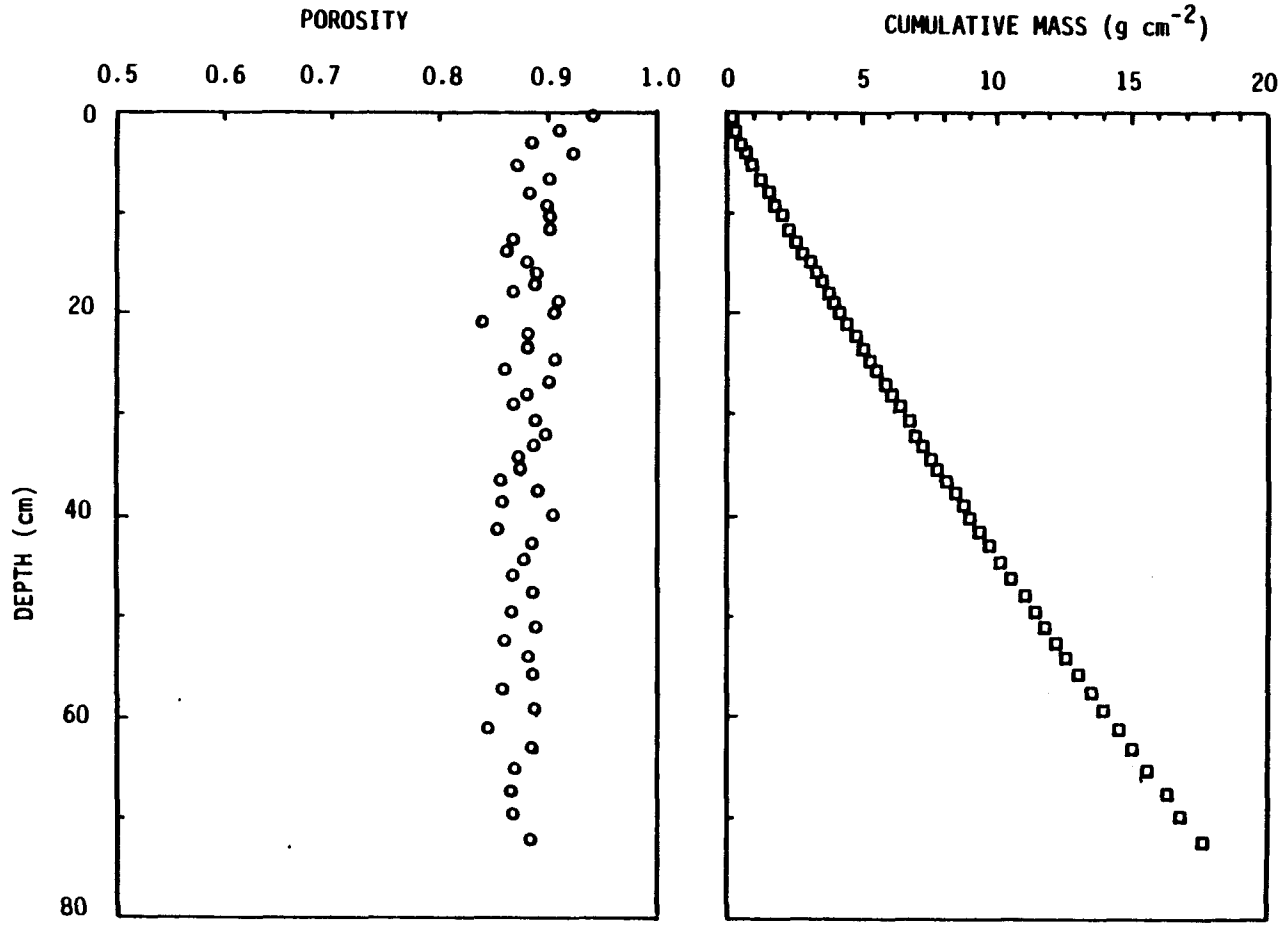

Fig. 3.7. Depth profiles of porosity and cumulative mass in the sediment at BQ9G.

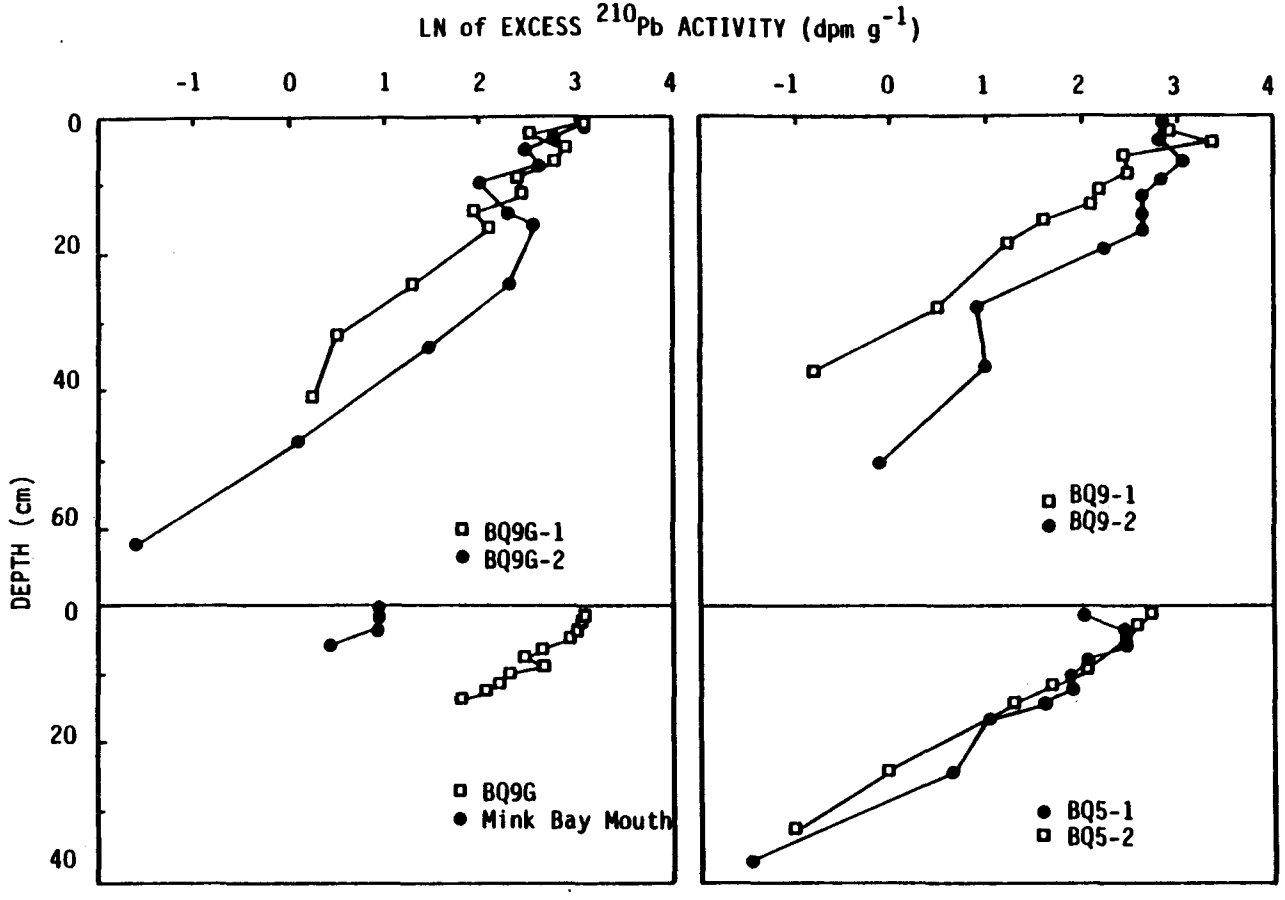

Fig. 3.8. Vertical distributions of unsupported ^{210}Pb in the sediments.

yr^{-1}, as summarized in Table 3.2. Variability of sedimentation rates at the same station may be due partly to the complex bottom topography. The surface ^{210}Pb activity is about tenfold smaller at the mouth of Mink Bay than at the basin floor (Fig. 3.8).

DISCUSSION

Optical Properties of SPM

The theory of light attenuation caused by SPM in marine waters well reviewed recently by Baker and Lavelle (1984), and is only summarized briefly here. Beam transmission (T) is dependent on the light path length (z) and attenuation coefficient (C):

$$T = e^{-Cz} \qquad (3.2)$$

C is a combination of three major components: water (C_W), SPM (C_{SPM}), and dissolved organic matter. The attenuation due to dissolved organic matter is considered to be negligible at the 660 nm wavelength (Jerlov, 1976) used by the Sea Tech transmissometer. C_{SPM} has a linear relationship to the concentration of SPM provided that optical properties such as distribution patterns of size, refractive index, and shape of SPM in the waters are constant or mutually compensating (Peterson, 1978).

Table 3.2. Sedimentation rates in the central basin.

Station	Depth (m)	Sedimentation Rate (cm yr^{-1})	(g m^{-2} yr^{-1})	Inventory (dpm cm^{-2})
BQ5 (basin)	275	0.21	414±93	41.7±0.4
BQ9 (basin)	372	0.25±0.06	556±154	105.9
BQ9G (basin)	380	0.27±0.06	612±143	74.7±7.3
Mink Bay mouth	125	0.13		

Then:

$$C = Cw + K \times (\text{Concentration of SPM}) \qquad (3.3)$$

The absolute value of Cw at a wavelength of 660 nm is reported to be from 0.25 to 0.5 m^{-1} (Spinard *et al.*, 1983). The proportionality constant, K, could vary depending on particle size. Smaller size particles attenuate more efficiently than do larger particles. K is lower in a high energy environment, where mean particle size is larger, and higher in a low energy environment where the mean particle size is smaller (Baker and Lavelle, 1984). Bishop (1986) introduced a temperature correction for the Sea Tech transmissometer applicable for use in a strong thermocline.

Although the available data are limited, a few important inferences may be drawn. Since the K value (slope) for SPM in the inner basin is nearly identical to that of bottom sediment dispersed in filtered seawater in a laboratory tank (Fig. 3.1), most SPM in the inner basin may be composed of resuspended sediment. Inner basin sediments are lower in organic carbon content compared with those of the central basin (Burrell, 1983b). Electron microscopic examination shows that most particles are non-biogenic below the surface layer (see

also Robb, 1981), and resuspension of bottom sediments is clearly shown in the inner basin of Boca de Quadra (Fig. 3.9). The fact that K values for the central basin and outer basin were very similar to each other in June 1983 (Fig. 3.2) suggests that the optical properties of the SPM may have been similar at that time, and that SPM in both these basins differs from that in the inner basin (Table 3.1). K values for the inner basin fall within a range typical of estuarine environments, and K values for the central and outer basin are similar to those reported for Puget Sound (Baker and Lavelle, 1984).

No significant correlation was found between beam attenuation and concentration of SPM during April 1983 in the central basin (Table 3.1). Burrell (1983b) has shown that primary production peaks between mid-March and early April. Scanning electron microscopic examination of material from the sediment traps deployed during March and April showed that most sinking particles throughout the entire water column consisted of intact diatoms or fragments, other biogenic debris and fecal pellets. Poor correlation between beam attenuation coefficients and biogenic particle mass concentrations have been noted by a number of workers (*e.g.*, Peterson, 1978; Baker *et al.*, 1983). Such poor correlation may be due to the patchiness of particulates of varying composition and

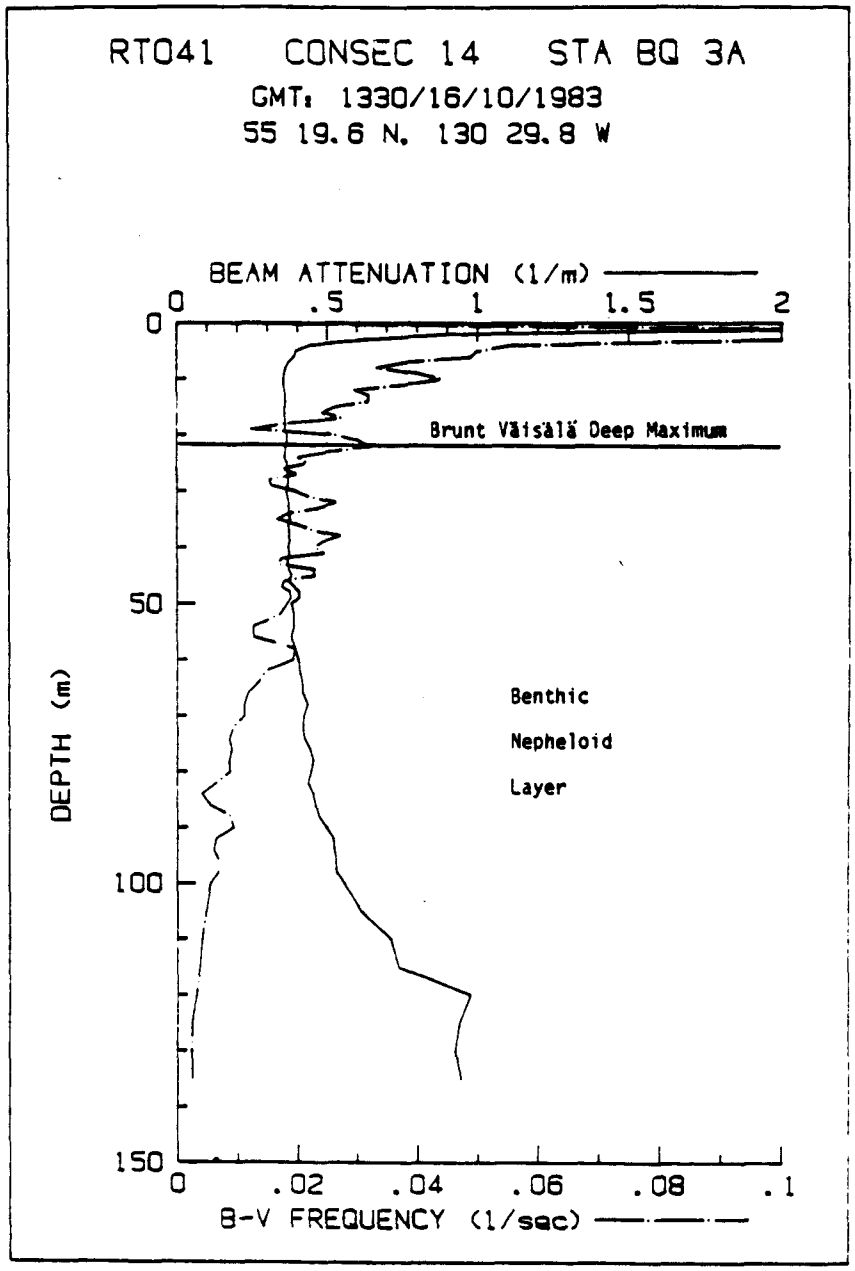

Fig. 3.9. Vertical profiles of attenuation coefficient and Brunt-Väisälä frequency in the inner basin (Station BQ3A).

size distributions (Shanks and Trent, 1980), or may result from a sampling error in collecting simultaneous data in regions of steep particulate concentration gradient. Another cause of the lack of correlation between the two parameters may be due to a scavenging effect, as large particles impact the slower sinking, smaller, but more abundant particles. In this case, smaller particles tend to adhere to larger particles and are carried down at a faster speed than predicted by Stokes Law (Lal, 1980). This results in an "optically clean" water column by skewing the size spectrum of SPM, since large particulates attenuate light less effectively. Similar arguments were made by Honjo (1982) to explain the relationship between the flux of lithogenic particles and surface primary production. Honjo concluded that suspended clays are effectively scavenged from the water column by rapidly sinking organic aggregates in the Panama Basin. In the present study, the beam attenuation coefficients approached the value of pure seawater (0.4 m^{-1}) in April 1983 in the central basin of Boca de Quadra (Fig. 3.3).

SPM Distribution Patterns

Eq. 3.3 was modified to convert the beam attenuation coefficient (m^{-1}) to the SPM mass concentration (mg l^{-1}) using the regression equations of Table 3.1 and beam attenuation profiles. Conversion results (Fig. 3.10) generally agree with observed trends for previous years which have been obtained using discrete sampling (Figs. 3.11 and 3.12). For example, for beam attenuation profile obtained on 7 August 1983 (Fig. 3.3), choosing 1, 0.5, and 0.6 m^{-1} as representative beam attenuation values for the surface 10 m, the clear water minimum (30 m deep), and the near bottom (350 m deep) regions, respectively, results in mass concentration values of 1.19, 0.40, and 0.56 mg l^{-1} (regression equation given in Table 3.1). The continuous increase in turbidity below the clear water minimum is more pronounced in beam attenuation profiles (Fig. 3.3) than in the discrete SPM measurements (Fig. 3.12). However, the computed surface SPM concentrations (Fig. 3.10) were generally too high, and attenuation profiles in April 1983 cannot be converted to SPM mass concentration values due to the lack of correlation (Table 3.1).

A systematic conversion of the transmissometer profiles to yield mass concentrations of SPM has not been made in the present study due to the lack of suitable

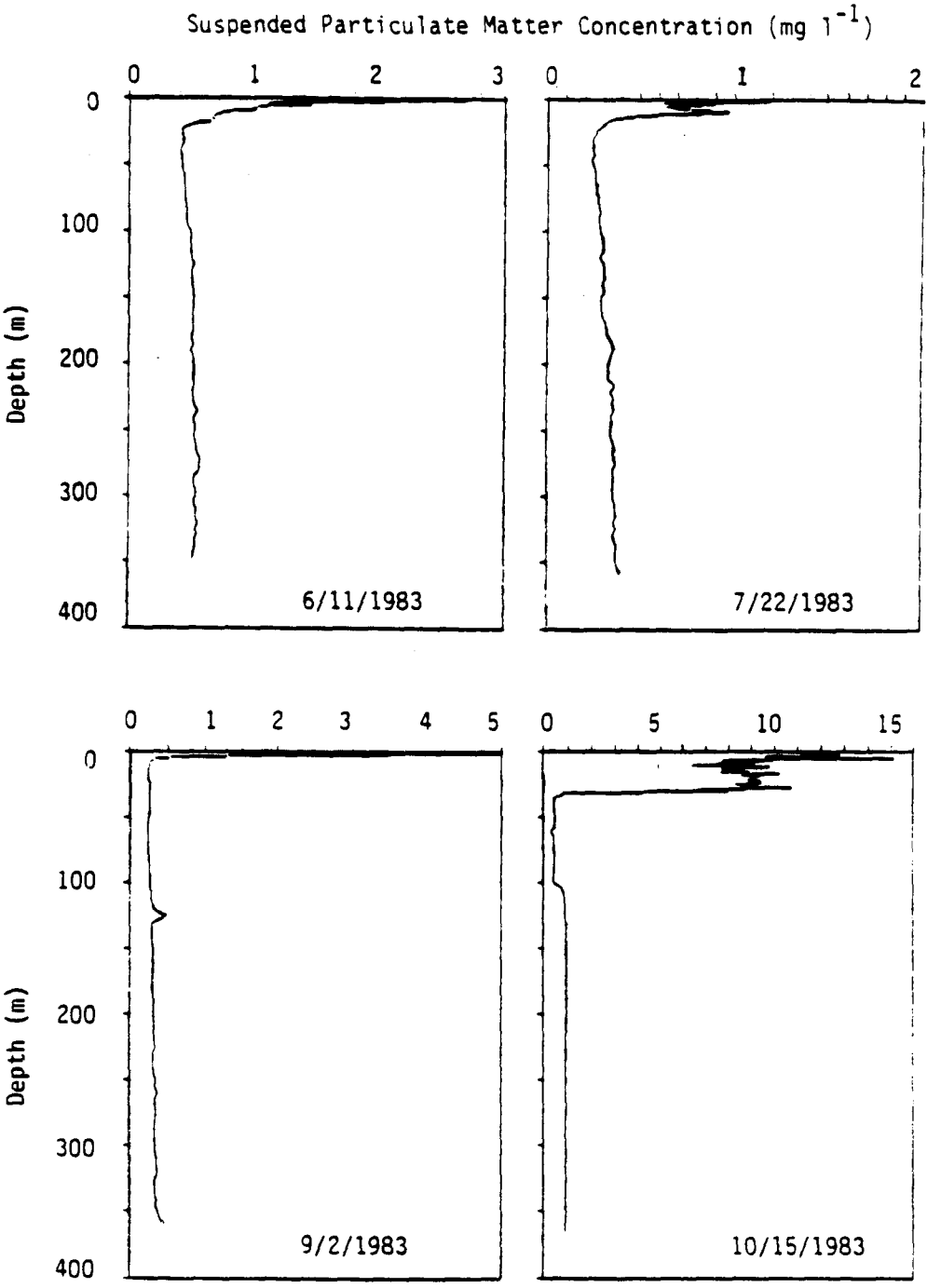

Fig. 3.10. Continous SPM profiles using the attenuation profiles in Fig. 3.3 and the calculated regressions of Table 3.1.

calibration data in each SPM reservoir. The optical properties of SPM are expected to differ in the mid-water clear zone, in the near bottom, and especially in the surface layer. Instead, previous data for discrete SPM concentration distribution (Burrell, 1983b) relevant to the objectives of this chapter are briefly summarized here.

Multiyear discrete sampling of SPM demonstrated that there is an annual bimodal pattern of SPM concentration maxima in the surface zone (Fig. 3.11). The spring and fall turbidity maxima coincide with the spring phytoplankton bloom, and with the period of maximum freshwater discharge in fall to early winter, respectively. However, particle mass concentrations in the BNL, unlike those in the surface plume, did not show significant temporal variability, except for a slight increase in the fall. Typical vertical distribution patterns of SPM are shown in Fig. 3.12. In general, surface loads are high, sometimes exceeding 2.0 mg l^{-1} during the spring bloom and the heavy rainfall season (2.3 mg l^{-1} at 10 m depth in April 1983). SPM decreases downwards from the surface to a depth of 50-75 m (0.3 mg l^{-1}), just below the euphotic zone and the pycnocline. The restricted vertical penetration of the surface SPM

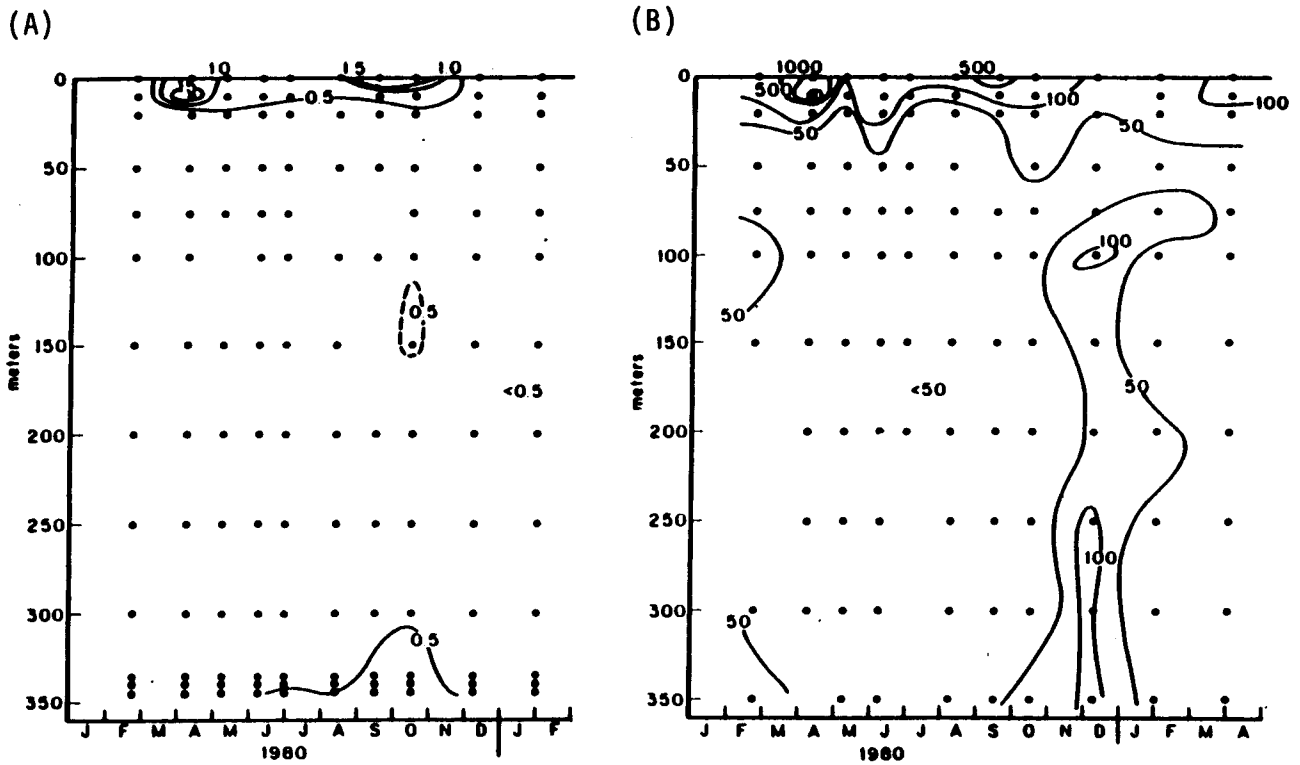

Fig. 3.11. Seasonal variations in SPM (mg l^{-1}) distribution (A) and in POC (ug l^{-1}) distribution (B) within the central basin (Station BQ9; from Burrell, 1983b).

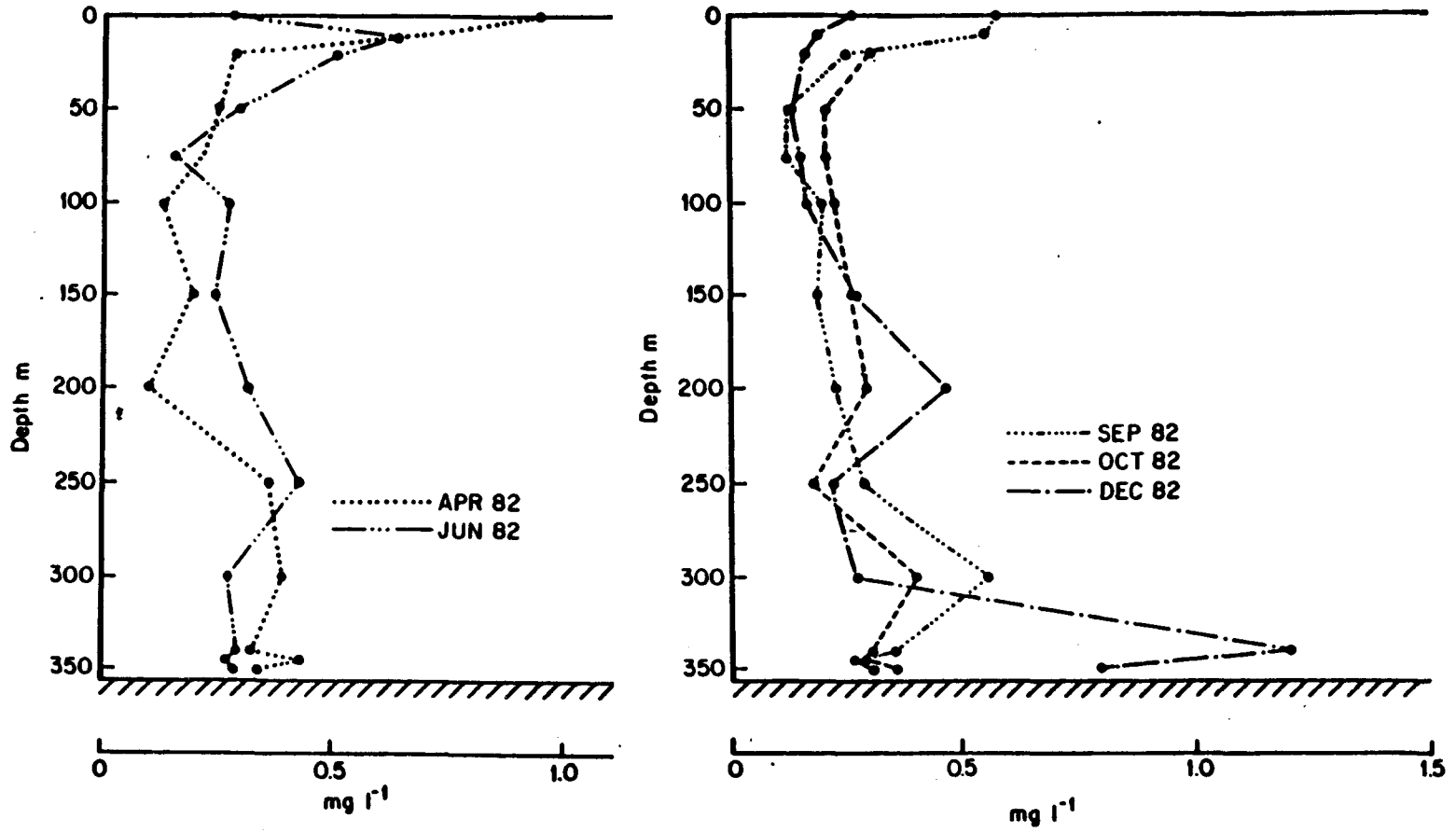

Fig. 3.12. Seasonal vertical profiles of SPM within the central basin (Station BQ9; from Burrell, 1983b).

plume may be due to sharply limited vertical mixing. This is reflected by the Brunt-Väisälä frequency distribution, which in turn is probably caused by the inflow of "clear water" from the outer basin as indicated in the temperature profiles shown in Fig. 3.3. The BNL can be described as a turbulent boundary layer where stratification is weak (low Brunt-Väisälä frequency). This zone is separated from the mid-depth minimum, which is indicative of a region of relatively low eddy diffusion. However, there is an increase of SPM below this minimum concentration zone. High values (1.20 mg l^{-1} in December 1982) were recorded around 30-50 m above the bottom, below which depth there is again a marked decrease. The current regime near the bottom may be responsible for the observed decrease of SPM in this region.

Standing stocks of SPM in the deep central basin are more uniform throughout the year at around 0.3 mg l^{-1}, with a slight increase in late summer-fall. The increase in SPM in the vicinity of the sea floor is more clearly seen in particulate organic carbon (POC) profiles (Fig. 3.11).

SPM Input to the Surface Layer

Sources of SPM to the upper reaches of the Boca de Quadra fjord system may be divided into two types: autochthonous and allochthonous. The most important allochthonous input of SPM is *via* river runoff, which carries terrestrial SPM. Although the central basin is protected from the outer basin by the Kite Island sill, water circulation characteristics suggest that exchange of SPM probably occurs especially during the deep water renewal period. A numerical modeling effort is being undertaken to estimate the exchange of SPM across the Kite Island sill during the summer deep-water renewal and winter isolation period. The primary source of autochthonous SPM is due to phytoplankton production since the littoral plant community is negligible in this fjord (Burrell, 1983b). The autochthonous SPM input would be largest during the phytoplankton bloom period in spring, and riverine SPM input is likely to be important in late summer-fall in this fjord, as suggested by the primary productivity and river runoff patterns (see Chapter 1). Riverine *versus* autochthonous SPM input will now be discussed.

SPM Production in Situ

Annual primary production within the central basin is around 140 g C m^{-2} yr^{-1} (Burrell, 1983b), and biogenic Si production is estimated to be 45 g Si m^{-2} yr^{-1} (Chapter 4). Approximately 10% and 70% of C and Si production, respectively, in the surface layer were measured at 40 m depth as a settling flux out of the euphotic zone, assuming that all the POC and Si flux at 40 m depth during the spring phytoplankton bloom period was phyto-detritus, and further assuming the complete remineralization of riverine biogenic silica in the freshwater zone (Anderson, 1986; see Chapter 4). These fluxes would be 35 g $(CH_2O)_{106}$ m^{-2} yr^{-1} of organic phyto-detritus, assuming the organic material has Redfield stoichiometry (Redfield *et al.*, 1963), and 71 g SiO_2 m^{-2} yr^{-1} assuming biogenic Si is in the form of SiO_2 (Banahan, 1983). Thus a total of approximately 106 g m^{-2} yr^{-1} of biogenic material is falling through the 40 m depth horizon. If half of the POC and biogenic Si undergo decomposition and dissolution within the water column (see discussion in Chapter 3), then approximately 53 g m^{-2} yr^{-1} of biogenic material at 40 m will be transported down to the basin surface sediment. The areal flux of the biogenic particulates formed *in situ* would be 3.6×10^9 g yr^{-1} at the 40 m depth within the

central basin.

Riverine Input of SPM

The Keta River is the major source of SPM in the surface waters of the inner basin during the high freshwater discharge period. The SPM originating from the Keta River is initially confined to a relatively thin, approximately 10 m thick brackish surface layer, which extends downfjord at least to Station BQ5 (Robb, 1981). Resuspension of bottom sediment is a consistent feature of the inner basin (Fig. 3.9). Robb (1981) concluded that it was highly unlikely that riverine suspended sediment would mix down and settle rapidly. Mn/Al ratios of suspended particulate matter in the Keta River also have been reported to be fairly constant (0.015-0.021) throughout the year (Robb, 1981), and similar values (0.09-0.032) have been determined for sediment trap samples collected at the 40 m depth (Chapter 4). These observations support the idea that the riverine particulates from the Keta River are largely transported to the central basin within the surface layer. Similarly, most of the riverine SPM discharged by the Marten River is expected to be transported through Marten Arm into the central basin.

Burrell (1983b) estimated the total quantity of

particulate sediment transported into Boca de Quadra by the combined Keta and Marten Rivers in 1980 to be around 7.8×10^9 g yr^{-1}. (The suspended sediment mass discharge rates are 100 and 145 g s^{-1} for the Keta and Marten Rivers, respectively). The total SPM flux into the fjord may be estimated at 9.2×10^9 g yr^{-1} if the contribution from the Red River (47 g s^{-1} discharge rate; Burrell 1983b) is included, using the mean monthly river flow rate in 1980 and monthly SPM load measurements in 1980-1982 (Burrell, 1983b). Burrell (1983b) also pointed out that this estimate should be at least doubled to include bed-load transport. Bed-load material is assumed to be deposited initially primarily adjacent to the river discharge zones at the heads of the inlets.

From these computations, the riverine particulate suspended sediment flux, if spread uniformly over the central basin of Boca de Quadra, and using the horizontal area at each depth (Fig. 3.13), would be of the order of 240 and 320 g m^{-2} yr^{-1} at the 40 m and 120 m depth horizons, respectively, and 680 g m^{-2} yr^{-1} at the basin floor. For the latter value, the sedimentation area was estimated by excluding the area where the bottom slope is greater than about 20 degrees (Hakanson and Jasson, 1983). Of course, these values can only be first order

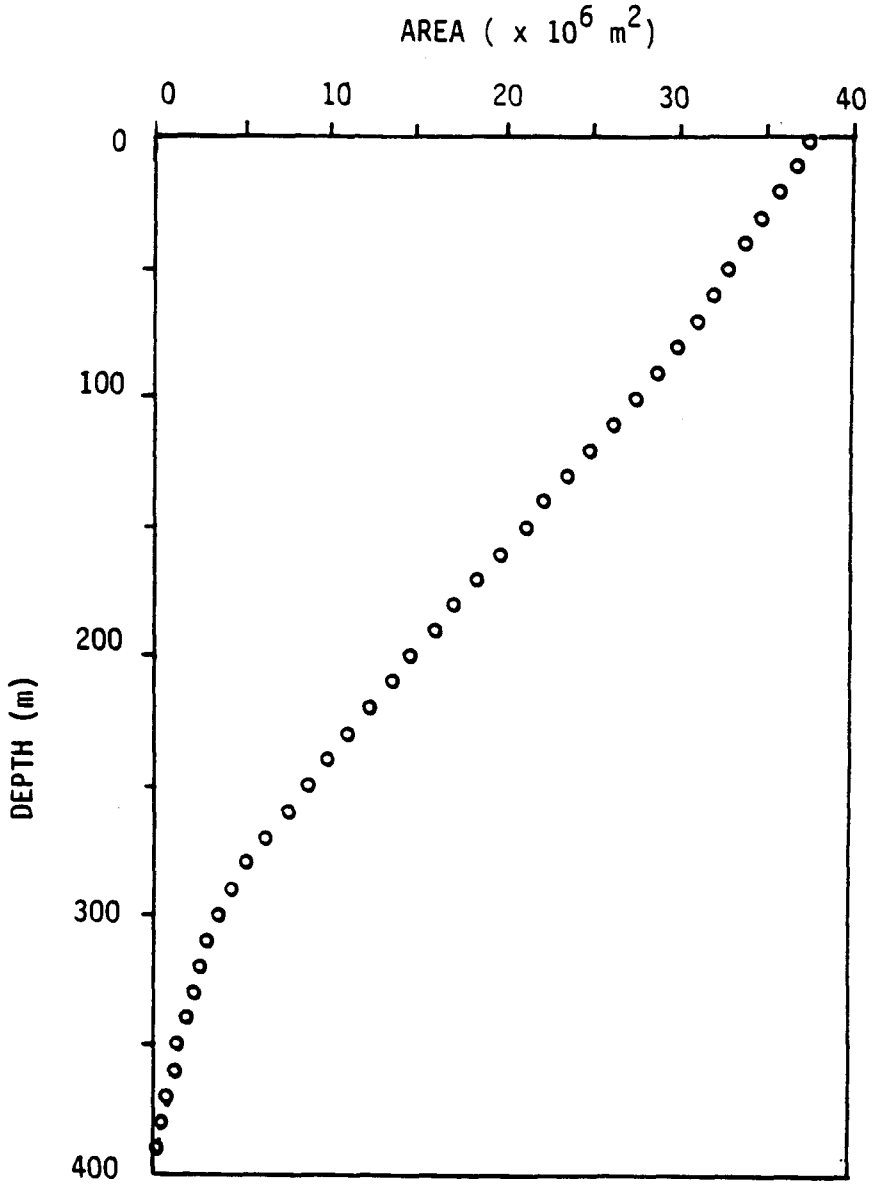

Fig. 3.13. Vertical distribution of horizontal areas in the central basin (original data from W. Lee, Univ. Alaska, pers. comm., 1983).

approximations, since some fine particulates are also sedimented in Marten Arm and in the inner basin. But it is of interest to compare these estimates with the direct flux measurements (Table 3.3). There is very close agreement with measured fluxes of SPM at 40 m depth, given the sediment trap flux precision of about 17%. It should also be noted that the measured vertical flux of SPM at 120 m depth is very similar to the long-term sedimentation rate (Table 3.2).

Further information about the total amount of SPM deposition within the fjord is given by considering ^{210}Pb sedimentation rate measurements, the estimated input of SPM from the rivers, and *in situ* production of SPM in the upper parts of Boca de Quadra, *i.e.*, within the inner and central basins and Marten Arm (Table 3.4). Since comprehensive bathymetry is unavailable, the sedimentation area of Marten Arm is here estimated at 1/3 of the surface area. The annual total suspended sediment deposition rate in the entire upper reach of Boca de Quadra above the Kite Island sill is then around 13×10^9 g yr^{-1} which is close to the estimated amount of sediment input from the rivers, 18×10^9 g yr^{-1} (Burrell, 1983b), plus 2×10^9 g yr^{-1} of *in situ* biogenic particulate production.

Table 3.3. Sources of SPM flux at depth (g m^{-2} yr^{-1}).

Depth	Measured Flux	Flux Estimated From Input and Production Rates		
(m)		Riverine	Autochthonous	Total
40	290 - 332	240	106	346
120	519	320	-	-
375	1151	680	53	733

Table 3.4. The total deposition rates of suspended particulate sediments in Boca de Quadra and Marten Arm.

Station	--Sedimentation -- Rate ($g\ m^{-2}\ yr^{-1}$)	Area ($\times 10^6\ m^2$)	Areal Deposition Rate ($\times 10^9 g\ yr^{-1}$)
BQ3 (inner basin)	1370*	3.82	5.2
BQ5 (central basin) (<260 m)	414	8.59	3.6
BQ9 (central basin) (360 m)	556	3.13	1.7
MA1A (Marten Arm)	910*	2.5	2.3
Total deposition rates			12.8

*Data from Sugai (1985)

Vertical Flux Patterns of Settling Particulates

The increase in SPM concentration and in vertical flux of SPM with increasing depth both require an additional source of SPM besides that dispersed downwards from the overlying mixed layer. Resuspension from the floor is the most likely primary mechanism. But other factors may be important, such as fecal pellet production by migrating zooplankton, the morphology of the basins (sediment focusing), and the hydrography and current regime. Fecal pellet production below the euphotic zone probably can be largely excluded since it has been shown that the organic carbon content of the sediment trap samples decreases with depth (Chapter 4). The large basins of Marten Arm (sill depth 170 m) and Mink Bay (120 m depth at the mouth) are connected to the central basin of Boca de Quadra, suggesting the strong possibility of additional advective transport of SPM into the central basin. Also, the "V" shape of the basin (Fig. 3.13) must result in downward sediment focusing, although the SPM content obtained using discrete sampling does not show a significant increase until very close to the bottom and even decreases toward the bottom in some cases (Fig. 3.12). The relative importance of sediment focusing, resuspension, and sediment input from the adjacent bays will now be discussed.

SPM Input to Mid-Depth (below 100 m) within the Central Basin from the Side Arms

SPM mass balance computations, based on the results of sediment trap deployments and sedimentation rate measurements at the bottom of the central basin, suggest an intermittent input from the benthic layers of Marten Arm and Mink Bay to the central basin of Boca de Quadra. The supporting evidence is:

1. The measured vertical flux at 40 m depth of about 300 g m^{-2} yr^{-1} cannot account for the long-term sedimentation rates of 500 to 600 g m^{-2} yr^{-1} determined by ^{210}Pb dating of the underlying sediment. The Brunt-Vaisala maximum during the deep renewal period is at 40 m, which is also the depth of the clear water minimum, and is just below the 1% light level during the productive season. Therefore, input in addition to the presently measured material fluxes from the surface layer (<40 m) is apparently required to make up the SPM mass balance (taking sediment focusing into account, but here not allowing for possible input of SPM from the outer basin).

2. The vertical flux at 120 m of 500 g m^{-2} yr^{-1} is nearly identical to the long-term sedimentation rate.

3. The mouths of Mink Bay and Marten Arm are about 120 m and 170 m deep, respectively, which is close to the

horizon where sediment fluxes increase. In fact, the mouth areas of Marten Arm and Mink Bay are relatively large, around 60% of the width of the central basin, and perpendicular to the central basin. This configuration may induce higher turbulence at the mouths of Mink Bay and Marten Arm (D. Nebert, Univ. of Alaska, 1984, pers. comm.). Consequently, the SPM influx from both side reservoirs may be rapidly dissipated within the central basin. This is believed to be the main reason why a direct influx from the side arms has not been positively verified (*i.e.*, in the transmissometer profiles).

Monthly variations of water column temperature and beam attenuation (turbidity) have been monitored from the start of deep water renewal (June) through the high precipitation season (October) at the mouths of Mink Bay (Fig. 3.14A) and Marten Arm (Fig. 3.14B). Although attenuation profiles at the mouth of Mink Bay show small maxima in June and in September 1983 at around 120 m depth (which corresponds to the bottom of Mink Bay), such a peak is not evident in October 1983. The cause of the subsurface maxima may be related to the density structure of the water column, as well as to the influx of sediment from Mink Bay. At the mouth of Marten Arm, there is no noticeable vertical change of attenuation, such as local

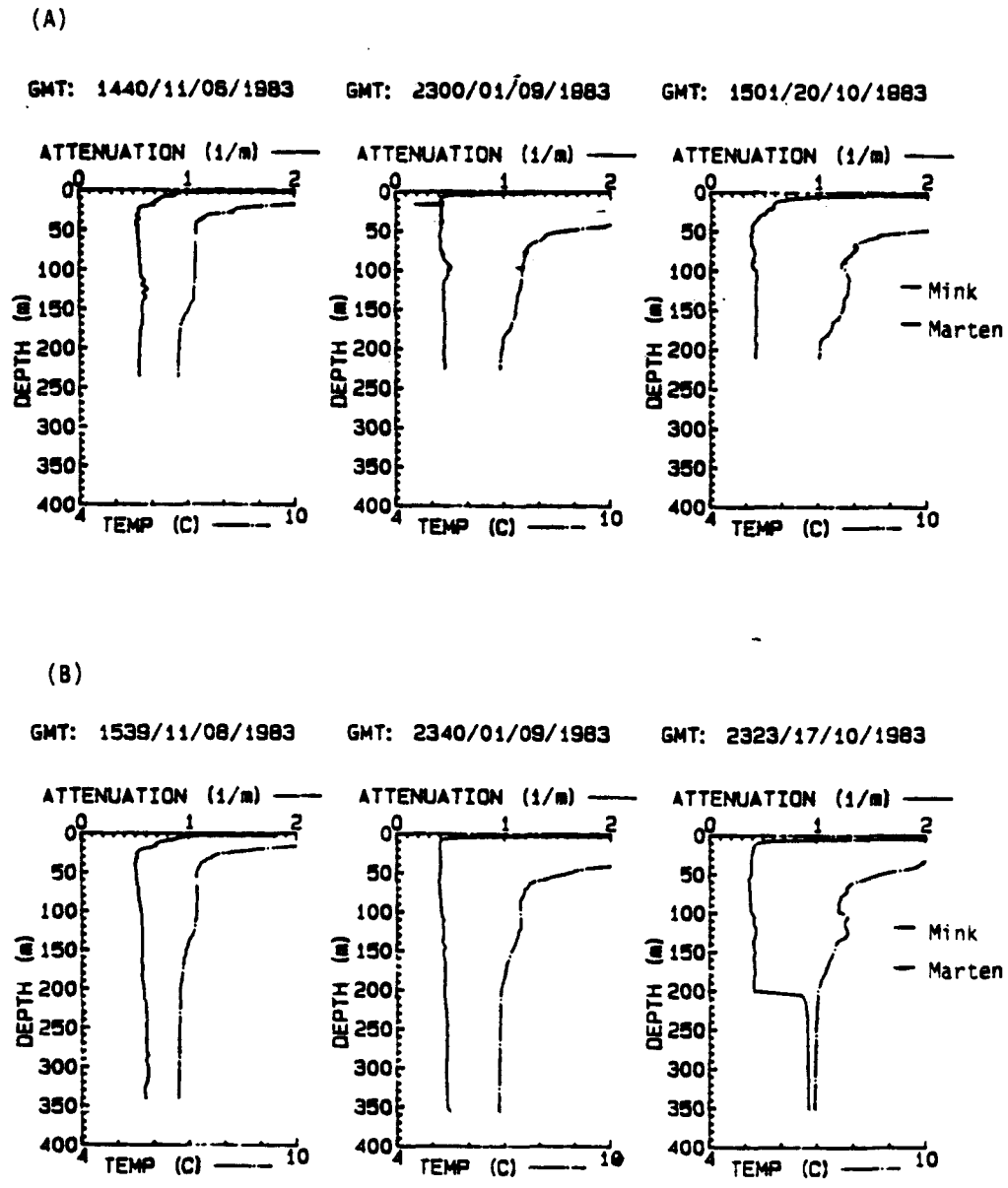

Fig. 3.14. Time series distribution of attenuation coefficient and temperature at the mouths of Mink Bay (A) and Marten Arm (B), June-October 1983.

maxima in June and September, but there is a marked increase of attenuation below 100 m depth. An additional feature was noted in October 1983: STD/transmissometer casts were conducted sequentially on October 15, 18 and 20. On October 15, a sudden increase in attenuation appeared at 100 m depth. Three days later the peak moved down to 230 m, and after 5 days to 300 m depth (Fig. 3.15). These phenomena could be the result of episodic slumping of SPM from Marten Arm. Pak and Zaneveld (1977) show that the formation and dissipation of the benthic nepheloid layer (BNL) on the continental shelf off Oregon is the result of the advection of turbid water from an adjacent coastal source. Likewise advection of turbid water from Marten Arm and Mink Bay is a potential source of the BNL within the central basin. More frequent casts, or a moored transmissometer, would be required to determine whether these phenomena are persistent in late fall to early winter or are short term features, possibly associated with local weather conditions. The primary energy for transporting SPM is probably provided by the turbulence generated by injecting river water, and by tidal waves which can winnow the bottom sediments at the mouths of Marten Arm and Mink Bay.

The reduced content of sand-sized material in the surface sediment (Burrell, 1983b) shows that the central

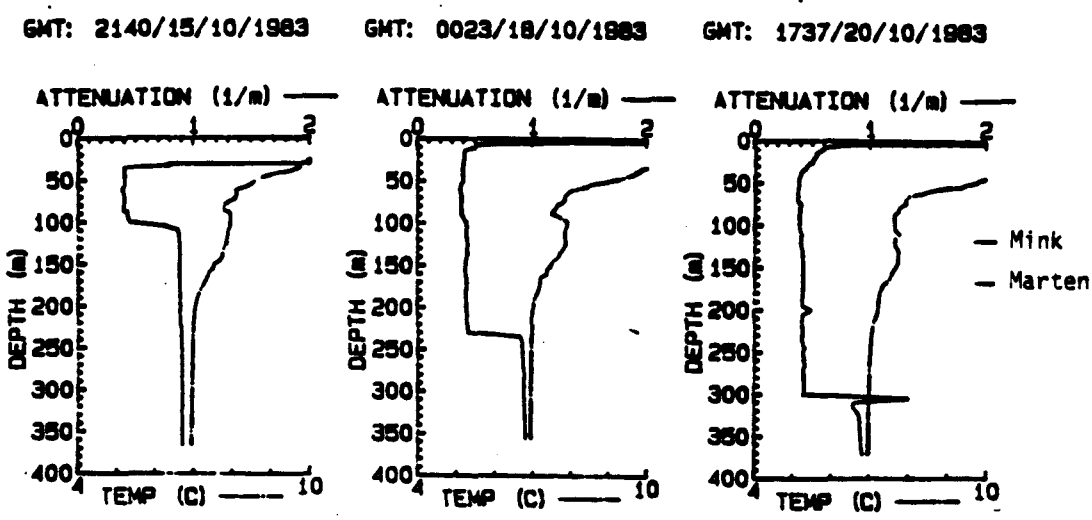

Fig. 3.15. Time series distribution of attenuation coefficient and temperature in the central basin (Station BQ9) during October 1983.

portion of Marten Arm is a deposition site for finer grained sediments. This is demonstrated by the sedimentation rates (Table 3.5) and also by the higher content of total organic carbon in the surface sediments (Burrell, 1983b). Since the coarser grain size material at the entrance sill area (Station MA1) also indicates a high energy environment, transport of previously deposited particulates across the mouth may be possible *via* the winnowing effect of currents and waves.

Since the sediment trap array was located adjacent to Mink Bay, and only slightly down-fjord from Marten Arm, traps at 120 m depth should be particularly influenced by these sediment sources. Fig. 3.16 is a comparison of the measured flux at 120 m (or 100 m), and that which should occur if there were no additional inputs of material between 40 m and that horizon. The estimated flux is computed using the vertical flux at 40 m, and allowing for the decreased horizontal area at 120 m (100 m). It is proposed that the additional material required for the flux actually measured is primarily derived from the adjacent arms, and that influx is greatest during the fall-winter period when high precipitation and runoff conditions prevail.

The presence of SPM input to mid-depths (below 100

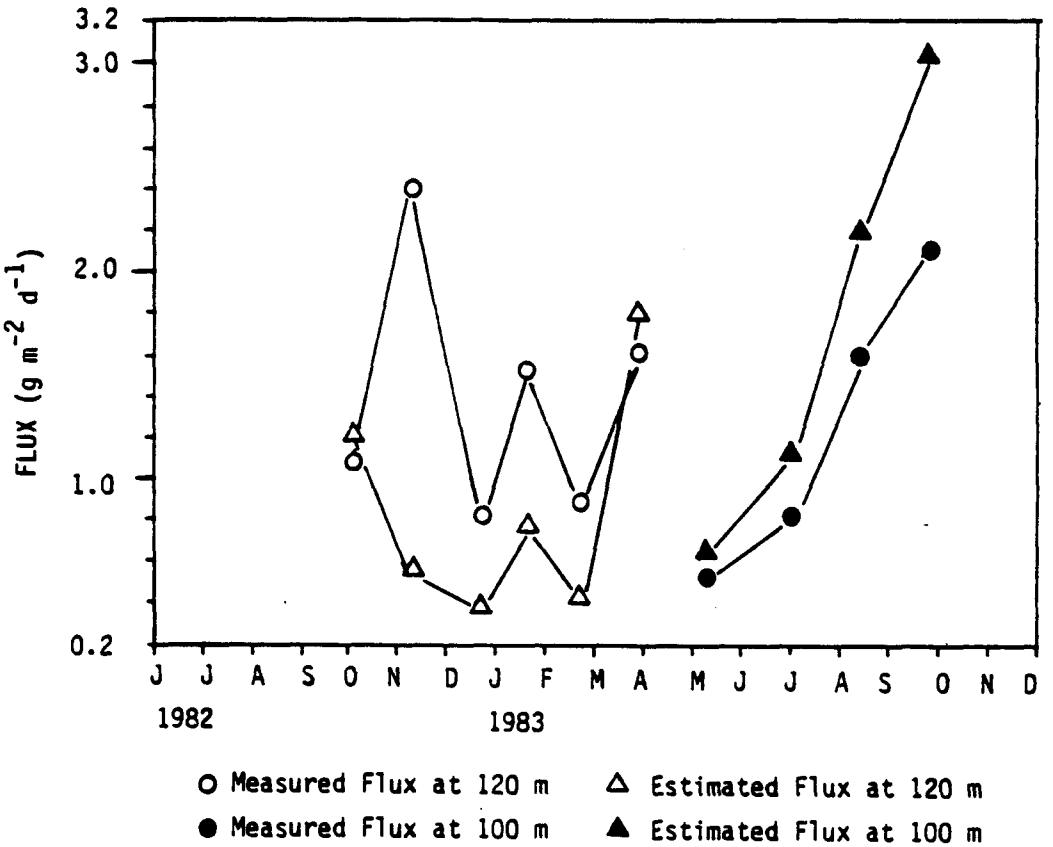

Fig. 3.16. Measured versus estimated settling flux at 120 m (100 m) depth.

m) from the side arms prevents use of the flux at 40 m as the designated "primary flux" to the basin waters. Therefore, the SPM flux observed at 120 m is used as the primary flux to the waters below in all following computations.

Sediment Focusing

Sediment focusing must occur given the morphology of the Boca de Quadra fjord basins. The horizontal area at 100 m is about 74%, at 250 m about 24%, and at 360 m only about 3% of the total surface area of the central basin (Fig. 3.13). The inner basin is located at the mouth of the Keta River, and Marten Arm at the mouth of the Marten River. Both bodies of water are separated from the central basin by deep sills at 100 m and 170 m depth for the inner basin and Marten Arm, respectively. These sills may restrict flushing of sediments out of the basins. Thus most sediment carried by rivers, especially the coarser material, should be deposited in these two basins and only the finer particles transported out to the central basin as described previously.

The manner of sediment focusing in small lakes has been well presented by Hilton (1985). By definition, sediment focusing is the phenomenon of greater sediment accumulation in the deep part of lakes than in the

shallows. This feature has been documented by Hargrave and Nielsen (1977), who observed that the concentration of sediment organic matter with increasing depth was inversely related to the bottom slope gradients in a Canadian fjord.

There is no clear trend of increasing sedimentation rate with depth in Boca de Quadra; nor an increase in organic carbon content; nor an increase in the portion of finer grain sized particulates in the bottom sediments of the central basin (Table 3.5). However, the Pb-210 inventory (Table 3.2) suggests that sediment deposited initially at Station BQ5 (located 100 m above the Station BQ9 area in the upper central basin) may be resuspended and transported to deeper areas in the vicinity of Station BQ9. (The ^{210}Pb inventory may also be affected by the scavenging rate of ^{210}Pb; *e.g.* Carpenter *et al.*, 1981.) However, it should be noted that the Station BQ5 area is located far (about 10 km) from the influence of Marten Arm, and is 16 km away from the Keta River. In addition, there is the presence of the inner sill. Thus the original SPM input may be smaller than in the BQ9 area which is closer to the mouth of Marten Arm.

Although the extremely complicated basin topography renders an exact assessment of the sediment focusing phenemenon nearly impossible using the present

Table 3.5. Sediment parameters in Boca de Quadra.

Station	Depth (m)	Sedimentation rate ($g\ cm^{-2}\ yr^{-1}$)	TOC (%)
BQ3 (basin)	156	* 0.137	
BQ5 (basin)	275	0.041	5
BQ9 (basin)	368	0.056	4-5
BQ9G (basin)	380	0.061	4-5
MA1 (sill)	174	* 0.023	^ 1.4
MA1A (basin)	208	* 0.091	^ 5.7

* Data from Sugai (1985)

^ Data from Burrell (1983b)

information, the continuous increase of vertical flux below 120 m depth cannot be due to sediment focusing alone (see Fig. 3.16). In fact, Table 3.3 shows that the projected SPM flux at 375 m depth is less than half of the measured flux, which in turn is twice the long term sedimentation rate.

Resuspension

From the preceding discussion it would appear that resuspension must be the predominant process responsible for the increase of SPM below 50 m depth; and especially below 120 m depth. The bottom topography is very steep, and around 65% of the floor has a slope of more than 20 to 35 degrees where net sedimentation of suspended particulate matter cannot occur (Hakanson and Jasson, 1983). Thus, particles initially deposited on this slope are likely to become water-borne again due to the steepness of the floor and the particularly low water column stability of the deep basin waters. This resuspended material is subsequently mixed with primary settling material. Turbulent water movements also cause settling material to pass the same depth horizon many times in the course of its overall progress downwards. The consequences of resuspension are an overall increase in both SPM content and the vertical flux of SPM with

depth.

The relationship between near-bottom current speeds and sediment suspension or deposition is not well known (Burrell, 1981). Recently Lavelle *et al.*(1984) studied the erosional response of a fine-grained sediment to bottom stress. These workers observed that currents 5 m above the bottom, having speeds exceeding 40 cm s^{-1}, cause a six-fold increase in SPM concentrations. Because of the power (2-4) dependence of bottom sediment erosion on current speed, even occasional high-speed currents (>50 cm s^{-1}) at 378 m depth (2 m above the bottom at BQ9G; see Chapter 1) may drastically increase the erosion rate of the basin floor. Davis (1971) shows that current velocities around 15 cm s^{-1} at 15 cm above the bottom are probably sufficient to resuspend unconsolidated surficial sediment composed of silty clay and having high water content (90%). However, sediments within the central basin of Boca de Quadra are organic-rich and cohesive. Unsupported ^{210}Pb and ^{137}Cs data indicate that the top few centimeters of the sediment layer are being mixed, but this may not be entirely due to the resuspension activity; bioturbation is another possibility.

Other supporting evidence for the resuspension of bottom sediments is the poorly stratified deep layer of

the central basin, as discussed earlier. Strong density gradients occur at around 40 m depth in the renewal period and about 120 m depth during the isolated period. The relatively small density gradients below the pycnocline must enhance the upward turbulent diffusional transport of fine SPM. Since the increase of SPM concentration around the bottom is more pronounced after the period when deep renewal events take place (Fig. 3.11), turbulent mixing may be more effective then in inducing and maintaining the resuspension of particulates in the central basin of Boca de Quadra.

The major causes of resuspension of bottom sediment in the central basin of Boca de Quadra have not been determined. Resuspension may be triggered by external factors, such as storms or episodic slumping from the flanks of the fjord due to the steep slope and strong bottom currents associated with tides. Turbulence from breaking internal waves may influence redistribution of SPM. The model of Stigebrandt (1976) shows that internal waves caused by a barotrophic tide oscillating across a sill can create boundary turbulence throughout the basin below sill depth.

All measured particulate Al fluxes below 300 m depth in the spring-summer period and below 120 m depth in the fall-winter period exceed the long-term Al

deposition rate. This also suggests that resuspension activity (including resuspension from the side walls) is great in the deep basin (Fig. 3.6). Since Al can be assumed to be completely refractory during residence in the water column and in the surface layer of sediments (Mackin and Aller, 1984), particulate Al can serve as a conservative tracer of the bulk SPM, in contrast to the biogenic particulates. The resuspension flux of Al can be obtained using the following simple relation:

(Resuspension Flux)=(Total Flux)-(Primary Flux) (3.4)

The primary flux is taken as the Al flux measured at 100 or 120 m depth. The relative contributions of resuspension flux for Al are given in Table 3.6. Table 3.6 shows that the resuspension fluxes comprise about half or more of the total flux of Al below 300 m depth. It further suggests that resuspension becomes more important during the period of low Al input to the surface layer or 120 m depth (spring-summer) than in the higher Al input season (fall-early winter), as discussed earlier. High Al fluxes in the fall-winter period suggest an increased input of inorganic minerals from land and probably of terrestrial POC as well. The magnitude of resuspension in the central basin of Boca de

Table 3.6. Temporal variations of the contribution of resuspension flux of Al at depths (%).

Date (1983)	3/3-4/9	4/11-6/7	9/2-10/18	10/18-12/1*
Depth (m)				
280	31	-	-	-
300	36	81	49	4
365	52	87	59	32
375	56	87	51	2

* 1982

Quadra is very small compared to other similar environments such as the main basin of Puget Sound where the magnitude of resuspension is well over ten times higher (Baker *et al.*, 1985).

Sedimentation Rates and Sediment Mixing

^{210}Pb profiles show complex features in the surface layer of the sediments (Fig. 3.8). Although the apparent mixing of the surface layer prohibits the direct application of ^{210}Pb geochronology, modern sediment accumulation rates (on a time scale of a few hundred years) can be estimated *via* analysis of the distribution of ^{210}Pb activity below the mixed layer. The top 10 or 20 cm of mixed surface sediment represents the present, and each point below this represents an increment of sediment a number of years in the past (Nittrouer *et al.*, 1979). However, it may be inferred that the mixed layer and sub-mixed layer sediment accumulation rates are similar in this mature fjord, because porosity does not change significantly, and the cumulative mass of bulk sediment increases in a fairly consistent manner with depth within the about upper 60 cm or so of sediment (Fig. 3.7). It should be noted also that active glaciers have been absent since the Pleistocene epoch, and that the fjord is pristine and surrounded by heavily forested

land (Chapter 1). Therefore, there is no good reason to believe that the mean sedimentation rate has changed significantly over the past few hundred years.

However, the ^{210}Pb method to determine sedimentation rates does not permit, in itself, discrimination between sedimentation and particle mixing from a linear plot of the natural logarithm of ^{210}Pb activity (Kipphut, 1978; Officer, 1982). Also, the presence of sediment mixing leads to overestimation of the sediment accumulation rate. Therefore, an alternative approach is needed to determine the mean sedimentation and mixing rates. The measurement of a sediment constituent, ^{137}Cs, which has a time dependent input different from that of ^{210}Pb, can be a useful complement to the ^{210}Pb sedimentation rate measurements.

The ^{137}Cs activity profiles in the central basin of Boca de Quadra are illustrated in Fig. 3.17. The deepest level at which the ^{137}Cs activity was detected was around 12 cm below the sediment-water interface. The general trend is an exponential-like increase in activity from 12 to 4 cm depth, followed by a decrease to the surface of the sediment.

The ^{137}Cs activities of approximately the upper 12 cm of these cores show a pattern which is probably due to mixing, and this can be semi-quantified. Such mixing may

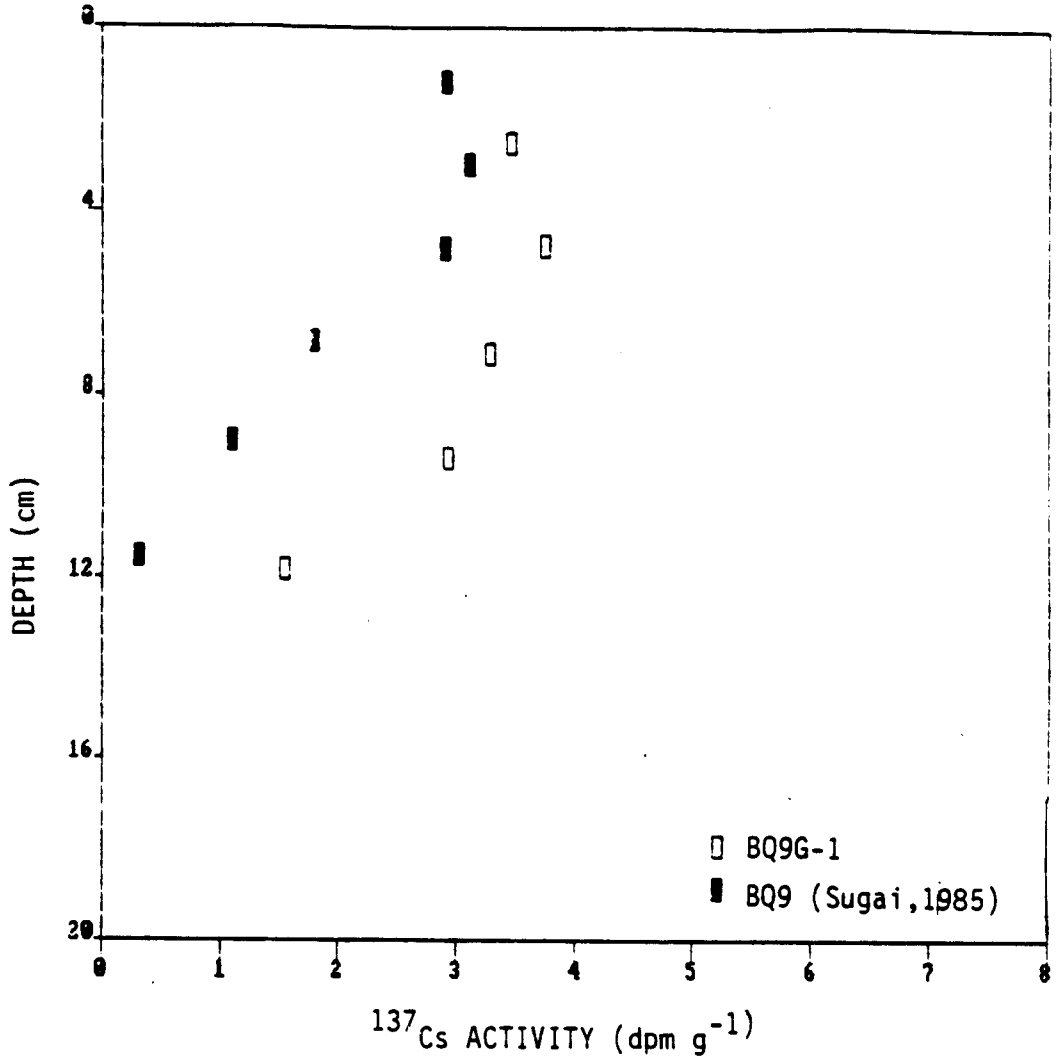

Fig. 3.17. Vertical profiles of ^{137}Cs in the sediments.

be caused by bottom turbidity currents, biological activity, gas ebullition, coring artifacts, radiocesium diffusion, or a combination of these (Scholkovitz and Mann, 1984; Torgersen and Longmore, 1984). The close reproducibility of the ^{137}Cs data for the two cores collected at separate times reduced the likelihood of mixing by coring. It is therefore probable that bioturbation, plus occasional strong currents, especially during the deep-water renewal period, is responsible for mixing the surface sediments.

Guinasso and Schink (1975) have developed a model in which vertical mixing can be expressed as a function of both depth and time. Kipphut (1978) has given a simplification of the Guinasso and Schink model for a pulse of material moving with constant sedimentation rate (w) and with a rate of sediment mixing (coefficient K). In this case distribution of the material, C, at some later time (t) will be given by:

$$C = Q/[2(\pi K)^{1/2}]\exp[-(z-wt)^2/(4Kt)] \qquad (3.5)$$

where Q is the amount of material (mass cm^{-2}) deposited at z = 0 and t = 0. Since depth-activity (concentration) profiles are available (Fig. 3.17), Eq. 3.5 can be solved for K. The dependence of the activity distribution of

^{137}Cs upon K was graphically presented by Torgersen and Longmore (1984). The ^{137}Cs fallout pattern in the vicinity of Boca de Quadra is assumed to follow the general trend for the northern hemisphere (Robbins and Edginton, 1975). Also, ^{137}Cs is assumed to have been introduced continuously for about 30 years with a maximum rate of injection about 20 years before core collection. Thus t was assigned a value of 20 years, and Q was obtained by summing up the total amount of ^{137}Cs activity in the sediment column (data from Sugai, 1985). From the ^{210}Pb data, w is about 0.2 to 0.3 cm yr^{-1}. Eq. 3.5 and ^{137}Cs profiles constrain the sedimentation rate (w). A maximum value of ^{137}Cs activity should be present where depth, z, is equal to w.t in Eq. 3.5. Thus w is chosen to be 0.2 cm yr^{-1}, and the calculated value of K is 5.8 x 10^{-9} cm^2 s^{-1}. Kipphut (1978) shows further that ^{210}Pb profiles are only slightly altered for K values less than 1 x 10^{-8} cm^2 s^{-1}. Since most ^{210}Pb distributions with depth in the central basin of Boca de Quadra show little mixing in the surface few centimeters, the ^{210}Pb activity profiles give an accurate estimation of the sediment accumulation rate.

CONCLUSIONS

This present study of the bulk suspended particulate dynamics has produced a number of findings which will provide the basis for understanding the behavior of particulate organic matter and particulate biogenic silica in the central basin of Boca de Quadra:

1. The SPM distribution patterns are closely related to the hydrography and circulation pattern.

2. The similar optical properties of SPM in the outer and central basin in summer suggest an exchange of SPM between the two basins. The SPM in the inner basin is optically different from that in the rest of Boca de Quadra, and this is probably due to the proximity of the river, and presence of the inner sill.

3. The vertical fluxes of particulates near the surface (40 m depth) correlate very well with the fluxes at depth, indicating that particles are largely transported vertically.

4. The SPM being introduced by the rivers (the Keta, Marten, and Red Rivers) appears to account for almost all of the sediment deposition on the basin floor of the upper reaches of Boca de Quadra above the Kite Island sill.

5. Although it is very difficult to assess sediment

focusing by the "V-shaped" basin morphology, it appears not to be important. The intermittent input of SPM from the benthic nepheloid layer of Marten Arm and Mink Bay could to be significant. Thus the vertical flux at 120 m is regarded as the primary flux within the basin below sill height. In the deep basin, resuspension is thought to be primarily responsible for the increased vertical flux and concentration of SPM. Resuspension may account for up to 50-80% of settling particulates at 300 m depth.

6. Sedimentation rates in the central basin of Boca de Quadra are 450 to 720 g m^{-2} yr^{-1}, or the equivalent of 0.2 to 0.3 cm yr^{-1}. The surface sediment mixing rate is estimated at 5.8×10^{-9} cm^2 s^{-1}.

CHAPTER 4. SOURCES, VERTICAL DISTRIBUTION, AND FLUX OF PARTICULATE C, N, BIOGENIC SI, MN AND FE WITHIN THE BASIN WATER COLUMN

INTRODUCTION

Settling particulate organic matter is a source of food for organisms living at mid-depths below the euphotic zone, and for the benthos (Angel, 1984). Metal transport is known to be intimately tied to that of the suspended matter, especially to the biogenic particulates (e.g. Collier and Edmond, 1984). Mn and Fe can be important scavenging agents for other trace metals (Olsen *et al.*, 1982) and are also involved in the oxidation of organic matter in the suboxic environment (Tebo and Nealson, 1984). Quantifying the transfer of biogenic matter and particulate Mn and Fe is hence very important to an understanding of many biological and geochemical processes occurring in the sea. In particular, the settling flux of particulate matter plays an important role in regulating the chemistry and biology within fjord basins, since the ratio of depth to width of such basins is much larger than in other types of estuaries.

The settling flux of organic matter has been measured directly in a number of non-glacial fjords: a Scottish sea loch (Davis, 1975); St. Margaret's Bay, Nova

Scotia (Webster *et al.*, 1975); Dabob Bay (Prahl *et al.*, 1980; Lorenzen *et al.*, 1981); and the main basin of Puget Sound (Baker *et al.*, 1985). The settling flux of biogenic Si is not known to have been measured previously in fjords. Settling fluxes of particulate Mn and Fe have been directly measured in a few fjords: for example, in the main basin of Puget Sound (Feely *et al.*, 1986) and the Laurentian Trough, Canada (Sundby and Silverberg, 1985).

In this chapter, the sources, composition and alteration of biologically produced particulate material and particulate Mn and Fe at various depths and times will be considered in detail. The primary objectives are:

1. To describe temporal variations in the settling flux of particulate organic C, N, biogenic Si, Mn and Fe.

2. To elucidate the sources of particulate organic matter in this fjord.

3. To determine the seasonal rates of energy and nutrient transfer from the euphotic zone to the deep basin and sea floor.

4. To investigate the non-conservative behavior of particulate organic C, N, biogenic Si, Mn and Fe.

The first and third objectives will be addressed using data from serial deployments of a sediment trap array (Chapter 2). Discussions related to the second

objective employ the $\delta^{13}C$ and C/N ratio of settling particulate organic matter. In addition, scanning electron microscopy was used to observe particulate morphology. The third objective will be addressed using a simple primary-resuspension-alteration model. This model may be the first one of its type applied to the marine environment. It was shown in Chapter 3 that the settling flux of SPM at 120 m (or sometimes at 100 m) depth may be regarded as the primary supply flux to the deep basin, and that particulate Al serves as a tracer for quantifying resuspension. In the model developed in this chapter, a transfer from a soluble to a particulate phase is called a "positive alteration flux", and a "negative alteration flux" is then the decompositon or dissolution of settling particulates. These "alteration flux" terms must also include any apparent compositional changes due to the lateral transport of particulates. However, the latter contribution is presumed to be small in the deep basin, as discussed in Chapter 3.

METHODS

Sampling Method

Settling particulates were collected using an array of sediment traps at Station BQ9G. Procedures have been described in detail in Chapter 2.

Elemental Analyses

Particulate organic carbon (POC) and particulate nitrogen (PN) contents of sediment trap samples were determined using a CHN analyzer (Perkin-Elmer model 240C) after treatment with HCl to remove carbonates (Tsunogai *et al.*,1980; S. Henrichs, 1982, Univ. of Alaska, pers. comm.). Biogenic Si content was determined by the procedure of DeMaster (1981). The precision of the POC, PN, and biogenic Si measurements is given in Appendix A. The content of Fe and Mn in sediment trap and bottom sediment samples was determined using a Kevex X-ray fluorescence (XRF) unit, calibrated against the NBS reference material #1646 (Estuarine Sediment). Analytical precision was 5% for Mn and 0.5% for Fe.

Scanning Electron Microscopy

Sediment samples obtained using water bottles, sediment traps, and the corer were examined *via* scanning electron microscopy (SEM). A small amount of sample (a few ml) was taken from the collection cup of the sediment trap, or from the top portion of the core and was fixed in the field with an equal volume of a mixture of 5% glutaraldehyde and 0.1 M cacodylate, and stored in a refrigerator (M. A. Borchert, 1983, Univ. of Alaska, pers. comm.). Following transportation to the

laboratory, the samples were dehydrated using both the CO_2 critical point drying method and air drying, and mounted on an Al stub. Discrete water samples were taken using Niskin bottles, and suspended sediments were collected on a 0.4 um Nuclepore filter. The filters were rinsed with distilled water several times, placed in individual petri dishes and frozen on board ship. On return to laboratory, the filters were dried in a desiccator. In the SEM laboratory (Geophysical Institute, University of Alaska), small disks were cut from the filter with a pair of scissors, and mounted on Al-stubs using double-sided tape. To minimize electron charging effects, and to improve image contrast and help stabilize the specimen, the samples were coated with a thin gold-palladium film using an ISI Sputter Coater. A JSM35U Scanning Electron Microscope was used to observe the samples. Identification of particulates rich in Fe and Mn was done using an energy dispersive X-ray microprobe (Kevex 7000 X-ray microanalyzer).

$\delta^{13}C$ Measurements

Stable carbon isotope ratios for organic matter collected in the sediment traps, from bottom sediments, and from leaves and twigs of the dominant land plants (Sitka spruce and western hemlock) were measured with a

SIRA-9 isotope ratio mass spectrometer on CO_2 prepared by combustion of the organic matter using the method of Craig (1953). All stable carbon isotope values reported here are relative to the PDB standard:

$$\delta^{13}C\ (^{0}/_{00}) = \left(\frac{^{13}C/^{12}C(\text{sample})}{^{13}C/^{12}C(\text{standard})} - 1\right) \times 1000 \quad (4.1)$$

RESULTS

Raw data on the concentrations and fluxes of particulate organic carbon, nitrogen, and biogenic Si are tabulated in Appendix A, and particulate Mn and Fe data are listed in Appendix B.

Particulate Organic Carbon (POC)

Concentrations (%) and vertical fluxes (mg C m^{-2} yr^{-1}) of particulate organic carbon at various depths are shown as depth profiles in Figs. 4.1 and 4.2, respectively. The points mark the mid-point of each sampling period. The sediment trap located at 40 m depth, just below the 1% light level and just below the surface mixed layer, will be discussed first. The POC content in settling particulates decreased from June-July 1982 (13%) toward a minimum value (9%) in late September 1982, subsequently increased to over 15% in December 1982, and decreased again to 7% in March 1983. Finally,

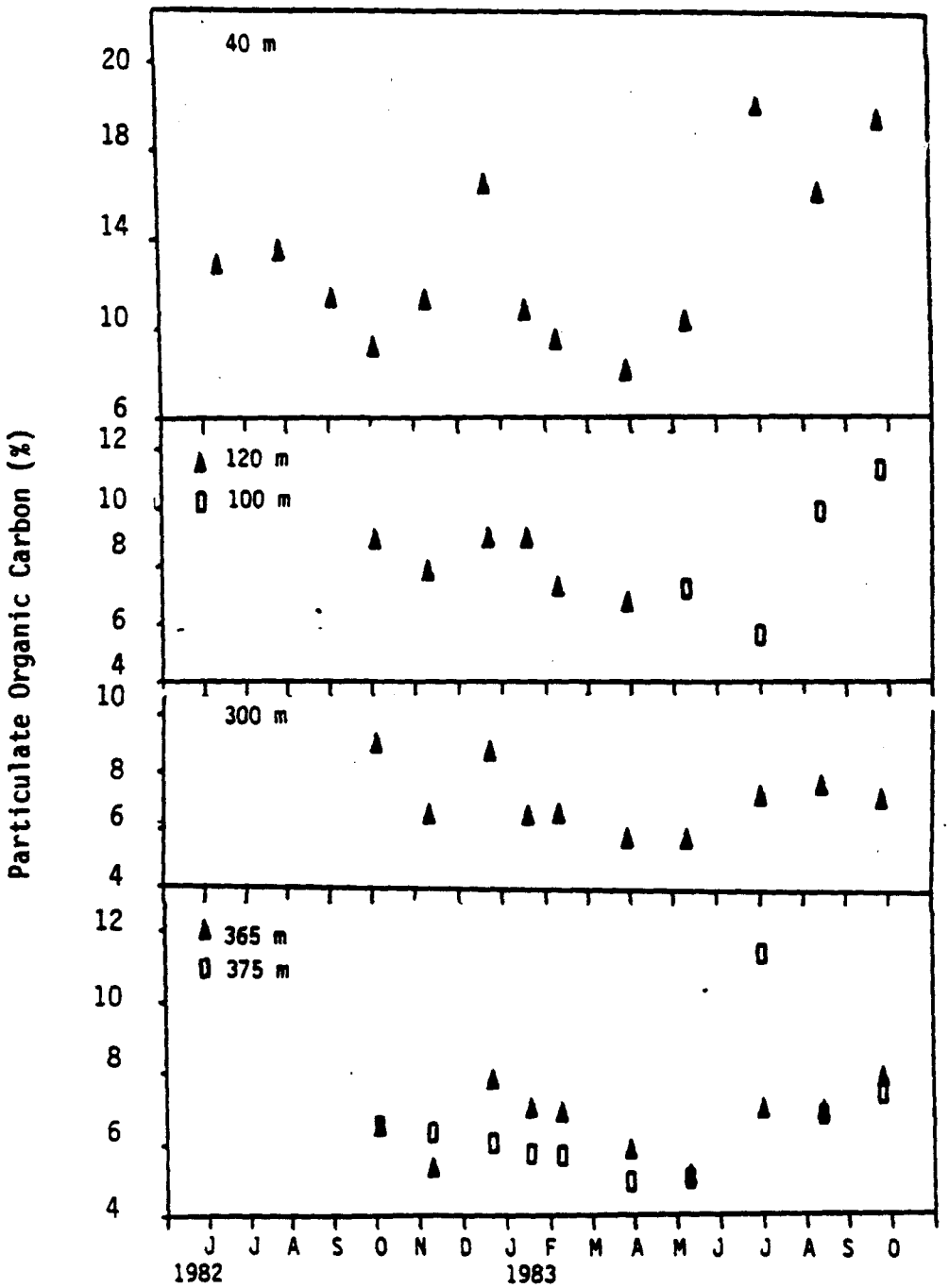

Fig. 4.1. POC content (%) of the settling particulates at various depths.

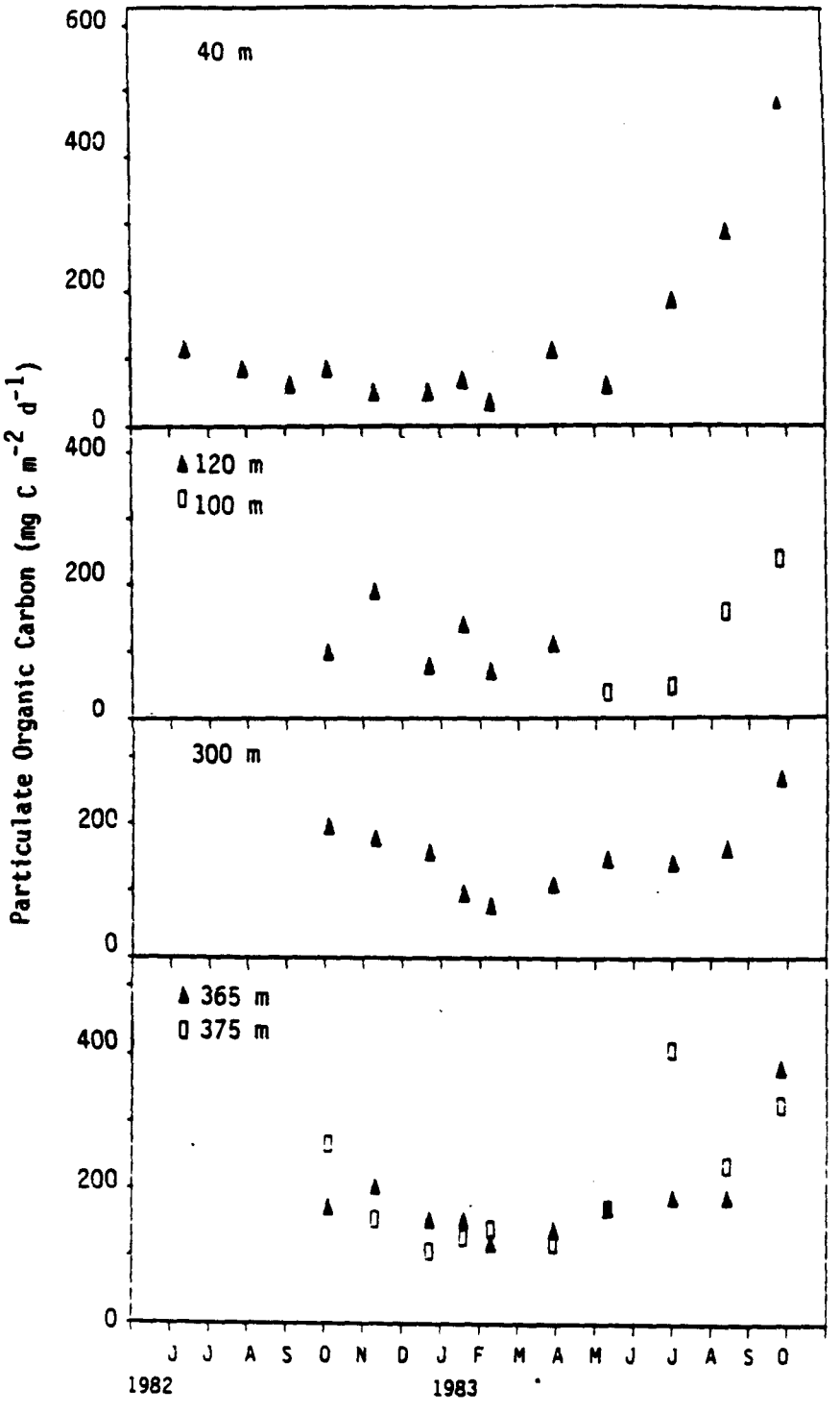

Fig. 4.2. Settling flux of POC (mg m^{-2} d^{-1}) at various depths.

concentrations gradually increased to more than 18% in July 1983. The settling particulates in the deeper layers of the basin essentially followed the trend observed at the 40 m depth, except that the mean percentages of POC were considerably less than those at 40 m depth. At 375 m depth, POC concentrations in the settling particulates were 5.0-7.8% with a single maximum value of 11.3% in the June-July 1983 sampling period.

The vertical fluxes of POC were about 50 mg C m^{-2} d^{-1} at 40 m and less than 200 mg C m^{-2} d^{-1} at 375 m during the winter months (approximately from October 1982 to April 1983). During the summer-fall period (before October 1982 and after May 1983), the settling flux values at 40 m ranged from 50 in May to more than 450 mg C m^{-2} d^{-1} in August 1983, and at 375 m from 150 in May to 450 mg C m^{-2} d^{-1} in June 1983.

Particulate Nitrogen (PN)

Concentrations and vertical fluxes of total nitrogen in the settling particulates are shown in Figs. 4.3 and 4.4. Concentrations of PN ranged from 0.9 to 2.5% in the settling particulates collected at 40 m depth, and from 0.6 to 0.8% in those sediment samples collected in the deeper layers, with maximum values during the June-July 1983 sampling period. The variability of PN in settling

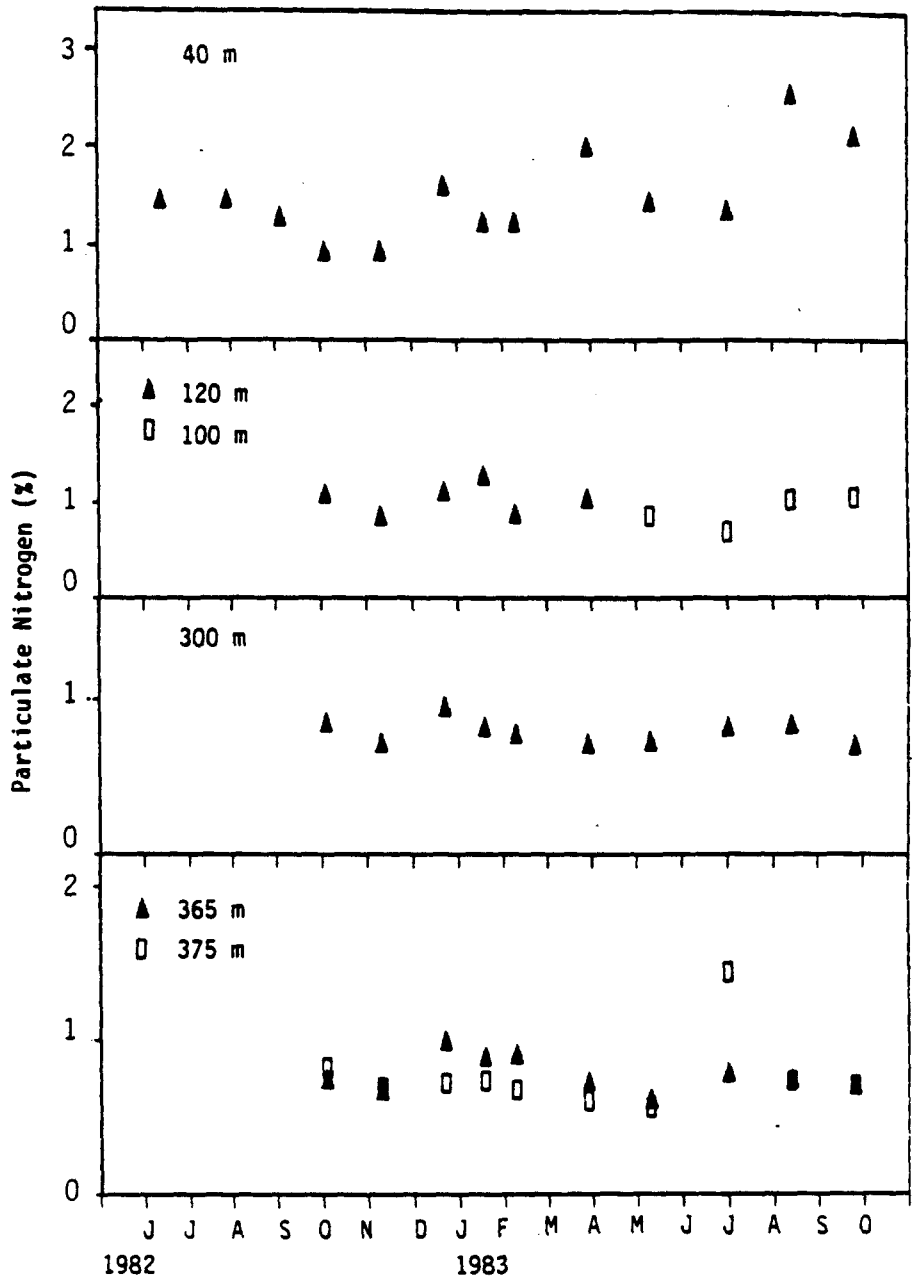

Fig. 4.3. PN content (%) of the settling particulates at various depths.

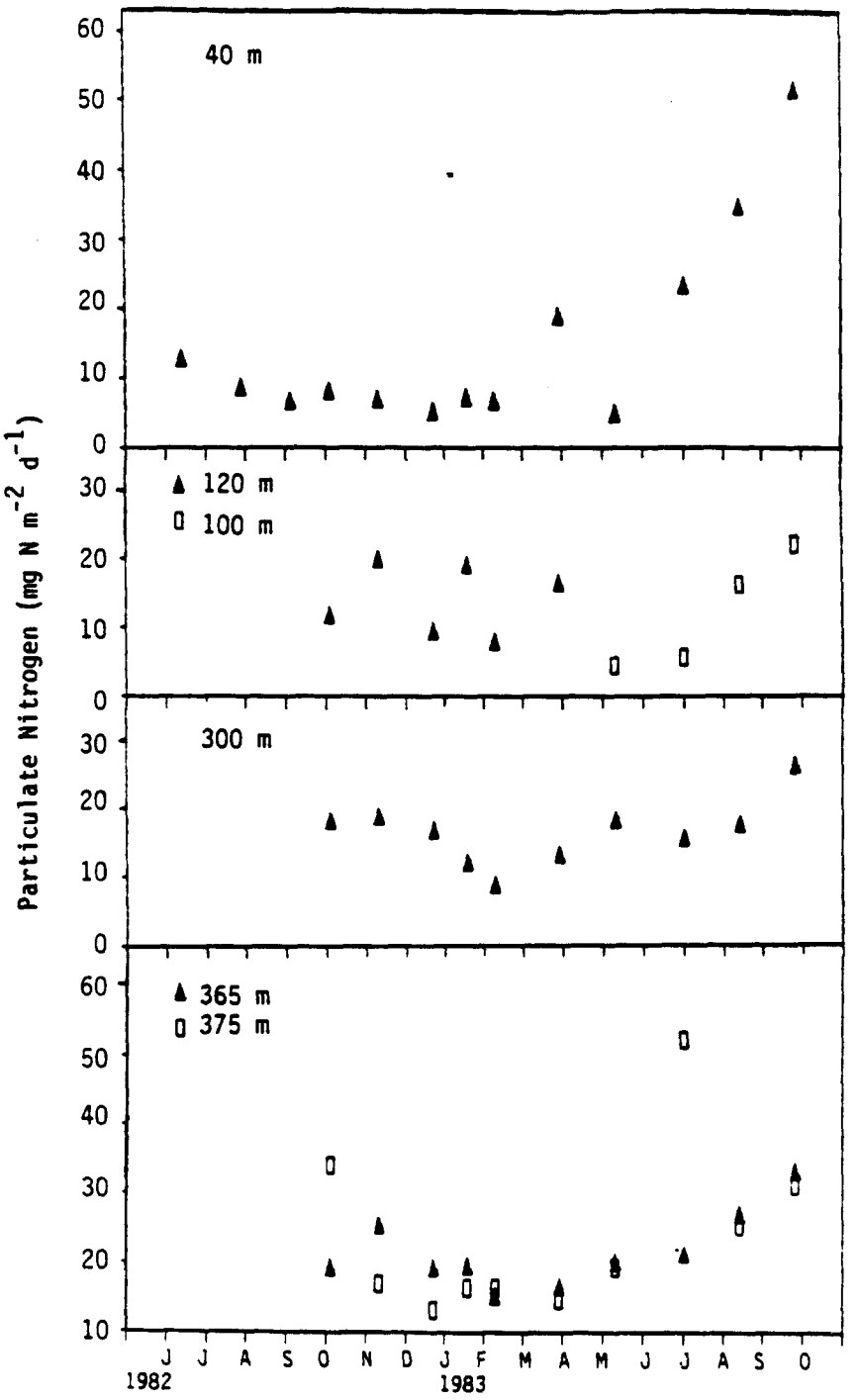

Fig. 4.4. Settling flux of PN (mg m^{-2} d^{-1}) at various depths.

particulate matter is significantly lower in the deeper layers than at the shallower depths.

The settling fluxes of PN were low in the winter period (about 10 mg N m^{-2} d^{-1}), but increased to 22 mg N m^{-2} d^{-1} in spring (March to May 1983), and then remained constant until the end of the sampling period. The annual average settling flux of total particulate nitrogen was 16.2, 12.6 and 100.8 mg N m^{-2} d^{-1} at depths of 40 m, 120 m and 375 m, respectively.

C/N Ratio

Mole ratios of POC and PN in the settling particulates through the sampling period are shown in Fig. 4.5. At 40 m depth, the particulate C/N ratio was 10-11 from June to August, increasing to >12 in October. Values decreased to 8 in November 1982, but increased again to 10-11 in January 1983. After January the C/N ratio decreased dramatically to reach minimum values of 5-6.5 during the sampling period of 30 January-9 April 1983, after which C/N ratios again increased. The C/N ratios of the settling particulates in the deep layers more or less follow the trend described at the 40 m depth horizon, but with smaller seasonal variability. In deep water the C/N ratios gradually decreased from more than 12 in the low primary productivity season to around 9 at

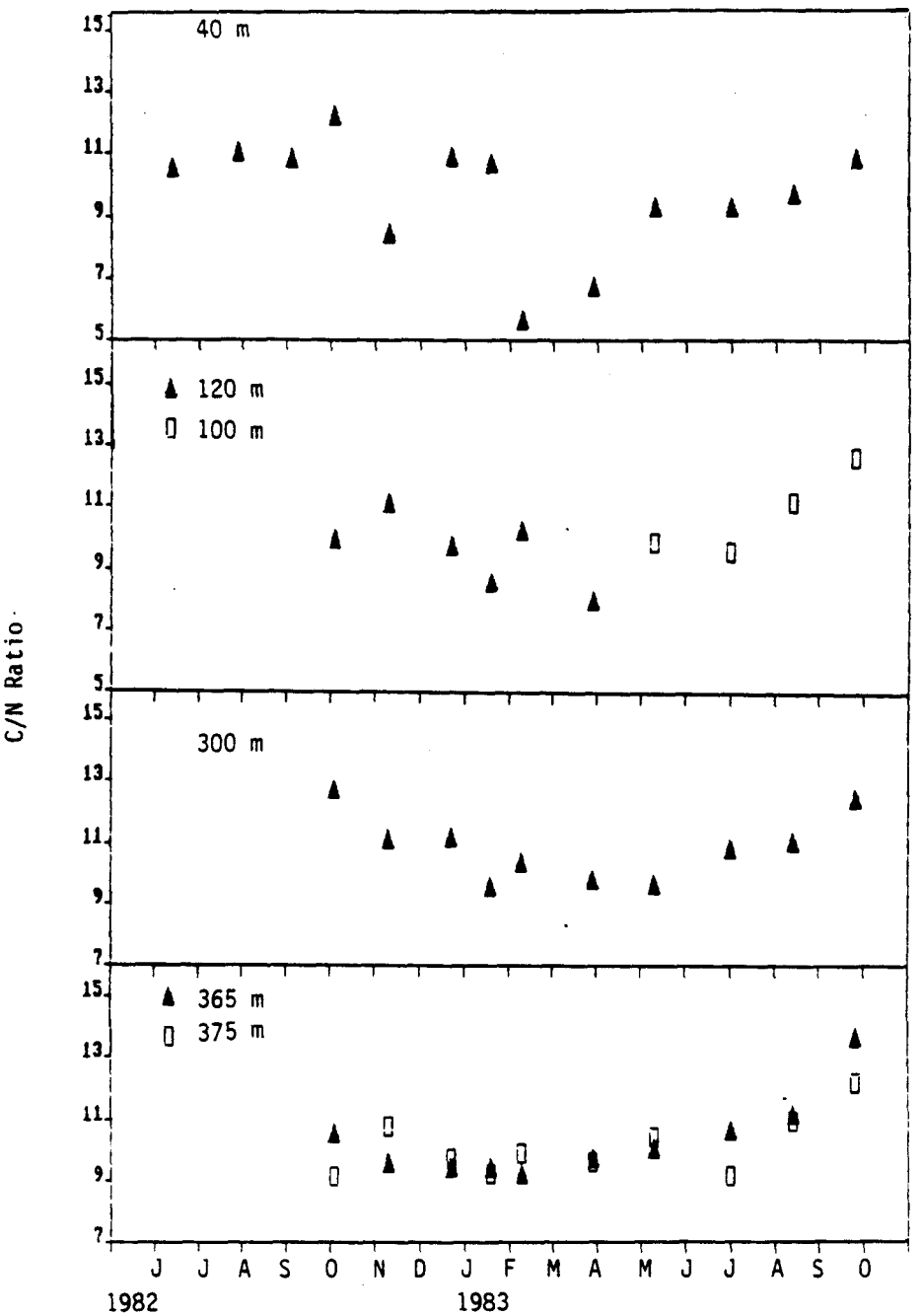

Fig. 4.5. C/N mole ratio in settling particulates at various depths.

375 m depth during the March to April spring bloom period.

Particulate Biogenic Silica

Concentrations and vertical fluxes of particulate biogenic silica are shown in Figs. 4.6 and 4.7. A nearly tenfold change in particulate biogenic Si concentration was observed during the total sampling period; the overall range was 3-22%. An increase of particulate biogenic silica concentration was observed from August (5%) to September (12%) 1982, and relatively small concentrations (3-4%) were maintained through February 1983. During March-April 1983, there was a sudden increase to more than 20% of the total particulate dry weight. After spring, concentrations decreased gradually to reach a local minimum (about 8%) around July 1983, slightly increased again in August (to 11%), and then decreased. Minimum values were observed in February 1983. At the 375 m depth horizon, concentration of biogenic Si in settling particulates was 5 to 7% with a minimum of 3.9% in February 1983 and a maximum of 11.3% in the March-April 1983 sampling period. The variability of particulate biogenic Si concentration was less at the deeper layers compared with the 40 m horizon.

Vertical fluxes of particulate biogenic Si at 40 m

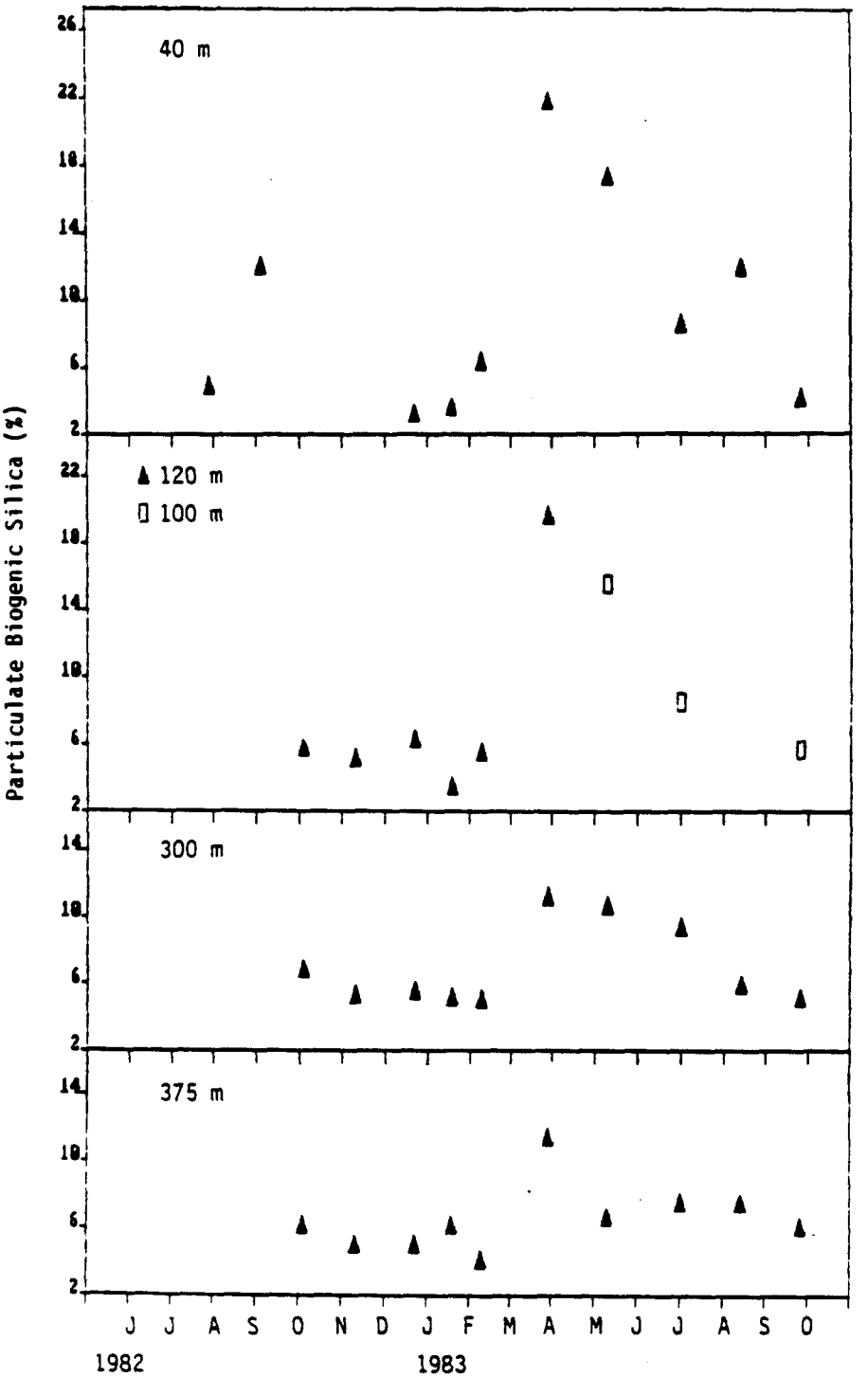

Fig. 4.6. Particulate biogenic Si content (%) of the settling particulates at various depths.

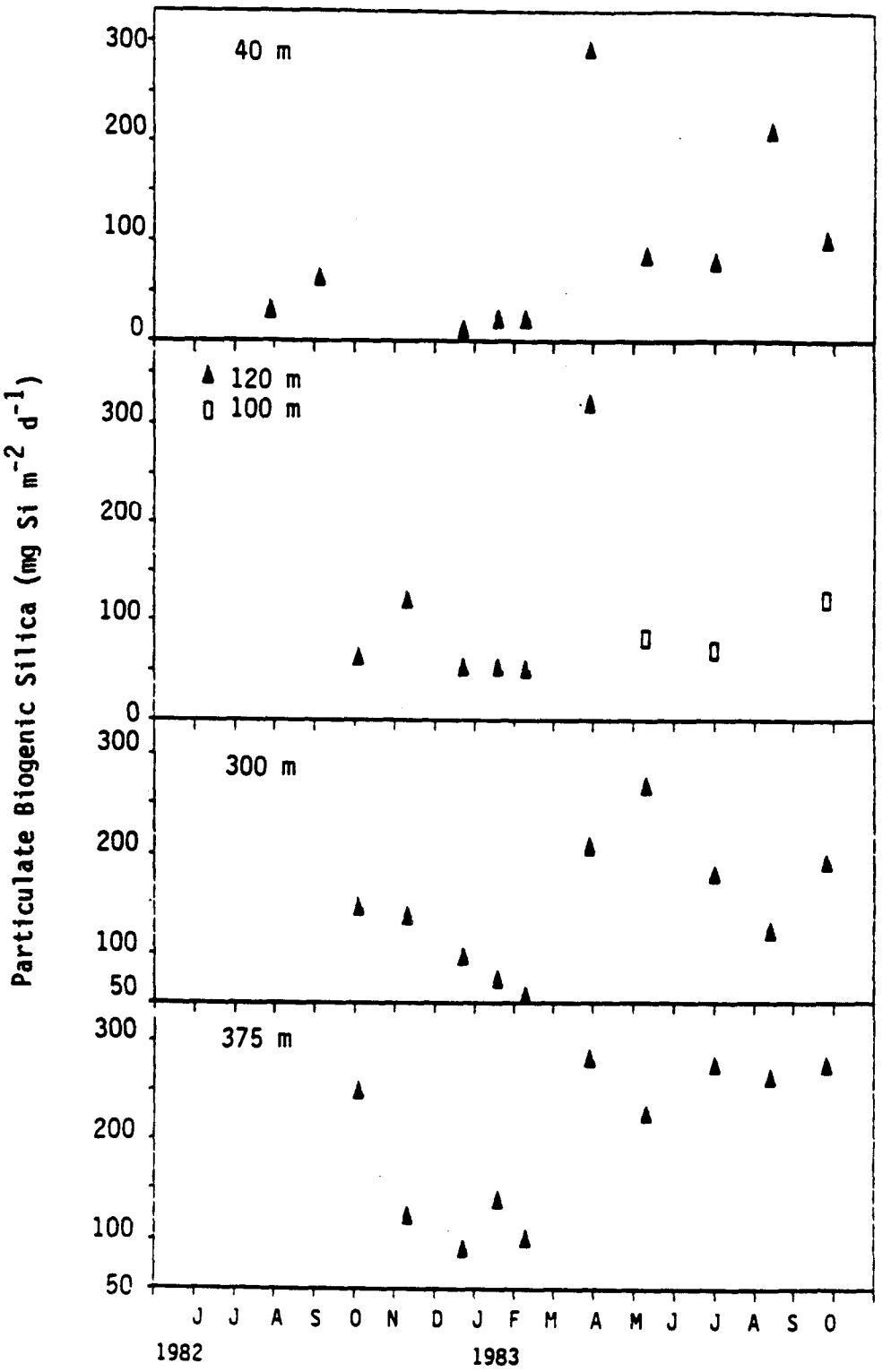

Fig. 4.7. Settling flux of biogenic Si (mg m^{-2} d^{-1}) at various depths.

depth ranged from 9 to 290 mg Si m^{-2} d^{-1}, with a minimum during December 1982-January 1983 and a maximum during the March-April 1983 sampling period. A smaller second maximum was also observed in early fall. At 375 m depth - just 5 m above the bottom - settling rates of biogenic Si ranged from 87 to 278 mg Si m^{-2} d^{-1} with a minimum in December 1982-January 1983 and a maximum in March-April 1983. Seasonal variability is significantly reduced at depth.

$\delta^{13}C$ of Settling Particulate Organic Carbon

Stable carbon isotope ratios for organic matter were obtained for selected sediment trap samples, major terrestrial plants from around the Boca de Quadra fjord, and for bottom sediments collected at BQ9G (Table 4.1). Most samples were collected in 1983. POC at 40 m depth was isotopically heavier in the spring-summer period (13 March-7 June 1983) than in the fall-winter period (18 October-1 December 1982 and 2 September-18 October 1983). This pattern, although less pronounced, was also observed at 375 m depth. Particulate sediment at shallower depths was usually isotopically heavier than was material in deep waters, especially through the spring-summer period. The $\delta^{13}C$ values were -19.7 to -19.6 (40 m) and -21.5 to -21.4 $^{o}/_{oo}$ (375 m) in the spring-summer period, and -21.4

Table 4.1. $\delta^{13}C$ values in various components.

Settling particulates				
Date	3/13 - 4/19	4/11-6/7	9/2-10/18	*10/18-12/1
Depth (m)				
40	-19.7 ± 0.3	-19.6 ± 0.2		-21.4 ± 0.2
120			-23.0 ± 0.2	
375	-21.5 ± 0.4	-21.4 ± 0.3	-22.9 ± 0.2	-21.5 ± 0.0
Surface bottom sediments			-21.2 to -22.6	
Western hemlock (*Picea sitchensis*)			-29.2 ± 0.8	
Sitka spruce (*Tsuga heterophylla*)			-28.0 ± 0.7	

* samples were taken in 1982.

(40 m) and -21.5 to -23.0 °/oo (375 m) in the fall-winter period. The $\delta^{13}C$ of bottom surface sediments was -21.2 to -22.6 °/oo, very close to the $\delta^{13}C$ of particulates collected in the trap at 375 m depth.

The $\delta^{13}C$ values obtained for surface sediments from the central basin (Station BQ9G) fall within the range reported for the southcentral Alaska sediments by Peters *et al.* (1978). Needles and twigs (green tissue) of Sitka spruce and western hemlock, which locally dominate the terrestrial vegetation (Sugai, 1985), had $\delta^{13}C$ values of -29.2 and -28.0 °/oo, respectively. These values are well within the ranges reported for C-3 plants (higher land plants) by Fry and Sherr (1984).

Particulate Mn

The concentrations of Mn in settling particulates and settling fluxes of Mn at several depths are shown in Fig. 4.8. Particulate Mn concentrations obtained at the 40 m depth horizon show a pronounced seasonal pattern: lower values (175-183 ppm) in the spring-summer period (13 March-9 April and 11 April-7 June 1983) and higher values (260-618 ppm) in the fall-winter period (2 September-18 October 1983 and 18 October-1 December 1982). In general, particulate Mn concentrations increase with depth. Down to 300 m depth, Mn

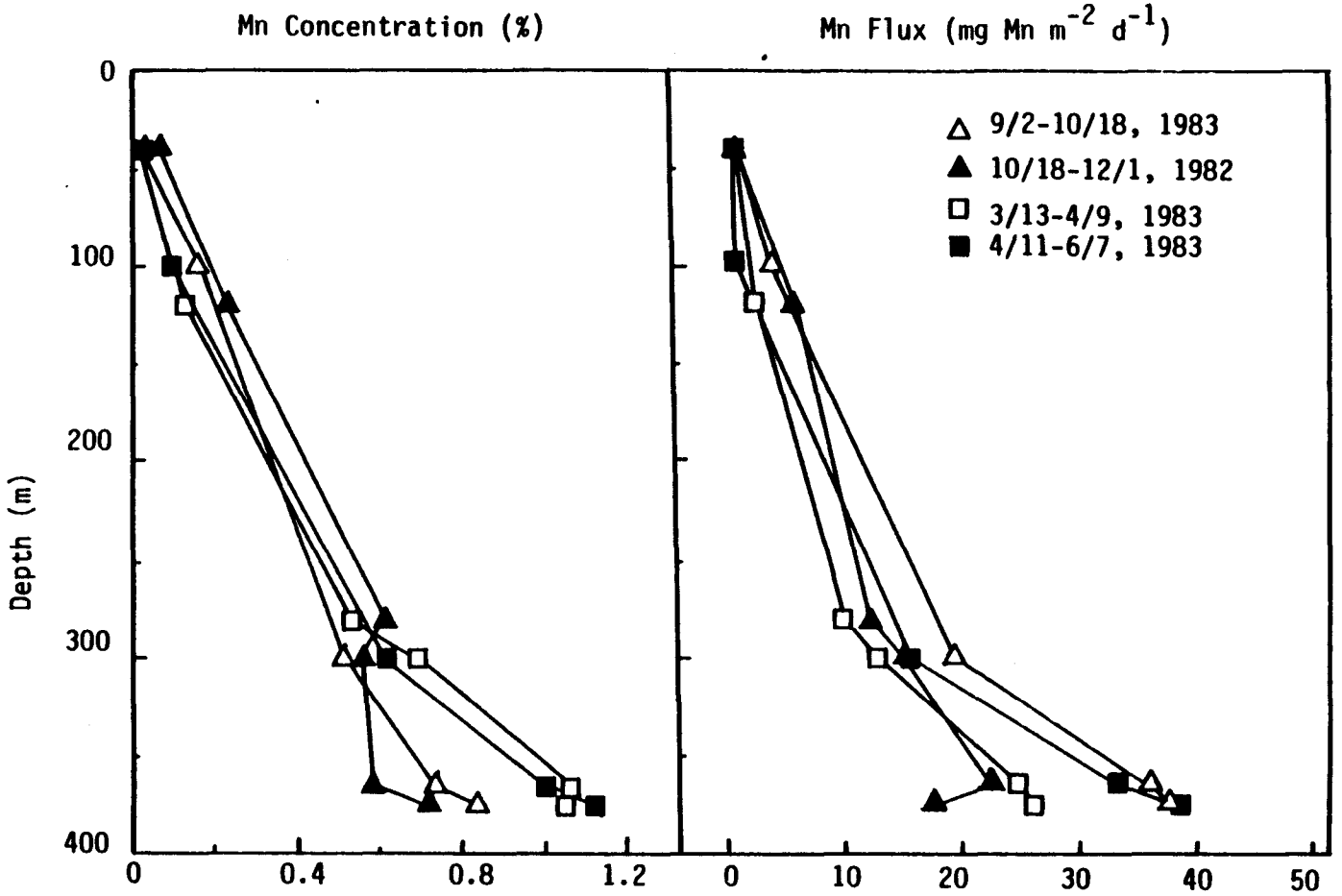

Fig. 4.8. The content (%) and flux (mg m^{-2} d^{-1}) of particulate Mn at various depths.

concentrations in the fall-winter period are higher than those in the spring-summer period. This trend is reversed, however, at depths below 300 m.

Settling fluxes of particulate Mn at 40 m depth ranged from 0.25-0.65 and 0.09-0.24 mg Mn m^{-2} d^{-1} in the fall-winter and spring-summer periods, respectively. The same trend was observed at 120 m depth, where Mn fluxes were 3.4-5.4 and 0.5-2.0 mg Mn m^{-2} d^{-1} in the fall-winter and spring-summer periods, respectively. Mn settling fluxes were 12-20 mg Mn m^{-2} d^{-1} at 300 m depth, but almost doubled to 17-40 mg Mn m^{-2} d^{-1} at 375 m. Since Mn concentrations of the bulk SPM are around 1%, particulate Mn settling fluxes at depth are essentially governed by bulk SPM fluxes. Therefore, seasonality of Mn fluxes is not apparent in Fig. 4.8.

Particulate Fe

Concentrations of Fe in settling particulates and the settling fluxes of Fe at various depths are shown in Fig. 4.9. Fe concentrations in particulate sediment collected at 40 m depth ranged from 1.4-1.6% and 0.8-1.1% in the fall-winter (2 September-18 October 1983 and 18 October-1 December 1982) and in the spring-summer periods (11 March-7 June 1983), respectively. Particulate Fe concentrations gradually increased with depth in the

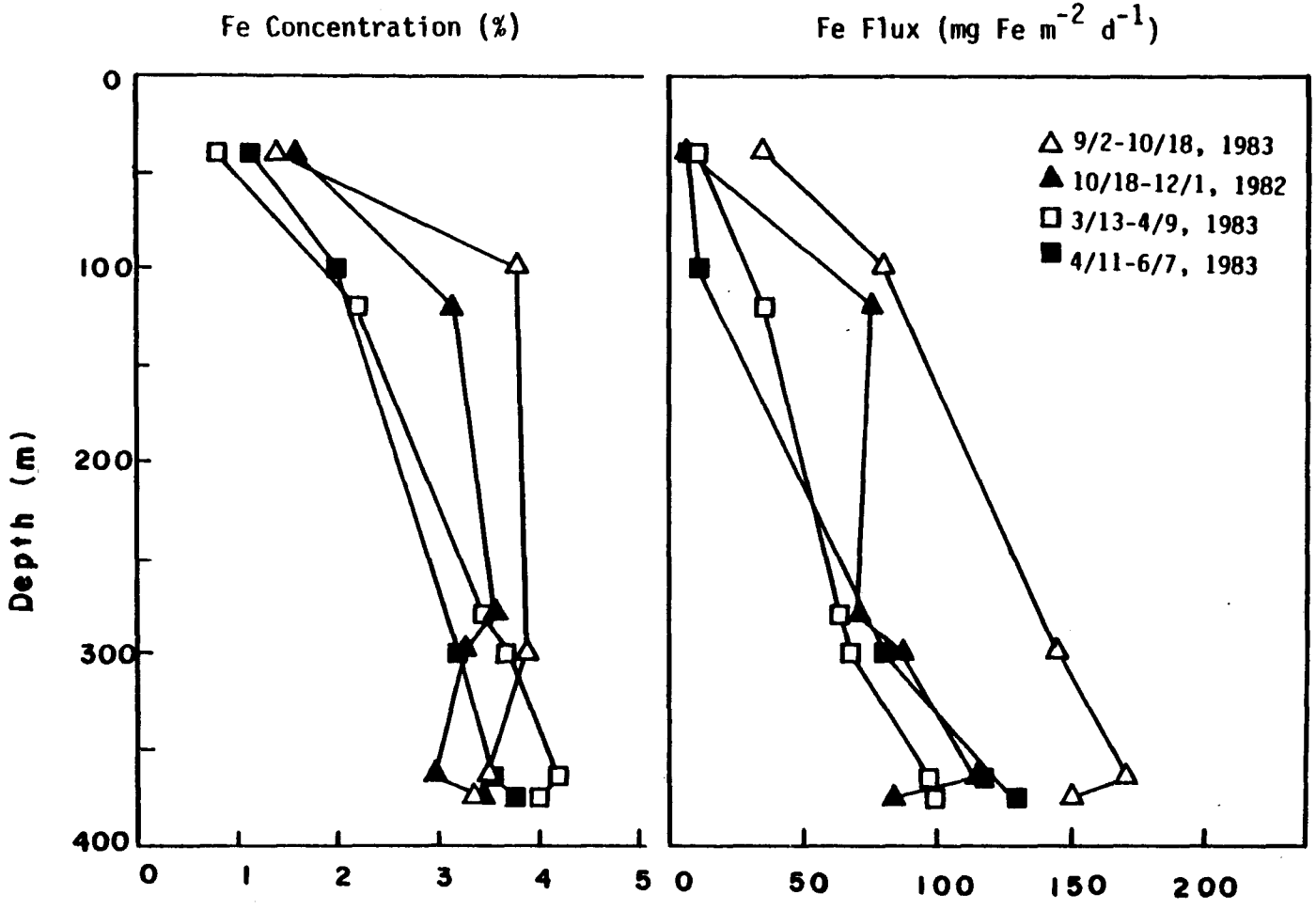

Fig. 4.9. The content (%) and flux (mg m^{-2} d^{-1}) of particulate Fe at various depths.

spring-summer period, but values were nearly constant below 100 or 120 m depth in the fall-winter period. Fe concentrations were 3.14-3.78 and 1.97-2.18% at 120 m, and 3.35-3.44 and 3.76-4.01% at 375 m depth in the fall-winter and spring-summer periods, respectively. Fe concentrations were higher in the fall-winter period than during the spring-summer period above the 300 m depth horizon, but this trend was reversed below 300 m depth.

In general, Fe settling fluxes increased with depth, and the gradient of Fe flux with depth was smaller in the spring-summer period than it was in the fall-winter period. An increase of particulate Fe was seen from 40 m depth to 100 or 120 m depth in the fall-winter period. Settling fluxes of Fe at 40 m depth ranged from 6.35-34.7 and from 6.03-10.63 mg Fe m^{-2} d^{-1} in the fall-winter and spring-summer periods, respectively. Fe fluxes at 120 m depth were 75.4-79.8 during the fall-winter and 10.43-35.2 during the spring-summer. At 375 m, the fluxes were 84 to 150 and 99-129 mg Fe m^{-2} d^{-1} in the fall-winter and spring-summer periods, respectively.

Mn/Al and Fe/Al Ratios in the Settling Particulates

Weight ratios of Mn/Al and Fe/Al in the settling particulates are shown in Fig. 4.10. Mn/Al ratios are low in settling particulates at 40 m depth: 0.009-0.012

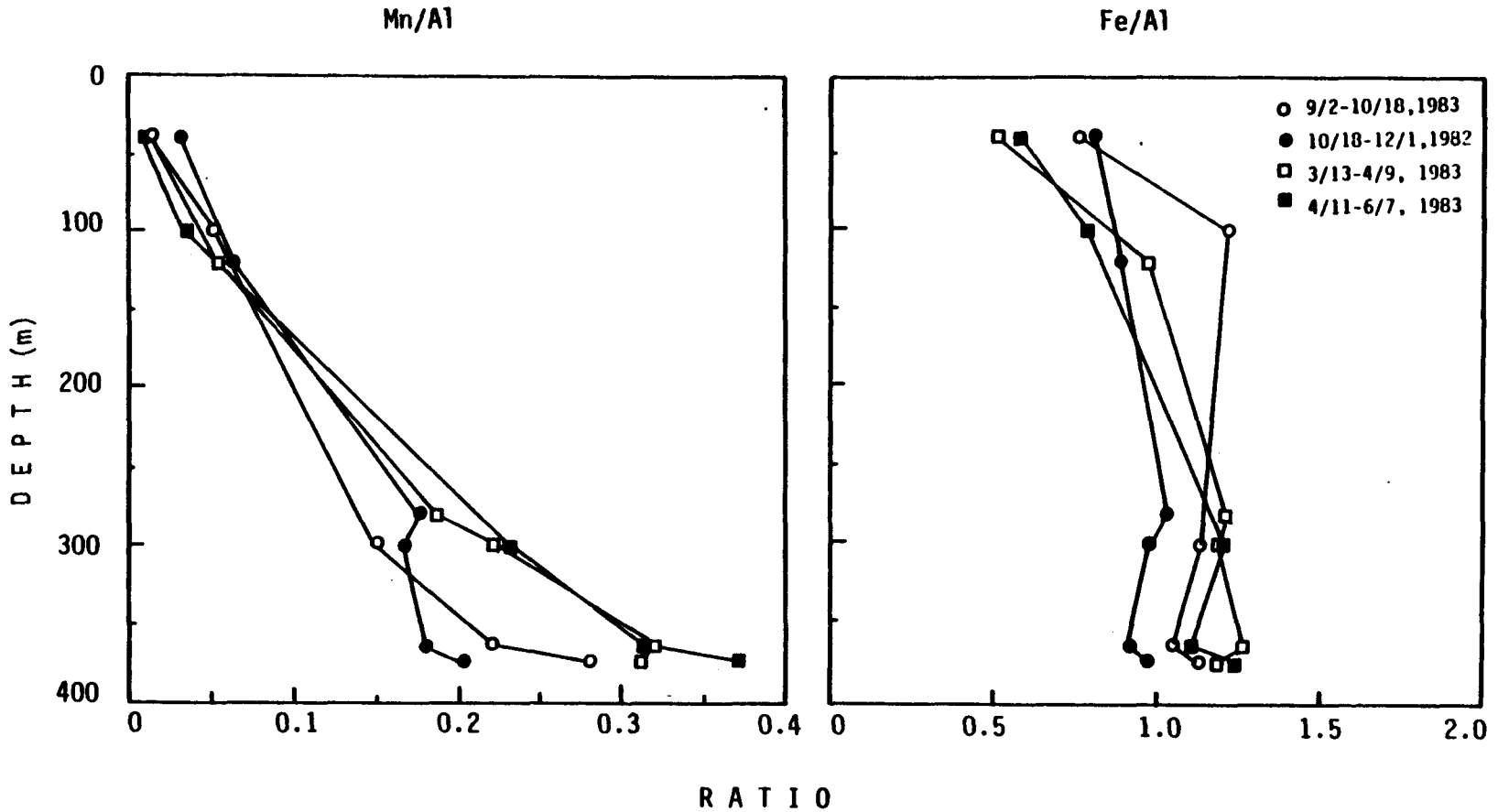

Fig. 4.10. Mn/Al and Fe/Al ratios by weight in the settling particulate matter.

in summer and 0.014-0.032 in winter, similar to values (0.016-0.023) previously reported for the Keta River mouth (Robb, 1981). This reinforces the idea that riverine particulates reach the central basin of Boca de Quadra as noted previously. The Mn/Al ratios increased with depth, especially in summer. Fe/Al ratios essentially followed the trend of Fe concentration with depth (Fig. 4.10).

Scanning Electron Microscopic Observations

Several examples of particulate morphology are shown in Plates 4.1-4.2. All samples appeared to be composed entirely of phytoplankton detritus in the spring-summer period (Plate 4.1C and 4.1D). However, inorganic particles were frequently noticed in fall (October 1983) samples (Plate 4.1A and 4.1B). Biogenic fragments, intact cells, and fecal pellets were found throughout the water column and in bottom surface sediment during April-May 1983 (Plate. 4.2). Nearly intact cells and frustules of diatoms were dominant, with infrequent silicoflagellates present throughout the water column. Particle sizes ranged from 10 to 80 um in diameter. Pellets were observed which consisted mainly of diatom frustules. These were spherical or elongate, ranging in diameter from 40 to 60 and 160 to 650 um

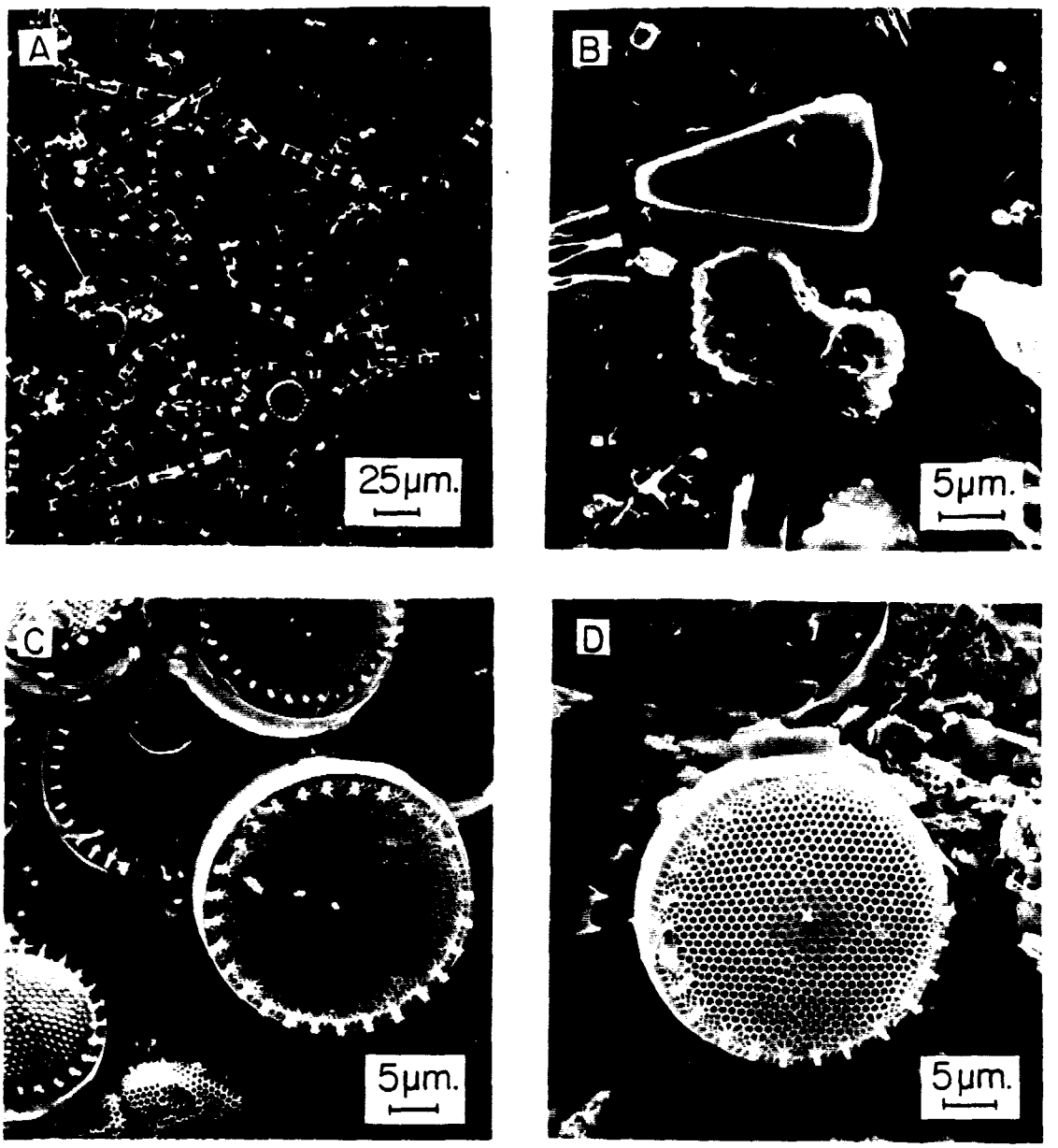

Plate 4.1. Scanning electron micrographs of SPM and bottom sediments.
A. 20 m, October 1983, BQ9.
B. 20 m, October 1983, BQ9.
C. 30 m, April 1983, BQ9.
D. 286 m (surface sediments), May 1983, BQ5.

Plate 4.2. Scanning electron micrographs of settling particulates.
A. 365 m, April 1983, BQ9G.
B. 280 m, April 1983, BQ9G.
C. 375 m, April 1983, BQ9G.
D. 365 m, April 1983, BQ9G.

(longest axis), respectively.

Mn and Fe rich particulates are shown in Plates 4.3 -4.4. Fe-rich particulates were usually discrete. However, Mn-rich particulates usually also contained Fe and were associated with fragments of diatom cells. The size of Fe particles ranged from about 2 to 10 um, whereas the Mn-enriched particulates were around 5 um in size.

DISCUSSION

Temporal Variations in the Concentration and Settling Flux of Particulate Organic C, N, Biogenic Si, Mn and Fe

The sediment trap array was deployed for 1-2 month periods, and the average values for each sampling interval are reported here. Thus variations on shorter time scales than the sampling period were not observed, although short-term variations are expected to be large in this type of estuary (*e.g.*, Baker *et al.*, 1986).

In general, the variability of POC and PN concentrations (Figs. 4.1 and 4.3) in the settling particulates was considerably less in deeper layers than in those collected at 40 m throughout the sampling period. The vertical fluxes of POC and PN (Figs. 4.2 and 4.4) significantly increased with depth, which is the

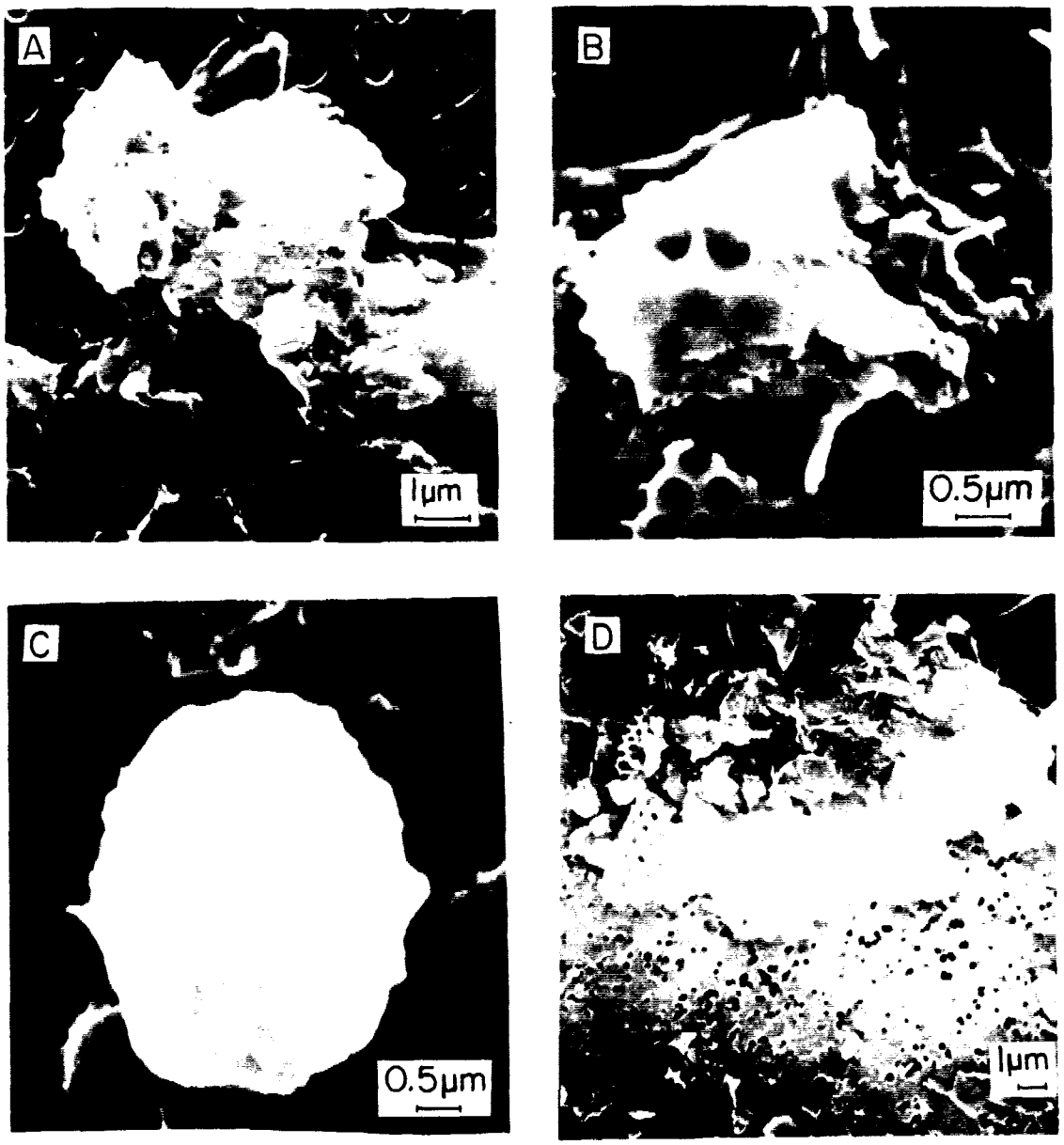

Plate 4.3. Manganese and iron enriched particles subjected to SEM-EDS.
A. 100 m, October 1983, Mn/Al = 0.38, Fe/Al = 1.75.
B. 300 m, October 1983, Mn/Al = 0.63, Fe/Al = 1.89.
C. 300 m, October 1983, Mn/Al = 0.47, Fe/Al = 1.99.
D. 375 m, October 1983, Mn/Al = 0.61, Fe/Al = 0.82.

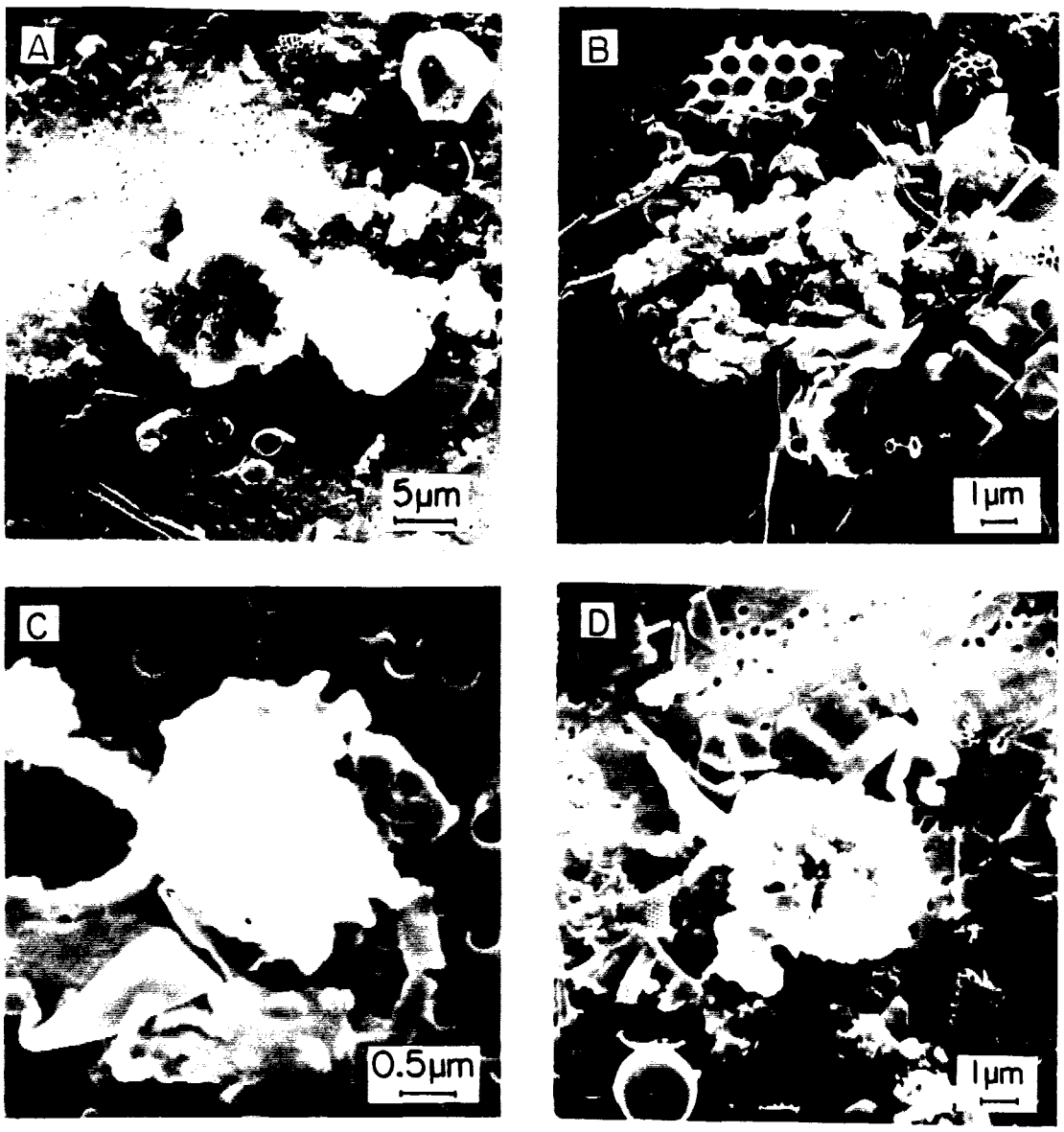

Plate 4.4. Iron enriched particles subjected to SEM-EDS.
A. 50 m, April 1983, Fe/Al = 17.41.
B. 40 m, October 1983, Fe/Al = 15.66.
C. 347 m, April 1983, Fe/Al = 0.13.
D. 375 m, October 1983, Fe/Al = 11.46.

reverse of the trend observed for the distribution of POC concentrations (Fig. 3.11 in Chapter 3). This is due to the increase of bulk SPM settling fluxes with depth in the central basin of Boca de Quadra, as described in Chapter 3. The small temporal variability in POC flux at 40 m depth was magnified in deeper water, so that seasonal changes in the surface layer generally were more pronounced at depth in the basin. However, there were some deviations from this general trend, such as in November 1982 when the vertical flux of POC at 40 m decreased while that at 120 m increased. Such discrepancies may be due to additional input from the adjacent basins through the bottom nepheloid layer, as discussed in Chapter 3.

Minimum C/N values of settling particulates (Fig. 4.5) are very close to those determined for the principal diatom species which are responsible for the spring bloom of phytoplankton (VTN, 1982; Harrison *et al.*, 1977). The C/N ratio of diatoms was 4.6-7.7 in the euphotic zone of the study area during the bloom period (Burrell, 1983b).

The distribution of biogenic silica concentrations in settling particles (Fig. 4.11) in deep water below 40 m followed the trend observed at the 40 m depth horizon in the summer (March-July 1983). However, through the

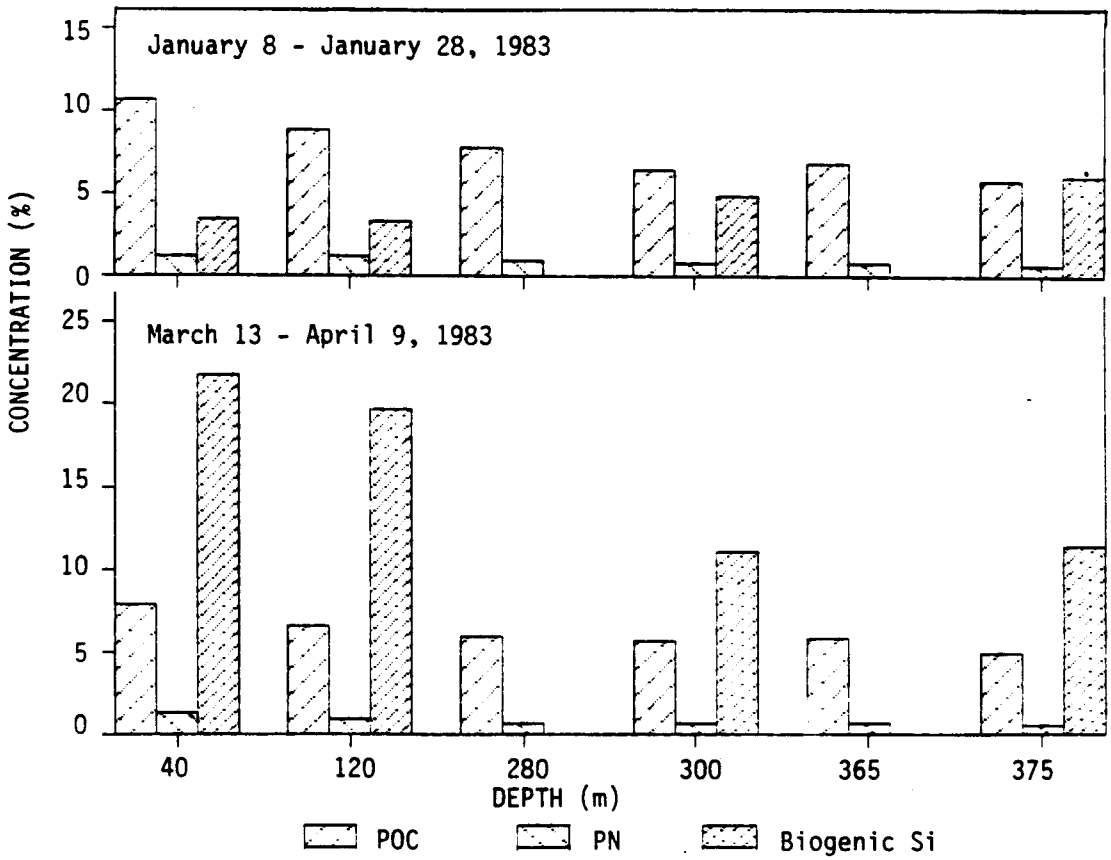

Fig. 4.11. Composition of biogenic matter during January 8-28, and March 13-April 9, 1983.

winter period (October 1982 to early March 1983) settling particulates in deeper layers had higher concentrations than those at shallower depths because biogenic silica production is nearly halted during this period. This trend may provide additional evidence of resuspension within the basin. The extreme seasonality is due to the limited period of diatom growth in this area. Because of the general increase in the vertical flux of bulk sediments with depth described in the previous chapter, fluxes of biogenic silica (Fig. 4.7) in the shallower depths were usually smaller than those in deeper layers. However, this trend was not apparent during the March-April 1983 period, when fluxes of biogenic silica were relatively homogeneous throughout the entire water column due to the intense production of biogenic silica in the surface layer.

Mn concentrations in the particulate sediment (Fig. 4.8) were greater in the spring-summer period than in the fall-winter period because the diagenetic efflux of dissolved Mn from the sediments increased following the sedimentation of fresh organic matter in the spring-summer season (see Chapter 5). The waters below 300 m depth appear to be strongly affected by the benthic regime in this period. It was observed that settling particulates had a considerably higher Mn concentration

than had the bottom surface sediment. It should be emphasized that the concentration of an element is determined by its concentration relative to the rest of the particulate constituents. Therefore, concentration changes may be due to changes in the other constituents, rather than the specific element under consideration.

The qualitative SEM observations (Plates 4.1-4.2) show that a substantial downward flux during the spring-early summer period can be attributed to consolidated fecal pellets, intact cells, and aggregates of phytoplankton skeletons. One of the reasons why a significant number of intact cells was found throughout the entire water column and surface sediment may be because there is some evidence showing that zooplankton populations do not start to increase until later, after the phytoplankton bloom (VTN, 1982). The VTN data are incomplete for regions below 25 m depth, however.

Sources of Particulate Organic Matter

The strong seasonality in the rainfall, river runoff patterns, and *in situ* primary productivity (Figs. 1.2 and 1.4) suggests that the flux and composition of POC in surface waters should also exhibit distinct seasonal patterns. High concentrations of inorganic particulates in the surface layer of the central basin during the fall

high runoff period show that there is an increased influx of terrestrial POC (Plates 4.1A and 4.1B), while in spring SPM was almost entirely composed of diatoms (Plates 4.1C and 4.1D). A more quantitative estimate of the terrestrial contribution to the settling fluxes of POC in the central basin of Boca de Quadra was attempted using C/N ratios and $\delta^{13}C$ values of particulate organic matter in conjunction with the estimated riverine POC influx data.

C/N Ratios

The biological origin of organic detritus may often be inferred from its elemental composition. The mean C/N ratio of open ocean biogenic particulates is 6.6 (Redfield *et al.*, 1963), whereas in land-derived organic debris this ratio is usually larger than 12 (Meyers *et al.*, 1984). Differences in the C/N ratios of aquatic and terrigenous organic matter reflect the presence of nitrogen-poor cellulose and lignin in land plants (Stuermer *et al.*, 1978; Hedges *et al.*, 1984). The C/N ratios of the sediment trap material collected at 40 m depth were as low as 5.5-6.5 during 30 January to 9 April 1983 and as high as 12.2 during 22 September-17 October 1982 (Fig. 4.5). As a first-order interpretation, the former observation indicates the dominance of aquatic

organic matter, and the latter suggests the presence of a greater amount of terrestrial organic matter.

However, there is controversy concerning the factors which control the C/N ratio of bulk organic matter. Preferential removal of nitrogenous organic compounds in the water column has been reported by Marinucci *et al.* (1983) and Prahl *et al.* (1980). (However, Prahl *et al.* have also shown a decrease in C/N ratios of the sediment organic matter with depth below the sediment-water interface, which appears to contradict their arguments.) Stuermer *et al.* (1978) show that C/N ratios of organic matter are not altered during diagenesis in various marine sediments. In Boca de Quadra, there are large differences between the C/N ratios of settling particles and the surface sediments, suggesting that settling particulates are relatively less affected by decomposition. Hence, it is believed that in this environment the C/N ratios of settling organic matter can be used as a provenance indicator for the settling particulates.

Autochthonous and River Input of POC

Phytoplankton primary production increases sharply in March and April but is relatively low during the rest of the summer except for a small increase in late summer

(Chapter 1). Since Boca de Quadra is very deep and has steep-sided walls, particulate organic matter production by the littoral plant community is insignificant compared with phytoplankton production (Burrell, 1983b).

In general, organic carbon constitutes a larger fraction of total riverine SPM in the fall than during the other seasons (Note that SPM load and POC content were separately determined. Original data from Burrell, 1983b). POC content in the riverine SPM ranges widely from 2 to more than 20% by weight and reaches 100% in the SPM collected in the Keta River during August 1982. The mean monthly flux of POC in the fall season is large: as much as 10 times that in winter and about 4 times that in the spring and summer season due to the combined effects of high river runoff and higher POC content.

River runoff is capable of contributing substantially to the fall POC flux, but only a small amount to the spring and summer flux because of the seasonality of phytoplankton productivity. The seasonal supply of riverine POC from the Keta and Marten Rivers was estimated from daily flow rate records for 1980 and monthly determinations of POC content during 1981-1982 by Burrell (1983b). By this method of computation, 1.2-4.8 x 10^8 g of POC was estimated to be discharged annually

into Boca de Quadra. Spread uniformly over the upper reaches of Boca de Quadra (above the Kite Island sill), this riverine POC influx could support fluxes of 3-14 and 5-20 g C m^{-2} yr^{-1} at 40 m and 120 m, respectively, taking into account the respective horizontal areas at each depth (Chapter 3). Also, this riverine POC would supply 7-26 g C m^{-2} yr^{-1} at the basin floor given the likely primary sedimentation area (Chapter 3). A comparison of the computed river contribution with direct measurements made at several depths is summarized in Table 4.2. Riverine POC input appears to make a greater contribution to the POC settling flux in the fall than that in spring. The mean annual, terrestrial POC influx may contribute around 7-30% of the total POC rain at the 40 m depth horizon in the central basin of Boca de Quadra.

$\delta^{13}C$ of Particulate Organic Matter

Stable isotope ratios of carbon are different for C-3 plants, phytoplankton and C-4 plants because of the different photosynthetic pathways (O'Leary, 1981). The resulting isotopic compositions are often preserved in organic detritus with little change during subsequent chemical and metabolic processes in the natural environment (Fry and Sherr, 1984).

A two end-member mixing model (Eq. 4.2) can be used

Table 4.2. Computed riverine contributions to the total POC flux at several depths within the central basin.

(a). Monthly average

Depth (m)	Riverine Flux' (mg C m^{-2} d^{-1})		Measured Flux (mg C m^{-2} d^{-1})		River Contribution (%)	
	September	April	September	April	September	April
40	123	31	80* - 473^	125	26* - 100^	24
120	174	44	74* - 238^	107	43* - 74^	41
375	229	57	268* - 329^	121	70* - 85^	57

* 9/22 - 10/17, 1982

^ 9/2 - 10/18, 1983

(b). Annual average

Depth (m)	Riverine Flux' (g C m^{-2} yr^{-1})	Measured Flux (g C m^{-2} yr^{-1})	River Contribution (%)
40	3.6* - 14.4^	49.2	7* - 30^
120	4.8* - 20.4^	42.0	12* - 49^
375	7.2* - 26.4^	79.2	9* - 36^

* using a minimum of 1.2 x10^8 moles of POC

^ using a maximum of 4.8 x 10^8 moles of POC

' data from Burrell (1983b)

to calculate the relative importance of the marine and terrestrial sources of organic matter. $\delta^{13}C$ values of marine phytoplankton at latitudes similar to Boca de Quadra are reported to be -20.0 ± 1.6 °/oo in Hood Canal (Simenstad and Wissmar, 1985) and -21.3 ± 1.1 °/oo off New England (Gearing *et al.*, 1984). Since the largest value of -19.6 °/oo was observed during the March-April sampling period, which is the primary phytoplankton bloom period, the -19 °/oo value is chosen here to represent marine organic matter. The $\delta^{13}C$ value of -28 °/oo obtained from the two dominant land plants (Sitka spruce and western hemlock) was chosen as the terrestrial end-member, because sampling of riverine particulates was not a part of this study.

$$\% \text{ Terrestrial POC} = \frac{(\delta^{13}C)s - (\delta^{13}C)m}{(\delta^{13}C)t - (\delta^{13}C)m} \times 100 \qquad (4.2)$$

The subscripts of s, m, t refer to sample, marine, and terrestrial, respectively. Results obtained by applying Eq. 4.2 suggest that the terrestrial POC contributes about 7% in spring-summer seasons and about 27% in the fall-winter period at 40 m depth (Table 4.3). These results suggest that *in situ* phytoplankton production is the most important source of organic matter in the central basin of Boca de Quadra.

Table 4.3. Computed fraction (%) of terrestrial POC in the settling particulates within the central basin.

Date	1983			1982
	3/13-4/19	4/11-6/7	9/2-10/11	10/18-12/1
Depth				
40 m	8	7	-	27
120 m	-	-	44	-
375 m	28	27	43	28

By correlating $^{13}C:^{12}C$ *versus* $^{15}N:^{14}N$, Peters *et al.* (1978) showed that the major factor controlling the $\delta^{13}C$ of organic matter in sediments is the input ratio of marine and terrestrial organic matter. However, a number of factors limit the accuracy of the quantitative $\delta^{13}C$ interpretation in terms of sources of organic matter. The exact $\delta^{13}C$ values used for the sources cannot be determined easily. Recently Cooper (1986) showed that not only may $\delta^{13}C$ value vary in the different parts of a plant but also among individuals of higher plant species. Isotopic changes due to heterotrophic metabolism during decompostion may also affect the results, since the $\delta^{13}C$ values of the residual fraction may increase as a result of kinetic isotope fractionation (Eadie and Jeffrey, 1973), or decrease due to the decarboxylation of amino acids and carbohydrates (summarized in Miller, 1980). Since occasional low C/N ratios of riverine particulates have been observed (Burrell, 1983b; possibly the result of freshwater planktonic detritus), the estimate of terrestrial organic matter input could be low. Overall, however, the results of the 2-end member model (Eq. 4.2) are fairly insensitive to small to moderate errors due to these factors.

Using more than one chemical tracer or method can help to resolve the complex sources of organic matter in

coastal environments, despite questions regarding the preservation of the source signals. All of the methods employed here favor the conclusion that terrestrial input of organic matter is significant in fall during the period of high runoff and heavy precipitation. However, the annual average contribution of terrestrial POC to the surface layer (40 m depth) would be, though still substantial, at most, 30% of the total settling POC flux. Similar observations and arguments - *i.e.*, that most POC is likely to have been produced and deposited *in situ* - were made for Hood Canal by Simenstad and Wissmar (1985) and for the St. Lawrence Estuary by Tan and Strain (1983).

Alteration of Settling Particles

One of the merits of measuring elemental fluxes is that it provides a direct means of estimating chemical changes (decomposition or dissolution, and authigenic production) as the particulates sink through the water column. Many studies have examined changes in elemental ratios of metals in marine SPM through the water column (*e.g.*, Lambert *et al.*, 1984). However, it should be noted that concentration ratios inherently reflect changes in the fractions of other constituents as well as in the specific elements of interest. Settling POC, PN,

particulate biogenic Si, and particulate Mn and Fe may be considered in terms of three mass flux fractions: primary, resuspension and alteration. Here "positive alteration" refers to the precipitation of dissolved phases onto settling particulates, while a "negative alteration" flux results from decomposition or dissolution. Al is generally assumed to be refractory during early diagenesis in the surface sediments (Mackin and Aller, 1984) and may thus be as a tracer for the resuspension flux (Chapter 3). Further, it is assumed that elements in surface sediments do not undergo appreciable diagenetic change when they are resuspended; a contention which seems to be justified by the short residence time of settling particulates in the water column. A working hypothesis for a three-component distribution system may then be constituted for the chemical element M:

$$T_z = P + R_z + A_z \qquad (4.3)$$

$$R_z = (Al_z - Al_P) \times (M/Al)_s \qquad (4.4)$$

where T_z is the total flux at depth z which is taken from the settling flux at depth z. P is the primary flux which is taken from the settling flux at 120 m or 100 m depth as discussed in Chapter 3. R_z is the resuspended

flux at depth z, which is calculated according to Eq. 4.4. A_z is the "alteration flux" integrated to depth z from the depth at which primary flux is taken. Al_z and Al_P are the Al fluxes at depth z, and the primary flux of Al, respectively. The subscript s refers to surface sediment. Surface sediment end-member concentrations are given in Appendix C. The results of the application of Eqs. 4.3 and 4.4 to POC, PN, biogenic Si, particulate Mn and Fe distributions are listed in Appendix C. In evaluating the results of this model, the nature of resuspension and microbial metabolism in the marine environment must be considered. Resuspended material is usually enriched in light and finer-sized material; this category includes organic matter. In addition, microbial activity is likely to be different at the sediment-water interface compared with in the water column. The alteration flux may also include any lateral transport.

The most interesting data set computed using this model was obtained during the 13 March-9 April 1983 sampling period, just before the onset of deep water renewal, and during the intense spring phytoplankton bloom (Fig. 4.12). The major features here are probably partly due to the reduced horizontal transport of SPM along the bottom of the fjord, but also to the availability of fresh organic matter.

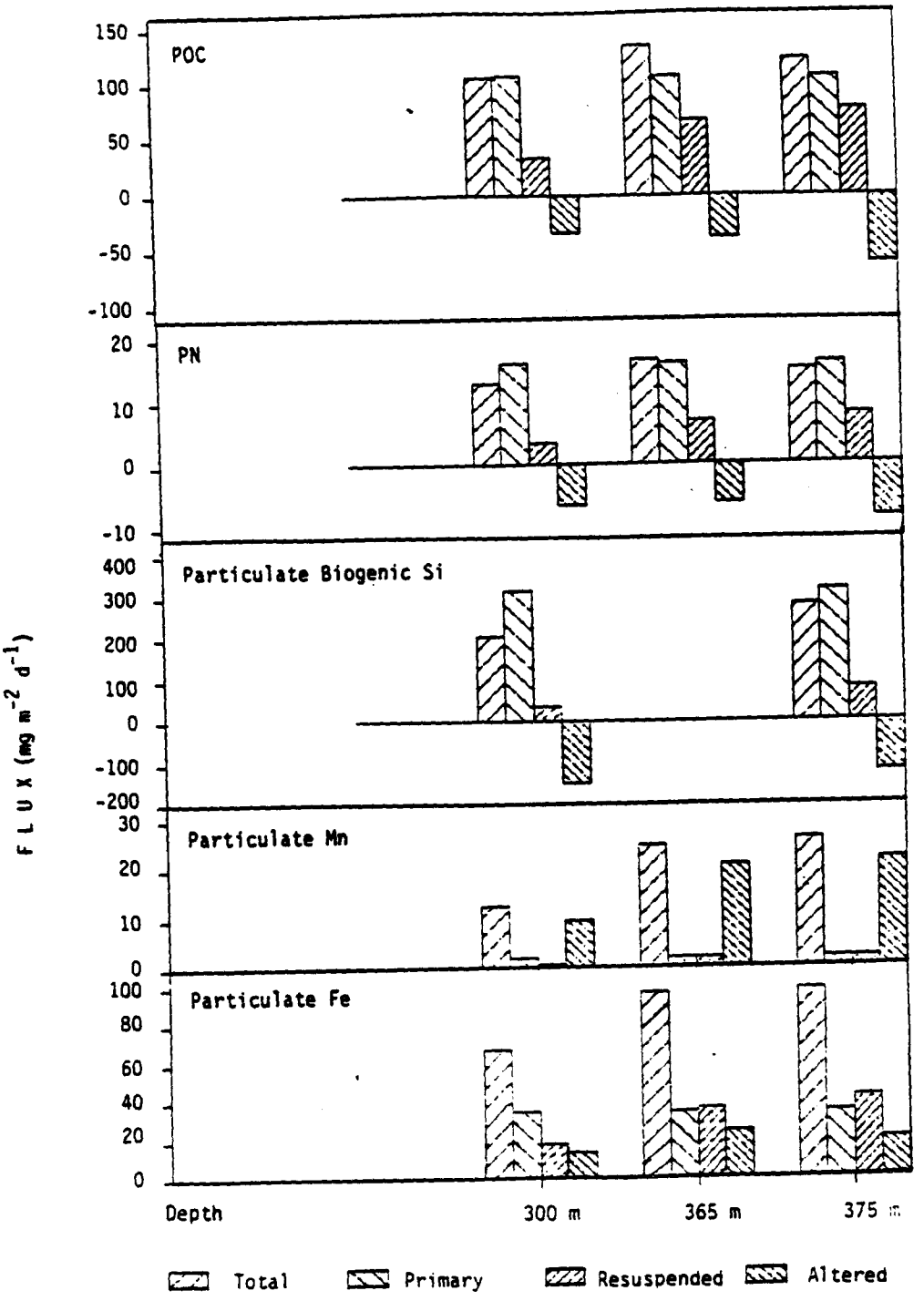

Fig. 4.12. The three components of settling particulates during the 13 March-9 April 1983 sampling period.

A significant amount of decomposition of POC and PN, and dissolution of biogenic Si is seen in Fig. 4.12. During the sampling period of 13 March to 9 April 1983, more than half of the total POC, PN and biogenic Si sinking between 100 or 120 m and 375 m depth is decomposed, which is in turn more than half of the primary flux at 120 m depth. However, substantially reduced decomposition of these components was observed during the rest of the sampling period. These factors are thought to be attributable mainly to the limited bloom period of phytoplankton in the spring such that the settling flux of fresh phytodetritus is substantially reduced during the rest of the year and subsequently reduces the decomposition rates. Overall annual decompositon rates are 10.2 $\pm$ 9.0 g C m^{-2} yr^{-1}, 1.5 $\pm$ 1.3 g N m^{-2} yr^{-1}, which are remarkably close to the values estimated in Chapter 5. It is not reasonable to directly compare these estimates with those in other environments where pelagic communities, and factors such as the temperature and depth, would greatly differ.

The rate of dissolution of biogenic Si in the water column is dependent upon the dissolved silicate concentration and water temperature. Thus the dissolution rate of biogenic Si usually will be higher in surface waters than in deep waters (Hurd, 1973; Lawson *et*

al., 1978). Direct measurements of dissolution rates have been reported to be 8.43-14.05 g Si m^{-2} yr^{-1} in surface layers off northeast Africa (Nelson and Goering, 1977) and 11.23-30.90 g Si m^{-2} yr^{-1} in the upper 100 m of the Antarctic Circumpolar Current zone (Nelson and Gordon, 1982). In the central basin of Boca de Quadra using the model given by Eq. 4.3, the dissolution rate of biogenic Si is estimated to be 0.08-53.65 g Si m^{-2} yr^{-1}, with an average of 16.01 $\pm$ 25.28 g Si m^{-2} yr^{-1} during the sampling period. These estimates fall within the range reported for elsewhere, and also agree well with the values estimated in Chapter 5.

Most of the settling flux of particulate Mn is attributable to a "positive alteration flux" (>80 %), which is probably due to authigenic formation of Mn oxides. Since the primary flux of particulate Mn is similar to the Mn accumulation rate in the sediment, this large positive alteration flux suggests that manganese oxide plays an important role in the early diagenesis of organic carbon in sediments. This recycling of Mn would also play a significant role in the trace metal chemistry of this region (Hunt, 1983). The authigenic Mn flux *i.e.*, the computed "positive alteration flux" of Eq. 4.3, varies from 12 to 34 mg Mn m^{-2} d^{-1}, with a maximum in the

period from 11 April to 7 June 1983 and minimum values during 18 October-1 December 1982. Higher POC fluxes seem to correspond to higher authigenic Mn fluxes. Migration of the redox boundary induced by variations in the primary productivity in overlying waters has been observed in Boca de Quadra (Sugai, 1986). The annual average authigenic flux at 375 m depth is 9.34 $\pm$ 3.85 g Mn m^{-2} yr^{-2}, which is about half of the predicted production of dissolved Mn (20.33-31.32 g Mn m^{-2} yr^{-1}) from the interstitial water profiles (Chapter 5; though the benthic flux may vary areally since only limited number of interstitial water profiles are available). However, these estimates seem very reasonable since the greatest precipitation of dissolved reduced Mn occurs right at the surface of the sediments (above the redox boundary) and decreases exponentially upwards into the water column.

The authigenic contribution to the settling flux of particulate Fe is much smaller than that for Mn due to the rapid oxidation of dissolved Fe in oxic waters (Murray and Gill, 1978). It comprises about 6 to 30% of the total flux, with a maximum values through the spring-summer period and a low in the fall-winter period. The annual average authigenic flux at 375 m depth is 6.70 $\pm$ 5.03 g Fe m^{-2} yr^{-1}; a relatively high value compared to

estimated values from the interstitial water profiles (0.22-0.56 g m^{-2} yr^{-1}; Chapter 5). This may be partly due to the complex iron chemistry in the sediment. Early diagenesis of Mn and Fe oxides in the sediments is discussed further in Chapter 5.

POC Budget

Mean annual primary productivity over a three-year period in the central basin of Boca de Quadra was around 140 g C m^{-2} yr^{-1} (Burrell, 1983b). Since productivity measurements were not a part of this study, it was assumed that *in situ* primary production during the study period was similar to that of the previous years.

Of particular interest in examining the POC budget is an estimate of what portion of the daily primary productivity escapes downwards from the euphotic zone. The variable influx of terrestrial POC makes a determination more uncertain in estuaries than in the open ocean. Comparison of the POC flux at the 40 m depth horizon with the primary productivity showed a marked seasonal trend (Table 4.4). The loss term was hence calculated by dividing the POC flux at 40 m depth by primary productivity during the same period (the primary productivity data used were from VTN; 1982). Loss of POC from the euphotic zone by settling particulates was

Table 4.4. Loss of POC from the euphotic zone.

Date	Primary Productivity* (Euphotic zone)	Vertical Flux (40 m depth)	Loss
	(mg C m^{-2} d^{-1})		(%)
1982			
6/9 - 6/12	920	109	12
8/15 - 9/22	110	57	52
1983			
3/13 - 4/9	1170	106	9

* data from VTN (1982)

greater than 50% of primary productivity in fall when river runoff was high but only 9-12% in the spring-summer period. During April 1983, in particular, the material caught in sediment traps at 40 m depth had a C/N ratio of 6.7; the combustion residue was white without the reddish brown tint which was usually observed for the rest of the sampling period; and the $\delta^{13}C$ values were nearly identical to typical marine phytoplankton. These observations suggest that settling material in April 1983 was composed entirely of autochthonous organic material. Therefore, loss of POC from the main pulse of primary production *in situ* is on the order of 10% in the central basin of Boca de Quadra. Although primary productivity was measured over three years (1980-1982), the timing of sampling appeared to inadequately cover the short and intense vernal bloom of phytoplankton. Therefore the estimates given here must be considered to be preliminary.

The annual mean loss of primary production below the euphotic zone in Puget Sound (Baker *et al.*, 1985), Dabob Bay (Lorenzen *et al.*, 1981) and in the Bedford Basin (Hargrave and Taguchi, 1978) has been measured directly at 5 $\pm$ 4, 10 and 6%, respectively. However, about 1/3 or 1/2 of the annual production of carbon has

been reported to settle to the bottom in shallow (<50 m depth) waters (Davis, 1975; Wassmann, 1983) and in the deeper (280 m) Resurrection Bay, Alaska (Burrell, 1983a).

The seasonal trend of the "loss term" in Table 4.4 in the central basin of Boca de Quadra agrees well with the few other available estuarine studies in which both POC flux and primary production were measured under conditions where traps were placed far enough above the bottom so that contamination from resuspension was negligible, but deep enough so that the traps collected only particulates settling out of the euphotic zone. The ratio of POC flux to the C fixation rate can exceed 90% in winter, but is less than 10% in summer in the main basin of Puget Sound (Baker *et al.*, 1985). In lower Cook Inlet, Alaska, about 12% of the total primary production leaves the euphotic zone during summer months (Chester and Larrance, 1981).

Seasonal variability in the source and flux of settling POC may be expected to have a direct effect on the metabolic activity of the benthos (Hargrave, 1973). In Boca de Quadra seasonal variability in the measured sea-bed oxygen consumption (Chapter 5) agrees with the trend in C fixation in the euphotic zone and subsequent loss from this zone (Figs. 1.4 and 4.2). O_2 uptake rates were twice as high as in summer than in winter. On an

annual basis, oxygen consumption was 58 l O_2 m^{-2} yr^{-1}. Thus aerobic respiration accounts for about 24 g C m^{-2} yr^{-1}, which is a little less than half of the total flux arriving at the basin floor. In addition to O_2 uptake, however, POC is lost through diagenetic reactions and permanent burial within the sediments. Based on the POC contents of the ^{210}Pb dated cores, permanent burial accounts for 16.8-28.8 g C m^{-2} yr^{-1}. A more detailed discussion of the POC diagenesis in sediments is given in Chapter 5.

Particulate Biogenic Si Budget

A mole ratio of 7 for C:Si in diatoms (the average C:Si ratio for the dominant diatom species occurring in the 1980-1982 bloom periods; Harrison *et al.*, 1977) was used to convert carbon production to silica production. The resulting annual production of biogenic Si is about 44.94 g Si m^{-2} yr^{-1}. Of this input, 33.15 g Si m^{-2} yr^{-1} is settling out of the euphotic zone; *i.e.*, around 70% of the annual production. Approximately 16.01 g Si m^{-2} yr^{-1} is estimated to dissolve between 120 m and 375 m within the basin, based on the three component model (primary-resuspended-alteration) discussed earlier. The sediment incorporation rate of biogenic Si is estimated at 16.85 g Si m^{-2} yr^{-1}. Therefore, a total of 28.09 g Si m^{-2} yr^{-1} -

which is 60% of the total annual production - is dissolved in the water column.

CONCLUSIONS

This study of the composition and fluxes of settling particulate biogenic matter and particulate Mn and Fe within the Boca de Quadra basin demonstrates the temporal changes in production, sources and budgets. Major findings are:

1. The fluxes and composition of settling POC, PN and biogenic Si at 40 m are strongly controlled by the sources of particles to the surface waters. Major sources are primary production and terrigenous influx. The vertical fluxes increase with depth. This is believed to be primarily due to resuspension of bottom sediments.

2. A strong seasonality was evident in the settling fluxes of POC, PN, biogenic Si, particulate Mn and Fe. In particular, a sharp primary production peak in the early spring was reflected nearly simultaneously in the settling fluxes throughout the water column. Decomposition of POC, PN and dissolution of biogenic Si reached a maximum shortly following the bloom period. Authigenic formation of particulate Mn and Fe was also

pronounced during this period of the year.

3. Algal primary production *in situ* provides the major portion of settling particulate organic matter, with minor terrestrial contributions (at most 30%) from river input.

4. About 10% of the annual *in situ* C production and 70% of the annual Si production settles out of the euphotic zone.

5. The major mode of transporting phytodetritus from the surface waters to deep waters was via settling of large intact cells, fecal pellets, and aggregates of cells.

6. Decomposition rates of settling POC and PN are estimated to be 10.20 $\pm$ 9.00 and 1.54 $\pm$ 1.26 g m^{-2} yr^{-1}, respectively. The dissolution rate of biogenic Si is estimated to be 16.01 $\pm$ 25.28 g Si m^{-2} yr^{-1} in the water column.

7. Annual fluxes at 40 m depth, just below 1% light level and in the major pycnocline; at 120 m depth, which is close to the depth of mouths of Mink Bay and Marten Arm; and at 375 m depth, just 5 m above the bottom are summarized in Table 4.5.

8. Most of the particulate Mn settling below 120 m depth is of authigenic origin, and the rate of authigenic Mn formation is estimated to be 12 to 34 mg Mn m^{-2} d^{-1}.

Table 4.5. Annual fluxes of biogenic particulates at depths.

Depth (m)	POC	PN	Particulate biogenic Si
		($g\ m^{-2}\ yr^{-1}$)	
40	48.84	5.88	33.15
120	41.40	4.62	36.24
375	78.60	8.96	73.88

However, a significantly lowered authigenic contribution of particulate Fe was observed within the basin water column.

CHAPTER 5. EARLY DIAGENESIS OF BIOGENIC MATTER IN THE SEDIMENTS

INTRODUCTION

Particulate biogenic matter arriving at the sediment-water interface is one of the major driving forces determining benthic metabolism and hence the fluxes of metabolite species from or to the sediments. However, the composition of organic matter raining to the sea floor is not well known. Considerable evidence indicates that the refractory particulate organic matter originates from phytoplankton materials, and forms very rapidly (Cronin and Morris, 1983). Recently, Westrich and Berner (1984) proposed that the pool of decomposable sedimentary organic carbon (plankton detritus) actually consists of various groups of compounds which are metabolized at different rates. However, very little information is available on the degradation of terrestrial organic matter, especially for the lignin-free fraction, in the marine environment (Hedges and Mann, 1979). Marine planktonic material is believed to be more labile than terrestrial organic matter.

There has been some controversy over whether the majority of POC raining to the sediment-water interface is predominantly oxidized at or near the sediment-water

interface (oxidation rate J_{pb}) or within the sediments (oxidation rate J_d). Reimers and Suess (1983) argue that resuspension near the sediment-water interface tends to increase J_{pb} and subsequently reduces J_d, because resuspension increases the residence time of POC in the water column. Emerson *et al.* (1985) show that J_d is dominant in the deep Pacific Ocean. Zeitzchel (1979) argued that J_{pb} is significantly larger than J_d in shallow waters (<200 m deep). J_{pb} has been measured using benthic chambers, and J_d has been estimated using diagenetic models of sediment organic carbon profiles and from interstitial water profiles (summarized by Reimers and Suess, 1983). Interstitial water concentration profiles have been used to examine sediment-water exchange, because relatively small changes in solid phase chemical compositions cause large changes in pore water solute concentrations (*e.g.*, Grundmanis and Murray, 1977).

The contemporaneous combination of direct measurements of the flux of biogenic material to the sea floor, and of studies on their subsequent diagenesis in sediments is very rare, as noted by Reeburgh (1983). This present work may be one of the few studies undertaken in a deep coastal environment. The fluxes and fate of settling biogenic matter, POC, PN and particulate

Si, in the water column have been discussed in Chapter 4. Since each sediment core section represents >10 years of deposition, processes occurring in sediments are integrated over a time span of years. The investigation of depth distributions of solid phases (TOC, TN, biogenic Si), pore water nutrients, and sulfate provides quantitative information on their early diagenesis. The important questions to be addressed in this chapter are:

1. What are the major sites for the oxidation of particulate organic matter and dissolution of biogenic silica arriving at the sediment-water interface?

2. How do decomposition rates of biogenic matter in sediments compare to rates of input from and removal within the water column?

3. What processes regulate pore water solute concentrations?

Consideration of the first and second questions makes use of oxygen uptake rates measured at the surface of sediment cores, sediment trap results, and computations based on the solid phase profiles. Diagenetic models are employed to provide insight into which process is the most significant for the oxidation of organic matter and dissolution of biogenic silica. Since significant recycling of Mn in the water column was

found (Chapter 4), the role of Mn and Fe oxides in the oxidation of sedimentary organic carbon is estimated using distributions of dissolved Mn and Fe in pore waters.

The final question will be addressed using measurements of nutrient fluxes from cores and by numerical modeling of pore water nutrient distributions. Such models can include terms for advection, diffusion, sediment mixing, bioturbation, and reaction between solids and solutions (Berner, 1980). A steady-state numerical model incorporating a nonlocal exchange mechanism (Emerson et al., 1984) is applied to the basin sediment and compared to the pore water profiles and direct nutrient flux measurements.

METHODS AND MATERIALS

Sampling Methods

The sediment and interstitial water samples were collected using a Benthos gravity corer with 6.7 cm i.d. plastic core liners used without core catcher, nose cone, or pipe barrel. Cores collected were immediately extruded into PVC squeezers (Reeburgh, 1967) constructed with an i.d. identical to that of the core liner, thereby minimizing atmospheric exposure. Interstitial water was

extracted from the sediment using 5-30 psi of ultrapure nitrogen gas. Two precombusted Whatman EPM 1000 filters were used in the squeezers. The initial few ml of interstitial water from each section were discarded. Samples for nutrient and sulfate analysis were collected in polyethylene bottles and frozen for later analysis. Sediment samples were also frozen immediately for later analysis of TOC, TN, and biogenic Si.

A Haps corer (Kanneworff and Nicolslausen, 1973) was used to collect cores for ship-board incubation measurements of fluxes of oxygen and nutrients. Thin vertical sections of sediment cores for later X-radiograph observation were obtained by cutting frozen cores.

Direct Flux Measurements

Core tops with their overlying waters were incubated in a refrigerator in the dark at the *in situ* temperature. The overlying water was aerated continuously and sampled daily with plastic syringes. Water samples were filtered immediately after collection, and frozen for later analysis of nutrients.

Separate cores with their overlying waters were incubated in a dark refrigerator at the *in situ* temperature for dissolved oxygen uptake measurements. A

plastic stirring blade was mounted on the stopper used to seal the tops of the cores. The size of the blade was adjusted to ensure homogeneity of overlying water, but to avoid resuspension of the bottom sediment. Oxygen concentrations were monitored using a dissolved oxygen probe (Wheaton 60 Second B.O.D. System) submerged in the overlying waters.

Analytical Methods

Sediment TOC, TN, and biogenic silica content were determined by the same procedures described in Chapter 4. Inorganic carbon in sediments was determined using a Carle GC 8700 gas chromatograph employing the procedure of Stainton (1973).

Dissolved inorganic nutrients were determined by autoanalyzer. For ammonium, the method used was that of Koroleff (1970), nitrate was determined by the Greiss reaction as described by Armstrong *et al.* (1967). Phosphate was quantitatively determined by the procedure of Murphy and Riley (1962). Silicic acid was determined by the molybdate method (Whitledge *et al.*, 1981). Sulfate concentrations were determined on a Dionex 2010i ion chromatograph using a HPIC Anion S4 separator column, a continuous flow suppressor column and a conductivity detector (Shaw *et al.*, 1984).

RESULTS

Sediment Chemistry

Sedimentary total organic carbon (TOC), nitrogen (TN) and biogenic silica profiles (on a dry weight basis), along with pore water profiles, for the central basin of Boca de Quadra, are shown in Figs. 5.1-5.7 (data listed in Appendix E), where BSi is sedimentary biogenic silica. Individual cores are named after their standard oceanographic station (Fig. 1.1), plus a sampling sequence number, unless specified otherwise (Table 5.1).

In general, TOC, TN and biogenic Si concentrations systematically decrease with depth, with some variability in the top layers of sediments. The average TOC and TN concentrations in the surface sediments are 4.8 $\pm$ 0.3 % and 0.44 $\pm$ 0.02%, respectively. The C/N ratio of organic matter in the surface sediments ranges from 9.9 to 14.3 (average 12.3 $\pm$ 1.8). The average content of biogenic Si is 4.02 $\pm$ 0.15% in the surface sediments.

Dissolved Oxygen Uptake

Oxygen uptake measurements were conducted twice: once in the oceanographic winter (March 1984) and again in summer (August 1984). The mean oxygen uptake was 0.16 $\pm$ 0.03 and 0.43 $\pm$ 0.30 mmol O_2 m^{-2} hr^{-1} in winter and in summer, respectively.

Table 5.1. Core samples.

Name	Sampling Date
BQ9G	January 1983
BQ9G*	June 1983 (Hogarty, 1985)
BQ9G-1	October 1983
BQ9G-2	October 1983
BQ9-1	October 1983
BQ9-2	October 1983
BQ9-3	March 1984
BQ9-4	March 1984
BQ5-1	October 1983
BQ5-2	October 1983

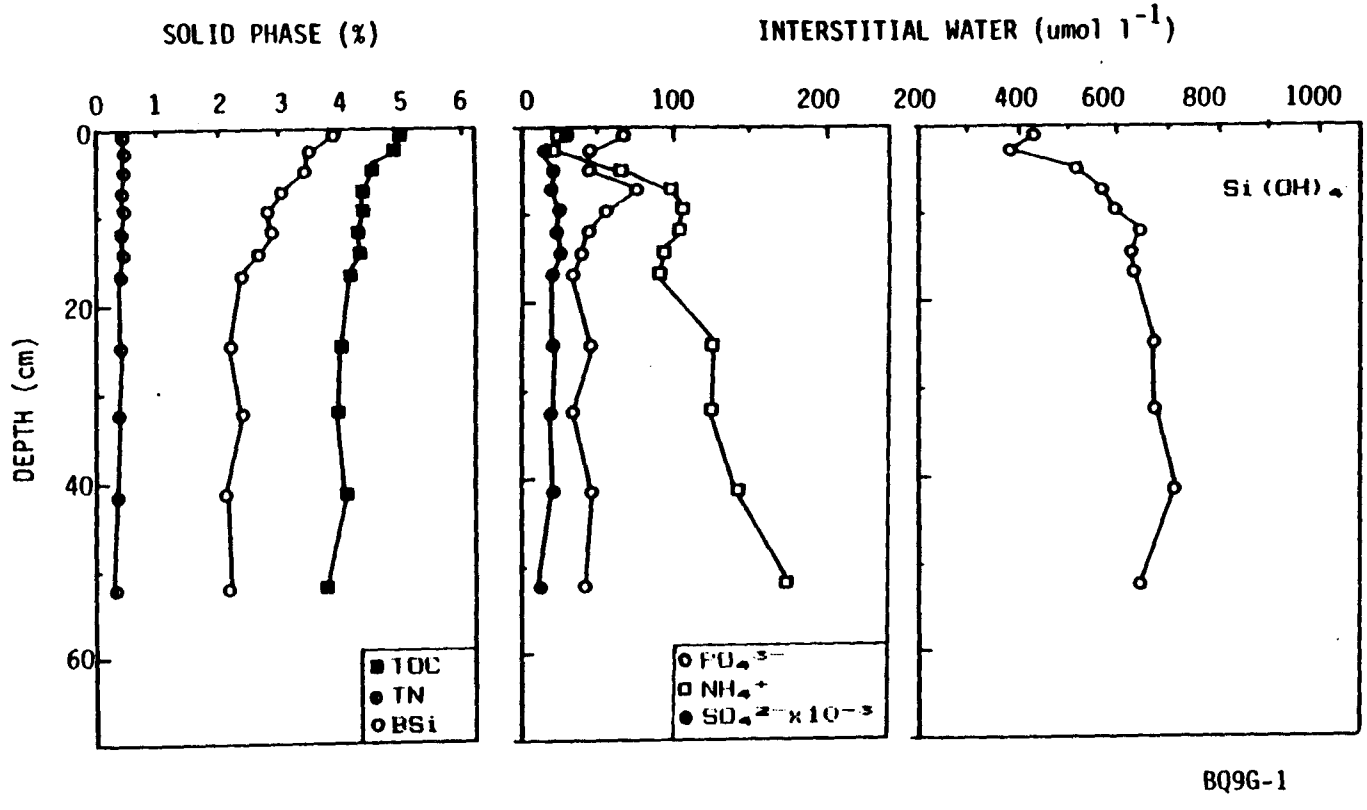

Fig. 5.1. Plots of solid phase (%) and pore water concentration (umol l^{-1}) data versus depth in core samples.

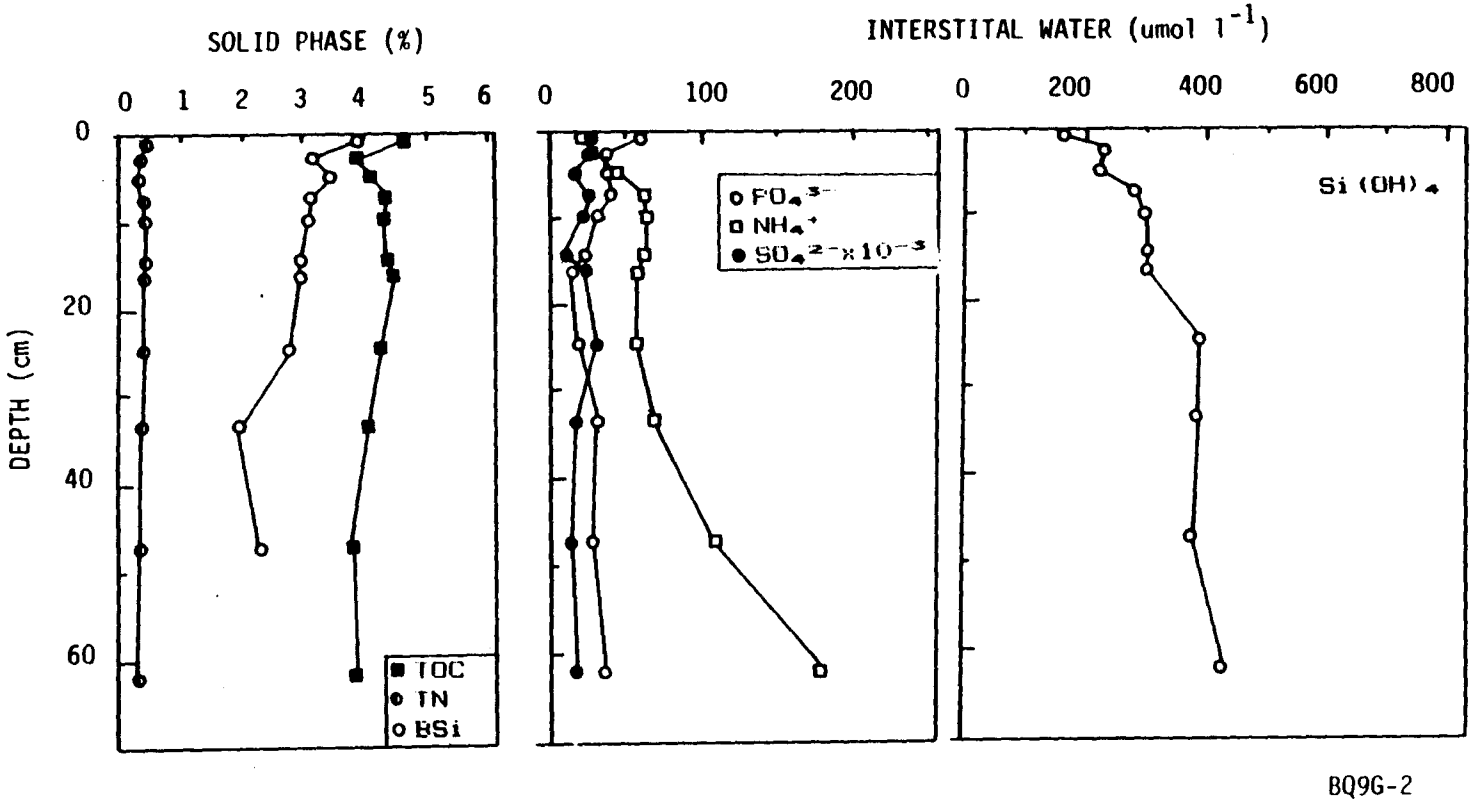

Fig. 5.2. Plots of solid phase (%) and pore water concentration (umol l^{-1}) data versus depth in core samples.

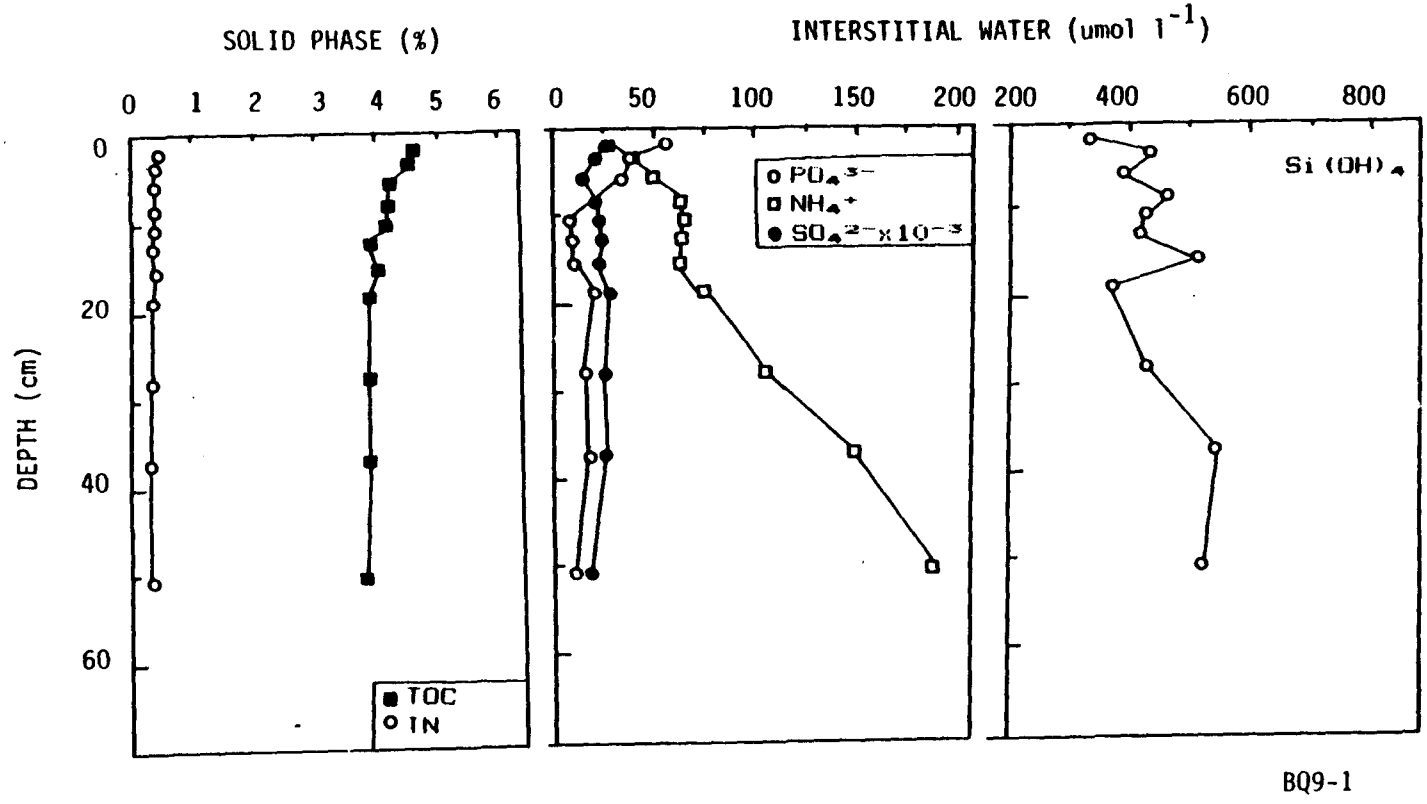

Fig. 5.3. Plots of solid phase (%) and pore water concentration (umol l^{-1}) data versus depth in core samples.

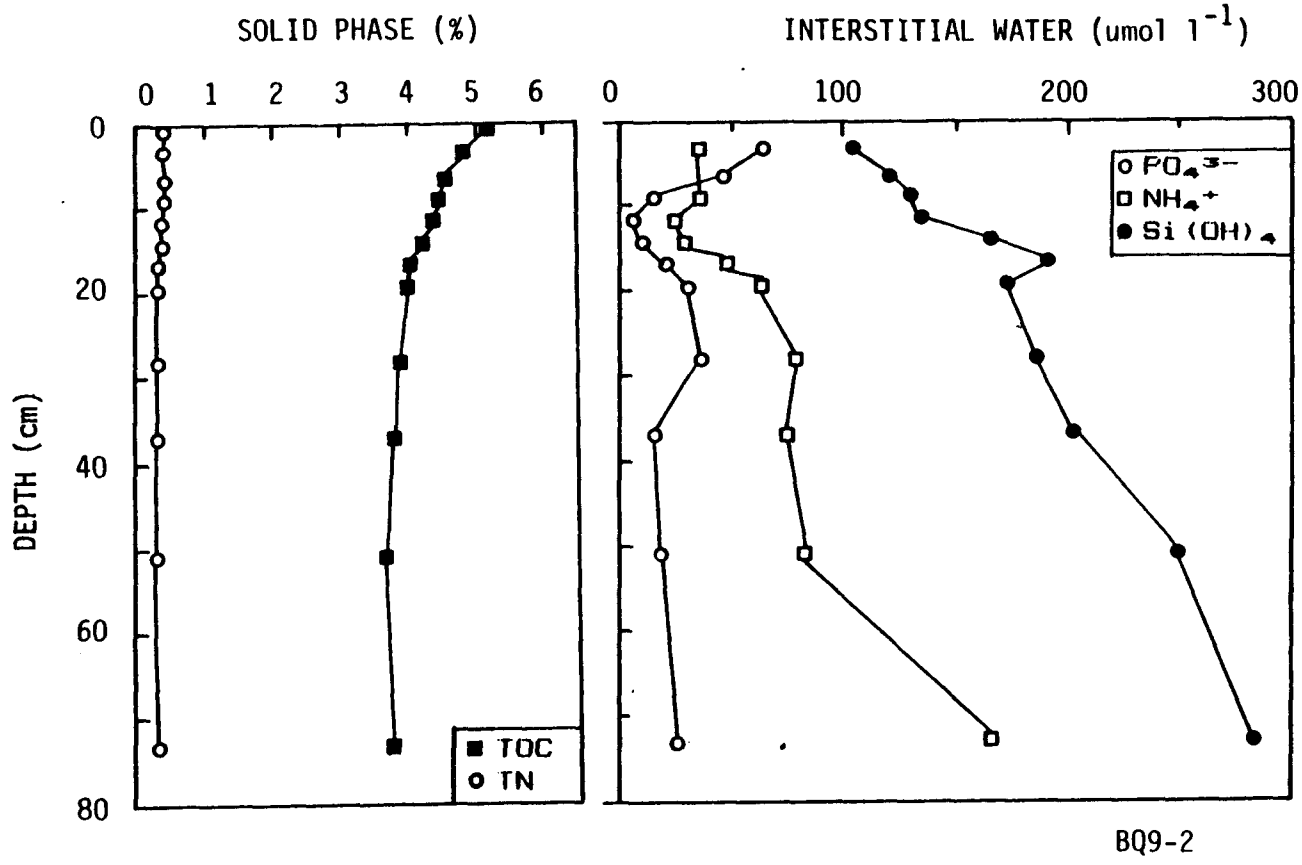

Fig. 5.4. Plots of solid phase (%) and pore water concentration (umol l^{-1}) data versus depth in core samples.

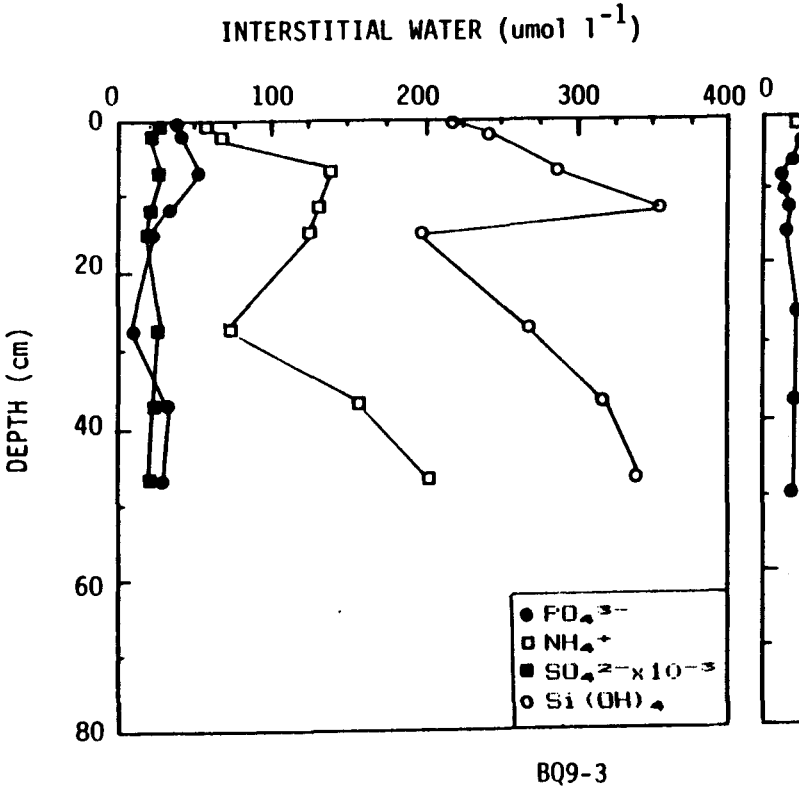

Fig. 5.5. Plots of pore water concentration (umol l

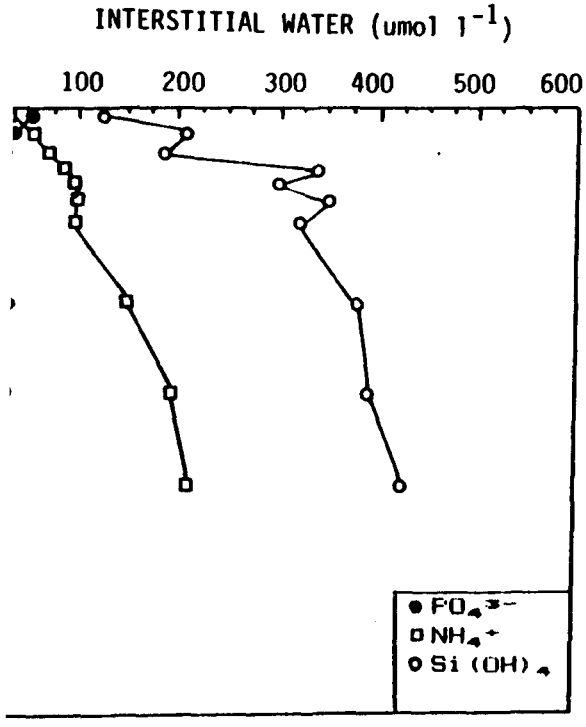

BQ9-4

$^{-1}$) data versus depth in core samples.

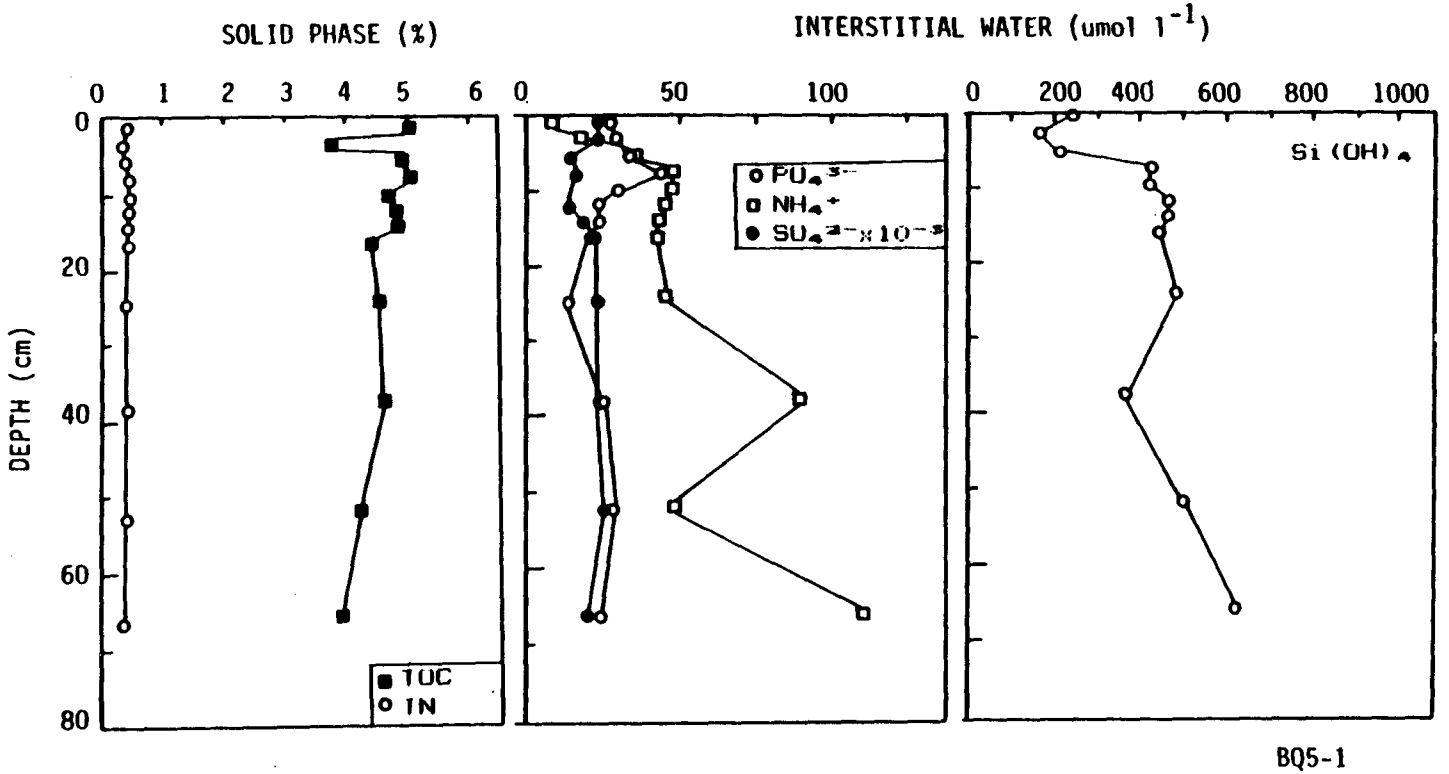

Fig. 5.6. Plots of solid phase (%) and pore water concentration (umol l^{-1}) data versus depth in core samples.

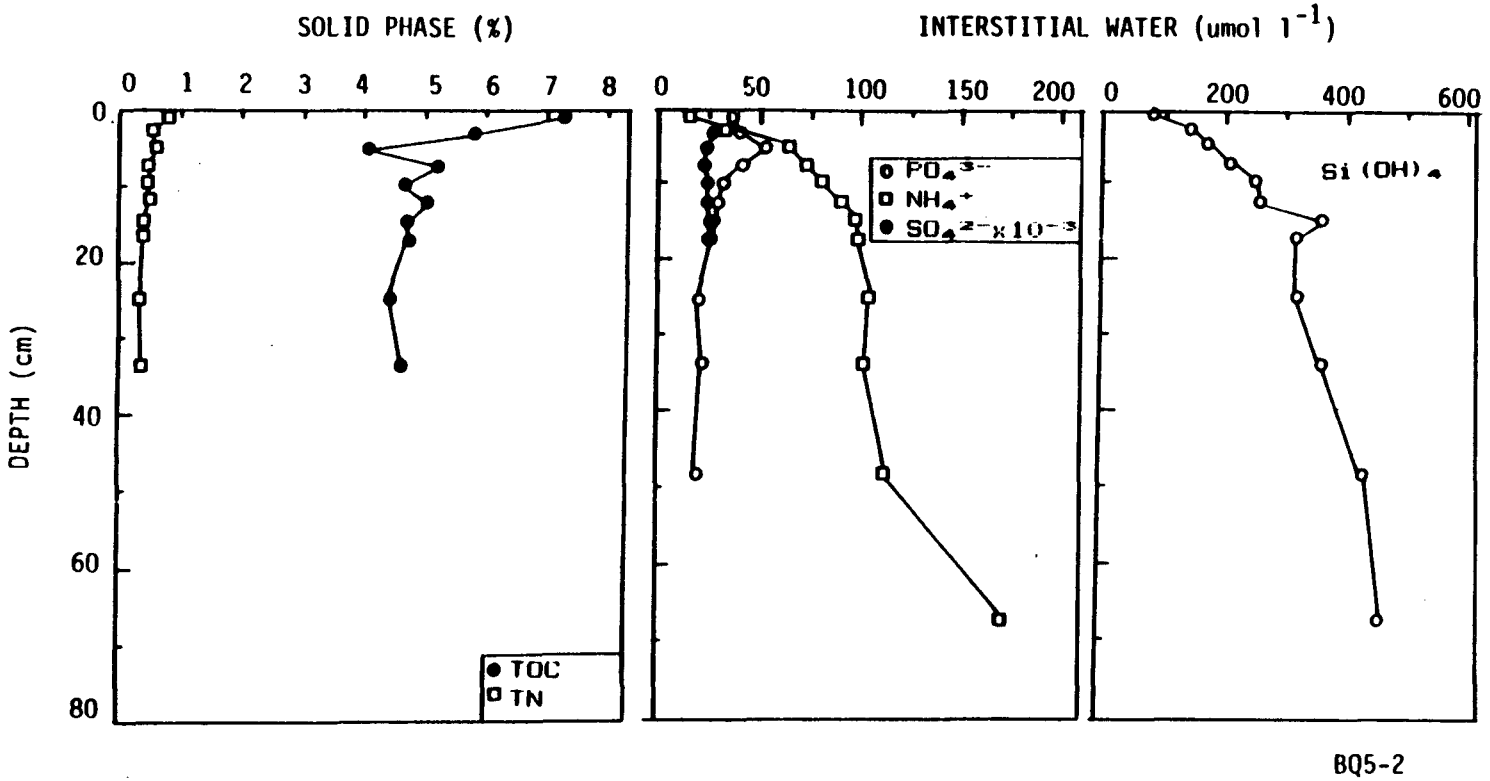

Fig. 5.7. Plots of solid phase (%) and pore water concentration (umol l^{-1}) data versus depth in core samples.

Nutrient Flux Measurements

Results of direct nutrient flux measurements are plotted in Fig. 5.8. as the change in mass of solutes per unit area (umol cm^{-2}) in overlying waters as a function of time. Volume changes due to sampling are small enough so that data in umol cm^{-2} in Fig. 5.8 essentially reflect changes in concentration with time. $Si(OH)_4$ concentrations increased with time, NO_3^- concentrations decreased with time, and there were no appreciable changes in PO_4^{-3}, NH_4^+ and NO_2^- concentrations. The rate of $Si(OH)_4$ flux across the sediment interface ranged from 0.103 to 0.131 umol cm^{-2} d^{-1}, and the NO_3^- consumption rate was 0.021 to 0.035 umol cm^{-2} d^{-1}.

DISCUSSION

Input of POC to the Sediment

The rate of POC incorporation into the sediment, J_s, can be obtained using Eqs. 5.1 and 5.2, which describe sediments without and with sediment mixing, respectively (Walsh *et al.*, 1985).

$$J_{s1} = w\rho G_0(1-\phi) \tag{5.1}$$

$$J_{s2} = w\rho G_0(1-\phi) + K\rho(\partial G/\partial z)_{z=0}(1-\phi) \tag{5.2}$$

where w is the sedimentation rate, ϕ the porosity, G_0 the

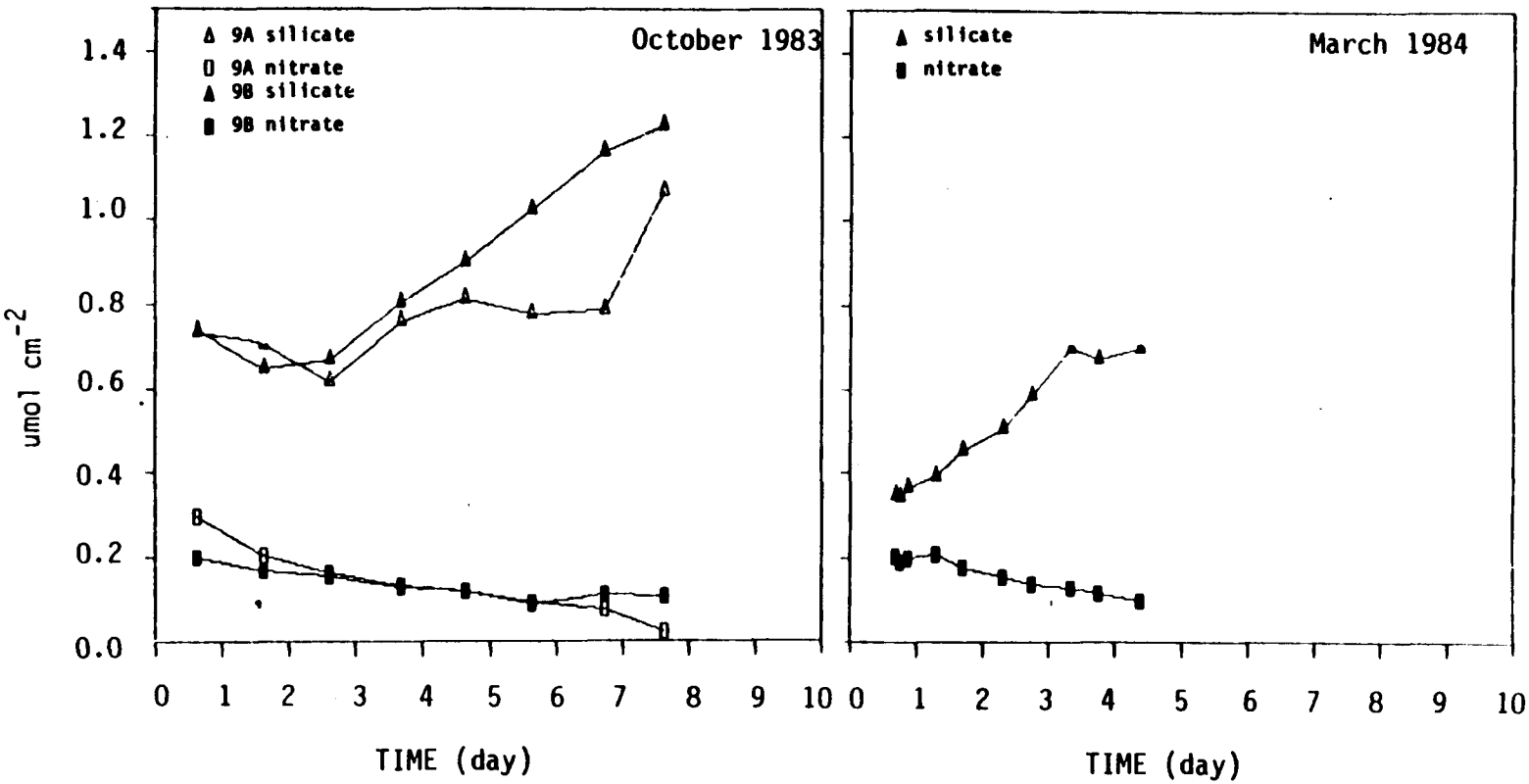

Fig. 5.8. Changes in mass of nutrients as a fuction of time in core overlying waters.

surficial TOC concentration taken from the top section of sediment core, K a sediment mixing coefficient, and $(\partial G/\partial z)_{z=0}$ is the TOC concentration gradient at the sediment-water interface. For the purposes of this discussion, sediment particle mixing is assumed to be a Fickian type diffusive process. Based on the data in Figs. 5.1-5.4 and Figs. 5.6-5.7, each parameter was calculated using sediment mixing coefficients (K) estimated from ^{137}Cs profiles (0.18 cm^2 yr^{-1}; Chapter 3). The results are tabulated in Table 5.2. As seen in Table 5.2, J_S can be approximated as J_{S1} in Eq. 5.1 because $(\partial G/\partial z)_{z=0}$ is relatively samll compared to G_0 and K is very small. Overall, the contribution of sediment mixing to J_S is at most 10% in the BQ5 area and much less in the vicinity of BQ9. The incorporation rate of POC into the sediment is about 2 moles C m^{-2} yr^{-1}.

TOC Decomposition Rate in the Sediment

An estimate of the oxidation of TOC within the sediment is attempted here without taking into account sediment mixing, because the sediment mixing effect is quite small as noted above. The total amount of TOC remineralized, G_r, over a depth interval down to 50 - 70 cm depth would be:

$$\%G_r = (G_0 - G_b)/G_0 \times 100 \qquad (5.3)$$

Table 5.2. The relative importance of sediment mixing to the incorporation rate of POC into the sediment. w is 0.2 cm yr^{-1}, ρ is 2.5 g cm^{-3}, and ϕ is 0.92 at the sediment surface. K is 0.18 cm^2 yr^{-1}.

Station	$(\partial G/\partial z)_{z=0}$ (x 10^{-2} cm^{-1})	Flux (mol C m^{-2} yr^{-1}) A	D	Js
BQ9G-1	0.034	1.83	0.01	1.84
BQ9G-2	0.426	1.56	0.13	1.69
BQ9-1	0.075	1.72	0.02	1.74
BQ9-2	0.126	1.71	0.04	1.75
BQ5-1	0.581	1.67	0.17	1.84

$A = w\rho G_0 (1-\phi)$, $D = k\rho(1-\phi)(\partial G/\partial z)_{z=0}$, $Js = A + D$.

and the decomposition rate of TOC, J_d, is

$$J_d = w\rho(G_o - G_b)(1-\phi) \qquad (5.4)$$

where G_o and G_b are the concentrations of surficial and core bottom TOC, respectively (Martens and Klump, 1984). G_o ranges from 4.79 $\pm$ 0.23 to 6.14 $\pm$ 1.59 %, and G_b from 3.78 $\pm$ 0.06 to 4.18 $\pm$ 0.37 % in the BQ9 and BQ5 areas, respectively. Applying Eq. 5.3 to TOC profiles yields a G_r value of 17-28% in the BQ9 and 22-36% BQ5 areas. The J_d values obtained using Eq. 5.4 is 0.5 $\pm$ 0.1 and 1.0 $\pm$ 0.2 mol C m^{-2} yr^{-1} in the BQ9 and BQ5 areas, respectively. However, seasonal variations in surficial TOC concentration complicate the choice of a representative G_o value. The POC concentration in the settling particulates varies from 4.99 in winter to 11.28% in summer at 375 m depth, 5 m above the bottom (see Chapter 4). The large organic carbon concentration difference between settling particulates and the surface sediments should be noted. Also, surface sediment carbon probably has been mixed with older sediment carbon and degraded at the sediment-water interface. Therefore the J_d values obtained here should be regarded as a minimum range for the TOC remineralization rate.

A first-order reaction rate constant for the oxidation of organic matter in the sediment was estimated

using the steady-state diagenetic model of Berner (1980):

$$K\frac{\partial^2 G}{\partial z^2} - w\frac{\partial G}{\partial z} - k_c G = 0 \qquad (5.5)$$

where K is the sediment mixing coefficient, z the depth in sediments (positive downward), w the sedimentation rate, and k_c is a first order rate constant for the oxidation of organic matter, G. The analytical solution of Eq. 5.5 for the boundary conditions

$$G = G_o \text{ at } z = 0$$

$$G \to 0 \text{ at } z \to \infty$$

is:

$$G_z = G_o \exp(B_c z) \qquad (5.6)$$

$$\text{where } B_c = (w-(w^2 + 4k_c K)^{1/2})/2K \qquad (5.7)$$

and G_o is the TOC concentration at the sediment-water interface. However, TOC concentrations decrease to an "equilibrium" concentration rather than to zero. This background concentration is generally regarded as non-metabolizable carbon. It should be noted that the term "metabolizable" and "non-metabolizable" are strictly operationally defined, based on TOC profiles. The presence of non-metabolizable carbon is included in Eq. 5.8.

$$G_z = G_{nm} + G_{m,o}\exp(B_c z) \qquad (5.8)$$

where $G_z = G_{nm} + G_{m,z}$ at z (5.9)

G_{nm} is non-metabolizable TOC, and $G_{m,o}$ and $G_{m,z}$ are the metabolizable TOC concentration at the sediment-water interface and at depth z, respectively. If sediment mixing can be ignored (see discussion above), Eq. 5.5 becomes:

$$-w\frac{\partial G}{\partial z} - k_c G = 0 \qquad (5.10)$$

Solving Eq. 5.10 for the boundary conditions:

$$G = G_{m,o} \text{ at } z = 0$$

$$G_{m,o} \rightarrow 0 \text{ at } z \rightarrow \infty$$

gives $G_z = G_{n,m} + G_{m,o}\exp(B_c z)$ (5.11)

where $B_c = -k_c/w$. (5.12)

Values for B_c were obtained by a least squares fit to the TOC data shown in Figs. 5.1-5.7, and subsequently the TOC degradation rate, k_c, was computed using Eq. 5.7 for the upper 20 cm and Eq. 5.12 for deeper sediment, since the upper 20 cm of sediment appears to be mixed. The residence time (T) of the TOC was taken as the inverse of k_c (Table 5.3). However, it is noted that sediment mixing has little effect on TOC decomposition at the small rate value (0.18 $cm^2\ yr^{-1}$) used here (see Chapter 3). Applying the k_c values listed in Table 5.3, J_d

Table 5.3. Parameters for the fit of Eq. 5.8 to the TOC data. B_c is taken as Eq. 5.7 in the surface 20 cm layer and Eq. 5.12 in the deeper layer of sediments. w is 0.2 cm yr^{-1}. R is the correlation coefficient.

Surface layer

Station	$G_{n,m}$ (%)	$G_{m,o}$ (%)	K (cm^2 yr^{-1})	B_c (cm^{-1})	k_c (yr^{-1})	T (yr)	R
BQ9G-1	3.77	1.14	0.18	-0.0729	0.016	62	-0.91
BQ9-1	3.78	0.85	0.18	-0.1035	0.023	44	-0.96
BQ9-2	3.72	1.42	0.18	-0.0686	0.015	68	-0.98

Deep layer

BQ9G-1	3.77	0.24	0	-0.05	0.01	100	
BQ9G-2	3.86	0.46	0	-0.067	0.013	75	
BQ9-1	3.78	0.10	0	-0.025	0.005	200	
BQ9-2	3.72	0.19	0	-0.75	0.015	67	

values above the 20 cm depth horizon range between 0.33 and 0.45 mol C m^{-2} yr^{-1}. J_d integrated over a depth of 50-70 cm within the sediment is estimated at 0.38 to 0.64 mol C m^{-2} yr^{-1}, which are remarkably close to the values estimated using Eq. 5.4.

Dissolved Oxygen Uptake at the Sediment-Water Interface

Oxygen consumption by undisturbed sediment cores is the result of both C-oxidation and S-oxidation (or oxidation of other reducing substances, such as Mn and Fe). Jorgensen (1978; 1982) found that in Danish coastal waters about 50% of the total oxygen uptake was used for sulfide oxidation, and 50% for aerobic respiration. Hargrave (1978) similarly found 40% of the total oxygen uptake to be chemical oxidation in the Bedford Basin (Nova Scotia). These workers compared sediment oxygen uptake rates with and without added formalin. Sediment oxygen uptake rates have been obtained in Puget Sound, a temperate fjord environment, at depths up to 180 m deep. Here bottom water temperature was 8-9 ^{o}C and the bottom dissolved oxygen content was 0.17-0.25 mmol O_2 l^{-1} (Pamatmat and Banse, 1969). Measured consumption rates were 0.18-1.79 mmol O_2 m^{-2} hr^{-1}. Hargrave (1978) reported rates of 0.18-1.25 ml O_2 m^{-2} hr^{-1} in Bedford Basin.

The rates of total oxygen uptake in the central basin of Boca de Quadra are lower than those determined in the other fjord environments cited above. One reason for this may be that only two measurements are presently available, and taking into account the annual variations in primary productivity and in bottom water temperatures (Hargrave, 1969) (see Chapter 1), the peak period of oxygen consumption was probably missed. The consumption of O_2 by reduced sulfur was not estimated in this region. Care must be exercised in extrapolating a few measurements to the annual budget. Nevertheless, it is instructive to estimate annual O_2 uptake rate by the sediments in the basin. The rate is 2.68 mol O_2 m^{-2} yr^{-1} which is equivalent to *ca.* 2 mol C m^{-2} yr^{-1}, assuming Redfield stoichiometry (Froelich *et al.*, 1979).

The Role of Mn and Fe Oxides in TOC Diagenesis in Sediments

Dissolved Mn and Fe production rates may be determined from the sum of the flux to the overlying water and the flux to the underlying pore water, assuming Fickian-type diffusion (Martin, 1985). The data used here are from Hogarty (1985).

Although an estimate of the production rate of dissolved Mn in the sediment is severely limited due to

the coarse sampling interval used, preliminary calculations were made in order to obtain the Mn(IV) contribution to the oxidation of organic carbon in sediments of the central basin. The production rate of dissolved Mn at Station BQ9 ranged from 0.4 to 0.6 mol m^{-2} yr^{-1} which is equivalent to a TOC oxidation rate of 0.2 to 0.3 mol m^{-2} yr^{-1}, using a sediment diffusion coefficient (D_s) of 3.65 x 10^{-6} cm^2 s^{-1} (Sugai, 1985) and the dissolved Mn profiles shown in Fig. 5.9. These estimated values account half of the J_d of TOC estimated earlier, which is unusally high in the marine environments. The average Mn burial rate (based on the apparent ^{210}Pb sedimentation rate and the solid phase Mn content below the reaction zone in the sediments) is 0.007 mol m^{-2} yr^{-1}. The average primary flux (at 120 m depth) in the water column is about 0.019 mol m^{-2} yr^{-1} (Chapter 4). Even if all the solid Mn raining to the sediment surface were available for the oxidation of organic matter, only 0.008 mol m^{-2} yr^{-1} of TOC can be oxidized without recycling of Mn, assuming Redfield stoichiometry (Froelich *et al.*, 1979). Therefore, the role of recycled diagenetic Mn in the oxidation of TOC is probably to be significant in the central basin of Boca de Quadra.

An estimation of dissolved Fe production was also

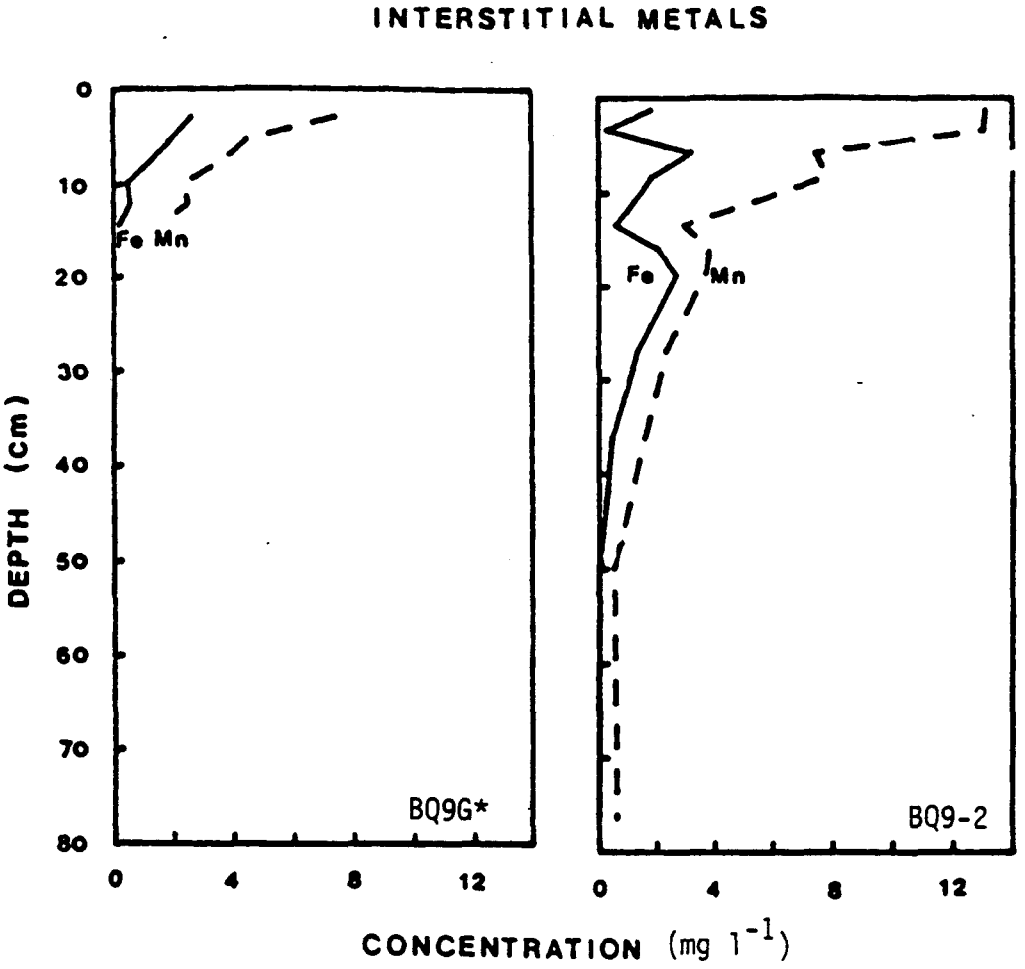

Fig. 5.9. Pore water concentration (mg l^{-1}) of Mn and Fe of two cores (from Hogarty, 1985).

made, in order to obtain a value for the rate of TOC oxidation by iron oxides, using a sediment diffusion coefficient (D_s) of 2.8 x 10^{-6} cm^2 s^{-1} at 6.5 °C of bottom water (Martin, 1985). It was assumed that dissolved iron was produced entirely through Fe(III) reduction, since the production rate of dissolved Fe *via* oxidation of sulfides is not known. The computed range of dissolved iron production rates is from 4.3 to 10.5 x 10^{-3} mol m^{-2} yr^{-1}, equivalent to a TOC oxidation rate of 1 to 2 x 10^{-3} mol m^{-2} yr^{-1}, but much less than that due to Mn reduction. The O_2 requirement would be 1.8 to 5.1 x 10^{-3} mol m^{-2} yr^{-1}, as calculated from the dissolved Fe flux out of the sediments, assuming that all the dissolved Fe is oxidized to Fe_2O_3.

The Fate of POC in the Benthic Regime

Fluxes of POC in the benthic regime can be divided into three compartments: J_{pb}, J_d, and J_b (Reimers and Suess, 1983). J_{pb} is the consumption rate of organic carbon at or near the bottom, and J_d is the rate of organic carbon consumed within the sediment. Both are mediated by respiration of the macro-benthos and micro organisms.

J_b is the carbon accumulation rate below the reaction zone. Thus, the flux of POC to the sediment-

water interface (J_f) is:

$$J_f = J_{pb} + J_d + J_b. \quad (5.13)$$

In this scheme the total benthic utilization (J_u) is

$$J_u = J_{pb} + J_d. \quad (5.14)$$

Also, the incorporation rate of POC into the sediment (J_s) can be described as

$$J_s = J_d + J_b. \quad (5.15)$$

There has been some controversy over whether the majority of POC raining to the sea floor is consumed at or near the sediment-water interface or within the sediment column. Emerson *et al.* (1985) showed that most POC raining to the deep Pacific Ocean is degraded within the sediment column rather than at or near the sediment-water interface. These investigators used three independent methods of estimating POC flux to the sediment-water interface: sediment traps, pore water O_2 profiles, and sedimentary organic carbon data. Reimers and Suess (1983) argued that resuspension near the sediment-water interface tends to increase J_{pb} and subsequently reduces J_d, because resuspension increases the residence time of POC in the water column. An

enhancement of POC degradation due to resuspension has been proposed also by Gardner (1977). Resuspension activity on the sea floor may increase J_{pb} significantly in a low sedimentation area, while it may not be significant in a high sedimentation area. Zeitzschel (1979) argued that the decomposition of sedimentary organic material occurs mainly at the sediment-water interface in shallow water (<200 m). It is also suggested that J_d can be increased if the benthic fauna are largely burrowers, because the burrows can increase the transport of oxidants and organic matter into the deeper layer (Emerson *et al.*, 1985).

The factors which affect the relative importance of J_d and J_b have been discussed by many scientists. Muller and Suess (1979) proposed that the sedimentary organic carbon content can be related to the bulk sedimentation rate and primary productivity in the overlying surface waters. Toth and Lerman (1977) showed empirically that the average reactivity of organic matter is proportional to a power of the sedimentation rate. Recently Aller and Mackin (1984) demonstrated theoretically that sedimentation and reactive organic carbon burial rates are not necessarily coupled. Preservation of organic matter in sediments depends on the relative importance of electron acceptor concentration, advection due to

sedimentation, solute diffusion, and the supply and reaction rate of metabolizable organic matter.

The relative importance of the various fluxes of sedimentary organic carbon in the benthic regime may be resolved by constructing a budget. J_f is taken as the settling rate of POC at the 375 m depth horizon (see Chapter 4). J_{pb} is computed by subtracting J_s from J_f. J_f can be corrected for resuspension using the average resuspension rate (64%) at 375 m depth estimated in Chapter 3. J_b is calculated using Eq. 5.16, assuming no mixing below the 50 to 70 cm depth in the sediment.

$$J_b = w\rho G_{nm}(1-\phi) \qquad (5.16)$$

An annual TOC budget is depicted in Fig. 5.10 and listed in Table 5.4. The measured mean annual POC supply rate to the sediment (J_f) is 6.6 mol m^{-2} yr^{-1}. Of this input, resuspension may account for 4.2 mol m^{-2} yr^{-1}. The rate of incorporation into the sediment (J_s) has been computed at about 2 mol m^{-2} yr^{-1}. Thus the aerobic respiration rate (J_{pb}) accounts for the remaining 0.4 mol m^{-2} yr^{-1} at the sediment-water interface and 4.2 mol m^{-2} yr^{-1} near the bottom (resuspension). Respiration within the sediment (J_d) is estimated to be greater than 0.5 mol m^{-2} yr^{-1}. The burial rate of TOC (J_b) is 1.4-2.4 mol m^{-2}

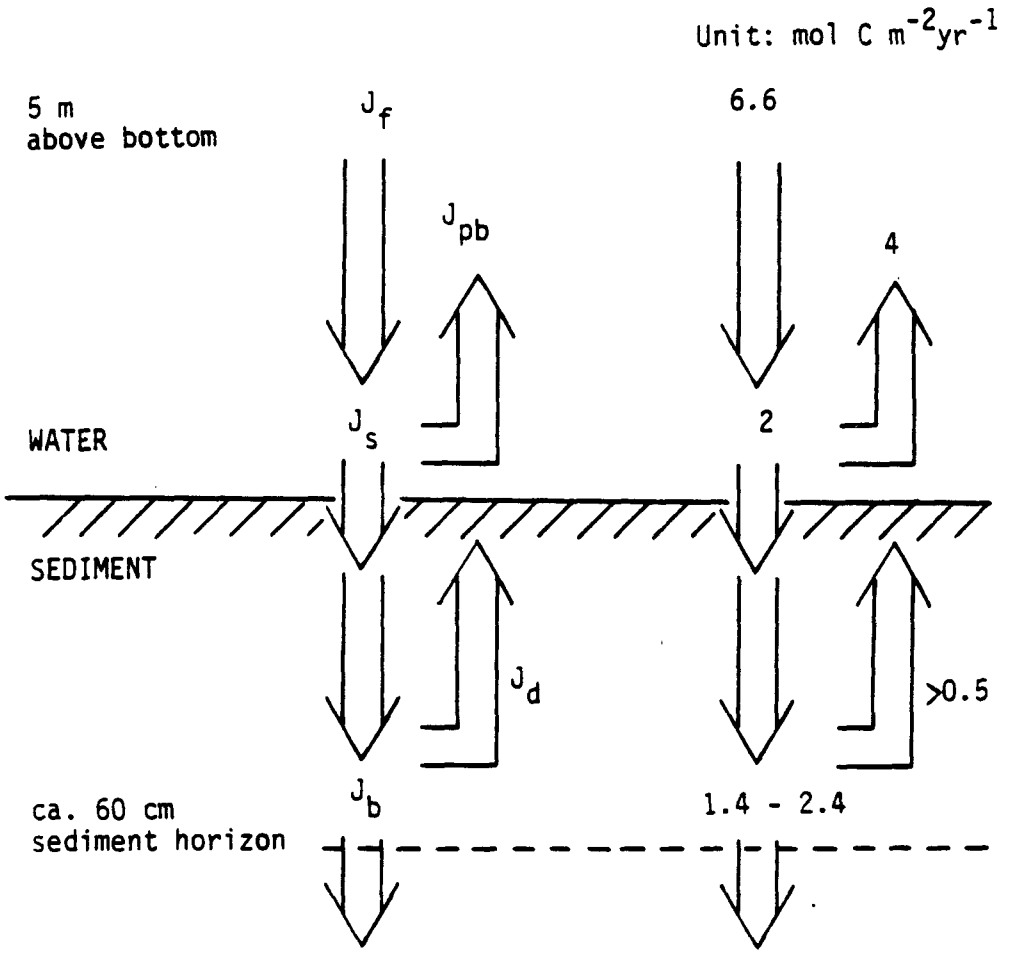

Fig. 5.10. A preliminary annual sedimentary organic carbon budget.

Table 5.4. Annual budget of sedimentary biogenic matter.

mol m^{-2} yr^{-1}

	J_f	J_{pb}	J_s	J_d	J_b
TOC	6.6	4.4	2	>0.5	1.4 - 2.4
TN	0.65	<0.5	>0.14	>0.03	0.11
Biogenic Si	2.64	2	>0.64	>0.32	0.31 - 0.35

yr^{-1}. J_{pb} appears to be much greater than J_d in this environment. The lower limit of the residence time of TOC is about 70 years in the upper 20 cm layer and 100 years in deeper sediments.

A preliminary annual budget of TN may be constructed in a similar manner to that presented for the TOC budget. Computed parameters are listed in Table 5.4.

The Fate of Biogenic Silica in the Benthic Regime

A particulate biogenic Si budget has also been constructed following the same methods used for the TOC budget discussed above (Table 5.4). The particulate biogenic Si supply rate to the sediment (J_f) was determined to be 2.6 mol m^{-2} yr^{-1} from the sediment trap data. Of this, resuspension may account for 1.7 mol m^{-2} yr^{-1}. The rate of incorporation into the sediment (J_s) is estimated to be more than 0.6 mol m^{-2} yr^{-1} using Eq. 5.1. Thus, the remaining 0.3 mol m^{-2} yr^{-1} of biogenic Si dissolves at the sediment-water interface, and J_{pb} would be 2 mol m^{-2} yr^{-1}. The burial rate of biogenic silica is 0.31-0.35 mol m^{-2} yr^{-1} at 30-50 cm sediment depth using Eq. 5.16. The dissolution rate within the sediment (J_d) would be greater than the 0.3 mol m^{-2} yr^{-1} value estimated by subtracting J_b from J_s. J_d agrees well with the measured efflux of dissolved $Si(OH)_4$ in the

flux cores and estimates from the nonlocal exchange model discussed below (Table 5.5). J_{Pb} is apparently greater than J_d in this environment, probably due to resuspension and higher pH, and lower concentration of $Si(OH)_4$ in the water column than in the sediments.

Distribution Patterns of Interstitial Water Solutes

Differences in the concentrations of dissolved constituents among cores are probably due to the horizontal inhomogeneity of sediments. Samples in the top 20 cm layer revealed a large variability from core to core, and significant gradients in the top 2 sections. At most sites the profiles show some common features, however. PO_4^{3-} concentrations were usually higher than NH_4^+ concentrations. This peculiar feature was noted also in the cores collected in previous years (Sugai, 1985). In most cases, there are maxima or minima in the profiles. For example in core BQ9G-1, PO_4^{3-} minima at 4 cm and 20 cm coincide closely with those for NH_4^+ and weakly with those for $Si(OH)_4$ and SO_4^{2-}. Also, in core BQ9-1, PO_4^{3-} minima correlate strongly with those of $Si(OH)_4$ and SO_4^{2-} but relate only weakly to those of NH_4^+. These features suggest that irrigation processes occur in the sediment, although the X-ray radiograph does not show any recognizable features such as slumping or

turbidity structure. Deep-burrowing (more than 10 cm) *Polychaetae* and *Nematertea* have been found in the floor of the central basin (VTN, 1982; C. Winiecki, 1985, Univ. of Alaska, pers. comm.).

NO_3^- and NO_2^- concentrations were below the analytical detection limit in all the cores. Sulfate reduction occurs above the subsurface nutrient maximum as indicated by strong gradients in the SO_4^{-2} concentrations with depth. Concentrations of organic matter decay products such as NH_4^+ and PO_4^{-3} are high, and the electron acceptors O_2, NO_3^-, NO_2^- are exhausted. Biogenic silica dissolution occurs in the sediments. Dissolved Mn and Fe distributions obtained by Hogarty (1985) in the same locality show that the upper layer above the subsurface maximum of nutrients is anoxic enough to maintain high levels of reduced metals. However, below this depth dissolved Mn and Fe show a common trend of a weak minimum and maximum and then decrease with depth (Fig. 5.9).

Sediment-Water Exchange Based on Flux Measurements

Direct flux measurements (Fig. 5.8) were compared to the linear vertical diffusion of dissolved silicate, [Si], using Eq. 5.17.

$$F = M/At = - \phi D_B (\partial [Si]/\partial z)_{z=0} \qquad (5.17)$$

where F = flux of solute across the sediment-water interface
M = mass of solute
A = cross-sectional area of flux cores
t = time
ϕ = porosity
D_s = sediment diffusion coefficient

Values of D_s (4.47×10^{-6} cm^2 s^{-1}) were estimated using the measured porosity (0.92) in the top portion of cores, and an empirical tortuosity correction, $D_s = \phi^2 D_o$ (Lerman, 1979) to the free solute diffusion coefficent for dissolved silicate, $D_o = 5.28 \times 10^{-6}$ cm^2 s^{-1} (corrected for temperature of 6.5 ^oC using the Stokes-Einstein relation, from the value of 5×10^{-6} cm^2 s^{-1} given by Wollast, 1974). Bottom water concentrations of dissolved Si were 60 to 70 uM. Taking the average dissolved Si concentration just below the sediment-water interface (0.75 cm) to be about 200 uM (Figs. 5.1-5.7), the diffusive flux would be around 800×10^{-9} umol cm^{-2} s^{-1}. However, this calculation is subject to considerable error because of the difficulty of estimating the concentration gradient at the interface.

A continuous decrease of NO_3^- in the overlying water of incubated cores is probably due to diffusion into the sediment and subsequent utilization as an electron acceptor for bacterial decay of organic matter. A similar trend of nitrate flux into the sediment was

observed *in situ* in San Clemente Basin by Jahnke *et al.* (1985), who suggested that nitrification is not rapid enough, relative to denitrification, to produce a nitrate maximum in the near-surface pore waters. They further suggested that NH_4^+ diffusing upward from the sulfate reduction zone is not escaping into the overlying water.

Sediment-Water Exchange Based on Modeling

The absence of a diffusion-type gradient in the pore water solute profiles in the near-surface sediment suggests that random Fickian-type diffusive mixing is not the dominant process transporting solute species. However, there is a possibility of non-steady-state deposition of sediment, such as slumping, in the fjord. Recently Hay *et al.* (1983) observed the meandering of subaqueous bottom channels in Rupert Inlet, British Columbia. However, Sugai (1985) found evidence for a particle by particle sedimentation in the central basin of Boca de Quadra, based on the ^{210}Pb and ^{137}Cs profiles. Also, the central basin is isolated from the direct influence of rivers and adjacent bays by the sills. It should be noted that non-steady-state deposition would result in fluctuations in the pore water profiles being preserved only if deposition were very rapid (>1 cm yr^{-1}), otherwise diffusion would smooth the profiles

(Lasaga and Holland, 1976). The shape of the cumulative mass *versus* depth (Figs. 3.7) may be further evidence that non-steady-state sedimentation of bulk sediment and organic matter would be unlikely in the BQ9G area.

The subsurface maxima and minima observed in the pore water profiles here are not unique. Similar profiles have been observed elsewhere. Grundmanis and Murray (1977) noted that silicate concentrations in the pore water profiles from 200 m depth of Puget Sound has a minimum at about 20-30 cm. This weak minimum in silicate concentration coincided with the nitrate maximum. They suggested that this silicate sink is due to the injection of low silicate bottom water by burrowing organisms. McCaffrey *et al.* (1980) also observed a $Si(OH)_4$ concentration profile with a maximum at 7 cm and minimum at 20 cm depth in shallow Naragansett Bay, Rhode Island sediments caused by polycheate worms. Emerson *et al.* (1984) have noted similar interstitial water profiles in the shallow waters (15 m deep) of Puget Sound.

In order to understand the complex features of the pore water profiles, a more sophisticated model is required to allow exchange between nonadjacent volume elements (in particular, pore water well below the sediment-water interface and overlying waters). The

connection allowing direct exchange is usually burrows of macrofauna. Aller (1980) developed a model in which exchange between pore water and overlying water is achieved by radial diffusion into vertically oriented burrows. The diagenetic equation which he developed is two-dimensional, and the transport process is molecular diffusion. Enhanced exchange over vertical molecular diffusion is achieved by decreasing the diffusion distance due to burrows below the sediment-water interface. That is, burrows hold water which is rapidly exchanged with overlying water. Aller found that his model predicts both pore water concentration profiles and fluxes across the sediment-water interface. However, his model requires substantial knowledge of the local fauna, such as the radius and length of burrows, their spacing and their density. Another model which describes nonlocal exchange is the "biopumping" model (McCaffrey *et al.*, 1980). Biopumping implies that pore water is vertically advected toward the sediment-water interface to balance the input of water through burrows. This model has been applied as a box model, predicting fluxes using transport parameters derived from the pore water profiles (*e.g.* Grundmanis and Murray, 1977); from *in situ* incubations of ^{22}Na (McCaffrey *et al.*, 1980), or using the ^{222}Rn radiotracer (e.g. Callender and Hammond, 1982).

Boudreau (1984) demonstrated that, if a linear approximation to dC/dr (Aller, 1980) at the burrow wall holds, Aller's radial diffusion model reduces to a nonlocal source model with an irrigation term similar to that in the biopumping models.

A positive feature of the model proposed by Emerson *et al.* (1984) is that it is relatively simple to apply to pore water profiles without requiring comprehensive knowledge of burrowing organisms. The simplified model presented by Emerson *et al.* for a dissolved constituent of concentration C is used here:

$$\frac{\partial C}{\partial t} = w\frac{\partial C}{\partial z} + D_s\frac{\partial^2 C}{\partial z^2} - \alpha(C - C_o/\phi) + R \qquad (5.18)$$

where w is the sedimentation rate, and D_s the Fickian-type sediment diffusion coefficient. α is a rate parameter used to evaluate the nonlocal source or sink which is assumed to be depth independent. C_o is the concentration in the overlying water, ϕ the porosity and R the reaction rate term. In Eq. 5.18, pore water transport is divided into three types: advection, diffusion and nonlocal exchange. The nonlocal source or sink is analogous to biopumping or to the radial diffusion term in the models noted previously. The nonlocal term simply means any mode of transport that is

capable of exchanging material between nonadjacent points in the sediments or between the overlying water and points in the sediments away from the sediment-water interface.

Since the concentration of $Si(OH)_4$ depends only on the mixing and dissolution of biogenic silica, silicate profiles are used to apply Eq. 5.18. Steady-state conditions, and a first-order dissolution of biogenic silica with respect to the difference between the local concentration [Si] and the asymptotic value $[Si]_a$ (Hurd, 1973) are assumed. Opal dissolution rates have been compiled by Emerson *et al.* (1984). Advection due to burial may be ignored since the sedimentation rate is low (0.2-0.3 cm yr^{-1}) compared with the other transport mechanisms. Eq. 5.18 may then be written:

$$0 = D_s \frac{\partial^2[Si]}{\partial z^2} - \alpha([Si] - [Si]_o/\phi) + k([Si]_a - [Si]) \quad (5.19)$$

For the boundary conditions:

$$[Si]_{z=o} = [Si]_o/\phi$$

$$\left.\frac{\partial[Si]}{\partial z}\right|_{z_1} = 0$$

where z_1 is the depth of minimum silicate concentration. A value for $[Si]_a$ of 800 uM has been estimated from profile BQ9G-1, and $[Si]_o$ here is 70 uM (measured). The biogenic silica dissolution rate is calculated to be 2 x

10^{-7} s^{-1} from the best fit of the dissolved Si profiles in the sediments. This rate lies within the range reported by Emerson et al. (1984). Eq. 5.19 was solved numerically using a finite difference method. Figs. 5.11 -5.13 give $[Si(OH)_4]$ profiles derived from Eq. 5.19 for different values of D_s. According to this model, silicate profiles near the sediment-water interface are produced only if a D_s value of 4.5 x 10^{-6} cm^2 s^{-1} is used (D_s is the molecular diffusion coefficient corrected for the tortousity). But to fit the subsurface minima of silicate, D_s must be enhanced to 2-3 x 10^{-5} cm^2 s^{-1}. The most likely explanation for this is that molecular diffusion process dominates transport near the sediment-water interface, while a non-local process controls the points well below the sediment-water interface. The nonlocal term required to fit the $[Si(OH)_4]$ profile at subsurface minima is 1 to 4 x 10^{-7} s^{-1}.

Silicate fluxes across the sediment-water interface resulting from diffusion, and from nonlocal processes, may be computed using the data of Figs. 5.11-5.13, and the integrated form of the right hand side of Eq. 5.19. That is:

$$F_T = F_D + F_{NL} \qquad (5.20)$$

where $$F_D = \phi D_s \frac{\partial [Si]}{\partial x}\Big|_{x=0} \qquad (5.21)$$

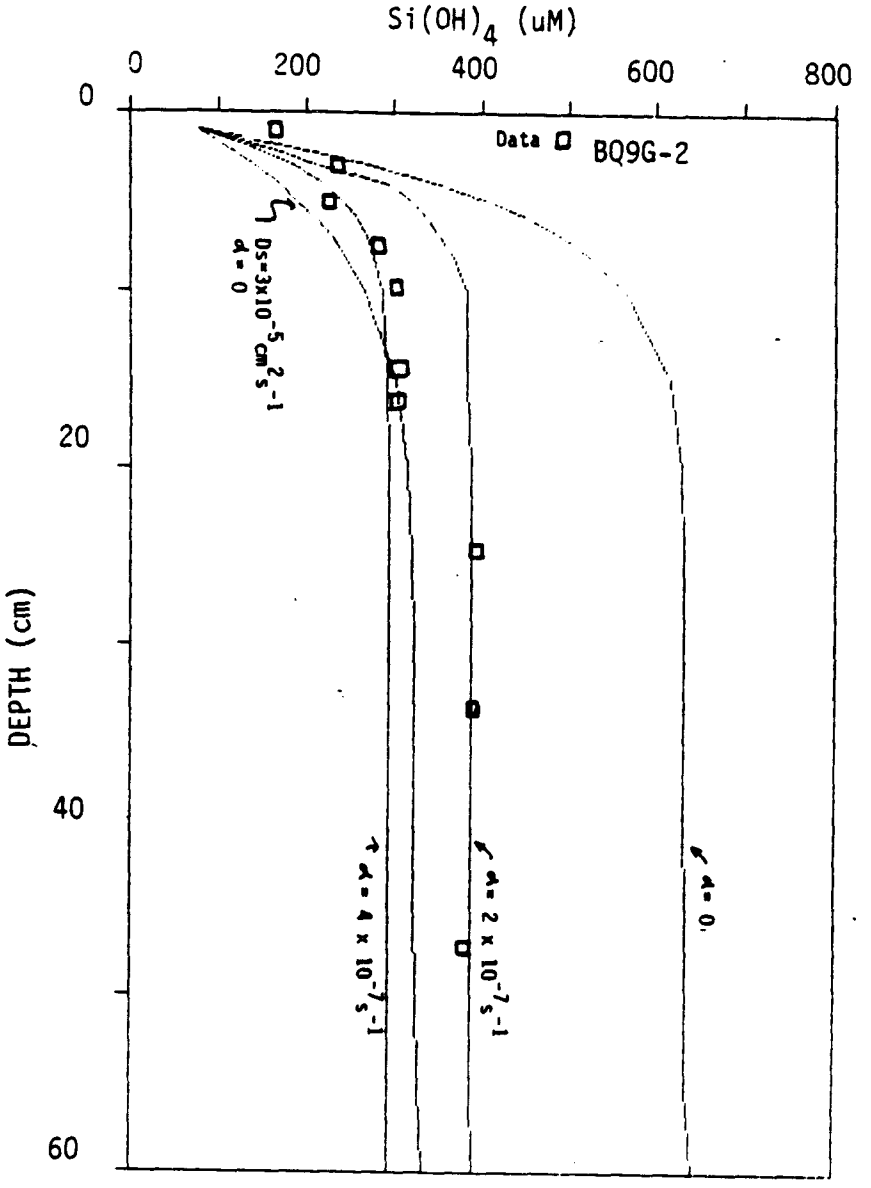

Fig. 5.11. Solutions to fit the model (see text) to the depth distribution of silicate for enhanced mixing with no nonlocal transport and molecular diffusion.

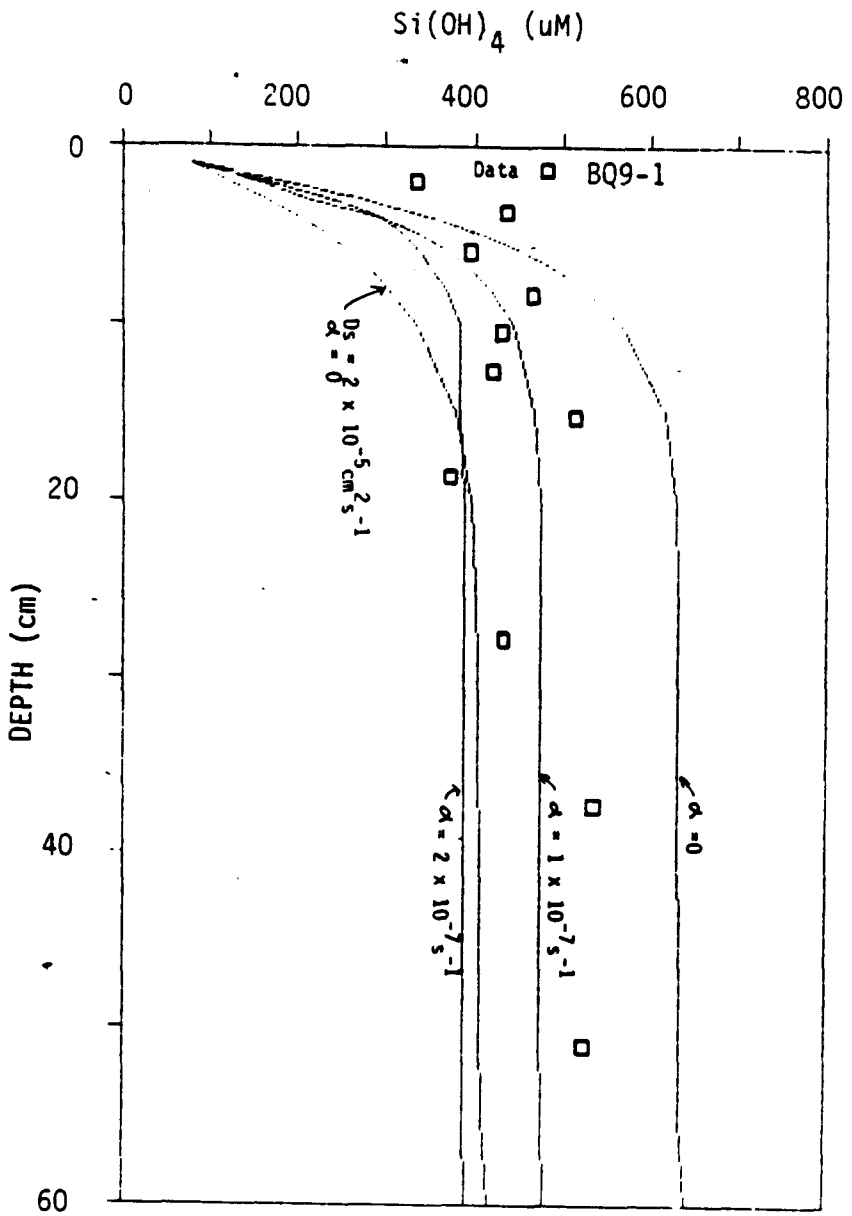

Fig. 5.12. Solutions to fit the model (see text) to the depth distribution of silicate for enhanced mixing with no nonlocal transport and molecular diffusion.

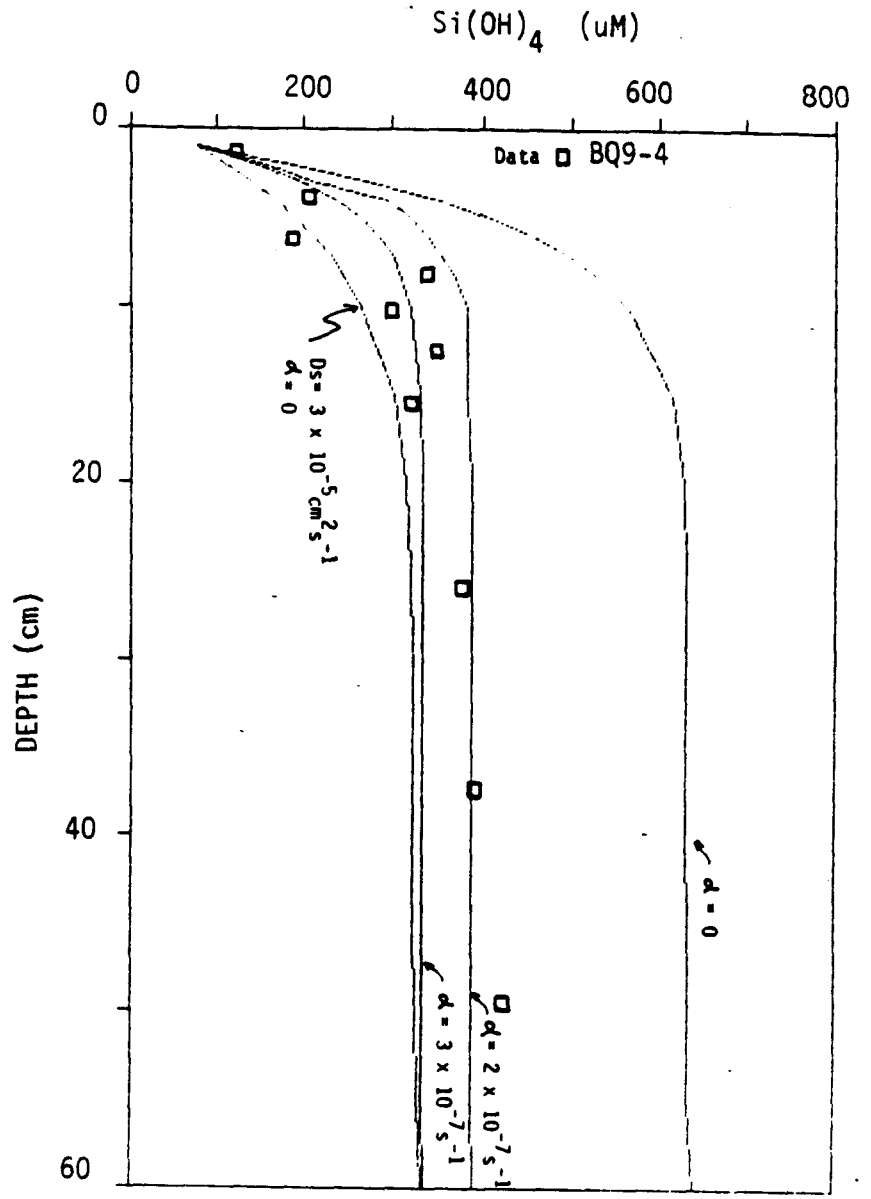

Fig. 5.13. Solutions to fit the model (see text) to the depth distribution of silicate for enhanced mixing with no nonlocal transport and molecular diffusion.

$$\text{and } F_{NL} = \alpha\left(\int_{z_1}^{0}(\phi[Si]dz - [Si]_0 \cdot \Delta z)\right) \qquad (5.22)$$

where F_T is the total flux combined flux due to diffusion (F_D) and nonlocal exchange (F_{NL}). The [Si] in each sampling interval was used to compute the F_{NL}. Flux computations for these cores using those equations are given in Table 5.5. $Si(OH)_4$ efflux from the sediment in the flux cores appears to agree with those calculated using this model. However, the great variability of $[Si(OH)_4]$ observed in Figs. 5.1-5.7 suggests that more comprehensive sampling would be required to estimate the areal fluxes in this study area. A comprehensive summary of the nonlocal effects in a number of other coastal environments has been compiled by Emerson *et al.* (1984). The magnitude of the nonlocal term in the central basin is similar to that found in Puget Sound. Nonlocal transport enhances the removal of breakdown products of oxidation of organic matter, and simultaneously supplies higher energy yield electron acceptors to the deeper part of the sediments. This should result in reduction of organic matter in the sediments (Aller and Mackin, 1984).

CONCLUSIONS

The major findings of this study on the early diagenesis of biogenic matter in sediments in terms of their relationship to settling fluxes in the water column

Table 5.5. Comparison between molecular diffusion and nonlocal transport of [$Si(OH)_4$] across the sediment-water interface. Bottom water [$Si(OH)_4$] is 70 uM. D_s is 4.5 x 10^{-6} cm^2 s^{-1} and ϕ is taken as 0.92.

		Flux (x 10^{-9} umol cm^{-2} s^{-1})				
Station	$\frac{d[Si]}{dz}\Big\|_{z=0}$ ($\times 10^{-3}$ umol cm^{-4})	F_D	z_1 (cm)	α	F_{NL}	F_T
BQ9G-2	164	677	17.4	1-4	235-940	912-1617
BQ9-1	258	1067	14.1	1-2	381-762	1448-1829
BQ9-4	100	413	17.3	1-3	331-993	744-1406

are:

1. Most of the particulate organic matter raining to the sediment-water interface appears to be decomposed at or near the sediment-water interface rather than in the sediment. Sediment resuspension contributes greatly to the oxidation of organic matter in the benthic regime. Most biogenic silica raining to the basin floor also appears to dissolve at or near the sediment-water interface rather than within the sediments.

2. Reduction of manganese oxides in the sediments appears to account for a half of sedimentary organic matter oxidation (0.2–0.3 mol C m^{-2} yr^{-1}). This is a result of active cycling of dissolved Mn in the benthic boundary layer. The sediment column is anoxic with a very thin oxic layer at the top. Sulfate reduction appears to occur also close to the sediment-water interface, which suggests the presence of micro-redox environments caused by sediment mixing and irrigation processes.

3. The distribution of pore water solute concentrations is strongly regulated by nonlocal mechanisms, probably caused by deep burrows. The transport process of sediment pore water is dominated by molecular diffusion in the top few centimeters and probably by animal activity in the deeper layers. The

value of the transport parameter for the nonlocal process is 1 to 4 x 10^{-7} s^{-1}. Nonlocal process is comparable to diffusion process as means of exchange of interstitial water with overlying water column.

CHAPTER 6. SUMMARY AND CONCLUSIONS

The primary goals of this work were to characterize the natural sedimentation dynamics in a non-glacial Alaskan fjord. This has included an investigation of the physical, chemical and biological processes controlling the fate of particulate organic carbon, nitrogen, biogenic silica, manganese and iron in the water column and in the bottom sediments. The study has been based on frequent collection of settling particulates using sediment traps, but interpretation has required a vast amount of ancillary oceanographic information gathered previously and concurrently in the study area.

A hypothesis was made concerning the factors controlling the increase of SPM concentration and flux with depth: lateral input, fecal pellet production in the deeper layer due to the migrating zooplanktons, hydrographic and current regimes, sediment focusing due to the "V" shaped basin, and resuspension from the bottom. It was tested based on the physical oceanography of the basin, elemental composition of SPM (Al, C, N and biogenic Si), elemental settling fluxes in the water column, and sedimentation rates and solid phase Al concentration in the sediments. A substantial lateral input of SPM from the bottom of the side arms was noted

at the around 120 m depth horizon. SPM production *via* zooplankton which feed in the shallow waters and defecate in the deeper waters was ruled out because the decrease in POC concentration in the settling particulates with depth. Sediment focusing due to the decreasing horizontal area with depth was not seen in the settling SPM flux data, nor in the sedimentation rate and concentration of organic matter in the basin floor sediment. Therefore, resuspension was appeared to be primarily responsible for increasing the concentration and vertical flux of SPM in the deep basin below 120 m depth, probably due to the occasional strong currents along the bottom and the poorly stratified deep basin water column.

The most important conclusion from this study is that understanding the bulk SPM sedimentation dynamics is a prerequisite to an interpretation of the behavior of non-conservative constituents of the particulate matter. A mass balance approach to the SPM dynamics allows an investigator to know what the quantitatively important processes are. Even a moderate amount of resuspension regulates the degradation of biogenic matter in a fjord basin to a significant degree. Well defined primary and resuspended fluxes permit semi-quantification of the degradation of organic matter, and biogenic silica and

authigenic formation of Mn and Fe containing particles in the benthic nepheloid layer. This approach may be applicable in many marine environments other than fjord basins.

Since the Boca de Quadra fjord is pristine, natural sedimentation processes may be particularly sensitive to the development of the environment in the future. The major specific findings are summarized below.

1. SPM being introduced by the rivers (primarily the Keta, Marten, and Red Rivers) would account for almost all the sediment deposited on the basin floor above the Kite Island sill. The SPM in the inner basin is optically different from that in the other Boca de Quadra basins, due probably to the proximity of the river and the presence of the inner sill.

2. In the central basin, the settling flux of particulates in the surface zone (at 40 m depth) is very well correlated with the flux at deeper depths, emphasizing the dominance of vertical transport. Although it is very difficult to assess sediment focusing resulting from the "V" shaped basin morphology, it does not appear to be important in the central basin. But the intermittent input of SPM from the benthic nepheloid layer of Marten Arm and Mink Bay does appear to be

significant. In the deep basin, resuspension seems to be primarily responsible for the increase in vertical flux and concentration of SPM. Thus, the vertical flux measured at the 120 m depth horizon may be regarded as the primary flux for the basin below the sill height. Resuspension may then account for 50-80% of settling particulates at 300 m depth.

3. Algal primary production *in situ* provides the major portion of settling particulate organic matter with a minor contribution from terrestrial input *via* rivers (about 30%). The major means of transporting phytodetritus from the surface waters to deep waters appear to be *via* settling of large intact cells, fecal pellets, and aggregates of cells. A strong seasonality was evident in the settling fluxes of POC, PN, biogenic Si, particulate Mn and Fe. In particular, a sharp primary production peak in spring was reflected nearly simultaneously in the settling fluxes throughout the water column, and subsequently decomposition of POC, PN and dissolution of biogenic Si reached a maximum. Authigenic formation of particles containing Mn and Fe was also pronounced at this time of the year.

4. The decompositon rates of settling POC and PN are estimated to be 0.85 ± 0.75 and 0.11 ± 0.09 mol m^{-2} yr^{-1}, respectively. The dissolution rate of biogenic Si is

estimated to be 0.57 ± 0.90 mol m^{-2} yr^{-1} in the water column using a primary-resuspended-altered flux model. Most particulate Mn settling below 120 m depth is believed to be of authigenic origin, and the rate of authigenic Mn formation is estimated to be 12 to 34 mg Mn m^{-2} d^{-1}. However, a significantly smaller authigenic contribution of particulate Fe was observed. This may be attributed to the active recycling (reduction of Mn in sediment and subsequent reoxidation in the water column) of dissolved Mn in the benthic boundary later.

5. Particulate organic matter raining to the sediment-water interface appears to be decomposed largely at or near the sediment-water interface rather than within the sediment. Sediment resuspension activity would greatly contribute to the oxidation of organic matter in the benthic boundary layer. Also, most of the biogenic silica raining to the basin floor appears to be dissolved at or near the sediment-water interface rather than within the sediments.

6. The sediment column is predominately anoxic with a very thin oxic layer at the top. Sulfate reduction appears to occur close to the sediment-water interface. The distribution of pore water concentrations appears to be strongly regulated by nonlocal mechanisms, probably

deep burrows. The transport process of sediment pore water may be dominated by molecular diffusion in the top few centimeters, but probably is mostly due to animal activity in the deeper layers. The value of the transport parameter for the nonlocal exchange process is estimated at 1-4 X 10^{-7} s^{-1}.

FUTURE WORK

The next step in understanding the sedimentation dynamics within the fjord environment would be to address a number of questions raised by this study. Three major questions are: (i) a quantitative evaluation of the sources of SPM to the deep basin; (ii) potential exchange of SPM across the Kite Island sill; (iii) a quantitative estimation of oxygen and nutrient fluxes across the sediment-water interface.

A simultaneous measurement of primary productivity in the basin proper and in the river, together with $\delta^{13}C$ measurements of seawater phytoplankton, freshwater phytoplankton, and various terrestrial plants (and different parts of the plants) might help to delineate the various particulate organic matter sources more clearly. Also, it was not possible to discriminate quantitatively between suspended sediment input *via* the bottom of the adjacent bays, resuspension from the

bottom, and sediment focusing in the central basin of Boca de Quadra. However, comparison of the observed vertical flux patterns and sedimentation rate measurements at the basin floor suggested that significant input of SPM *via* the bottom of the adjacent bays and resuspension activity are largely responsible for the depth distribution of the settling flux of SPM. A more precise evaluation of the magnitude of each of the three - inputs from the adjacent bays, resuspension, and sediment focusing - could be made in the following way. Since strong temporal changes in environmental conditions occur in this type of estuary, a sampling interval shorter than half the period of the variation must be employed in order to observe the temporal changes. In order to do this, the following instruments should be deployed: (i) a time-series sediment trap whose sampling interval can be appropriately set. At least two traps are needed, one at the just above the benthic nepheloid layer and the other close to the bottom; and (ii) transmissometers moored just below the pycnocline, at the 1% light level, at the depth of mouth of the adjacent bays, and close to the basin floor with concurrent STD and current measurements. An echo sounder would be a good alternative for the light transmissometer, provided

that it could be moored, because it could cover the entire water column unlike the transmissometer which can only "see" short distances.

It was not possible to determine the import and export of SPM across the Kite Island sill. A numerical effort to estimate this is underway. However, synoptic measurements of concentration and size distribution of SPM would enhance the reliability of the model prediction.

Since benthic organisms are probably patchily distributed and the bottom is complex, a large number of core-top incubations on the oxygen and nutrient fluxes, or similar measurements made using a bottom lander (Janke *et al.*, 1985) type *in situ* device, would enhance understanding of the energy and material transfer across the sediment-water interface. Information on the benthic organisms in the deep basin floor will also increase understanding of the pore water solute concentration depth profiles.

REFERENCES

Aller, R. C. 1980. Quantifying solute distributions in the bioturbated zone of marine sediments by defining an average micro environment. Geochim. Cosmochim. Acta. 44:1955-1966

Aller, R. C. and J. E. Mackin. 1984. Preservation of reactive organic matter in marine sediments. Earth Planet. Sci. Lett. 70:260-266.

Anderson, G. F. 1986. Silica, diatoms and a freshwater productivity maximum in Atlantic coastal plain estuaries, Chesapeake Bay. Estuar. Coast. Shelf Sci. 22:183-197.

Angel, M. V. 1984. Detrital organic fluxes through pelagic ecosystems. In Fasham, M. J. R. (ed.), *Flows of Energy and Materials in Marine Ecosystems. Theory and Practice.* Plenum Press.

Armstrong, F. A. J., C. R. Stearns, and J. D. H. Strickland. 1967. The measurement of upwelling and subsequent biological processes by means of the Technicon Auto-Analyzer and associated equipment. Deep-Sea Res. 14:381-389.

Baker, E. T., G. A. Cannon, and H. C. Curl, Jr. 1983. Particle transport processes in small marine bay. J. Geophys. Res. 88:9661-9669.

Baker, E. T., R. A. Feely, M. R. Landry and M. Lamb. 1985. Temporal variations in the concentration and settling flux of carbon and phytoplankton pigments in a deep fjordlike estuary. Estuar. Coast. Shelf Sci. 21:859-877.

Baker, E. T. and J. W. Lavelle, 1984. The effect of particle size on the light attenuation coefficient of natural suspensions. J. Geophys. Res. 89:8197-8203.

Banahan, S. 1983. The uptake of silicic acid by diatoms in the Bering Sea. M.S. Thesis. Univ. of Alaska, Fairbanks. 121p.

Bartz, R., J. R. Zaneveld and H. Pak. 1978. A transmissometer for profiling and moored observations in water. SPIE Vol. 160. Ocean Optics V:102-108.

Berger, W. H. and G. R. Heath. 1968. Vertical mixing in pelagic sediments. J. Mar. Res. 26:134-143.

Berger, W. H. and J. W. Piper. 1972. Planktonic foraminifera: differential settling, dissolution, and redeposition. Limnol. Oceanogr. 17:275-287.

Berner, R. A. 1980. *Early Diagenesis: A Theoretical Approach.* Princeton Univ. Press. 241p.

Biscaye, P. G. and S. L. Eittreim. 1977. Suspended particulate loads and transports in the nepheloid layer of the abyssal Atlantic Ocean. Mar. Geol. 23:155-172.

Bishop, J. K. 1986. The correction and suspended matter calibration of Sea Tech transmissometer data. Deep-Sea Res. 33:121-134.

Blomqvist, S. and L. Hakanson, 1981. A review on sediment traps in aquatic environments. Arch. Hydrobiol. 91:101-132.

Blomqvist, S. and C. Kofoed. 1981. Sediment trapping - A subaquatic *in situ* experiment. Limnol. Oceanogr. 26:585-590.

Boudreau, B. 1984. On the equivalence of nonlocal and radial-diffusion models for porewater irrigation. J. Mar. Res. 42:731-735.

Brewer, P. G., D. W. Spencer, P. E. Biscaye, A. Henley, P. L. Sachs, C. L. Smith, S. Kardarand and J. Fredericks. 1976. The distribution of particulate matter in the Atlantic Ocean. Earth Planet. Sci. Lett. 32:393-402.

Bruland, K. W., R. P. Franks, W. Landing and A. Soutar. 1981. Southern California inner basin sediment trap calibration. Earth Planet. Sci. Lett. 53:400-408.

Bruland, K. W. and M. W. Silver. 1981. Sinking rates of fecal pellets from gelatinous zooplankton (Salps, Pterpods, Dolloids). Mar. Biol. 63:295-300.

Burrell, D. C. 1981. Marine environmental studies in Boca de Quadra and Smeaton Bay: Chemical and Geochemical, 1980. Unpublished Report. Inst. Mar. Sci. Univ. of Alaska, Fairbanks.

Burrell, D. C. 1983a. Patterns of carbon supply and distribution and oxygen renewal in two Alaskan fjords. Sediment. Geology. 36:93-115.

Burrell, D. C. 1983b. The biogeochemistry of Boca de Quadra and Smeaton Bay, southeast Alaska. A summary report on investigations 1980 - 1983. Unpbulished Report. Inst. Mar. Sci. Univ. of Alaska, Fairbanks.

Burrell, D. C. 1986. Interaction between silled fjords and coastal regions of the Gulf of Alaska. In Hood, D. W. (ed.) *The Gulf of Alaska: Physical Environment and Biological Resources.* (in press)

Burrell, D. C., H. J. Niebauer, and D. Nebert. 1980. Marine environmental studies in Boca de Quadra and Smeaton Bay: Physical and Chemical, 1979. Unpublished Report. Inst. Mar. Sci. Univ. of Alaska, Fairbanks.

Callender, E. and D. E. Hammond. 1982. Nutrient exchange across the sediment-water interface in the Potomac River estuary. Estuarine Coast. Shelf. Sci. 15:395-413.

Carpenter, R., J. T. Bennett and M. L. Peterson. 1981. ^{210}Pb activities in and fluxes to sediments of the Washington continental slope and shelf. Geochim. Cosmochim. Acta 45:1155-1172.

Chester, A. J. and J. D. Larrance. 1981. Composition and vertical fluxes of organic matter in a large Alaskan estuary. Estuaries 4:42-52.

Collier, R. and J. Edmond. 1984. The trace element geochemistry of marine biogenic particulate matter. Progr. Oceanogr. 13:113-199.

Cooper, L. C. 1986. Stable carbon isotope ratio variations within marine macrophytes from the Northeast Pacific. Ph.D. Thesis. Univ. of Alaska, Fairbanks. 134p.

Craig, H. 1953. The geochemistry of the stable carbon isotopes. Geochim. Cosmochim. Acta 3:53-92.

Cresswell, G. R. and D. L. Nebert. 1986. Temperature and salinity features of Boca de Quadra, a fjord in southeast Alaska (in preparation).

Cronin, J. R. and R. J. Morris. 1983. Rapid formation of humic material from diatom debris. In Suess, E. and J. Thiede (eds.). *Coastal Upwelling: Its Sediment Record.* Part A. pp485-496. Plenum.

Davis, J. M. 1975. Energy flow through the benthos in a Scottish Sea Loch. Mar. Biol. 31:353-362.

Davis, R. A. 1971. *Coastal Sedimentary Environment.* Springer Verlag, 420p.

DeMaster, D. J. 1981. The supply and accumulation of silica in the marine environment. Geochim. Cosmochim. Acta. 45:1715-1732.

Eadie, B. J. and L. M. Jeffrey. 1983. $\delta^{13}C$ analysis of oceanic particulate organic matter. Mar. Chem. 1:199-209.

Emerson, S., R. Jahnke and D. Heggie. 1984. Sediment-water exchange in shallow water estuarine sediements. J. Mar. Res. 42:709-730.

Emerson, S., K. Fisher, C. Reimers and D. Heggie. 1985. Organic carbon dynamics and preservation in deep-sea sediments. Deep-Sea Res. 32:1-21.

Fauchald, K, and P. A. Jumars. 1979. The diet of worms: a study of polychaete feeding guilds. Oceanogr. Mar. Biol. Ann: Rev. 17:193-284.

Feely, R. A. 1976. Evidence for aggregate formation in a nepheloid layer and its possible role in the sedimentation of particulate matter. Mar. Geol. 20:M7-M13.

Feely, R., G. J. Massoth, E. T. Baker, J. F. Gendron, A. J. Paulson and E. A. Crecelius. 1986. Seasonal and vertical variations in the elemental composition of suspended and settling particulate matter in Puget Sound, Washington. Estuar. Coast. Shelf Sci. 22:215-239.

Froelich, P. N., G. P. Klinkhammer, M. L. Bender, N. A. Luedtke, G. R. Heath, D. Cullen, P. Dauphin, D. Hammond, B. Hartman, and V. Maynard. 1979. Early oxidation of organic matter in pelagic sediments of the eastern Equatorial Atlantic: suboxic diagenesis. Geochim. Cosmochim. Acta. 43:1075-1090.

Fry, B. and E. B. Sherr. 1984. $\delta^{13}C$ measurements as indicators of carbon flow in marine and freshwater ecosystems. Contrib. Mar. Sci. 27:13-47.

Gardner, W. D. 1977. Fluxes, dynamics and chemistry of particulates in the ocean. Ph.D. Thesis, MIT/WHOI. 394p.

Gardner, W. D. 1980. Field assessment of sediment traps. J. Mar. Res. 38:41-52.

Gardner, W. D. 1985. The effect of tilt on sediment trap efficiency. Deep-Sea Res. 32:349-361.

Gearing, J. N., P. J. Gearing, D. T. Rudnick, A. G. Requejo and M. J. Hutchins. 1984. Isotopic variability of organic carbon in phytoplankton - based temperate estuary. Geochim. Cosmochim. Acta 48:1089-1098.

Grundmanis, V. and J. W. Murray. 1977. Nitrification and denitrification in marine sediments from Puget Sound. Limnol. Oceanogr. 22:804-813.

Grundmanis, V. and J. W. Murray. 1982. Aerobic respiration in pelagic marine sediments. Geochim. Cosmochim. Acta. 46:1101-1120.

Guinasso, N. L. Jr. and D. R. Schink. 1975. Quantitative estimates of biological mixing rates in abyssal sediments. J. Geophys. Res. 80:3032-3043.

Hakanson, L. M. Jansson. 1983. *Principles of Lake Sedimentology*. Springer Verlag. Berlin. 316p.

Hargrave, B. T. 1969. Similarity of oxygen uptake by benthic communities. Limnol. Oceanogr. 14:801-805.

Hargrave, B. T. 1973. Coupling carbon flow through some pelagic and benthic communities. J. Fish. Res. Bd. Can. 30:1317-1326.

Hargrave, B. T. 1978. Seasonal changes in oxygen uptake by settled particulate matter and sediments in a marine bay. J. Fish. Res. Board Canada. 35:1621-

Hargrave, B. T. and N. M. Burns. 1979. Assessment of sediment trap collection efficiency. Limnol. Oceanogr. 24:1128-1136.

Hargrave, B. T. and L. K. Nielsen. 1977. Accumulation of sedimentary organic matter at the base of steep bottom gradients. In Golterman, H. L. (ed.), *Interactions Between Sediments and Freshwater*, Dr. W. Junk B. V. Publ. The Hague.

Hargrave, B. T. and S. Taguchi. 1978. Origin of deposited material in a marine bay. J. Fish. Res. Bd. Can. 35:1604-1613.

Harrison, P. J., H. L. Conway, R. W. Holmes and C. O. Davis. 1977. Marine diatoms grown in chemostats under silicate or ammonium limitation. III. Celluar chemical compostion and morphology of *Chaetoceros debilis, Skeletonema costatum*, and *Thalassiosira gravida*. Mar. Biol. 43:19-31.

Hay, A. E. Burling, R. W. and J. W. Murray. 1982. Remote acoustic detection of a turbidity current surge. Sci. 217:833-835.

Heggie, D. T. 1977. Copper in the sea: a phsical-chemical study of reservoirs, fluxes and pathways in an Alaskan fjord. Ph. D. Thesis. Univ. of Alaska. 214p.

Hedges, J. I. and D. C. Mann. 1979. The lignin geochemistry of marine sediments from the southern Washington coast. Geochim. Cosmochim. Acta. 43:1809-1818.

Hilton, J. 1985. A conceptual framework for predicting the occurrence of sediment focusing and sediment redistribution in small lakes. Limnol. Oceanogr. 30:1131-1143.

Hogarty, B. J. 1985. The fate of molybdenum and other heavy metals in two southeast Alaska Fjords. M.S. Thesis. Univ. of Alaska, Fairbanks, 151p.

Honjo, S. 1982. Seasonality and interaction of biogenic and lithogenic particulate flux at the Panama Basin. Sci. 218:883-884.

Hoskin, C. W., D. C. Burrell and G. R. Freitag. 1976. Suspended sediment dynamics in Queen Inlet, Glacier Bay, Alaska. Mar. Sci. Comm. 2:95-108.

Hoskin, C. M., D. C. Burrell and G. R. Freitag. 1978. Suspended sediment dynamics in Blue Fjord, western Prince William Sound, Alaska. Estuar. Coast. Mar. Sci. 7:1-16.

Hunt, C. D. 1983. Incorporation and depostion of Mn and other trace metals by flocculent organic matter in a controlled marine ecosystem. Limnol. Oceanogr. 28:302-308.

Hurd, D. C. 1973. Interactions of biogenic opal sediment and seawater in the central Equatorial Pacific. Geochim. Cosmochim. Acta 37:2257-2282.

Jahnke, R. A., R. F. Weiss, C. E. Reimers, M. L. Bender, D. T. Heggie, S. R. Emerson and D. C. McCorkle. 1985. Exchange of bioactive elements across the sediment-water interface in a deep coastal basin: *In situ* measurements. EOS 66:286.

Jerlov, N. G. 1976. *Marine Optics*. Elsevier, New York.

Jorgensen, B. B. 1978. A comparison of methods for quantification of bacterial sulfate reduction in coastal marine sediments. I. Measurement with radiotracer techniques. Geomicrobiol. J. 1:11-27.

Jorgensen, B. B. 1982. Mineralization of organic matter in the sea bed - the role of sulphate reduction. Nature 296:643-645.

Kanneworf, E. and W. Nicolaisen. 1973. The "Haps", a frame supported bottom corer. Ophelia 10:119-128.

Kipphut, G. W. 1978. An investigation of sedimentary processes in lakes. Ph.D. Thesis. Columbia Univ. 179p.

Knauer, G. A., J. M. Martin and K. W. Bruland. 1979. Fluxes of particulate carbon, nitrogen and phosphorous in the upper water column of the northeast Pacific. Deep-Sea Res. 26:97-108.

Komar, P. D. 1976. *Beach Processes and Sedimentation.* 426p. Prentice-Hall.

Komar, P. D., A. P. Morse, L. F. Small, and S. W. Fowler. 1981. An analysis of sinking rates of natural copepod and euphausiid fecal pellets. Limnol. Oceanogr. 26:172-180.

Koroleff, F. 1970. Information on techniques and methods for seawater analysis. Int. Counc. Explor. Sea Interlab. Rep. no. 3:10-22.

Kowalik, Z. 1984. The physical oceanography of Boca de Quadra: Numerical modeling of fjord circulation and submarine disposal of mine tailings in Boca de Quadra, southeast Alaska. Report for U. S. Borax. Institute of Marine Science, Univ. of Alaska, Fairbanks.

Lal, D. 1977. The oceanic microcosm of particles, suspended particulate matter. Sci. 198:997-1009.

Lal, D. 1980. Comments on some aspects of particulate transport in the ocean. Earth Planet. Sci. Lett. 49:520-527.

Lambert, C. E., J. K. Bishop, P. E. Biscaye and R. Chesslet. 1984. Particulate aluminium, iron and manganese chemistry at the deep Atlantic boundary layer. Earth Planet. Sci. Lett. 70:237-248.

Lambert, C. E., C. Jehanno, N. Silberberg, J. C. Brun-Cottan and R. Chesselet. 1981. Log-normal distributions of suspended particles in the open ocean. Deep-Sea Res. 39:77-98.

Lasaga, A. C. and H. D. Holland. 1976. Mathematical aspects of non-steady-state diagenesis. Geochim. Cosmochim. Acta 40:257-266.

Lau, Y. L. 1979. Laboratory study of cylindrical sedimentation traps. J. Fish. Res. Board Can. 36:1288-1291.

Lavelle, J. W., H. O. Mofjeld and E. T. Baker. 1984. An *in situ* erosion rate for a fine-grained marine sediment. J. Geophys. Res. 89:6543-6552.

Lawson, D. S., D. C. Hurd and H. S. Pankratz. 1978. Silica dissolution rates of decomposing phytoplankton assemblages at various temperatures. Am. J. Sci. 278:1373-1393.

Lee, C., S. G. Wakeham and J. W. Farrington. 1983. Variations in the composition of particulate organic matter in a time-series sediment trap. Mar. Chem. 13:181-194.

Lerman, A. 1979. *Geochemical Process: Water and Sediment Environments*. John Wiley and Sons. New York. 481p.

Lorenzen, C. J., F. R. Shuman and J. T. Bennet. 1981. *In situ* calibration of a sediment trap. Limnol. Oceanogr. 26:580-585.

Mackin, J. and R. C. Aller. 1984. Dissolved Al in sediments and waters of the East China Sea: Implications for authigenic mineral formation. Geochim. Cosmochim. Acta 48:281-297.

Marinucci, A. C., J. E. Hobbie, J. V. K. Helfrich. 1983. Effect of litter nitrogen on decompostion and microbial biomass in *Spartina alterniflora*. Microb. Ecol. 9:27-40.

Martens, C. S. and J. V. Klump. 1984. Biogeochemical cycling in an organic-rich coastal marine basin. 4. An organic carbon budget for sediments dominated by sulfate reduction and methanogenesis. Geochim. Cosmochim. Acta 48:1987-2004.

Martin, W. R. 1985. Transport of trace metals in nearshore sediments. Ph.D. Thesis. MIT/WHOI. 302p

McCaffrey, R. J., A. C. Myers, E. Davey, G. Morrison, M. Bender, N. Luedtke, D. Cullin, P. Froelich, and G. Klinkhammer. 1980. The relation between pore water chemistry and benthic fluxes of nutrients and manganese in Naragansett Bay, Rhode Island. Limnol. Oceanogr. 25:31-44.

McCave, I. N. 1975. Vertical flux of particles in the ocean. Deep-Sea Res. 22:491-502.

Meyers, P. A., M. J. Leenheer, B. J. Eadie and S. J. Mauk. 1984. Organic geochemistry of suspended and settling particulate matter in Lake Michigan. Geochim. Cosmochim. Acta 48:443-452.

Miller, L. G. 1980. Dissolved inorganic carbon isotope ratios in reducing marine sediments. M.S. Thesis. Univ. of Southern California. 101p.

Muench, R. D. and D. T. Heggie. 1978. Deep water exchange in Alaskan subartic fjords. In Kjertve (ed.), *Estuarine Transport Processes*, Univ. of South Carolina.

Muller, P. J. and E. Suess. 1979. Productivity, sedimentation rate and sedimentary organic matter in the oceans. I. Organic carbon preservation. Deep-Sea Res. 26:1347-1362.

Murphy, J. and J. P. Riley. 1962. A modified single solution method for the determination of phosphate in natural waters. Anal. Chim. Acta 27:31-36.

Murray, J. W. and G. Gill. 1978. The geochemistry of iron in Puget Sound. Geochim. Cosmochim. Acta 9-19.

Nelson, D. M. and J. J. Goering. 1977. Near-surface silica dissolution in the upwelling region off northwest Africa. Deep-Sea Res. 24:65-73.

Nelson, D. M. and L. I. Gordon. 1982. Production and pelagic dissolution of biogenic silica in the Southern Ocean. Geochim. Cosmochim. Acta 46:491-501.

Nebert, D. L. 1984. Physical Oceanography of Boca de Quadra. Unpublished report to U. S. Borax, Institute of Marine Science, Univ. of Alaska, Fairbanks.

Nittrouer, C. A., R. W. Sternberg, R. Carpenter and J. T. Bennett. 1979. The use of Pb-210 geochronology as a sedimentological tool: Application to the Washington continetal shelf. Mar. Geol. 31:297-316.

Officer, C. B. 1982. Mixing, sedimentation rates and age dating for sediment cores. Mar. Geol. 46:261-278.

O'Leary, M. 1981. Carbon isotope fractionation in plants. Phytochem. 22:553-567.

Olsen, C. R., N. H. Cutshall, and I. L. Larsen. 1982. Pollutant particle associations and dynamics in coastal marine environments: A review. Mar. Chem. 11:501-533.

Pak, H. and J. R. Janeveld. 1977. Bottom nepheloid layers and bottom mixed layers observed on the continental shelf off Oregon. J. Geophys. Res. 82:3921-3931.

Pamatmat, M. M. and K. Banse. 1969. Oxygen consumption by the sea bed. 2. *In situ* measurements to a depth of 180 m. Limnol. Oceanogr. 14:250-259.

Peters, K. E., R. E. Sweeney and I. R. Kaplan. 1978. Correlation of carbon and nitrogen isotope ratios in sedimentary organic matter. Limnol. Oceanogr. 23:598-604.

Peterson, R. L. 1977. A study of suspended particualte matter: Arctic Ocean and northern Oregon continental shelf. Oregon State Univ. 122p.

Peterson, B. J., R. W. Howarth and R. H. Garritt. 1985. Multiple stable isotopes used to trace the flow of organic matter in estuarine food webs. Sci. 227:1361-1363.

Pond, S. and G. L. Pickard. 1981. *Introductory Dynamic Oceanography*. Pergamon Press, Oxford. 241p.

Prahl, F. G., J. T. Bennett and R. Carpenter. 1980. The early diagenesis of aliphatic hydrocarbons and organic matter in sedimentary particulates from Dabob Bay, Washington. Geochim. Cosmchim. Acta 44:1967-1976.

Redfield, A. C., B. H. Ketchum and F. A. Richards. 1963. The influence of organisms on the composition of seawater. In Hill, M. N. (ed.). *The Sea*. Vol. 3. Wiley Interscience, New York.

Reeburgh, W. S. 1967. An improved interstitial water sampler. Limnol. Oceanogr. 12:163-165.

Reeburgh, W. S. 1983. Rates of biogeochemical processes in anoxic sediments. Ann. Rev. Earth Planet. Sci. 11:269-298.

Reimers, C. E. and E. Suess. 1983. The partitioning of organic carbon fluxes and sedimentary organic matter decomposition rates in the ocean. Mar. Chem. 13:141-168.

Robb, M. S. 1981. Composition and manganese association of suspended matter at the head of a southeast Alaskan fjord. M.S. Thesis. Univ. of Alaska, Fairbanks. 185p.

Robbins, J. A. 1978. Geochemical and geophysical applications of lead. In Niragu, J. O. (ed.) *The Biogeochemistry of Lead in the Environment.* pp285-293. Elsevier.

Robbins, J. A. and D. N. Edginton. 1975. Determination of recent sedimentation rates in Lake Michigan using Pb-210 and Cs-137. Geochim. Cosmochim. Acta 39:285-304.

Royer, T. C. 1975. Seasonal variations of waters in the northern Gulf of Alaska. Deep-Sea Res. 22:403-416.

Shanks, A. and J. Trent. 1979. Marine snow: microscale nutrient patches. Limnol. Oceanogr. 24:850-853.

Shaw, D. G., M. J. Alperin, W. S. Reeburgh and D. J. McIntosh. 1984. Biogeochemistry of acetate in anoxic sediments of Skan Bay, Alaska. Geochim. Cosmochim. Acta 48:1819-1825.

Sholkovitz, E. R. and D. R. Mann. 1984. The pore water chemistry of $^{239,240}Pu$ and ^{137}Cs in sediments of Buzzards Bay, Massachusetts. Geochim. Cosmochim. Acta 48:1107-1114.

Simenstad, C. A. and R. C. Wissmar. 1985. $\delta^{13}C$ evidence of the origins and fates of organic carbon in eaturies and nearshore food webs. Mar. Ecol. Prog. Ser. 22:141-152.

Soutar, A., S. A. Kling, P. A. Crill, E. Duffrin and K. W. Bruland. 1977. Monitoring the marine environment through sedimentation. Nature 266:136-138.

Spinard, R. W., J. R. V. Zaneveld and J. Kitchen. 1983. A study of the optical characteristics of the suspended particles in the benthic nepheloid layer of the Scotian Rise. J. Geophys. Res. 88:7641-7645.

Stainton, M. P. 1973. A syringe gas-stripping procedure for gas-chromatographic determination of dissolved inorganic and organic carbon in fresh water and carbonates in sediments. J Fish. Res. Bd. Can. 30:1441-1445.

Stigebrandt, A. 1976. Vertical diffusion driven by internal waves in a sill fjord. J. Phys. Oceanogr. 6:486-495.

Stuermer, D. H., K. E. Peters and I. R. Kaplan. 1978. Source indicators of humic substances and protokerogen. Stable isotope ratios, elemental compositions and electron spin resonance spectra. Geochim. Cosmochim. Acta 42:989-997.

Sundby, B. and N. Silverberg. 1985. Manganese fluxes in the benthic boundary layer. Limnol. Oceanogr. 30:372-381.

Sugai, S. F. 1985. Processes controlling trace metal and nutrient geochemistry in two Southeast Alaskan fjords. Ph.D. Theis. Univ. of Alaska. 139p.

Sugai, F. S. 1986. Temporal changes in the sediment geochemistry of two southeast Alaskan fjords. Deep-Sea Res. (in press).

Syvitski, J. P. M., K. W. Asprey, D. A. Clattenburg, and G. D. Hodge. 1986. The prodelta environment: Suspended particle dynamics. Sedimentology (in press)

Syvitski, J. P. M., D. C. Burrell and J. M. Skei. *Fjords: Processes and Products*. Springer-Verlag. (in press).

Syvitski, J. P. M. and J. W. Murray. 1981. Particle interaction in fjord suspended sediment. Mar. Geol. 39:215-242.

Tan, F. C. and P. M. Strain. 1983. Sources, sinks and distribution of organic carbon in the St. Lawrence Estuary, Canada. Geochim. Cosmochim. Acta 47:125-132.

Tebo, B. M. and K. N. Nealson. 1984. Microbial mediation of Mn(II) and Co(II) precipitation at the O_2/H_2S interfaces in two anoxic fjords. Limnol. Oceanogr. 29:1247-1258.

Torgersen, T. and M. E. Longmore. 1984. ^{137}Cs diffusion in the highly organic sediment of Hidden Lake, Fraser Island. Queensland. Australian J. Mar. Freshwater Res. 35:537-548.

Toth, D. J. and A. Lerman. 1977. Organic matter reactivity and sedimentation rates in the ocean. Am. J. Sci. 14:129-137.

Tsunogai, S., M. Uematsu, N. Tanaka and K. Harada. 1980. A sediment trap experiment in Funka Bay, Japan: "Upward flux" of particulate matter in seawater. Mar. Chem. 9:321-334.

VTN. 1982. Boca de Quadra base line report. U.S. Borax and Chemical Co. Los Angeles.

Walsh, J. J. E. T. Premuzic, J. S. Gaffney, G. T. Rowe, G. Harbottle, R. W. Stoenner, W. L. Balsam. P. R. Betzer and S. A. Macko. 1985. Organic storage of CO_2 on the continental slope off the mid-Atlantic bight, the southeastern Bering Sea, and the Peru coast. Deep-Sea Res. 32:853-883.

Wassman, P. 1983. Sedimentation of oraganic and inorganic particulate material in Lindaspollene, a stratified, land-locked fjord in western Norway. Mar. Ecol. Prog. Ser. 13:237-248.

Webster, T. J. M., M. A. Paranjabe and K. M. Mann. 1975. Sedimentation of organic matter in St. Margaret's Bay, Nova Scotia. J. Fish. Res. Board Can. 32:1399-1407.

Westrich, J. T. and R. A. Berner. 1984. The role of sedimentary organic matter in bacterial sulfate reduction: The G model tested. Limnol. Oceanogr. 29:236-249.

Whitledge, T. E., S. C. Malloy, C. J. Patton and C. D. Wirick. 1981. Automated nutrient analysis in seawater. Brookhaven Nat. Lab. Pub. 51398. New York. 216p.

Wollast, R. 1974. Silica problem in the sea. In Goldberg, E. D. (ed.). *The Sea.* v.5. pp359-392.

Zeitzschel, B. 1979. Sediment-water interactions in nutrient dynamics. In Tenore, K. R. and B. C. Coull (eds.). *Marine Benthic Dynamics*. Univ. of South Carolina Press. pp195-213.

APPENDIX A: COMPOSITION AND FLUX OF SETTLING PARTICULATE MATTER.

BQ9G - 40m depth

Cruise No.	Deploy	Retrieve	Duration (days)	Net wt. of sediment caught (mg)	Mass flux (mg/m^2/day)
RT26	06-09-82	06-12-82	3	19.90	860.69
RT27/RT28	07-13-82	08-15-82	32	145.04	588.10
RT28/AM01	08-15-82	09-22-82	35	137.41	509.41
AM01/RT30	09-22-82	10-17-82	24	163.90	886.10
RT30/RT31	10-18-82	12-01-82	43	135.47	408.78
RT31/RT33	12-03-82	01-06-83	33	70.35	276.61
RT33/RT34	01-08-83	01-28-83	19	83.21	568.25
RT34/RT35	01-30-83	03-11-83	39	94.52	314.47
RT35/RT36	03-13-83	04-09-83	26	267.15	1333.20
RT36/RT38	04-11-83	06-07-83	56	228.13	528.58
RT38/RT39	06-08-83	07-20-83	41	288.77	913.87
RT39/RT40	07-21-83	09-01-83	41	565.61	1789.98
RT40/RT41	09-02-83	10-18-83	45	860.91	2482.33

Deploy	Retrieve	Duration (days)	Composition POC (%)	PON (%)	C/N	inorg C (%)	Biogenic Si (%)
06-09-82	06-12-82	3	12.73	1.42	10.46		
07-13-82	08-15-82	32	13.29	1.42	10.92	4.77 +- 2.68	4.67 +- 0.04
08-15-82	09-22-82	35	11.24	1.22	10.75	0.50 +- 0.22	11.79
09-22-82	10-17-82	24	8.96 +- 2.00	0.86 +- 0.01	12.16	0.54	
10-18-82	12-01-82	43	11.08 +- 0.84	1.56 +- 0.28	8.29	1.97 +- 0.21	
12-03-82	01-06-83	33	16.18 +- 0.87	1.75 +- 0.21	10.79	1.51	3.08
01-08-83	01-28-83	19	10.65 +- 1.27	1.17 +- 0.07	10.62	3.78	3.39
01-30-83	03-11-83	39	9.27 +- 0.04	1.96 +- 0.03	5.52	0.33 +- 0.16	6.20
03-13-83	04-09-83	26	7.92 +- 0.85	1.39 +- 0.11	6.65		21.73 +- 1.75
04-11-83	06-07-83	56	10.15 +- 0.31	1.29 +- 0.04	9.18		17.12 +- 2.28
06-08-83	07-20-83	41	19.66 +- 1.84	2.50 +- 0.28	9.17		8.36
07-21-83	09-01-83	41	15.80	1.92	9.60		11.66
09-02-83	10-18-83	45	19.09 +- 0.00	2.06 +- 0.03	10.81		3.97 +- 0.15

BQ96 - 40m depth

Deploy	Retrieve	Duration (days)	Flux POC (mg C/m²/day)	Flux PON (mg N/m²/day)	Flux Inorg C (mg C/m²/day)	Flux Biogenic Si (mg Si/m²/day)
06-09-82	06-12-82	3	109.57	12.22		
07-13-82	08-15-82	32	78.16	8.35	28.05 +- 15.76	27.46 +- 0.24
08-15-82	09-22-82	35	57.26	6.21	2.55 +- 1.12	60.06
09-22-82	10-17-82	24	79.39 +- 17.72	7.62 +- 0.09	4.78	
10-18-82	12-01-82	43	45.29 +- 3.43	6.38 +- 1.14	8.05	
12-03-82	01-06-83	33	44.76 +- 2.41	4.84 +- 0.58	4.18	8.52
01-08-83	01-28-83	19	60.52 +- 7.22	6.65 +- 0.40	21.48	19.26
01-30-83	03-11-83	39	29.15 +- 0.13	6.16 +- 0.09	1.04 +- 0.50	19.50
03-13-83	04-09-83	26	105.59 +- 11.33	18.53 +- 1.47		289.71 +- 23.33
04-11-83	06-07-83	56	53.65 +- 5.67	4.49 +- 0.73		83.04 +- 41.69
06-08-83	07-20-83	41	179.67 +- 16.82	22.85 +- 2.56		76.40
07-21-83	09-01-83	41	282.82	34.37		208.71
09-02-83	10-18-83	45	473.88	51.14		98.55 +- 3.72

BQ96 - 120 m depth

Cruise No.	Deploy	Retrieve	Duration (days)	Net wt. of sediment caught (mg)	Mass flux (mg/m^2/day)
AM01/RT30	09-22-82	10-17-82	24	199.35	1077.75
RT30/RT31	10-18-82	12-01-82	43	794.69	2397.97
RT31/RT33	12-03-82	01-06-83	33	208.07	818.11
RT33/RT34	01-08-83	01-28-83	19	223.21	1524.31
RT34/RT35	01-30-83	03-11-83	39	267.10	888.64
RT35/RT36	03-13-83	04-09-83	26	323.39	1613.87

Deploy	Retrieve	Duration	Composition				
			POC	PON	C/N	inorg C	Biogenic Si
		(days)	(%)	(%)		(%)	(%)
09-22-82	10-17-82	24	8.71 +-0.85	1.03 +-0.11	9.87	0.66 +-0.01	5.62 +-1.75
10-18-82	12-01-82	43	7.67 +-0.49	0.81 +-0.01	11.05	0.75 +-0.05	4.92 +-0.40
12-03-82	01-06-83	33	8.84 +-0.78	1.07 +-0.33	9.64	1.01 +-0.12	6.08
01-08-83	01-28-83	19	8.80 +-0.28	1.22 +-0.16	8.42	1.06	3.30 +-0.63
01-30-83	03-11-83	39	7.15 +-0.04	0.82 +-0.01	10.17	0.34 +-0.14	5.33 +-0.13
03-13-83	04-09-83	26	6.60 +-0.49	0.98 +-0.01	7.86	0.49 +-0.50	19.61 +-0.39

Deploy	Retrieve	Duration	Flux			
			POC	PON	Inorg C	Biogenic Si
		(days)	(mg C/m^2/day)	(mg N/m^2/day)	(mg C/m^2/day)	(mg Si/m^2/day)
09-22-82	10-17-82	24	93.87 +- 9.16	11.10 +-1.19	7.11 +- 0.11	60.57 +- 18.86
10-18-82	12-01-82	43	183.92 +-11.75	19.42 +-0.24	17.98 +- 1.20	117.98 +- 9.59
12-03-82	01-06-83	33	72.32 +- 6.38	8.75 +-2.70	8.26 +- 0.98	49.74
01-08-83	01-28-83	19	134.14 +- 4.27	18.60 +-2.44	16.16	50.30 +- 9.60
01-30-83	03-11-83	39	63.54 +- 0.36	7.29 +-0.09	3.02 +- 1.24	47.36 +- 1.16
03-13-83	04-09-83	26	106.52 +- 7.91	15.82 +-0.16	7.91 +- 8.07	316.48 +- 6.29

BQ96 - 100m Depth

Cruise No.	Deploy	Retrieve	Duration (days)	Net wt. of sediment caught (mg)	Mass flux (mg/m²/day)
RT36/RT38	04-11-83	06-07-83	56	228.13	528.58
RT38/RT39	06-08-83	07-20-83	41	258.49	818.04
RT39/RT40	07-21-83	09-01-83	41	505.68	1600.32
RT40/RT41	09-02-83	10-18-83	45	731.49	2109.16

Deploy	Retrieve	Duration (days)	Composition POC (%)	PON (%)	C/N	Biogenic Si (%)
04-11-83	06-07-83	56	7.22	0.85	9.91	15.71 +-0.17
06-08-83	07-20-83	41	5.63	0.68 +-0.05	9.66	8.56
07-21-83	09-01-83	41	9.86	1.02	11.28	
09-02-83	10-18-83	45	11.33	1.04	12.71	5.72

Deploy	Retrieve	Duration (days)	Flux POC (mg C/m²/day)	PON (mg N/m²/dday)	Biogenic Si (mg Si/m²/day)
04-11-83	06-07-83	56	38.16	4.49	83.04 +- 0.90
06-08-83	07-20-83	41	46.06 +- 0.00	5.56 +-0.41	70.02
07-21-83	09-01-83	41	157.79	16.32	
09-02-83	10-18-83	45	238.97	21.94	120.64

BQ9G - 280 m depth

Cruise No.	Deploy	Retrieve	Duration (days)	Net wt. of sediment caught (mg)	Mass flux mg/m²/day
AM01/RT30	09-22-82	10-17-82	24	418.26	2261.26
RT30/RT31	10-18-82	12-01-82	43	650.75	1963.63
RT31/RT33	12-03-82	01-06-83	33	386.48	1519.59
RT33/RT34	01-08-83	01-28-83	19	194.95	1331.33
RT34/RT35	01-30-83	03-11-83	39	296.57	986.68
RT35/RT36	03-13-83	04-09-83	26	370.85	1850.72

Deploy	Retrieve	Duration (days)	Composition POC (%)	PON (%)	C/N	inorg C (%)
09-22-82	10-17-82	24	7.19	0.74	11.34	0.60 +-0.16
10-18-82	12-01-82	43	6.60	0.68	11.32	0.49 +-0.02
12-03-82	01-06-83	33	7.26 +-0.01	0.86 +-0.04	9.85	0.75 +-0.00
01-08-83	01-28-83	19	7.76 +-0.68	0.96 +-0.05	9.43	1.49
01-30-83	03-11-83	39	6.81 +-0.15	0.72 +-0.06	11.03	0.25
03-13-83	04-09-83	26	5.97 +-0.08	0.76 +-0.01	9.16	0.13 +-0.02

Deploy	Retrieve	Duration (days)	Flux POC (mg C/m²/day)	PON (mg N/m²/dday)	Inorg C (mg C/m²/day)
09-22-82	10-17-82	24	162.58	16.73	13.57 +- 3.62
10-18-82	12-01-82	43	129.60	13.35	9.62 +- 0.39
12-03-82	01-06-83	33	110.32 +- 0.15	13.07 +-0.61	11.40 +- 0.00
01-08-83	01-28-83	19	103.31 +- 9.05	12.78 +-0.67	19.84
01-30-83	03-11-83	39	67.19 +- 1.48	7.10 +-0.59	2.47 +- 0.00
03-13-83	04-09-83	26	110.49 +- 1.48	14.07 +-0.19	2.41 +- 0.37

BQ96 - 300 m depth

Cruise No.	Deploy	Retrieve	Duration (Days)	Net wt. of sediment caught (mg)	Mass flux mg/m^2/day
AM01/RT30	09-22-82	10-17-82	24	396.54	2143.83
RT30/RT31	10-18-82	12-01-82	43	881.70	2660.52
RT31/RT33	12-03-82	01-06-83	33	445.60	1752.05
RT33/RT34	01-08-83	01-28-83	19	208.64	1424.82
RT34/RT35	01-30-83	03-11-83	39	333.27	1108.78
RT35/RT36	03-13-83	04-09-83	26	368.71	1840.04
RT36/RT38	04-11/83	06-07-83	56	1087.53	2519.81
RT38/RT39	06-08-83	07-20-83	41	603.01	1908.34
RT39/RT40	07-21-83	09-01-83	41	663.83	2100.81
RT40/RT41	09-02-83	10-18-83	45	1301.11	3751.60

Deploy	Retrieve	Duration (days)	Composition: POC (%)	PON (%)	C/N	inorg C (%)	Biogenic Si (%)
09-22-82	10-17-82	24	8.87	0.82	12.62	0.75 +-0.52	6.66 +-0.56
10-18-82	12-01-82	43	6.48	0.69	10.96	0.90 +-0.23	5.06
12-03-82	01-06-83	33	8.70 +-1.45	0.92 +-0.04	11.03	0.63 +-0.04	5.32 +-0.38
01-08-83	01-28-83	19	6.48 +-1.55	0.80 +-0.13	9.45	1.24 +-0.02	4.94 +-0.09
01-30-83	03-11-83	39	6.56 +-0.48	0.75 +-0.06	10.20	0.20 +-0.03	4.85 +-0.69
03-13-83	04-09-83	26	5.70 +-0.76	0.69 +-0.10	9.64	0.29	11.10 +-0.63
04-11-83	06-07-83	56	5.72 +-0.54	0.70 +-0.06	9.53		10.49
06-08-83	07-20-83	41	7.21	0.79	10.65		9.20 +-0.78
07-21-83	09-01-83	41	7.56	0.81	10.89		5.72 +-1.14
09-02-83	10-18-83	45	7.16	0.68	12.28		5.00

Deploy	Retrieve	Duration (days)	Flux: POC (mg C/m^2/day)	PON (mg N/m^2/day)	Inorg C (mg C/m^2/day)	Biogenic Si (mg Si/m^2/day)
09-22-82	10-17-82	24	190.16	17.58	16.08 +-11.15	142.78 +-12.01
10-18-82	12-01-82	43	172.40	18.36	23.94 +- 6.12	134.62
12-03-82	01-06-83	33	152.43 +- 25.40	16.12 +-0.70	11.04 +- 0.70	93.21 +- 6.66
01-08-83	01-28-83	19	92.33 +- 22.08	11.40 +-1.85	17.67 +- 0.28	70.39 +- 1.28
01-30-83	03-11-83	39	72.74 +- 5.32	8.32 +-0.67	2.22 +- 0.33	53.78 +- 7.65
03-13-83	04-09-83	26	104.88 +- 13.98	12.70 +-1.84	5.34	204.24 +-11.59
04-11-83	06-07-83	56	144.13 +- 13.61	17.64 +-1.51		264.33
06-08-83	07-20-83	41	137.59	15.08		175.57 +-14.89
07-21-83	09-01-83	41	158.82	17.02		120.17 +-23.95
09-02-83	10-18-83	45	268.61	25.51		187.58

BQ9G - 365m depth

Cruise No.	Deploy	Retrieve	Duration (days)	Net wt. of sediment caught (mg)	Mass flux (mg/m^2/day)
AM01/RT30	09-22-82	10-17-82	24	483.91	2616.18
RT30/RT31	10-18-82	12-01-82	43	1270.66	3834.21
RT31/RT33	12-03-82	01-06-83	33	491.49	1932.48
RT33/RT34	01-08-83	01-28-83	19	321.42	2195.00
RT34/RT35	01-30-83	03-11-83	39	501.53	1668.58
RT35/RT36	03-13-83	04-09-83	26	466.83	2329.70
RT36/RT38	04-11-83	06-07-83	56	1436.48	3328.33
RT38/RT39	06-08-83	07-20-83	41	864.16	2734.80
RT39/RT40	07-21-83	09-01-83	41	1168.65	3698.41
RT40/RT41	09-02-83	10-18-83	45	1704.80	4915.59

Deploy	Retrieve	Duration (days)	Composition POC (%)	PON (%)	C/N	inorg C (%)
09-22-82	10-17-82	24	6.39 +-2.00	0.72 +-0.01	10.35	0.70 +-0.04
10-18-82	12-01-82	43	5.24	0.65	9.41	0.82 +-0.10
12-03-82	01-06-83	33	7.71 +-0.55	0.97 +-0.01	9.27	0.65 +-0.16
01-08-83	01-28-83	19	6.90 +-0.25	0.87 +-0.06	9.25	1.12 +-0.08
01-30-83	03-11-83	39	6.81 +-0.11	0.88 +-0.04	9.03	0.46 +-0.04
03-13-83	04-09-83	26	5.76 +-0.43	0.70 +-0.04	9.60	0.21 +-0.09
04-11-83	06-07-83	56	5.00 +-0.11	0.59 +-0.01	9.89	
06-08-83	07-20-83	41	6.82	0.76	10.47	
07-21-83	09-01-83	41	6.77	0.72	10.97	
09-02-83	10-18-83	45	7.72	0.67	13.44	

Deploy	Retrieve	Duration (days)	Flux POC (mg C/m^2/day)	PON (mg N/m^2/dday)	Inorg C (mg C/a^2/day)
09-22-82	10-17-82	24	167.17 +- 52.32	18.84 +-0.26	18.31 +- 1.05
10-18-82	12-01-82	43	200.91	24.92	31.44 +- 3.83
12-03-82	01-06-83	33	148.99 +- 10.63	18.75 +-0.19	12.56 +- 0.00
01-08-83	01-28-83	19	151.45 +- 5.49	19.10 +-1.32	24.58 +- 1.76
01-30-83	03-11-83	39	113.63 +- 1.84	14.68 +-0.67	7.68 +- 0.67
03-13-83	04-09-83	26	134.19 +- 10.02	16.31 +-0.93	4.89 +- 2.10
04-11-83	06-07-83	56	166.42 +- 3.66	19.64 +-0.33	
06-08-83	07-20-83	41	186.51	20.78	
07-21-83	09-01-83	41	250.38	26.63	
09-02-83	10-18-83	45	379.48	32.93	

BQ96 - 375m depth

Cruise No.	Deploy	Retrieve	Duration (days)	Net wt. of sediment caught (mg)	Mass flux (mg /m^2/day)
AM01/RT30	09-22-82	10-17-82	24	762.84	4124.17
RT30/RT31	10-18-82	12-01-82	43	813.13	2453.61
RT31/RT33	12-03-82	01-06-83	33	462.26	1817.55
RT33/RT34	01-08-83	01-28-83	19	331.97	2267.04
RT34/RT35	01-30-83	03-11-83	39	744.78	2477.87
RT35/RT36	03-13-83	04-09-83	26	495.75	2474.02
RT36/RT38	04-11/83	06-07-83	56	1488.96	3449.92
RT38/RT39	06-08-83	07-20-83	41	1155.58	3657.05
RT39/RT40	07-21-83	09-01-83	41	1109.30	3510.59
RT40/RT41	09-02-83	10-18-83	45	1561.38	4502.05

Deploy	Retrieve	Duration (days)	Composition POC (%)	PON (%)	C/N	inorg C (%)	Biogenic Si (%)
09-22-82	10-17-82	24	6.52 +-2.00	0.83 +-0.01	9.16	0.84 +-0.11	5.96 +-0.03
10-18-82	12-01-82	43	6.36	0.69	10.75	1.16 +-0.03	4.88 +-0.76
12-03-82	01-06-83	33	6.02 +-0.71	0.72 +-0.01	9.75	0.97 +-0.06	4.80 +-0.49
01-08-83	01-28-83	19	5.76 +-0.32	0.73 +-0.01	9.21	1.14 +-0.13	6.02
01-30-83	03-11-83	39	5.66 +-0.06	0.67 +-0.01	9.86	0.39 +-0.03	3.89 +-0.19
03-13-83	04-09-83	26	4.93 +-0.08	0.60 +-0.02	9.59	0.23 +-0.09	11.27 +-1.22
04-11-83	06-07-83	56	4.99	0.56	10.40		6.48 +-0.74
06-08-83	07-20-83	41	11.28	1.44	9.14		7.44 +-0.35
07-21-83	09-01-83	41	6.81	0.73	10.88		7.40 +-0.43
09-02-83	10-18-83	45	7.31	0.70	12.18		6.07 +-0.29

Deploy	Retrieve	Duration (days)	Flux POC (mg C/m^2/day)	PON (mg N/m^2/ day)	Inorg C (mg C/m^2/day)	Biogenic Si (mg Si/m^2/day)
09-22-82	10-17-82	24	268.90 +- 82.48	34.23 +-0.41	34.64 +- 4.54	245.80 +- 1.24
10-18-82	12-01-82	43	156.05	16.93	28.46 +- 0.74	119.74 +-18.65
12-03-82	01-06-83	33	109.42 +- 12.90	13.09 +-0.18	17.63 +- 1.09	87.24 +- 8.91
01-08-83	01-28-83	19	130.58 +- 7.25	16.55 +-0.23	25.84 +- 2.95	136.48
01-30-83	03-11-83	39	140.25 +- 1.49	16.60 +-0.25	9.66 +- 0.74	96.39 +- 4.71
03-13-83	04-09-83	26	121.97 +- 1.98	14.84 +-0.49	5.69 +- 2.23	278.82 +-30.18
04-11-83	06-07-83	56	172.15 +- 0.00	19.32 +-0.00		223.56 +-25.53
06-08-83	07-20-83	41	412.52	52.66		272.08 +-12.80
07-21-83	09-01-83	41	239.07	25.63		259.78 +-15.10
09-02-83	10-18-83	45	329.10	31.51		273.27 +-13.06

APPENDIX B: CONCENTRATIONS OF AL, MN, AND FE IN THE SETTLING PARTICULATE MATTER AND IN THE SURFACE SEDIMENT.

		Al (%)	Mn (ppm)	Fe (%)	Mn/Al	Fe/Al
Surface sediment						
BQ96-2		3.03	880	2.69	0.029	0.889
BQ9-2		3.60	1084	3.32	0.030	0.923
BQ96*		3.18	1563	2.76	0.049	0.870
Sediment traps						
09/02/83 to 10/18/83	40 m	1.84	263	1.40	0.014	0.762
	100 m	3.11	1619	3.78	0.052	1.216
	300 m	3.41	5138	3.87	0.150	1.133
	365 m	3.30	7295	3.48	0.221	1.053
	375 m	2.98	8343	3.35	0.280	1.126
10/18/82 to 12/01/82	40 m	1.93	618	1.55	0.032	0.804
	120 m	3.53	2261	3.14	0.064	0.890
	280 m	3.44	6076	3.55	0.177	1.033
	300 m	3.31	5566	3.25	0.168	0.980
	365 m	3.25	5831	2.97	0.180	0.916
	375 m	3.52	7137	3.44	0.203	0.977
03/13/83 to 04/09/83	40 m	1.56	183	0.80	0.012	0.512
	120 m	2.24	1243	2.18	0.055	0.972
	280 m	2.83	5281	3.43	0.187	1.213
	300 m	3.08	6874	3.67	0.223	1.192
	365 m	3.31	10629	4.18	0.321	1.262
	375 m	3.38	10504	4.01	0.311	1.185
04/11/83 to 06/07/83	40 m	2.17	191	1.27	0.009	0.585
	40 m	1.75	159	1.01	0.009	0.579
	100 m	2.51	914	1.97	0.036	0.786
	300 m	2.64	6141	3.19	0.232	1.208
	365 m	3.20	10025	3.54	0.313	1.105
	375 m	3.03	11234	3.76	0.371	1.243

APPENDIX C: RESULTS OF THE PRIMARY-RESUSPENDED-ALTERED FLUX MODEL.

POC

13 March-9 April 1983

Depth (m)	Total	Primary	Resuspended	Altered
		(mg C m^{-2} d^{-1})		
300	104.88	106.52	33.16	-34.80
365	134.19	106.52	66.21	-38.54
375	121.97	106.52	76.92	-61.47

11 April-7 June 1983

Depth (m)	Total	Primary	Resuspended	Altered
		(mg C m^{-2} d^{-1})		
300	144.13	38.16	86.40	19.57
365	166.42	38.16	151.29	-23.03
375	172.15	38.16	147.83	-13.84

2 September-18 October 1983

Depth (m)	Total	Primary	Resuspended	Altered
		(mg C m^{-2} d^{-1})		
300	268.61	238.97	87.81	-58.17
365	379.48	238.97	136.06	4.45
375	329.10	238.97	96.07	-5.94

18 October-1 December 1982

Depth (m)	Total	Primary	Resuspended	Altered
		(mg C m^{-2} d^{-1})		
300	172.40	183.92	4.92	-16.44
365	200.91	183.92	55.93	-38.94
375	156.05	183.92	2.22	-30.09

PN

13 March-9 April 1983

Depth (m)	Total	Primary	Resuspended	Altered
		(mg N m^{-2} d^{-1})		
300	12.70	15.82	3.38	-6.50
365	16.31	15.82	6.75	-6.26
375	14.84	15.82	7.84	-8.82

11 April-7 June 1983

Depth (m)	Total	Primary	Resuspended	Altered
		(mg N m^{-2} d^{-1})		
300	17.64	4.49	8.77	4.38
365	19.64	4.49	15.41	-0.26
375	19.32	4.49	15.06	-0.23

2 September-18 October 1983

Depth (m)	Total	Primary	Resuspended	Altered
		(mg N m^{-2} d^{-1})		
300	25.31	21.94	8.59	-5.22
365	32.93	21.94	13.31	-2.32
375	31.51	21.94	9.40	0.17

18 October-1 December 1982

Depth (m)	Total	Primary	Resuspended	Altered
		(mg N m^{-2} d^{-1})		
300	18.36	19.42	0.48	-1.54
365	24.92	19.42	5.47	0.03
375	16.93	19.42	0.22	-2.71

Particulate Biogenic Si

13 March-9 April 1983

Depth (m)	Total	Primary	Resuspended	Altered
		(mg Si m^{-2} d^{-1})		
300	204.24	316.48	34.98	-147.22
375	278.82	316.48	81.13	-118.79

11 April-7 June 1983

Depth (m)	Total	Primary	Resuspended	Altered
		(mg Si m^{-2} d^{-1})		
300	264.33	83.04	91.13	90.16
375	223.56	83.04	155.92	-15.40

2 September-18 October 1983

Depth (m)	Total	Primary	Resuspended	Altered
		(mg Si m^{-2} d^{-1})		
300	187.58	120.64	80.20	-13.26
375	273.27	120.64	87.71	64.92

18 October-1 December 1982

Depth (m)	Total	Primary	Resuspended	Altered
		(mg Si m^{-2} d^{-1})		
300	134.62	117.98	4.50	12.14
375	119.74	117.98	2.03	-0.27

Particulate Mn

13 March-9 April 1983

Depth (m)	Total	Primary	Resuspended	Altered
		(mg Mn m^{-2} d^{-1})		
300	12.65	2.01	0.98	9.66
365	24.76	2.01	1.95	20.80
375	25.99	2.01	2.27	21.71

11 April-7 June 1983

Depth (m)	Total	Primary	Resuspended	Altered
		(mg Mn m^{-2} d^{-1})		
300	15.47	0.48	2.55	12.44
365	33.37	0.48	4.46	28.43
375	38.76	0.48	4.36	33.92

2 September-18 October 1983

Depth (m)	Total	Primary	Resuspended	Altered
		(mg Mn m^{-2} d^{-1})		
300	19.28	3.41	1.88	13.99
365	35.86	3.41	2.90	29.55
375	37.56	3.41	2.05	32.10

18 October-1 December 1982

Depth (m)	Total	Primary	Resuspended	Altered
		(mg Mn m^{-2} d^{-1})		
300	14.81	5.42	0.11	9.28
365	22.36	5.42	1.19	15.75
375	17.51	5.42	0.05	12.04

Particulate Fe

13 March-9 April 1983

Depth (m)	Total	Primary	Resuspended	Altered
		(mg Fe m^{-2} d^{-1})		
300	67.58	35.23	18.46	13.89
365	97.30	35.23	36.85	25.22
375	99.18	35.23	42.82	21.13

11 April-7 June 1983

Depth (m)	Total	Primary	Resuspended	Altered
		(mg Fe m^{-2} d^{-1})		
300	80.39	10.43	48.09	21.87
365	117.82	10.43	84.21	23.18
375	129.85	10.43	82.28	37.14

2 September-18 October 1983

Depth (m)	Total	Primary	Resuspended	Altered
		(mg Fe m^{-2} d^{-1})		
300	145.14	79.83	56.33	8.98
365	170.92	79.83	87.26	3.83
375	150.87	79.83	61.61	9.43

18 October-1 December 1982

Depth (m)	Total	Primary	Resuspended	Altered
		(mg Fe m^{-2} d^{-1})		
300	86.36	75.33	3.16	7.87
365	114.00	75.33	35.87	2.80
375	84.28	75.33	1.43	7.52

Surface Sediment Chemistry (%)

	Al	Mn	Fe	TOC	TN	Biogenic Si
Spring-summer	3.27	0.156	2.95	5.3	0.54	5.59
Fall-winter	3.27	0.098	2.95	4.6	0.45	4.20

APPENDIX D: POROSITY AND CUMULATIVE MASS DATA.

8090, January 1983

Top (cm)	Bottom (cm)	Interval (cm)	Mass (g)	Cummulative Mass (g/cm^2)	Porosity
0.0	1.4	1.4	4.35	0.116	0.94
1.4	2.8	1.4	8.56	0.345	0.91
2.8	3.5	0.7	6.05	0.507	0.89
3.5	5.0	1.5	7.42	0.705	0.92
5.0	6.0	1.0	9.92	0.971	0.87
6.0	7.5	1.5	10.68	1.256	0.90
7.5	8.7	1.2	10.68	1.542	0.88
8.7	9.9	1.2	8.61	1.772	0.90
9.9	11.1	1.2	8.57	2.001	0.90
11.1	12.5	1.4	9.56	2.257	0.90
12.5	13.5	1.0	10.33	2.533	0.87
13.5	14.5	1.0	10.89	2.825	0.86
14.5	15.5	1.0	9.08	3.067	0.88
15.5	16.7	1.2	9.93	3.333	0.89
16.7	17.5	0.8	6.8	3.515	0.89
17.5	18.5	1.0	10.34	3.791	0.87
18.5	19.5	1.0	6.47	3.964	0.91
19.5	20.7	1.2	8.04	4.179	0.91
20.7	21.5	0.8	10.48	4.460	0.84
21.5	23.0	1.5	13.46	4.820	0.88
23.0	24.1	1.1	9.96	5.086	0.88
24.1	25.2	1.1	7.32	5.282	0.91
25.2	26.2	1.0	10.94	5.574	0.86
26.2	27.8	1.6	11.38	5.879	0.90
27.8	28.6	0.8	7.25	6.073	0.88
28.6	29.9	1.3	13.25	6.427	0.87
29.9	31.6	1.7	14.1	6.804	0.89
31.6	32.6	1.0	7.29	6.999	0.90
32.6	33.8	1.2	9.96	7.265	0.89
33.8	34.9	1.1	10.71	7.552	0.87
34.9	36.1	1.2	11.51	7.860	0.88
36.1	37.2	1.1	12.36	8.190	0.86
37.2	38.4	1.2	9.76	8.451	0.89
38.4	39.4	1.0	11.28	8.753	0.86
39.4	40.9	1.5	10.1	9.023	0.91
40.9	42.2	1.3	15.2	9.429	0.85
42.2	43.7	1.5	12.69	9.769	0.89
43.7	45.4	1.7	15.74	10.190	0.88
45.4	46.9	1.5	15.63	10.608	0.87
46.9	48.7	1.8	15.6	11.025	0.89
48.7	50.3	1.6	16.91	11.477	0.87
50.3	51.6	1.3	10.88	11.768	0.89
51.6	53.2	1.6	17.53	12.237	0.86
53.2	54.9	1.7	15.17	12.643	0.88
54.9	56.6	1.7	14.38	13.027	0.89
56.6	58.3	1.7	19.2	13.541	0.86
58.3	60.4	2.1	17.6	14.011	0.89
60.4	62.0	1.6	20.2	14.551	0.84
62.0	64.2	2.2	19.09	15.062	0.89
64.2	66.2	2.0	20.31	15.605	0.87
66.2	68.9	2.7	28.43	16.365	0.87
68.9	70.5	1.6	16.63	16.810	0.87
70.5	74.2	3.7	32.23	17.672	0.88

APPENDIX E: SEDIMENT CHEMISTRY DATA.

B096, January 1983

Solid Phase

Top (cm)	Bottom (cm)	Cumulative mass (g/cm²)	Inorg C (%)	POC (%)	PON (%)	C/N	Biognic Si (%)
0.0	1.4	0.116	0.60 +- 0.01	4.60 +- 0.08	0.54 +- 0.01	9.94	4.2
1.4	2.8	0.345	0.44 +- 0.17	4.36 +- 0.00	0.49 +- 0.01	10.38	3.1
2.8	3.5	0.507	0.48 +- 0.05	4.40 +- 0.01	0.47 +- 0.01	10.92	2.6 +- 0.5
3.5	5.0	0.705	0.55 +- 0.04	4.18 +- 0.01	0.45 +- 0.02	10.84	2.1 +- 0.4
5.0	6.0	0.970	0.58 +- 0.13	4.02 +- 0.09	0.44 +- 0.00	10.66	2.7
6.0	7.5	1.256	0.47 +- 0.03	4.03 +- 0.01	0.44 +- 0.02	10.69	1.4
7.5	8.7	1.542	0.42 +- 0.01	3.99 +- 0.06	0.44 +- 0.04	10.58	1.6
8.7	9.9	1.772	0.37 +- 0.11	- -	- -	-	1.6
9.9	11.1	2.001	0.44 +- 0.06	3.81 +- 0.07	0.41 +- 0.00	10.84	2.0
11.1	12.5	2.257	0.50	3.80 -	0.39 -	11.37	1.5
12.5	13.5	2.533		- -	- -	-	
13.5	14.5	2.824		3.72 +- 0.01	0.42 +- 0.04	10.33	

Top (cm)	Bottom (cm)	Excess Pb-210 (dpm/g)
0.0	1.4	- -
1.4	2.8	21.76 +- 0.67
2.8	3.5	20.83 +- 1.45
3.5	5.0	19.70 +- 0.59
5.0	6.0	18.45 +- 1.40
6.0	7.5	13.80 +- 0.41
7.5	8.7	11.84 +- 0.48
8.7	9.9	14.30 +- -
9.9	11.1	9.67 +- 0.34
11.1	12.5	8.97 +- 0.60
12.5	13.5	7.53 +- -
13.5	14.5	5.98 +- -

BQ9G-1, October 1983

Solid Phase

Top (cm)	Bottom (cm)	Dry wt. (g)	POC (%)	PON (%)	C/N	Biogenic Si (%)	Total Pb-210 (dpm/g)
0.0	1.5	1.90	4.91 +- 0.07	0.45 +- 0.00	12.73	3.95 +- 0.02	23.54
1.5	3.5	10.05	4.85	0.45	12.57	3.52 +- 0.16	13.92
3.5	6.0	14.17	4.53	0.43	12.29	3.45 +- 0.50	19.71
6.0	8.2	16.58	4.39 +- 0.06	0.42 +- 0.00	12.19	3.08	17.69
8.2	10.6	18.26	4.38	0.44	11.61	2.81	12.56
10.6	13.1	8.45	4.29	0.42	11.92	2.89 +- 0.11	13.01
13.1	15.6	6.04	4.32	0.43	11.72	2.68 +- 0.01	8.58
15.6	18.0	17.28	4.16 +- 0.02	0.42 +- 0.01	11.56	2.42 +- 0.18	9.62
23.0	26.7	30.56	4.01	0.40	11.70	2.23 +- 0.29	5.22
31.1	33.6	21.36	3.93	0.39	11.76	2.41 +- 0.16	3.25
39.0	44.0	34.24	4.09	0.37	12.90	2.16 +- 0.21	2.89
50.2	54.3	35.36	3.77 +- 0.01	0.35 +- 0.03	12.57	2.22 +- 0.00	1.63

Interstitial Water

Top (cm)	Bottom (cm)	PO_4^{3-} (uM)	$Si(OH)_4$ (uM)	NO_3^- (uM)	NO_2^- (uM)	NH_4^+ (uM)	SO_4^{2-} (mM)
0.0	1.5	66.40	433.12	0.00	0.64	22.88	29.76 +- 0.30
1.5	3.5	44.80	383.84	0.32	0.32	18.24	14.52
3.5	6.0	43.20	509.76	2.24	0.32	63.68	20.03
6.0	8.2	75.20	564.80	1.28	0.32	97.12	18.63
8.2	10.6	55.52	591.68	0.64	0.32	105.12	23.01
10.6	13.1	43.20	643.84	0.80	0.32	102.40	22.78
13.1	15.6	39.04	627.36	0.80	0.32	91.68	24.42 +- 0.73
15.6	18.0	32.48	631.52	0.96	0.32	88.96	19.93
23.0	26.7	44.80	673.12	1.12	0.32	124.80	19.81
31.1	33.6	33.12	673.12	0.64	0.96	124.80	18.91
39.0	44.0	44.80	710.24	0.96	0.64	140.80	21.05 +- 0.29
50.2	54.3	41.92	641.76	1.12	0.64	173.92	12.64

BQ96-2, October 1983

Solid Phase

Top (cm)	Bottom (cm)	Dry wt. (g)	POC (%)	PON (%)	C/N	Biogenic Si (%)	Total Pb-210 (dpm/g)
0.0	2.0	1.53	4.66 +- 0.06	0.43 +- 0.03	12.64	3.92 +- 0.45	22.45
2.0	3.8	13.36	3.85 +- 0.19	0.36 +- 0.01	12.48	3.22 +- 0.07	16.64
3.8	6.2	19.21	4.08	0.33	14.42	3.47 +- 0.26	12.42
6.2	8.5	16.71	4.32 +- 0.10	0.42 +- 0.01	12.00	3.14 +- 0.08	14.47
8.5	11.0	17.62	4.31	0.40	12.57	3.11 +- 0.08	8.02
13.5	15.0	10.07	4.38	0.43	11.88	2.97 +- 0.07	10.33
15.0	17.4	17.79	4.46	0.42	12.39	2.96 +- 0.07	13.72
22.6	26.5	26.66	4.29	0.41	12.21	2.78 +- 0.04	10.30
31.6	35.5	30.18	4.05	0.38	12.43	1.96 +- 0.18	4.82
44.4	50.0	31.54	3.83	0.35	12.77	2.33 +- 0.28	1.64
60.2	64.0	35.65	3.86	0.35	12.87		0.75
68.8	72.4	36.10	3.94	0.35	13.13		0.55

Interstitial Water

Top (cm)	Bottom (cm)	PO_4^{3-} (uM)	$Si(OH)_4$ (uM)	NO_3^- (uM)	NO_2^- (uM)	NH_4^+ (uM)	SO_4^{2-} (mM)
0.0	2.0	59.84	163.62	1.76	1.76	20.96	
2.0	3.8	37.28	231.84	1.12	0.80	26.24	25.59 +- 1.96
3.8	6.2	38.88	224.64	0.00	0.48	44.00	14.96 +- 0.31
6.2	8.5	40.48	279.20	0.00	0.64	61.76	26.29
8.5	11.0	30.24	300.32	0.00	0.64	62.88	22.03
13.5	15.0	23.36	302.88	0.00	0.96	60.64	12.30
15.0	17.4	15.20	302.08	0.00	0.80	56.48	21.94
22.6	26.5	18.88	390.88	0.00	1.28	56.64	30.02
31.6	35.5	31.20	386.24	0.48	0.64	68.48	17.95
44.4	50.0	28.16	378.72	0.48	0.32	109.12	14.37
60.2	64.0	36.80	436.48	0.64	0.32	178.88	17.75 +- 0.90
68.8	72.4	44.16	524.00	0.00	2.40	272.02	23.43

BQ9-1, October 1983

Solid Phase

Top (cm)	Bottom (cm)	Dry wt. (g)	POC (%)	PON (%)	C/N	Total Pb-210 (dpm/g)
0.0	1.5					
1.5	2.6	5.98	4.63 +- 0.00	0.47 +- 0.01	11.49	19.16
2.6	4.7	13.47	4.51 +- 0.03	0.44 +- 0.01	11.96	29.72
4.7	7.1	17.33	4.23 +- 0.02	0.42 +- 0.00	11.75	12.23
7.1	9.8	19.50	4.19 +- 0.04	0.41 +- 0.00	11.92	12.80
9.8	11.3	12.40	4.14 +- 0.03	0.40 +- 0.00	12.07	9.80
11.3	14.1	19.21	3.89 +- 0.02	0.38 +- 0.00	11.94	9.03
14.1	16.6	19.18	4.02	0.41	11.44	5.74
16.6	20.8	34.77	3.88 +- 0.02	0.37 +- 0.00	12.23	4.21
25.8	29.9	32.17	3.85 +- 0.04	0.36 +- 0.00	12.48	2.47
35.3	39.5	34.49	3.88 +- 0.00	0.35 +- 0.00	12.93	1.28
49.3	52.5	22.70	3.78 +- 0.06	0.34 +- 0.00	12.97	0.83

Interstitial Water

Top (cm)	Bottom (cm)	PO_4^{3-} (uM)	$Si(OH)_4$ (uM)	NO_3^- (uM)	NO_2^- (uM)	NH_4^+ (uM)	SO_4^{2-} (mM)
0.0	1.5						
1.5	2.6	56.00	335.04	1.28	0.80	26.40	25.57 +- 0.21
2.6	4.7	38.40	434.88	1.44	0.64	37.12	22.12
4.7	7.1	34.08	394.24	0.96	0.32	48.64	15.32 +- 0.98
7.1	9.8	20.32	464.16	1.76	0.32	62.08	20.77 +- 0.24
9.8	11.3	8.32	430.24	1.44	0.80	64.80	23.18
11.3	14.1	9.60	421.28	1.60	0.64	62.08	24.18
14.1	16.6	10.24	514.72	0.48	1.12	61.12	23.00
16.6	20.8	20.32	373.92	1.76	0.96	72.64	28.28
25.8	29.9	15.84	433.40	0.32	0.64	103.36	25.66
35.3	39.5	18.56	536.96	0.96	1.44	146.88	25.76
49.3	52.5	10.72	526.88	0.00	3.68	184.00	17.30

BQ9-2, October 1983

Solid Phase

Top (cm)	Bottom (cm)	Dry wt. (g)	POC (%)	PON (%)	C/N	Total Pb-210 (dpm/g)
0.0	1.3	1.43	5.14 +- 0.03	0.42 +- 0.00	14.28	18.51
1.3	5.4	9.84	4.80 +- 0.21	0.42 +- 0.00	13.33	17.73
5.4	7.8	15.35	4.55 +- 0.02	0.40 +- 0.00	13.27	22.75
7.8	10.3	15.65	4.47 +- 0.02	0.41 +- 0.01	12.72	18.10
10.3	12.9	15.81	4.39 +- 0.08	0.38 +- 0.00	13.48	14.93
12.9	15.5	17.38	4.21 +- 0.01	0.37 +- 0.00	13.27	15.20
15.5	18.1	16.78	4.03 +- 0.16	0.36 +- 0.02	13.06	15.44
18.1	20.8	15.48	4.00 +- 0.02	0.36 +- 0.00	12.96	10.47
26.3	29.8	23.82	3.91 +- 0.00	0.35 +- 0.00	13.03	3.72
34.8	39.2	26.80	3.82 +- 0.00	0.34 +- 0.01	13.11	3.91
48.8	52.8	26.02	3.72 +- 0.01	0.33 +- 0.01	13.15	2.14
70.8	75.5	33.84	3.83 +- 0.02	0.34 +- 0.01	13.14	1.25

Interstitial Water

Top (cm)	Bottom (cm)	PO_4^{3-} (uM)	$Si(OH)_4$ (uM)	NO_3^- (uM)	NO_2^- (uM)	NH_4^+ (uM)
0.0	1.3					
1.3	5.4	64.32	103.84	0.00	0.32	34.40
5.4	7.8	45.76	120.80	0.00	0.32	46.24
7.8	10.3	15.52	130.56	0.00	0.48	35.52
10.3	12.9	6.40	134.72	0.00	0.48	25.12
12.9	15.5	10.56	165.76	0.00	0.64	28.96
15.5	18.1	21.12	191.68	0.00	0.32	47.52
18.1	20.8	29.76	172.80	0.00	0.48	63.84
26.3	29.8	36.80	186.24	0.00	0.48	78.40
34.8	39.2	15.52	203.20	0.00	0.48	74.08
48.8	52.8	19.84	249.76	0.00	0.48	82.88
70.8	75.5	26.88	283.20	0.00	0.64	165.44

BQ5-1, October 1983

Solid Phase

Top (cm)	Bottom (cm)	Dry wt. (g)	POC (%)	PON (%)	C/N	Total Pb-210 (dpm/g)
0.0	2.1	4.14	5.01	0.42	13.92	8.47 +- 0.58
2.1	4.3	13.57	3.76	0.34	12.90	12.23 +- 0.49
4.3	6.5	17.97	4.87	0.42	13.53	12.47 +- 1.32
6.5	9.0	18.40	4.99 +- 0.30	0.44 +- 0.01	13.23	8.69 +- 0.57
9.0	11.4	17.59	4.72	0.48	11.47	7.39 +- 0.40
11.4	13.0	11.77	4.75	0.43	12.89	7.83 +- 0.37
13.0	15.4	19.99	4.83	0.42	13.42	6.02 +- 0.23
15.4	18.0	18.77	4.40	0.44	11.67	3.84 +- 0.25
23.0	26.2	28.00	4.56	0.42	12.67	2.99 +- 0.08
36.0	40.0	35.26	4.65	0.43	12.62	1.35 +- 0.10
50.0	54.0	39.44	4.24	0.37	13.37	1.12 +- 0.07
64.0	67.8	42.54	3.92	0.36	12.70	1.10 +- 0.05

Interstitial Water

Top (cm)	Bottom (cm)	PO_4^{3-} (uM)	$Si(OH)_4$ (uM)	NO_3^- (uM)	NO_2^- (uM)	NH_4^+ (uM)	SO_4^{2-} (mM)
0.0	2.1	26.88	246.24	0.48	0.64	8.48	23.58 +- 1.93
2.1	4.3	29.44	174.72	0.00	0.96	17.28	22.74
4.3	6.5	33.92	218.88	0.00	2.24	33.44	13.24 +- 1.58
6.5	9.0	44.32	423.68	0.00	0.96	47.04	15.92
9.0	11.4	30.08	422.88	0.00	0.48	46.88	
11.4	13.0	23.52	470.08	0.00	0.80	44.96	13.28
13.0	15.4	24.16	469.28	0.00	0.48	43.36	18.72
15.4	18.0	21.44	450.24	0.00	0.48	42.24	22.10
23.0	26.2	14.08	480.00	0.00	0.96	45.44	23.36
36.0	40.0	25.12	361.92	0.00	0.64	88.64	24.01
50.0	54.0	29.44	503.68	0.00	0.64	48.14	25.73
64.0	67.8	25.28	620.16	0.00	0.48	111.84	19.85

BQS-2, October 1983

Solid Phase

Top (cm)	Bottom (cm)	Dry wt. (g)	POC (%)	PON (%)	C/N	Total Pb-210 (dpm/g)
0.0	1.8	2.42	7.26	0.83	10.20	15.87 +- 0.69
1.8	3.5	11.88	5.80 +- 1.15	0.60 +- 0.11	11.28	13.83 +- 0.78
3.5	6.0	23.21	4.08 +- 0.02	0.60 +- 0.01	7.93	12.45 +- 0.37
6.0	8.3	18.72	5.19 +- 0.70	0.50 +- 0.03	12.11	
8.3	10.7	19.23	4.69 +- 0.00	0.48 +- 0.03	11.40	8.46 +- 0.31
10.7	13.2	19.26	5.01 +- 0.04	0.54 +- 0.08	10.82	6.23 +- 0.42
13.2	15.7	19.58	4.71	0.42	13.08	4.52 +- 0.18
15.7	18.1	18.94	4.73 +- 0.08	0.40 +- 0.00	13.80	3.68 +- 0.23
23.0	26.8	38.35	4.44	0.36	14.39	1.99 +- 0.07
31.6	35.7	36.08	4.62	0.37	14.57	1.40 +- 0.10
45.7	50.3	38.18				1.04 +- 0.08
65.3	68.8	31.29				1.20 +- 0.07

Interstitial Water

Top (cm)	Bottom (cm)	PO_4^{3-} (uM)	$Si(OH)_4$ (uM)	NO_3^- (uM)	NO_2^- (uM)	NH_4^+ (uM)	SO_4^{2-} (mM)
0.0	1.8	36.80	82.08	0.64	0.80	14.72	
1.8	3.5	40.64	142.24	0.96	0.48	30.72	26.63
3.5	6.0	54.24	169.28	0.00	0.32	63.36	23.79
6.0	8.3	41.44	209.60	0.00	0.32	72.16	21.83
8.3	10.7	32.96	252.00	0.00	2.72	80.48	24.29
10.7	13.2	29.92	260.16	1.28	0.48	91.04	24.81
13.2	15.7	26.08	360.56	0.00	0.32	96.64	25.86
15.7	18.1	25.76	320.96	0.16	1.76	98.40	24.60
23.0	26.8	20.64	322.72	0.80	0.96	105.44	
31.6	35.7	22.88	368.32	1.12	0.80	102.40	
45.7	50.3	20.64	437.28	0.32	0.48	113.28	
65.3	68.8	23.68	469.12	0.16	0.80	170.56	24.53

BB9-3, March 1984

Interstitial Water

Top (cm)	Bottom (cm)	PO_4^{3-} (uM)	$Si(OH)_4$ (uM)	NO_3^- (uM)	NO_2^- (uM)	NH_4^+ (uM)	SO_4^{2-} (mM)
0.0	0.7	35.19	218.52	7.81	0.28	56.68	26.91
0.7	3.3	40.01	242.63	1.67	0.20	67.58	22.94
3.3	5.7						
5.7	8.5	51.32	287.15	0.50	0.08	138.43	24.75 +- 0.80
8.5	10.7						
10.7	13.0	33.38	354.46	0.31	0.02	131.89	21.06
13.0	17.1	17.78	197.38	0.24	0.00	126.44	21.93
25.5	29.5	8.53	268.30	0.00	0.29	74.12	25.33 +- 0.35
35.5	38.2	28.95	316.41	0.23	0.09	158.05	24.79
45.5	48.0	26.32	340.53	0.03	0.08	201.65	21.41

BB9-4, March 1984

Interstitial Water

Top (cm)	Bottom (cm)	PO_4^{3-} (uM)	$Si(OH)_4$ (uM)	NO_3^- (uM)	NO_2^- (uM)	NH_4^+ (uM)	SO_4^{2-} (mM)
0.0	2.5	51.02	124.76	0.06	0.08	31.61	20.22
2.5	5.0	36.12	207.68	0.14	0.00	54.50	21.91
5.0	7.3	29.06	187.39	0.07	0.06	71.94	23.79
7.3	9.0	15.12	339.91	0.00	0.26	87.20	21.04
9.0	11.4	20.09	300.43	0.13	0.00	97.01	23.55
11.4	13.5	22.29	350.94	0.13	0.00	101.37	24.10
13.5	17.3	20.77	322.26	0.09	0.04	99.19	23.27
23.5	28.0	31.80	379.97	0.08	0.05	152.00	23.47
35.0	39.5	27.66	392.09	0.09	0.03	195.12	20.29
47.5	51.3	26.27	424.61	0.07	0.05	215.82	23.55